Studies on the use of Peptide Auxiliaries in the *Meso*-desymmetrization of Epoxides, and the Kinetic Resolution of Secondary Alcohols

A thesis submitted to the

University of Cape Town

In fulfilment of the requirements of the

Degree of Doctor of Philosophy

By

Rudy Edgar Cozett

Supervisor: **Professor Roger Hunter**

Department of Chemistry

University of Cape Town

Rondebosch, 7701

Cape Town

April 2015

Declaration

I declare that "*Studies on the use of Peptide Auxiliaries in the Meso-desymmetrization of Epoxides, and the Kinetic Resolution of Secondary Alcohols"* is my own work and that all sources that I have used or quoted have been indicated and acknowledged by means of complete references.

_____

Rudy E. Cozett

Abstract

This thesis reports on the use of amino acids and peptides as chiral ligands/catalysts in two asymmetric processes: *Meso*-desymmetrization of an epoxide and the kinetic resolution of secondary alcohols. Chapter 1 comprises a literature review, which gives a general overview of methods of asymmetric synthesis, followed by an overview on the existing classes of asymmetric DMAP-type acyl-transfer catalysis as the major topic of the thesis. Chapter 2 describes the synthesis and evaluation of four peptide ligands used in combination with scandium(III) triflate for the *meso*-desymmetrization of cyclohexene oxide. Enantioselectivities were determined by chiral HPLC, and gave results of up to 41% ee.

Chapter 3 discusses the synthesis and characterisation of three classes of nucleophilic DMAP-type catalysts, in which various amino acid/peptide auxiliaries were attached either α, β, or γ- to the pyridine nitrogen. The peptides contained tryptophan, chosen to exploit a potential π–π stacking interaction with the acyl-pyridinium cation. Catalysts substituted at the α and *γ* positions gave no kinetic resolution for 1-(2-naphthyl)ethanol **121**; however, a dipeptide (Leu-Trp)-containing catalyst **128** substituted at the β-position gave an s-value of 5.3. In order to improve the selectivity, **128** was derivatised at the C-terminal to form two tripeptide-containing catalysts, and acylated at the NH group of the indole ring (**141**). A range of secondary alcohols were tested and selectivity factors increased to up to 10.7. A series of second-generation catalysts were synthesised, but s-values did not improve.

An NMR study was performed to reveal a possible conformational change during the stereoselective step. Computational modelling was performed using molecular mechanics (MMFF94) and quantum mechanics (B3LYP/6-31G, M06/6-31G*, ωB97X-D/6-31G) to determine a possible transition-state model, which indicated a π–cation interaction of the electron-rich indole ring of a tryptophan moiety with the electron-deficient pyridinium cation as a likely determinant of stereoselectivity.

Acknowledgements

I would like to thank the following people for their contributions to this thesis:

Professor Roger Hunter, for his guidance, motivation, and encouragement throughout the course of my PhD and the preparation of my thesis.

Dr. Gerhard Venter for assistance with molecular modelling experiments and helpful discussions.

Colleagues past and present in the Hunter/Gammon research groups, Ana Andrijevic, Dr. Yassir Younis, Wade Petersen, Cathryn Driver, Dr. Pieter Levecque, Dr. Sopie Rees-Jones, Athi Msutu, James Biwi, Shankari Nair, Taigh Anderson, Fabrizio L'Abbata, Daniel Kusza.

Pete Roberts, Noel Hendricks, Zac McDonald, Piero Benincasa, and Claire Lawrence-Naidoo for their analytical services.

The National Research Foundation and the University of Cape Town for their financial support.

My family for their constant support and encouragement throughout the course of my studies.

Abbreviations

AcOH	Acetic Acid
APT	Attached proton test
aq.	Aqueous
Ar	Aromatic
BnBr	Benzyl Bromide
Boc	di-*tert*-butyl dicarbonate
br.	Broad
br. s	Broad singlet
C	Conversion
cat.	Catalytic
CF_3COOH	Trifluoreoacetic acid
CH_2Cl_2	Dichloromethane / Methylene chloride
CH_3CN	Acetonitrile
COSY	Correlation spectroscopy
Cys	Cysteine
δ	Chemical shift in ppm
d	Doublet
dd	Doublet of doublets
dt	Doublet of triplets
DCC	1,3-Dicyclohexylcarbodiimide
DCM	Dichloromethane / Methylene chloride
DIAD	Diisopropylazodicarboxylate
DIEA	Diisopropylethylamine
DMAP	4-Dimethyamino pyridine / *N*,*N*-Dimethyamino pyridine
DMF	Dimethylformamide
DMSO	Dimethylsulfoxide
E1	Unimolecular elimination
E2	Bimolecular elimination
EDC	*N*-(3-Dimethylaminopropyl)-*N*′-ethylcarbodiimide hydrochloride
ee	Enantiomeric excess

Et_3N	Triethylamine
Et_2O	Diethyl ether
EtOAc	Ethyl acetate
EtOH	Ethanol
eq.	Equivalent
Fmoc	Fluorenylmethyloxycarbonyl
g	Grams
HCl	Hydrochloric acid
HOBt	1-Hydroxybenzotriazole
HPLC	High-performance liquid chromatography
hr.	Hour
HRMS	High-resolution mass spectrometry
HSQC	Heteronuclear single quantum coherence
Hz	Hertz
IR	Infrared spectrometry
J	Coupling constant
k_{rel}	Selectivity factor
LAH	Lithium aluminium hydride
Leu	Leucine
Lit.	Literature
m	*Meta*
m	multiplet
M^+	Molecular ion
MeOH	Methanol
mg	Milligram(s)
MHz	Megahertz
mL	Millilitre(s)
mmol	Millimole(s)
MMFF94	Merck molecular force field
m.p.	Melting point
m/z	Mass to charge ratio
NMM	*N*-Methylmorpholine
NR	No reaction
o	*Ortho*

p	*Para*
PG	Protecting group
Pd/C	Palladium-on-carbon
pet ether	Petroleum ether
PPh_3	Triphenylphosphine
PPY	4-Pyrrolidinopyridine
Pro	Proline
PT	Proton transfer
r.t.	room temperature
s	Singlet
S_N1	Unimolecular nucleophilic substitution
S_N2	Biomolecular nucleophilic substitution
s-value	Selectivity factor
t	Triplet
td	Triplet of doublets
TFA	Trifluoroacetic acid
THF	Tetrahydrofuran
TLC	Thin layer chromatography
Trp	Trytophan
Tyr	Tyrosine
q	Quartet
UV	Ultraviolet

Contents

Chapter 1: Literature Review

1.1 Asymmetric Synthesis

Asymmetric synthesis – the production of chiral compounds from prochiral substrates or racemic molecules – is one of the main areas of research in organic chemistry and has widespread industrial uses.[1] The production and sale of chiral molecules in enantiomerically pure form is a multibillion dollar industry that includes pharmaceuticals (e.g. **1** and **2**), agrochemicals (e.g. **3** and **4**), polymers, and starting material/intermediates for total synthesis (Fig. 1.1).

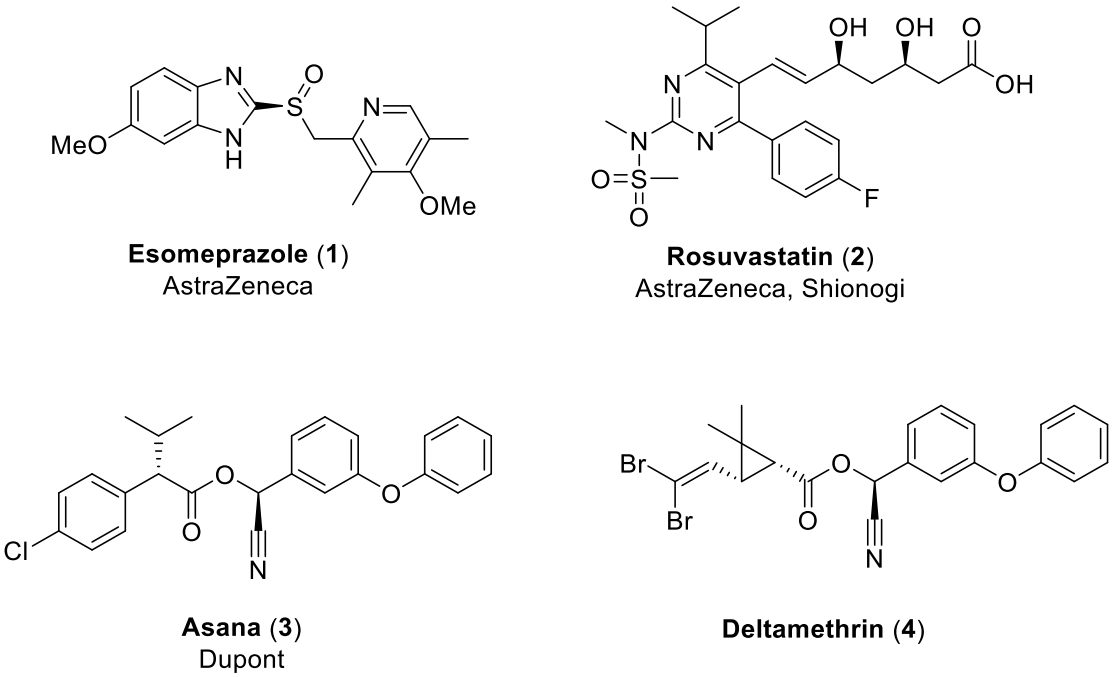

Figure 1.1. Examples of chiral pharmaceuticals and pesticides.

One of the main reasons for producing enantiopure compounds is that opposite enantiomers can have drastically different chemical reactivity;[2] this is especially true in the pharmaceutical and agrochemical industry. Since biological macromolecules in living systems are made up exclusively of one enantiomer, biologically active compounds like drugs can show different behaviours for opposite enantiomers. Other reasons for producing enantiopure compounds include the following: 1) Biological activity is usually only associated with one enantiomer. For example, deltamethrin (**4**) (Fig. 1.1) exists as eight stereoisomers, but only the isomer shown is biologically active;[2] 2) The presence of the inactive enantiomer may inhibit the active one; 3) Stereoisomers that may appear harmless in

the short-term could have long-term side effects; 4) Producing pharmaceutical drugs in enantiopure form is required by law.[3]

1.2 Methods for Asymmetric Synthesis

There are four general methodologies in asymmetric synthesis, namely:[2] 1) Substrate-controlled methodology in which stereocontrol is directed intramolecularly by a chiral entity present in the molecule from a chiral pool substrate such as an amino acid, carbohydrate, terperne etc.; 2) Auxiliary-controlled methods, in which stereocontrol is also directed intramolecularly but by a chiral auxiliary (attached to the substrate) that is removed after the reaction is complete;[4] 3) Reagent-controlled methods, in which stereocontrol is directed intermolecularly by a stoichiometric amount of a chiral reagent; and 4) Catalyst-controlled methods, in which stereocontrol is directed intermolecularly or intramolecularly (see organocatalysis) by a chiral catalyst in conjunction with a reagent (see section 1.3).[5] Additionally, racemic mixtures can be resolved in a classical resolution[6] by adding a stoichiometric amount of a chiral resolving agent and then separating the diastereomers, or by a kinetic resolution[7] in which the fast reacting enantiomer produces a product and the slow reacting enantiomer is resolved (discussed further in section 1.6). Ideally, if there is some way for the racemic starting material to racemize,[8] all of the substrate can be resolved into a single enantiomer, a process known as dynamic kinetic resolution.[6]

Of all the methods listed above, asymmetric catalysis (4) is the most favourable, since enantiomerically pure compounds can be formed using a small amount of recoverable catalyst at a lower cost, higher yield, and greater atom economy than with the other methods. In view of the research carried out in this thesis, only the latter type will be discussed.

1.3 Asymmetric Catalysis

In a chemical reaction, a catalyst speeds up a reaction by providing a lower activation-energy reaction path towards the product. Figure 1.2 shows a typical reaction-coordinate diagram for the conversion of substrate **A** into product **B**, for both the uncatalysed (i) and catalysed (ii) reactions in which transition-state free-energy changes ($\Delta G^{\ddagger}$) for the catalysed reaction are given for the two steps overall. The difference between the free energies of the reactants and products is given by $\Delta G°$.

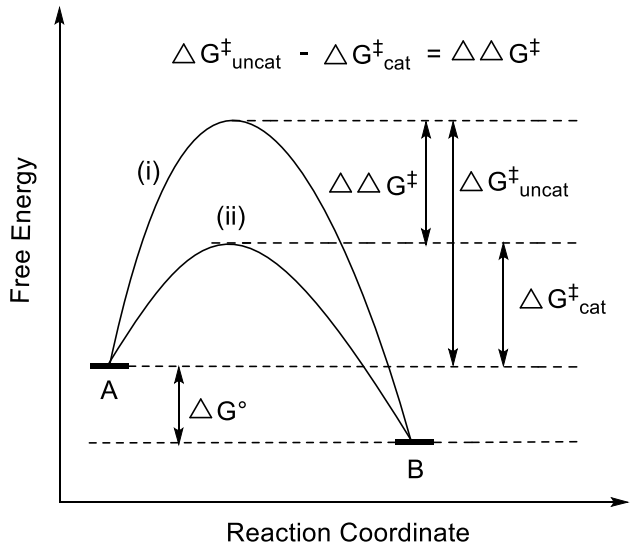

Figure 1.2. Reaction-coordinate diagram for (i) an uncatalysed and (ii) a catalysed reaction.

A catalytic asymmetric process (Fig. 1.3) relies on a kinetic phenomenon in which one enantiomer reacts faster than the other. Here it is assumed that the *R*-enantiomer is faster formed. Therefore, the transition states that lead to the two products, *R* and *S*, should have different activation energies by virtue of diastereomeric complex formation between the substrate and the catalyst.

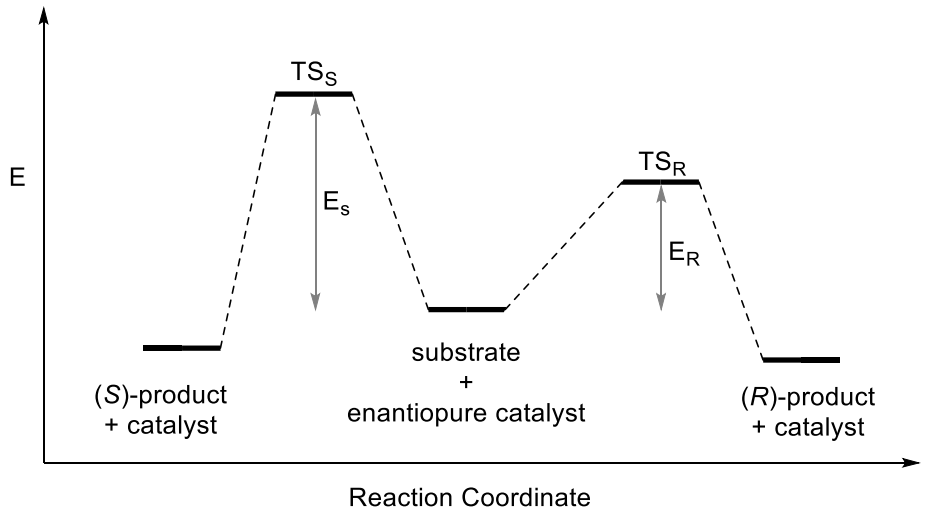

Figure 1.3. Reaction-coordinate diagram for a catalytic reaction.

Asymmetric catalysis has traditionally fallen into two general categories as involving either transition-metal complexes or enzymes. However, over the last decade a third category, coined organocatalysis, has emerged from a few interesting reactions to being a thriving area of research that include a wide range of reactions.[9-11]

1.4 Organocatalysis

Organocatalysis is asymmetric catalysis involving an organic catalyst consisting of the main elements of organic chemistry,[10] namely: carbon, hydrogen, oxygen, nitrogen, sulfur, and phosphorus. Figure 1.4 shows some examples of asymmetric organocatalysts.

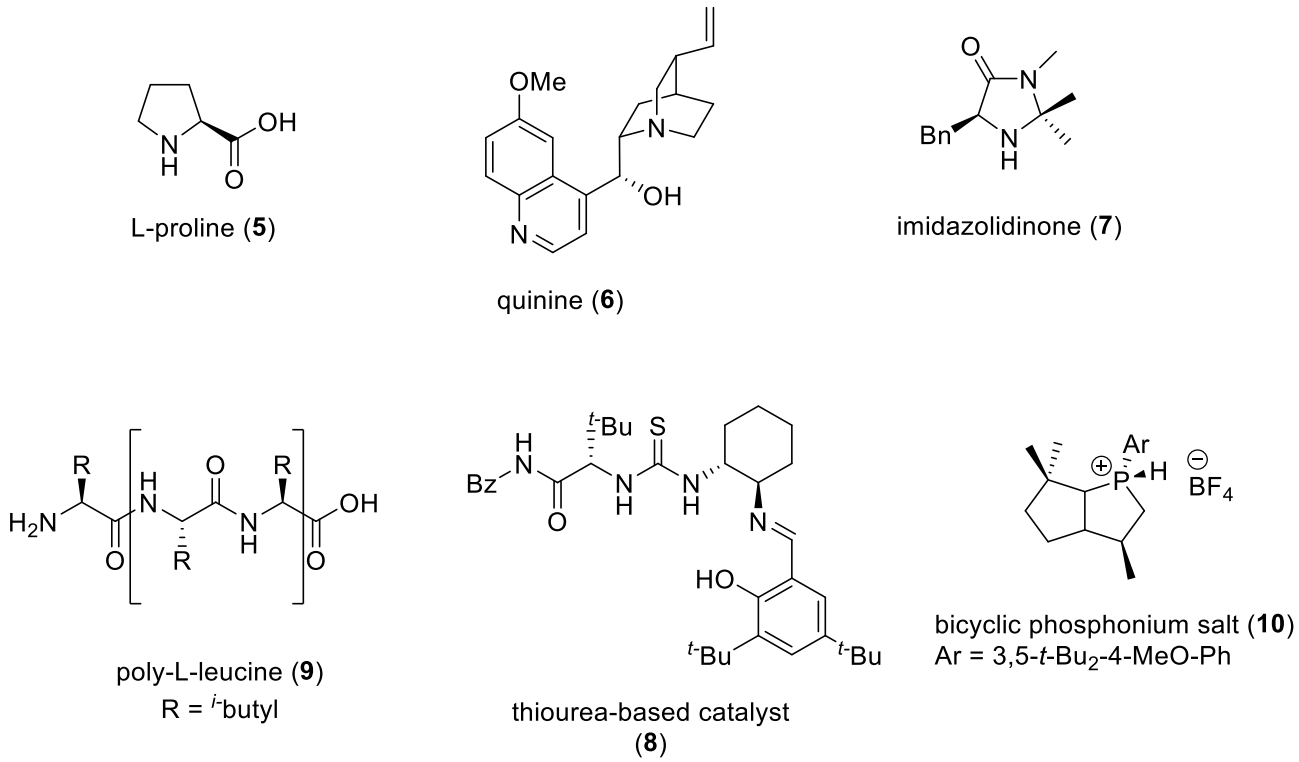

Figure 1.4. Examples of asymmetric organocatalysts (**5–10**).

There are certain advantages to using an organic catalyst over traditional asymmetric catalysts such as transition-metal catalysts and enzymes, since they are inexpensive, easily synthesised, stable in air or aqueous media, and do not result in undesirable by-products such as heavy metals.[10] Moreover, organic molecules such as amino acids, carbohydrates, and terpenes are available from the chiral pool as single enantiomers.

The earliest example of an asymmetric reaction catalysed by an organic molecule was reported by Bredig and Fiske in 1913 involving the addition of HCN to benzaldehyde in the presence of quinine (**6**).[12] Unfortunately, an ee of only 10% was obtained. Over the following 90 years there were sporadic reports of organic molecules catalysing asymmetric reactions. In 1998 MacMillan introduced iminium-ion activation – a mode of catalysis involving the use of a chiral amine – to catalyse the asymmetric Diels Alder reaction. Since then the field has grown to the extent that organic catalysts are used in a wide range of reactions, e.g.

oxidations,[13, 14] reductions,[15, 16] aminations, Strecker reaction (for amino acid synthesis),[17,18] halogenation,[19-21] Michael additions,[22,23] and others.[24-26]

Organocatalysis can be classified based on their mechanism of action into four types: Lewis acid, Lewis base, Brønsted acid, and Brønsted base.[27] This thesis focuses on the use of Lewis bases as catalysts, specifically the use of chiral 4-dimethylaminopyridine (DMAP)-type derivatives for the kinetic resolution of secondary alcohols, which will be discussed in the next section.

1.5. Review of DMAP Chemistry

1.5.1 Introduction

DMAP (**11,** Fig. 1.5) is a versatile, mild, and inexpensive nucleophilic catalyst used in a wide range of useful chemical transformations,[28-31] such as the acylation of alcohols, amines, and enolates, the Baylis-Hillmann reaction, the Dakin-West reaction, the protection of amines, C-acylations, silylations, and many others.

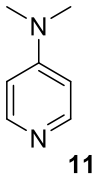

11

Figure 1.5. Structure of 4-dimethylaminopyridine (DMAP).

Its catalytic activity was first detailed in 1967 by Litvinenko and Kirichenko when they discovered that replacing pyridine with **11** caused a rate increase of 10^4 for the benzoylation of *m*-chloroaniline.[32] Independently, Steglich and Höfle showed in 1969 that **11** accelerates the acylation of the sterically hindered alcohol, 1-methylcyclohexanol.[33]

Since its discovery as a nucleophilic acyl transfer catalyst, a range of more reactive nucleophilic DMAP-derived catalysts have been reported. For example, 4-pyrrolidinopyridine (PPY, **12**) and the pyridonaphthyridine **13**, react 2.4 and 6 times faster than **11** respectively in the acylation of tertiary alcohols.[34] Han *et al.*[35] has also shown that the tricyclic triaminopyridines based on **14** – also called "super DMAP"[36] – are also more reactive than **11**.

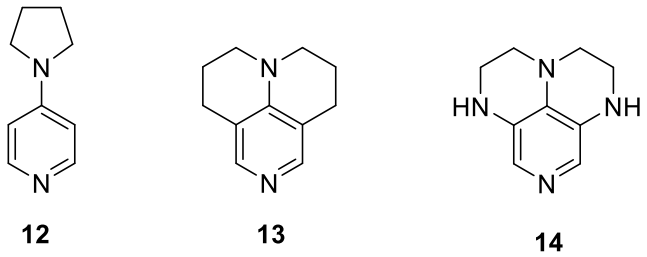

Figure 1.6. Nucleophilic acyl-transfer catalysts based on the DMAP concept.

Despite the availability of more efficient variants of **11**, it is still the reagent of choice for acyl transfer reactions. The availability of **11** in commercial quantities, its wide range of reported applications, and its low cost, have continued to stimulate great interest in its use as a catalyst, some examples of which are given in the following:

1.5.1.2 Steglich Esterification[28]

The esterification of carboxylic acids is a popular reaction employing **11** as a catalyst. Steglich *et al.* first described the reaction in 1978 using dicyclohexylcarbodiimide (DCC) and a catalytic amount of **11** as carboxylic acid activating agent (Scheme 1.1).

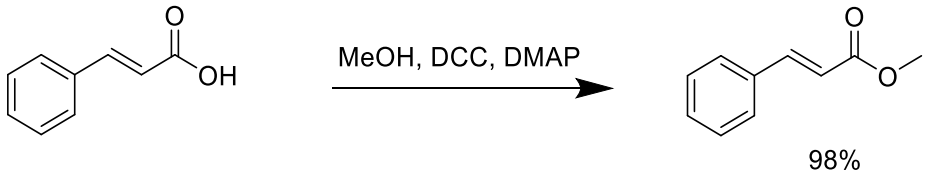

Scheme 1.1. Steglich Esterification using DMAP

1.5.1.3 Total Synthesis

In the synthesis of the CP molecule, Nicolaou included a report of a successful model study for the one-carbon homologation of an aldehyde into a nitrile by cyanohydrin formation and deoxygenation. One of the hydroxyl groups was acylated using DMAP and thiocarbonyldiiimidazole to form the thiocarbamate, while deoxygenation of the cyanohydrin was achieved via a radical reduction (Scheme 1.2).[37]

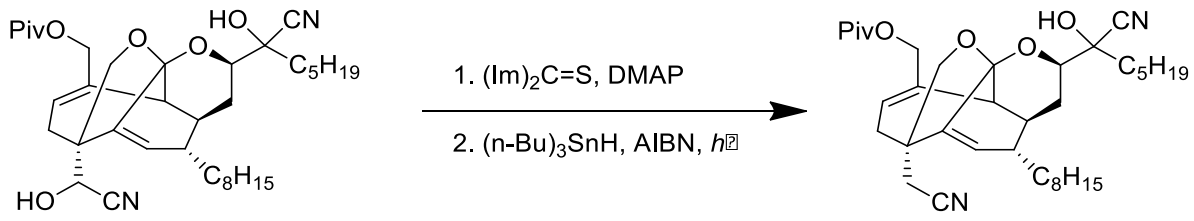

Scheme 1.2. One-carbon homologation of an aldehyde into a nitrile

1.5.1.4 Reagents Supported on DMAP

The ionic liquid [bmim]PF_6 has been employed as solvent for OsO_4 immobilised on DMAP as a catalyst in a simple and practical approach for olefin dihydroxylation (Scheme 1.3).[38] Isolated yields varied between 73 and 99 % for various substrates.

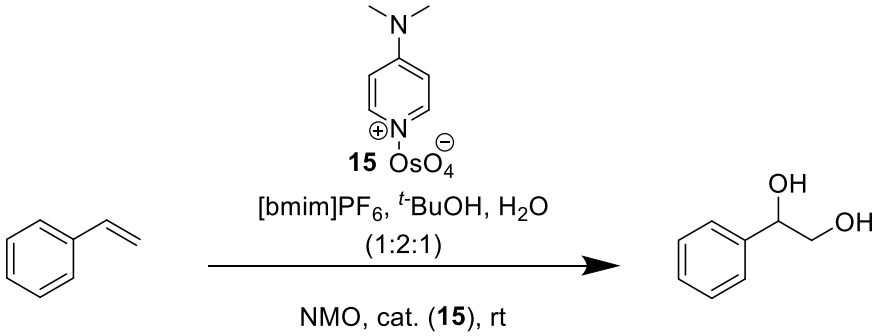

Scheme 1.3. Reagents Supported on DMAP

Similarly, chiral variants of **11** that promote a wide range of enantioselective transformations is an important topic in asymmetric catalysis, and has matured to the extent that developing effective chiral **11** analogues has become an active area of research.[39,40] The kinetic resolution of secondary alcohols provides a testing ground for applying new design principles for chiral catalysts of **11**, since optically active secondary alcohols are important starting materials and intermediates in the synthesis of natural products, bioactive non-natural products, and chiral ligands. This has led to a renewed interest in understanding the mechanism of DMAP catalysis and the factors that influence its reactivity. Thus, the next three sections will highlight the mechanism of DMAP catalysis, the general concept of kinetic resolution, and the use of chiral DMAP derivatives.

1.5.2 Mechanism of DMAP Catalysis

Scheme 1.4 shows the currently accepted mechanism of catalysed acylation using **11**. In the first step the pyridine nitrogen attacks the acylating agent (e.g. anhydride or acid chloride) to form an acyl-pyridinium cation **A**.[35]

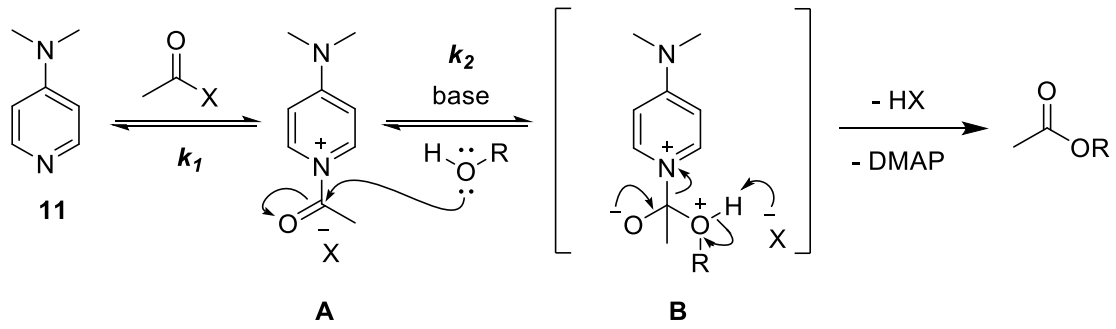

Scheme 1.4. Mechanism of DMAP Catalysis[34]

The next step, which is the rate-determining step k_2, involves nucleophilic attack of the hydroxyl group of the alcohol on the *N*-acyl-pyridinium ion **A** to form intermediate **B**. This is followed by rapid deprotonation of **B** to form the ester, with regeneration of the catalyst.[35] The HX is usually removed by an auxiliary base like triethylamine that does not participate in acyl-transfer. That way the DMAP can achieve turnover as a catalyst.

The development of chiral derivatives of **11** in order to achieve an asymmetric transformation has prompted researchers to pay closer attention to this seemingly straightforward process. [34] A recent review on the mechanism of acylation reactions of **11** has revealed interesting aspects about the factors that increase the catalyst efficiency, the deprotonation step, and solvent effects, which are now discussed.

The efficiency of the catalysis depends on the stability of the acyl-pyridinium salt.[28] Therefore, factors that lead to a more stable acyl-pyridinium salt such as electron-donation will enhance its concentration and accelerate the reaction. Similarly, factors that destabilize the acyl-pyridinium cation will decrease its concentration. The presence of an electron-donating group in the 4-position, greatly enhances the catalytic activity of **11** and other related pyridine compounds.[28] This can be rationalised using resonance theory, in which the lone pair on the exocyclic nitrogen overlaps with the π orbitals of the pyridine ring producing a number of canonical forms, four of which are shown in Scheme 1.5.

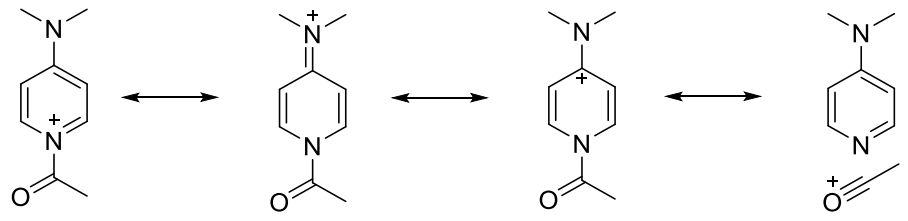

Scheme 1.5. Resonance structures of *N*-acyl-pyridinium cation

Thus the increased electronic communication between the exocyclic nitrogen and the carbonyl group, through the pyridine ring, increases the stability of the acyl-pyridinium cation;[34] this accounts for the improved nucleophilicity of DMAP derivatives such as **12**, **13** and **14**.

Inductively donating groups attached to nitrogen at the 4-position (e.g. alkyl groups), and directly to the pyridine ring in the 3- and 5-positions also stabilize the acyl-pyridinium cation, while any groups attached to the 2- and 6-positions destabilize the acyl-pyridinium cation due to steric interactions with the acyl group. Table 1.1 shows some acylation enthalpies for various pyridine catalysts calculated by Zipse *et al.*[41] As can be expected, extra substitution (4-substitution is there in each) at the 3- and 5-positions results in the highest exothermic acylation enthalpy, and the compounds are efficient catalysts; while introduction of substitution to the 2- and 6-positions results in a reduced exothermic acylation enthalpy and the resultant compounds are inefficient as acylation catalysts.[41]

Table 1.1. Acylation enthalpies for various catalysts.

catalyst	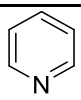	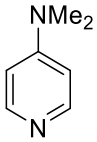	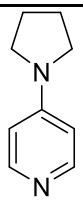	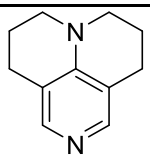	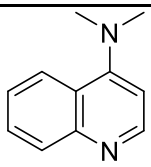	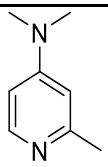
substitution position		4	4	3, 4, 5	2, 3, 4	2, 4
ΔH_{rxn} kJ/kmol	0.00	−82.2	−93.1	−108.9	−60.4	−66.2

The concentration of the acyl-pyridinium ion also depends on the nature of the acylating agent. When acetyl chloride is used the equilibrium of the reaction (Scheme 1.4, k_1) is shifted completely to the right, but when acetic anhydride is used only 5–10% (relative to DMAP) of an acyl-pyridinium cation is formed at any one time.[42] However, the rate of the reaction overall is faster when an acetate anion is present than when a chloride anion is present. This is due to a looser degree of binding between the pyridinium cation and the anion: “Loose binding” between mesomerically stabilized anion (e.g. acetates) and cation leads to faster reaction overall since the alcohol has better access to the carbonyl group, whereas “tight

binding", due to high ionicity between the anion (e.g. chloride) and the cation, leads to a decrease in the rate because access to the carbonyl is restricted (Fig. 1.7) probably due to steric hindrance by the bigger chloride group.[43]

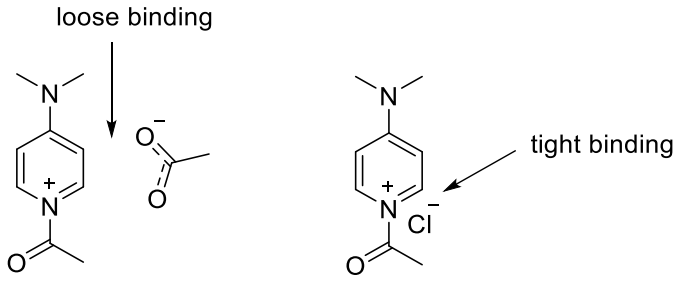

Figure 1.7. Loose binding and tight binding between acyl-pyridinium cation and anion.

In order to shed more light on the mechanism, Zipse *et al.*[44] used theoretical and kinetic methods to investigate the deprotonation step since three bases are present in the reaction, namely: **11** (DMAP), the anion (X^- of the acylating agent), and the auxiliary base. For this, they studied the acylation of *tert*-butanol with acetic anhydride in the presence of catalytic amounts of **11** (Scheme 1.6) together with triethylamine as the auxiliary base (for the AcOH formed).[44]

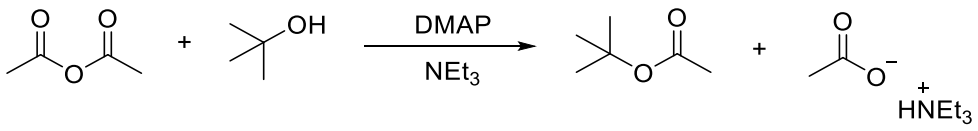

Scheme 1.6

Their theoretical results support the mechanism described in Scheme 1.4 in which there is no base catalysis on the hydroxyl hydrogen, and in which the acetate counterion is the most likely base in the "deprotonating step". Kinetic studies have shown that neither the auxiliary base nor catalytic DMAP removes the proton in intermediate **B** (Scheme 1.4), due to lack of correlation between the catalytic reactivity and their pK_a.[44] The choice of solvent also plays an important role in the rate of the reaction, which increases in non-polar solvents, while polar solvents result in lower rates.[43]

1.6 Kinetic Resolution using Chiral DMAP Catalysts

A kinetic resolution involves the use of a chiral agent (reagent, catalyst, solvent, etc.) to achieve partial or complete resolution due to the selective reaction of one enantiomer over the other, giving an enantioenriched staring material that can then be isolated (Scheme 1.7).[6,45] The kinetic resolution operates when $k_S \neq k_R$, and the reaction is stopped at some time so as to achieve about 50% conversion.

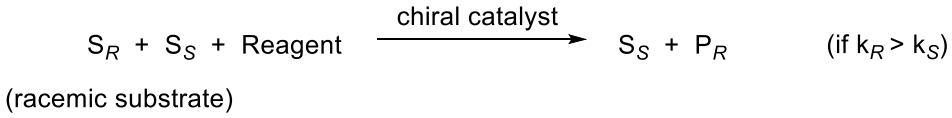

Scheme 1.7

Figure 1.8 shows a graphical representation of a general case for a kinetic resolution, highlighting the three relevant processes: the uncatalysed reaction; the catalysed reaction of the *R*-starting material; and the catalysed reaction of the *S*-starting material. In this idealized situation, the fast-reacting enantiomer (in this example, *R*) will have a lower energy barrier than the slow-reacting enantiomer (*S*) – i.e. $k_R >> k_S$ – and will react until it is consumed, yielding a higher percentage of the *R*-product.

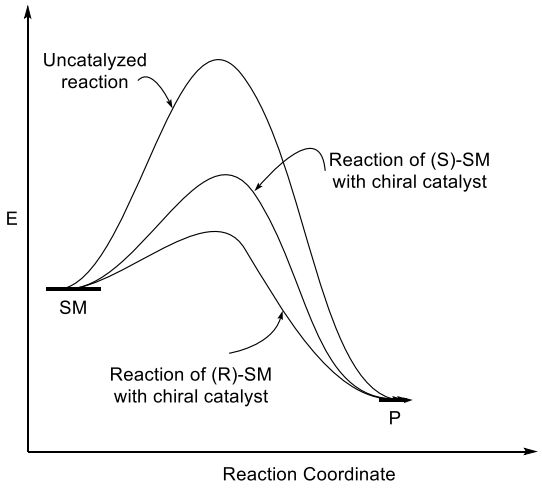

Figure 1.8. Kinetic Resolution[5]

The free energies of these competing transition states define the rate constants for the conversion of the fast-reacting and slow-reaction enantiomers, and the ratio, $k_{rel} = \frac{k_{fast}}{k_{slow}}$, controls the product distribution.[15] This is an important factor in kinetic resolution termed the selectivity factor (s) (i.e. $k_{rel} = s$).

Figure 1.9 shows a general reaction profile for a typical kinetic resolution reaction, for two enantiomers, S_S and S_R that cannot racemize (i.e., $k_{rac} = 0$, or k_R, $k_S >> k_{rac}$). In this example $k_R >> k_S$, so the *R* enantiomer of the substrate (S_R) will react faster than the *S* enantiomer (S_S), leaving S_S enriched. The selectivity factor (s) can be determined using the conversion (C) and the ee of the starting material and product.[46] At the start of the reaction $S_S = S_R = 0.5$ for time t_0. At time t

$$S_R + S_S + C = 1 \quad (1)$$

Rearranging gives, $S_R = 1 - C - S_S$ and $S_S = 1 - C - S_R$ (2)

For reactions that are first order or pseudo-first order in [S], with $k_R >> k_S$

$$\frac{d[S_R]}{dt} = k_R[S_R], \quad (3)$$

and $$\frac{d[S_S]}{dt} = k_S[S_S] \quad (4)$$

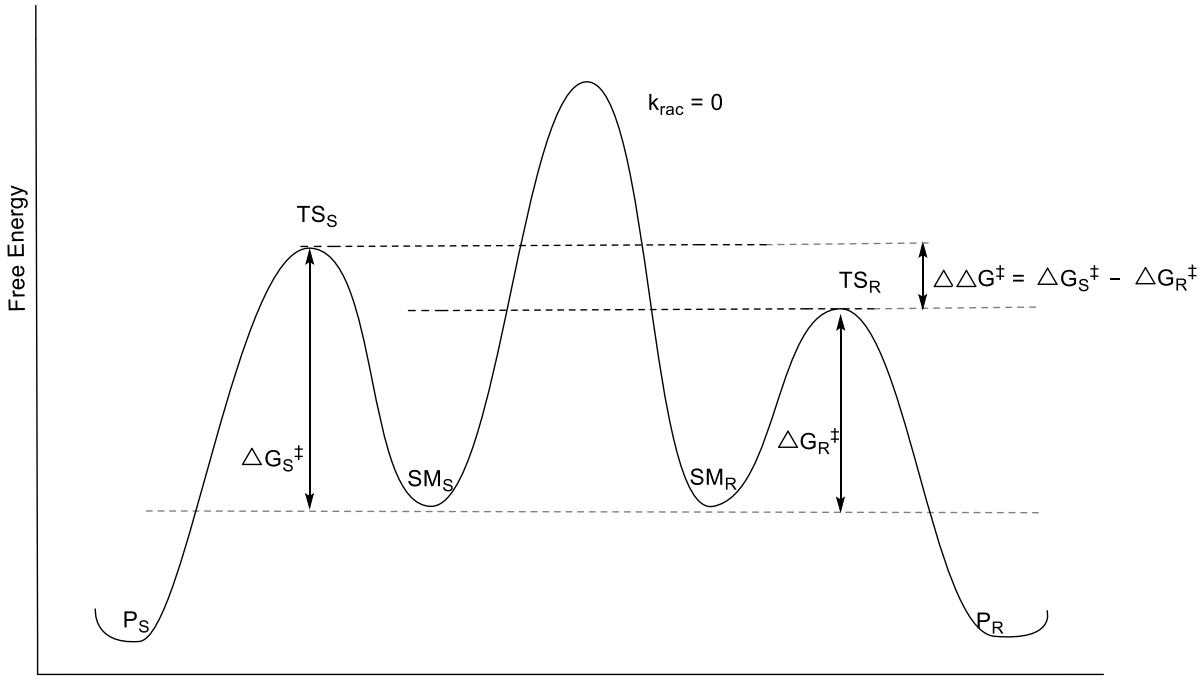

Figure 1.9. Relative rate constants in kinetic resolutions.[6,46]

Kagan[45] derived the expression for the selectivity factor using these equations, plus the definition of ee, to show that the selectivity factor (or s-value) is related to C and ee by

$$s = \frac{\ln[(1 - C)(1 - ee)]}{\ln[(1 - C)(1 + ee)]} \qquad \text{where } ee = S_S - S_R \qquad (5)$$

Figure 1.10 shows how the ee of the starting material (initially as a racemate) increases as the reaction progresses. High substrate enantiomeric excesses can be obtained by running the reaction to higher conversion to consume all of the fast-reacting enantiomer. Selectivity factors with s > 10 are generally considered useful for obtaining the product in an enantioenriched form (> 90 % ee) at 50% conversion.

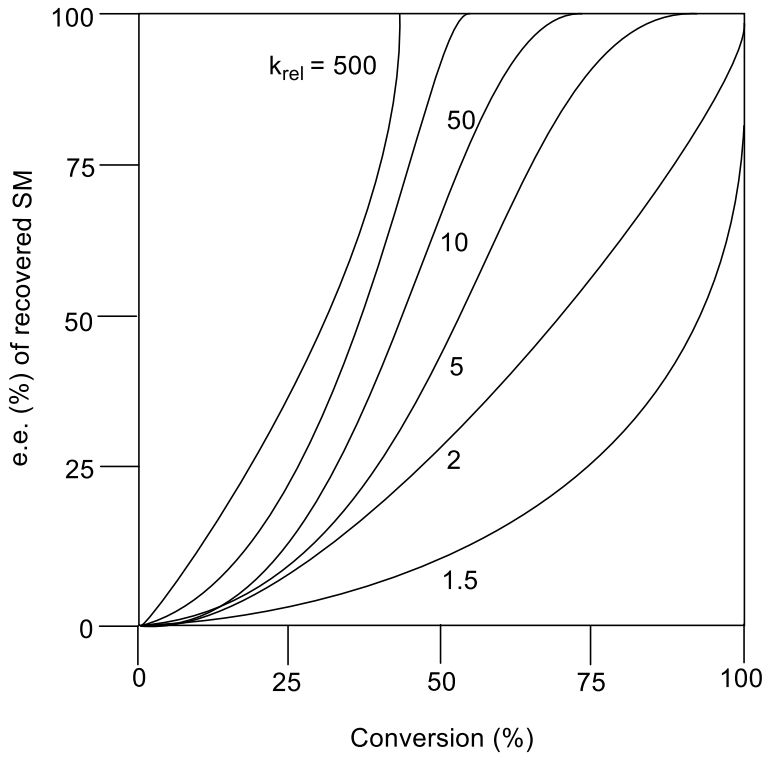

Figure 1.10. Variation of recovered starting material ee with conversion for different s-values.[45]

1.7 Chiral DMAP Derivatives

In 1996 Vedejs and Chen introduced the first chiral DMAP derivative **15** (Fig 1.11) for the kinetic resolution of secondary alcohols using stoichiometric quantities of **15**.[47]

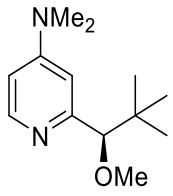

15

Figure 1.11. Structure of Vedejs and Chen's first chiral DMAP derivative.

They obtained s-values up to 53 for a range of benzylic alcohols and an s-value of 14 for an allylic alcohol. However, Vedjes and Chen were unable to use **15** in catalytic amounts, presumably due to steric congestion at the α-position, since Litvinenko and Kirichenko's initial report (section 1.5.1) showed that any steric bulk near the 2- or 6-position (even a methyl group) greatly diminishes DMAP's catalytic activity, referred to in future as its reactivity (as opposed to its enantiopromoting activity) (Scheme 1.8).[48]

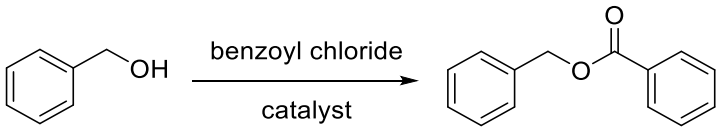

catalyst		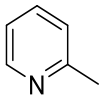	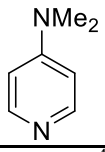
relative rates	1	0.047	3.7×10^4

Scheme 1.8[39]

An effective chiral DMAP catalyst therefore requires the chirality-directing group to get as close to the catalyst's active site (*N*-acyl-pyridinium) as possible without inhibiting its reactivity. Another aspect is to introduce steric effects to shield one face of the molecule, thereby controlling the approach of the nucleophile. Since too much steric bulk can inhibit the catalyst's reactivity, an alternative strategy would be to use a stereogenic group to desymmetrize DMAP through stacking interactions (π–π or π–cation) between the pyridine ring and the chiral side chain attached to either the β- or γ-positions. Scheme 1.9 shows how stacking interactions with a chiral stacking group (electron-rich) can result in

desymmetrization of one face of the pyridine ring, close to the active site following reaction of catalyst **A** with an acylating agent, **R**–**X**, to form intermediate **B**. This derivatisation brings about a conformational change in which an electron-rich functional group in the side chain interacts with the electron-deficient pyridine ring, thereby also stabilizing the acyl-pyridinium cation. The nucleophile (NuH) then attacks **B** in a chiral environment, resulting in the regeneration of **A** and the production of the product.

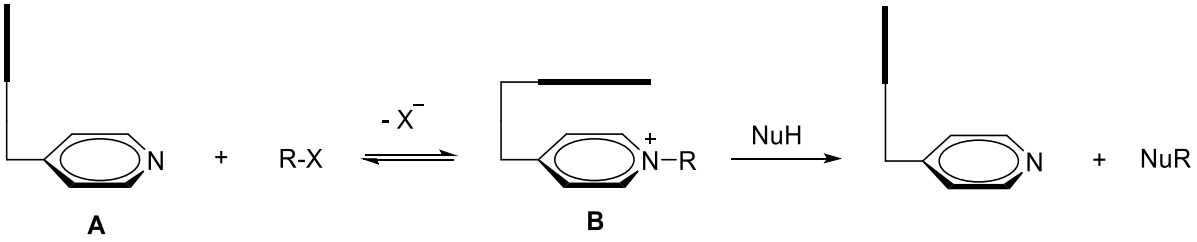

Scheme 1.9. Stacking interactions between the pyridinium ion and an electron-rich side chain[41]

Asymmetric DMAP catalysts can be classified according to the type of stereogenic unit present promoting the enantio-discrimination: axial (atropisomers), central, and planar. Another class of asymmetric acyl-transfer catalysis involves using achiral DMAP in the presence of a chiral H-bond donor; all the strategies will be discussed in the next four sections. The use of amino acids/peptides – which also contain central chirality, and is the focus of this thesis – will be discussed separately in section 1.8.

1.7.1 Central Chirality

4-Substituted DMAP Catalysis

In 1997, Kawabata et.al produced PPY-derived catalyst **16** that acts through an "induced fit" mechanism similar to the concept just introduced above in Scheme 1.9. In his case the 4-pyrrolidino substituent was annulated at its 2,3-positions with a chiral cyclopentanol ring bearing a 2-naphthylmethyl substituent. In the neutral state, the catalyst exists in an open conformation **A**, while in the acylated state the catalyst flips to a closed conformation **B** in which the naphthalene ring stacks over the active site, Figure 1.12.[49]

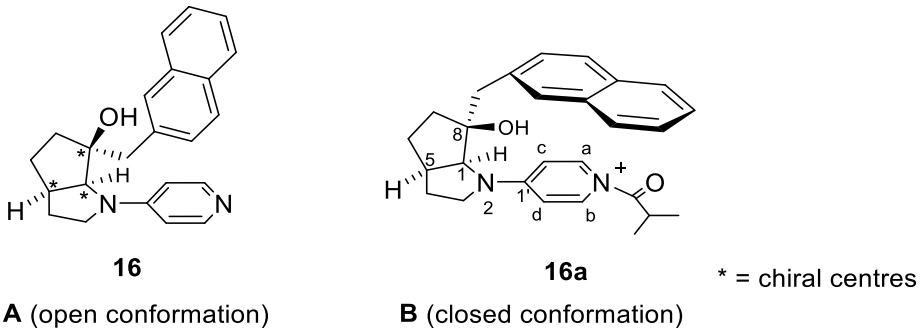

Figure 1.12. Open and closed conformations of Fuji's catalyst.

Mechanistic detail on the reaction was obtained from a ^{1}H NMR study of **16** and its *N*-acyliminion ion **16a** (Fig.1.12) – formed by mixing **16** and *iso*-butyryl chloride in $CDCl_3$. NOe measurements indicated the preferred conformation of **A** to be the "open conformation" in which the naphthyl ring and the pyridine ring lie apart from each other. Protons H_a and H_b are indistinguishable and appear at δ_H 8.01 ppm, while H_c and H_d appear at δ_H 6.37 ppm, suggesting that there is free rotation around the N(2)–C(1') bond. By comparison, in the *N*-acyliminium ion **B**, protons H_a, H_b, H_c, and H_d all appeared independently at δ_H 7.45 ppm, 8.73 ppm, 5.69 ppm, and 6.87 ppm respectively; H_a and H_c were shifed upfield (0.50–0.68 ppm), while H_b and H_d were shifted downfield (0.50–0.72 ppm), indicating a π–π interaction between the naphthalene ring and the acyl-pyridinium moiety predominantly on one side of the pyridine ring. Therefore, upon acylation the naphthyl ring transfers asymmetry from the chiral centres at C(1) and C(8) to the catalysts' active site via π–stacking to the pyridine ring. This intramolecular interaction shields one face of the catalyst and exposes the other to the attacking nucleophile, thus allowing a stereoselective process to occur.

The catalyst was tested in the kinetic resolution of a range of mono-acylated 1,2-diols and produced s-values in the range of 4.7 up to 12.3 (Scheme 1.10).[49]

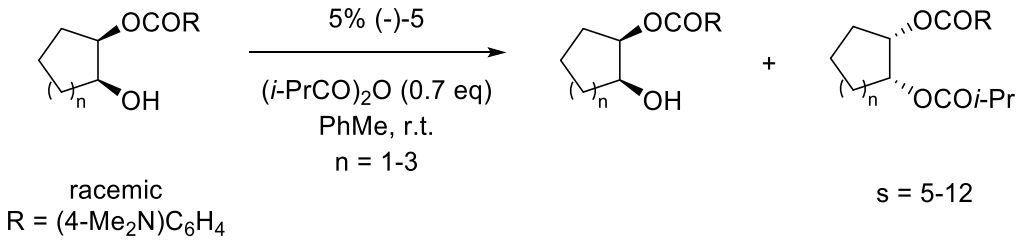

Scheme 1.10.

In 2000, Spivey *et al.* introduced a series of chiral, non-racemic *trans*-2,5-disubstituted C_2-symmetric PPY catalysts (Fig. 1.13).[50]

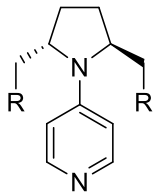

R = H (**17**), OBn (**18**), trityl (**19**), *p*-$NO_2C_6H_4$ (**20**), Ph (**21**), 2-naphthyl (**22**), *p*-$MeOC_6H_4$ (**23**)

Figure 1.13. Spivey's *trans*-2,5-disubstituted C_2-symmetric PPY catalysts.

Their catalyst design was based on molecular modelling studies that suggested that a π–π interaction would occur between the acyl-pyridinium ion and the aryl ether groups (in a similar way to Fuji's induced fit mechanism), attached to the pyrrolidine ring. They also rationalised that a C_2-symmetric catalyst would result in a lower number of diastereomeric transition-states in the stereodifferentiating step. The catalysts were tested in the kinetic resolution of 1-phenylethanol with acetic anhydride as the acyl donor in THF (Table 1.2), but s-values were low (< 2).

Table 1.2. Kinetic resolution of 1-phenylethanol using different catalysts.

catalyst	C	$ee_{(alcohol)}$	s-value
17	72.2	18.7	1.3
18	48.2	19.1	1.8
19	38.1	2.5	1.1
20	14.1	2.6	1.4
21	31.5	6.3	1.5
22	27.2	6.6	1.5
23	28.2	5.1	1.4

Spivey suggested that possible reasons could be that the desired π–π interaction did not take place, or that the chiral groups were ineffective in transferring chirality to the acyl-pyridinium ion. The authors also noted that two of the catalysts (**22** and **23**) had low THF solubility, which could have hampered the formation of the acyl-pyridinium ion. Thereafter, Spivey turned his attention to using axial chirality (see section 1.7.2)

Díez synthesised a C_2-symmetric catalyst **24** and two non C_2-symmetric sulfone-containing PPY catalysts, also incorporating the chirality into the pyrrolidine ring (Fig. 1.14).[51] Compounds **24** and **25** were not expected to produce much asymmetric induction, since the stereogenic centres are not near the active site. Therefore, a benzyl group was introduced

using the reactivity of the sulfone (of catalyst **25**) to form compound **26**. The catalysts were tested in the kinetic resolution of 1-phenylethanol **27** but s-values were also low (Table 1.3).

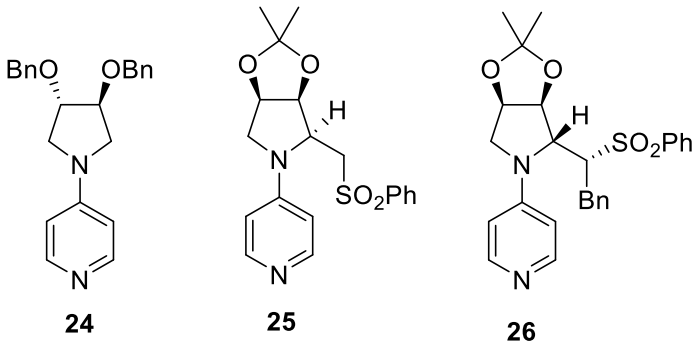

Figure 1.14. Díez' C_2-symmetric catalyst **22** and two sulfone-containing PPY catalysts **23**, **24**.

Table 1.3. Kinetic resolution of 1-phenylethanol using catalysts **22-24**.

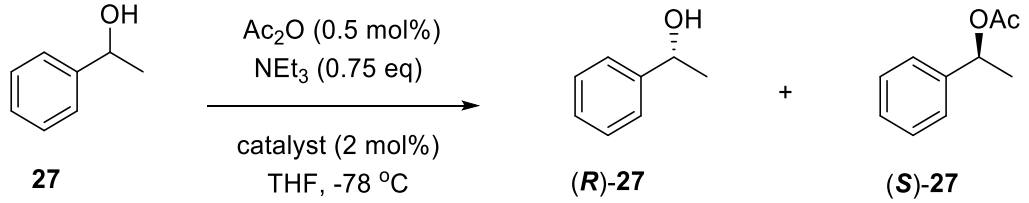

catalyst	C	$ee_{(alcohol)}$	s-value
(+)-24	28	0.8	1.8
(+)-24	40	1.8	2.1
(+)-25	8.6	6.9	1.6
(+)-25	21	4.1	1.4
(+)-26	57	1.2	1.5
(+)-26	62	2.5	1.4

Molecular modelling of the lowest-energy conformation of catalyst **26** (Fig. 1.15) revealed the reason for the low s-values.[51] Although the benzyloxy group's phenyl ring is positioned in the vicinity of the reactive centre, it is too far away to effectively shield one face of the catalyst.

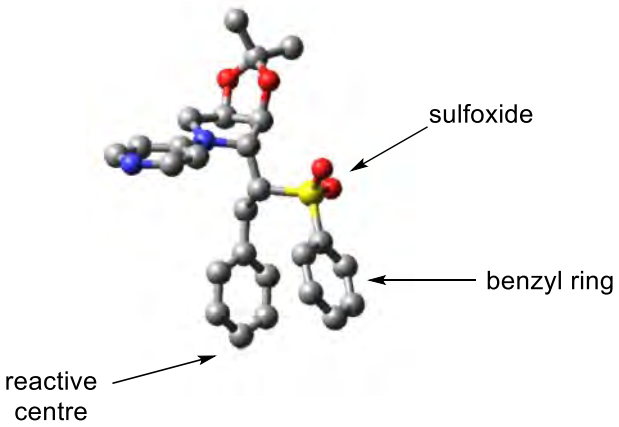

Figure 1.15. Lowest energy conformation for compound **26**.[51]

3-Substituted DMAP Catalysis

Other groups used a different approach and attached the chirality directing group to the β-position, closer to the pyridine nitrogen. In 2002, Jeong designed an interesting chiral DMAP catalyst containing Kemp's triacid as a linker (attached to the β-position to minimize steric repulsion), and a binaphthyl framework as the chiral atropisomeric subunit (Fig. 1.19).[52]

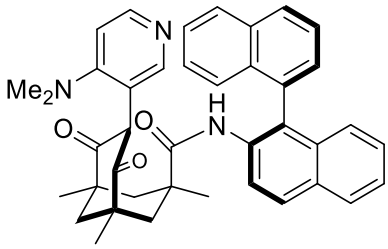

28

Figure 1.16. Jeong's β-substituted DMAP catalyst.

Molecular modelling revealed that in the energy-minimum structure the dimethylamino group points away from the binaphthyl group in order to minimize steric repulsion, while the pyridine nitrogen atom is close to the naphthyl ring of the chiral ligand. Presumably, the role of the linker is to allow the binapthyl group to reach the active site where it can provide shielding of one face of the catalyst. Catalyst **28** gave modest to excellent s-values (4–21) for the resolution of racemic secondary benzylic alcohols (Table 1.4).

Table 1.4. Kinetic resolution of various secondary alcohols with **28**.

unreacted alcohol (major product)	C	$ee_{(alcohol)}$	s-value
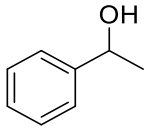	70	79	4.4
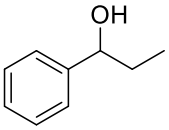	67	85	6.3
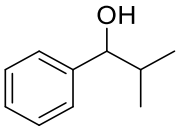	77	99	8.1
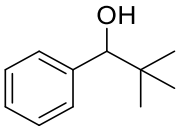	59	90	13.3
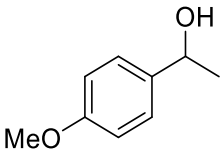	72	84	4.7
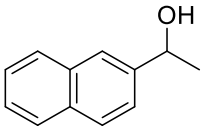	72	98	8.3
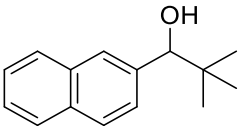	63	95	12.4
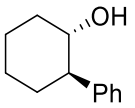	62	99	21.0

As Table 1.4 shows, the s-value increased with increasing steric bulk of the alkyl group of the alcohol, in which the best result was obtained for the acylation of racemic *trans*-2-phenylcyclohexanol, which proceeded with s = 21.

Other groups pursued this concept of remote asymmetric induction via conformational control. Yamada introduced a thiazolidine-2-thione (attached β to the pyridine nitrogen) catalyst **28** that functioned via a "conformational switch" system similar to Fuji's "induced fit" mechanism. On acylation, the thiocarbonyl (π-bond) is postulated to interact with the pyridine ring (cation), resulting in a conformational change in the molecule (Fig. 1.17).[53]

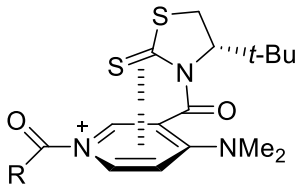

29

Figure 1.17. Yamada's catalysts upon acylation.

^{1}H NMR studies revealed that when the thiocarbonyl interacts with the pyridine ring it selectively shields one face of the molecule, transferring asymmetry to the catalyst's active site. This was determined by comparing the spectra of **29** and its *N*-methyl-pyridinium ion **29a** to corresponding reference compounds lacking the thiocarbonyl moiety (Fig. 1.18).

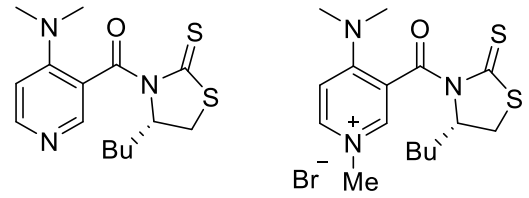

29 **29a**

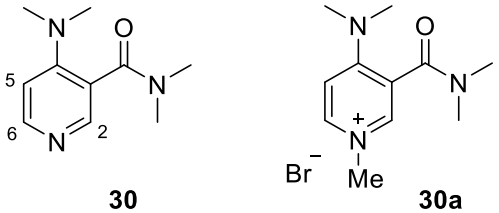

30 **30a**

Figure 1.18. Structural studies of catalyst **29**, its reference (**30**), and their corresponding methyl salts (**29a** and **30a**).

Table 1.5 shows the results of the ^{1}H NMR study, which indicated much greater shifts for the pyridine hydrogens going from catalyst **29** to its pyridinium salt **29a** compared to those for going from **30** to **30a** as monitored by Δδ and Δδa – the differences in chemical shifts between **29** and **30**, and chemical shift differences in the reference compounds **29a** and **30a** respectively. These results reflect the effect of the thiocarbonyl moiety on the chemical shifts of the pyridinium protons implying a proximity effect.

Table 1.5. Selected ^{1}H NMR chemical shifts (ppm) for **29**, **30** and methylated analogues.[53]

Proton	δ**29**	δ**30**	Δδ [c]	δ**29a**	δ**30a**	Δδa [c]
H-2 [a,b]	8.22	8.14	0.08	9.55	8.46	1.09
H-5 [a,b]	6.56	6.57	−0.01	6.87	7.11	−0.24
H-6 [a,b]	8.18	8.22	−0.04	8.08	8.52	−0.44

*a. Measured using $CDCl_3$ as solvent. b. All pyridine protons where unambiguously assigned by NMR spectroscopy (^{1}H, ^{13}C, HSQC, and COSY). c. The Δδ values were calculated using the equations, Δδ = δ**29** − δ**30**, and Δδa = δ**29a** − δ**30a**.*

These observations are consistent with Yamada's previously reported π–cation complex,[54] and indicate that **29a** has a fixed conformation in which there is close proximity of the C=S group with one face of pyridine ring. This interaction is absent in **29**. Therefore, the π–cation interaction allows the incoming alcohol to only approach the acyl-pyridinium ion from the opposite, exposed face. The catalysts produced s-values up to 13 for a range of secondary alcohols (Table 1.6).[53]

Table 1.6. Kinetic resolution of various alcohols catalysed by **29**.

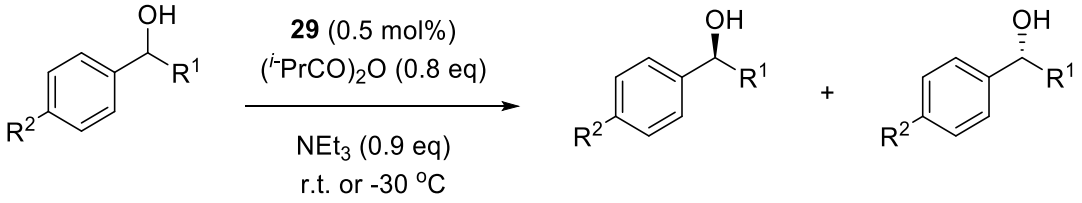

substrate	C	$ee_{(alcohol)}$	s-value
R^1 = Me, R^2 = H	65	89	7.3
R^1 = Me, R^2 = OMe	68	97	10
R^1 = Me, R^2 = NO_2	72	98	8.9
R^1 = ^{t}Bu, R^2 = H	62	88	9.6
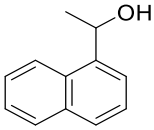	65	97	13
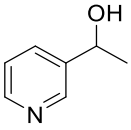	66	92	8.1
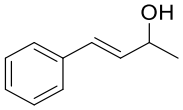	65	94	9.8
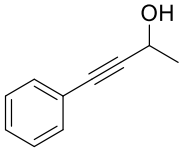	61	78	6.6

The Connon group synthesised the 3-substituted PPY derived catalysts, **31**, **32**, and **33** (Fig. 1.19) also with Fuji's "induced fit" concept in mind, but based on an amide without an extra (thio)carbonyl appendage. They rationalised that their catalyst would also undergo a conformational change upon acylation, causing the sterically demanding aromatic rings to shield one face of the catalyst.[55] Catalysts **30**–**32** were tested in the kinetic resolution of mono-acylated diols, but produced variable s-values (1.4–9.4).

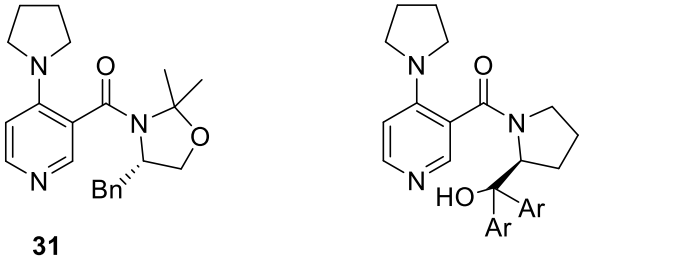

Figure 1.19 Connon's 3-substituted PPY derived catalysts.

NMR studies and molecular modelling by Connon revealed two important factors responsible for the stereoselectivity. These were π–π stacking between the pyridine ring and the aromatic groups in the side chain attached to the 3-position, as well as H-bonding interactions between the substrate and the hydroxyl group of the catalyst.

The most efficient catalyst **32** (of three) was tested in the kinetic resolution of various secondary alcohols (Table 1.7). Results were varied, but they did obtain an s-value of 30 for the *trans*-phenylcyclohexanol alcohol.

Table 1.7. Kinetic resolution of various alcohols catalysed by **32**.[55]

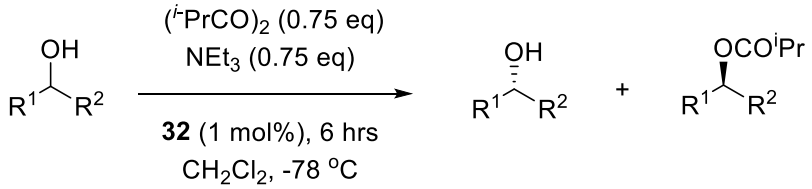

substrate	C	$ee_{(alcohol)}$	s-value
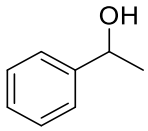	27.5	25	6.3
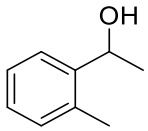	17	17	6.0
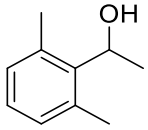	14.6	1	1.1
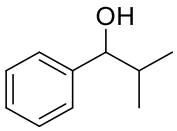	19	19	13.5
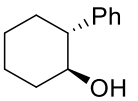	19	22	30.0

Levacher *et al.* created a DMAP catalyst bearing a chiral sulfoxide **33** at the 3-position via bromine-magnesium exchange on a 3-bromo-DMAP derivative followed by substitution with a chiral sulfinate via Anderson chemistry. Sulfoxide, **33,** was obtained as a pure enantiomer in a 60% yield (Scheme 1.10).[56]

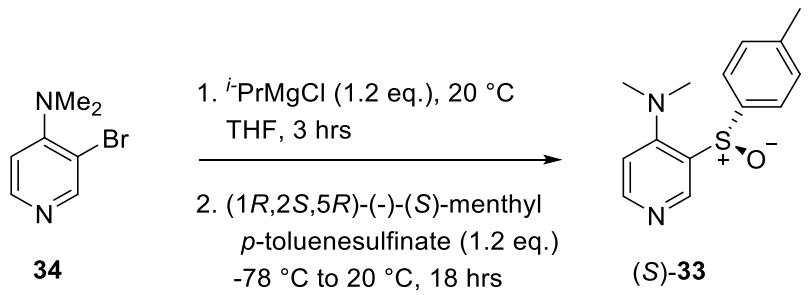

Scheme 1.10. Synthesis of Levacher's sulfoxide-containing DMAP catalyst

They rationalised that the proximity of the dimethylamino group to the sulfoxide would prevent free rotation around the C(3)-S bond. Molecular modelling showed that in the lowest energy conformation, the lone pair of the sulfoxide and the pyridine ring are in a co-planar arrangement. This constraint suggested sterodifferentiation between the two faces of the catalyst. The initial control reaction with DMAP took 2 hours (Scheme 1.11), but the reaction with **33** took 24 hours.

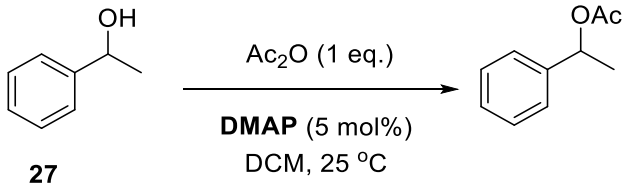

Scheme 1.11.

The authors suggested that the decrease in rate was due to the electron-withdrawing sulfoxide dipole, hampering the formation of the acyl-pyridinium salt. The sulfoxide presumably also did not provide good enough shielding of the face because only modest levels of selectivity (s-values up to 4.5) in the resolution of various secondary alcohols were obtained. Table 1.8 shows the results of the kinetic resolution of various secondary benzylic alcohols using **33** as a chiral catalyst.

Table 1.8. Kinetic resolution of various secondary alcohols with catalyst **33**.

unreacted alcohol (major product)	C	ee $_{(alcohol)}$	s-value
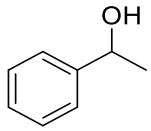	15.5	9.4	3.4
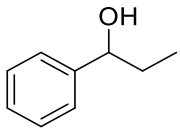	18.3	10.4	3.0
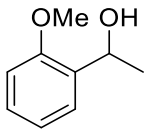	16.7	12.0	4.5
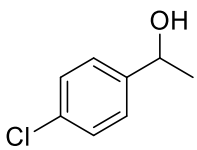	22.4	12.8	2.9

In 2007 the Richards group synthesised a C_2-symmetric organometallic DMAP catalyst with a chiral pyrrolidino group at C-4 incorporating two extra ferrocene groups attached to the β-positions.[57,58]

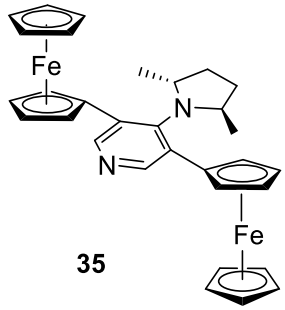

Figure 1.20. Richards' C_2-symmetric organometallic DMAP catalyst.

The iron-containing groups do not participate in the reaction, but provide steric bulk to the two faces. Catalyst **35** was tested in the kinetic resolution of the normal library of secondary alcohols that had become standard for catalyst evaluation (Table 1.9), but s-values were relatively modest, once again suggesting that proximity between chiral element and the active site was not optimal.

Table 1.9. Kinetic resolution of secondary alcohols with **35**.

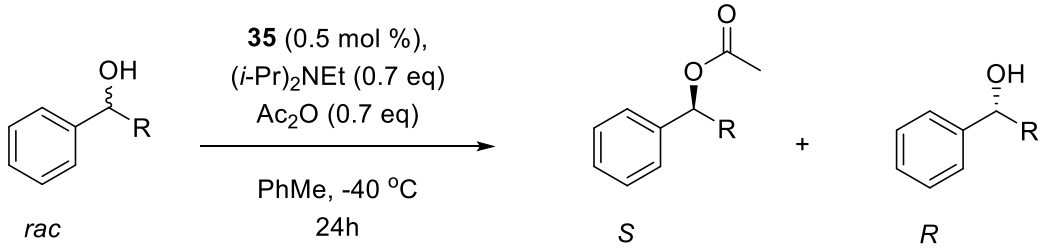

unreacted alcohol (major product)	C	$ee_{(alcohol)}$	s-value
R = Et	52	32	2.5
R = Et	22	16	4.5
R = Et	12	9	5.3
R = Et	8	6	5.8
R = ^{i}Pr	23	20	6.1
R = ^{i}Pr	32	25	4.1

Recently (2014) the Sibi group introduced a DMAP catalyst with fluxional chirality[59] – in which an achiral moiety is used to relay and amplify stereochemical information from existing chiral centres to a different site in the molecule[60] – for the kinetic resolution of

secondary alcohols and biaryl compounds. The catalyst design consisted of three main components: a DMAP moiety; a pyrazolidinone group (the chiral element developed by the group in 2003)[61] attached β to the pyridine nitrogen; and a fluxional substituent, which can be varied and functions as a blocking group (Figure 1.21).

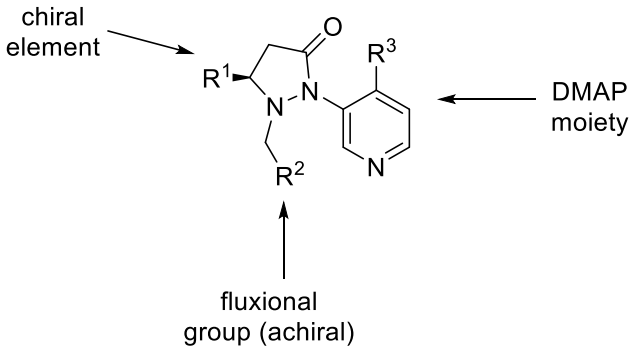

Figure 1.21. Catalyst design for the novel fluxionally chiral DMAP catalyst.

The results of a catalyst screening (varying R^1, R^2, and R^3) revealed **36**, with R^1 as *tert*-butyl, R^2 as 1-naphthyl, and R^3 as dimethylamino to be the best catalyst (Fig. 1.22). Catalyst **36** was tested in the kinetic resolution of a range of *sec*-alcohol; 1-(2-naphthyl)ethanol and 4-phenyl-3-butyn-2-ol gave the highest s-values of 17 and 37 respectively.

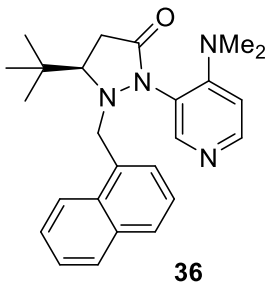

36

Figure 1.22

Next, they tested catalyst **36** in the kinetic resolution of axially chiral biaryl compounds, which had previously been tested only with biaryl-derived catalysts,[59] and only once using a chiral DMAP catalyst (s = 1.4).[62] A range of mono-protected bis-2-naphthols were evaluated and returned excellent results. Scheme 1.12 shows three of the highest s-values obtained.

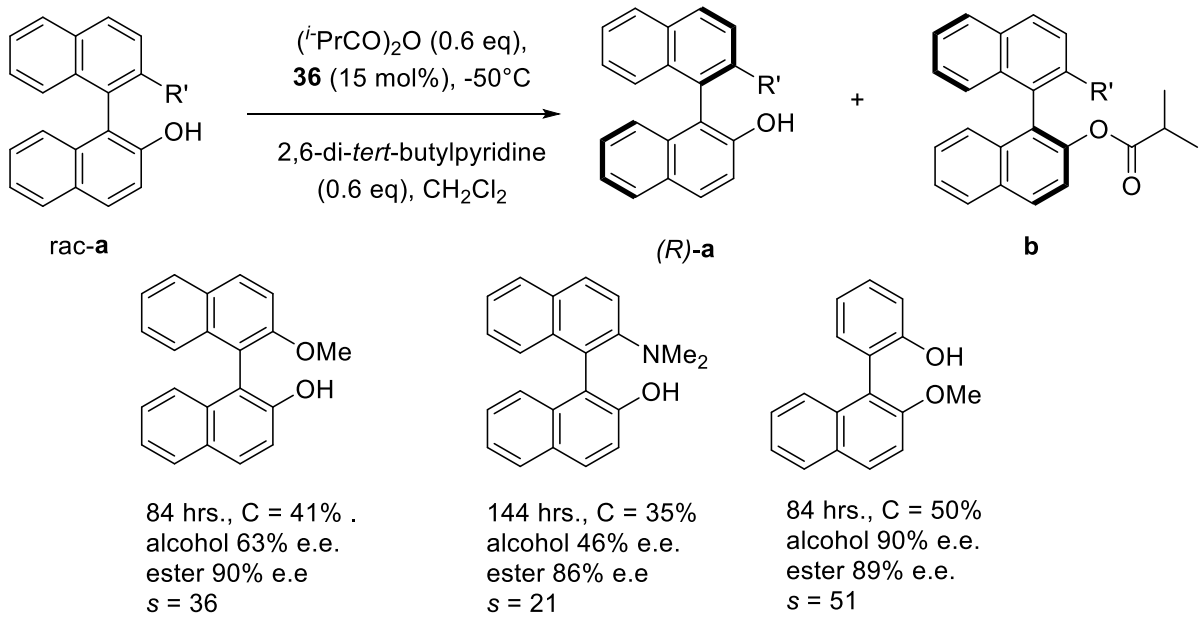

Scheme 1.12. Selected examples of the kinetic resolution of biaryls using catalyst **36**[59]

The origin of the stereoselectivity was determined by X-ray crystallography, which indicated that the *tert*-butyl group and the naphthyl ring are on opposite sides of the five-membered ring due to steric interactions. According to the researchers, the naphthyl substituent blocks the bottom face of the catalyst, as well as the back side – away from the pyridine nitrogen, and close to the dimethylamino nitrogen (Fig. 1.23).

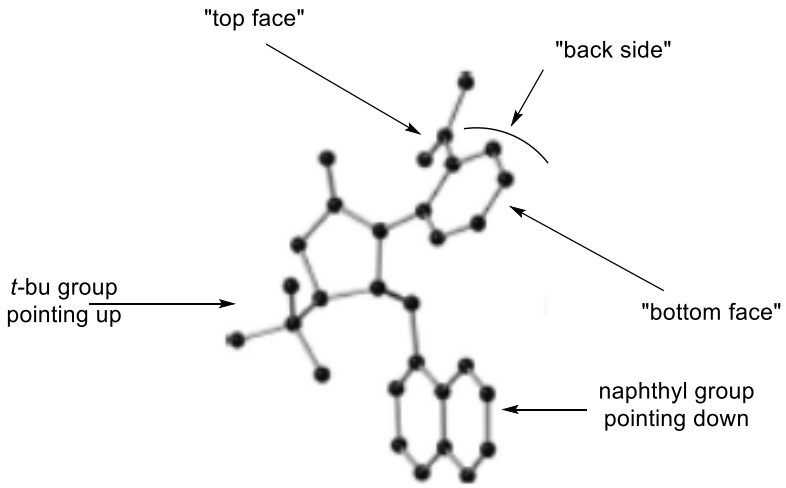

Figure 1.23. X-ray crystal structure of catalyst **36**.[59]

Therefore, in the stereoselective step the hydroxyl group of the biaryl substrate approaches the catalyst from the top face, while the other protected hydroxyl group (R') approaches from the backside (to minimize steric interactions between the naphthyl ring and the biaryl ring).

This approach is favoured in the *S*-enantiomer, resulting in a kinetic resolution of the *R*-enantiomer.

1.7.2 Axial Chirality

In 1998, Spivey introduced the first atropisomeric acyl-transfer catalysts, which consisted of a DMAP molecule attached to a hindered biaryl at the 3-position, with restricted rotation about the aryl-pyridine bond (Fig. 1.24).[63,64]

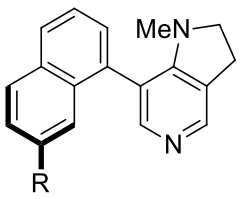

(+)-37 **R** = Me
(-)-38 **R** = Ph
(-)-39 **R** = 3,5-*bis*(3,5-dimethylphenyl)phenyl

Figure 1.24. Spivey's axially chiral acyl-transfer catalyst.

Initial tests showed that while the catalytic reactivity was comparable to that of DMAP (for the acylation of methyl cyclohexanol), the catalysts gave disappointing selectivities for the kinetic resolution of secondary benzylic alcohols (Table 1.10).

Table 1.10. Kinetic resolution of secondary benzylic alcohols with catalytic atropisomeric DMAP derivatives **37**–**39**.

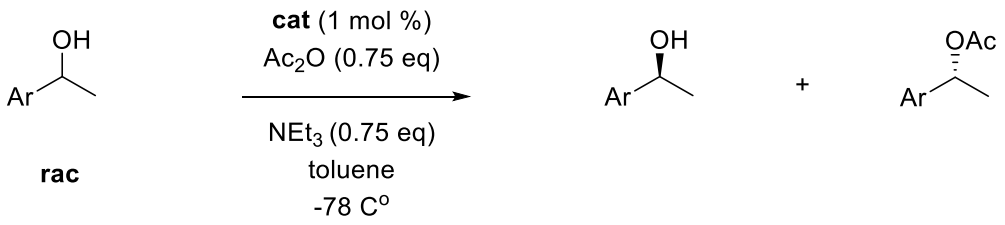

substrate	catalyst	C	$ee_{(alcohol)}$	s-value
Ar = Ph	**37**	35.0	9.1	1.5
Ar = Ph	**38**	26.0	11.6	2.2
Ar = 1-Nap	**38**	18.3	9.0	2.5
Ar = 1-Nap	**39**	17.6	13.1	4.7

To improve the selectivities, they synthesised compound **43** (R = Ph) in a short three-step synthesis from 3,5-dibromo-4-chloropyridine on a gram-scale (Scheme 1.13). Catalyst **43** (resolved by semi-preparative chiral HPLC) gave vastly improved results for the kinetic resolution for the same substrates (Table 1.11).[65]

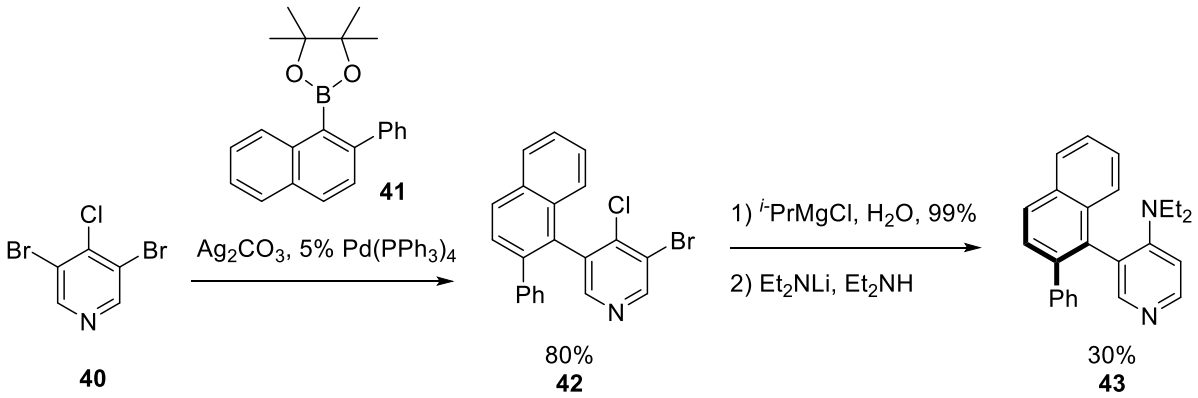

Scheme 1.13. Synthesis of Spivey's atropisomeric DMAP catalyst.

Table 1.11. Kinetic resolution of secondary benzylic alcohols with catalytic atropisomeric DMAP (-)-**43**.

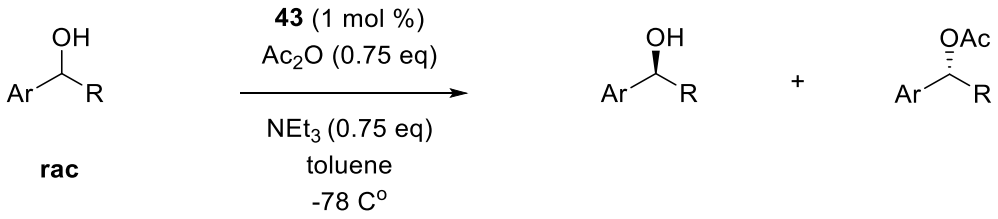

substrate	C	e.e$_{(alcohol)}$	s-value
Ar = 1-Nap , R = Me	17.2	18.6	21
Ar = 1-Nap , R = Me	22.3	26.3	29
Ar = Ph, R = Me	39.0	49.9	13
Ar = 2-Tol , R = Me	41.4	60.7	25
Ar = Ph, R = $^{t-}$Bu	17.5	18.8	20

They also reported that the nature of the *N*-alkyl group has an effect on the s-values (Table 1.12)[66] with the 4-dibutyl-substituted catalyst giving optimal reactivity and selectivity. However, possible reasons for the improved selectivities are not yet known.

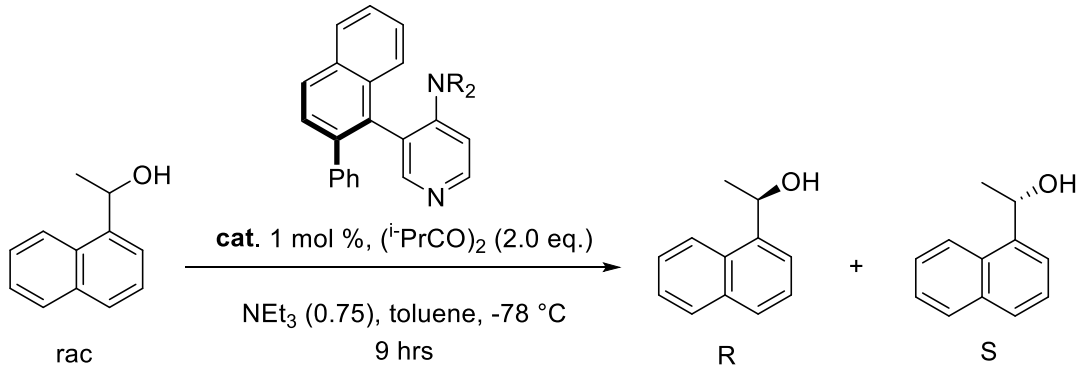

Table 1.12. Kinetic resolution of 1-(1-naphthyl)ethanol catalysed by atropisomeric DMAP derivatives.

catalyst	**R**	s-value
43a	Me	10
43b	Et	16
43c	$(CH_2)_4$	3.5
43d	Bu	31
43e	Pent	30
43f	Hex	39[a]

a. T = 93 °C, time = 14.3 hrs

Spivey then tried to improve the selectivity of **43** even further by adding a methyl group to the pyridine ring α-position to form **44**.[67] They rationalised that the presence of a methyl group α to the pyridine nitrogen would influence the conformation of the carbonyl group of the acyl-pyridinium intermediate.

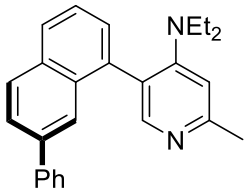

(-)-44

Even though α-substitution is known to strongly attenuate the nucleophilicity of pyridine catalysts, they hoped that the effect on the carbonyl would enhance enantiodiscrimination. Sammakia and Hurley showed that α-substituted 4-PPY catalysts can catalyse the methanolysis of α-hydroxy esters – though the mechanism is not nucleophilic.[68] Unfortunately, **44** gave a low selectivity in the kinetic resolution of 1-(1-naphthyl)ethanol (s = 2.0).

To explain the high s-values with catalyst **43** Spivey proposed a transition-state model based on the minimization of steric interactions:[65] The alcohol attacks the acyl-pyridinium ion – in an orientation that minimizes steric repulsion with both the naphthalene ring system (of the catalyst) and the isopropyl groups (of the acyl-pyridinium ion) – from the opposite face to the phenyl substituent (on the naphthalene). Importantly, the hydroxyl group adopts a stereoelectronically favoured colinear approach on the carbonyl. The groups at the stereogenic centre adopt a minimized steric trajectory in which the larger ligand points away from the pyridinium vicinity (Fig. 1.26).

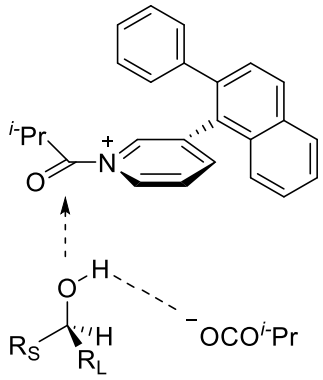

Figure 1.26. A transition-state representation of a kinetic resolution using Spivey's catalyst, isobutyric anhydride, and a secondary alcohol (NEt_2 group omitted for clarity).

In 2013, Spivey and Zipse[69] reported on using computational methods to predict that **45**, containing a 4-Bu_2N group and a 3,5-$(CH_3)_2C_6H_3$ "blocking group" (attached to the binaphthyl group) would exhibit high levels of selectivity for the kinetic resolution of 1-(1-naphthyl)ethanol. Here, they obtained an s-value of 44 with a 44% conversion. Computational modelling showed that the improved selectivity was most likely due to steric repulsion between the naphthyl ring of the *S*-alcohol and one of the methyl groups (*ortho* or *meta*) of the blocking group (blocking groups that were *para*-substituted did not improve the selectivity). Comparing the levels of enantioselecitvity that were predicted computationally with results obtained experimentally allowed the method to be validated.

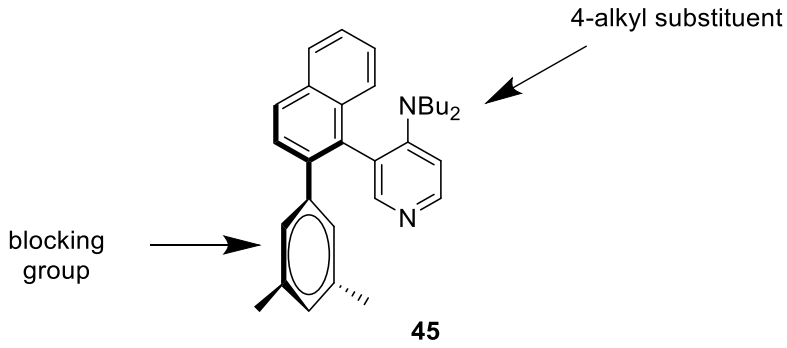

1.7.3 Planar-Chiral DMAP Catalysts

In 1996 Fu and Ruble introduced the first planar-chiral DMAP catalysts.[70] They based their design on desymmetrizing DMAP by incorporating the pyridine ring of the DMAP as a replacement for one of the rings of ferrocene, as well as adding a group to the pyridine 2-position (Fig. 1.27).[70] In such a way, as with previously described motifs in this review, facial discrimination on the pyridine faces would be achieved as well as sides.

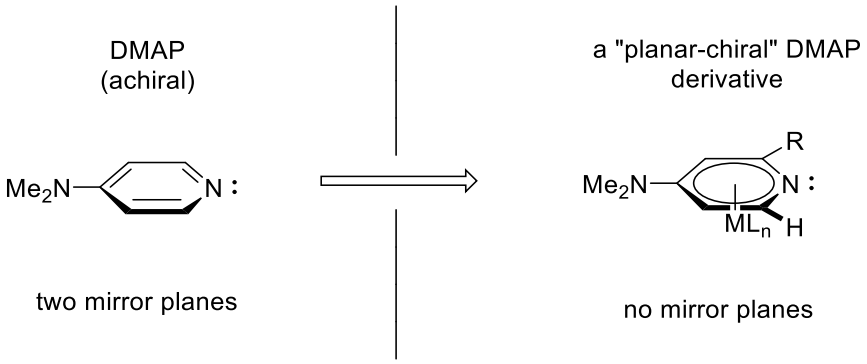

Figure 1.27. Fu's planar-chiral catalyst design.

Fu's catalysts consist of either a pentamethyl or pentaphenylcyclopentadienyl ligand complexed to the iron metal centre. The **R** group was varied from being a single substituent to an annulated ring. Iron is the preferred metal since it promotes electron-release into the pyridine ring, increasing the negative charge on the nitrogen atom.[40,71-76] Figure 1.28 illustrates the genesis of the catalyst design.

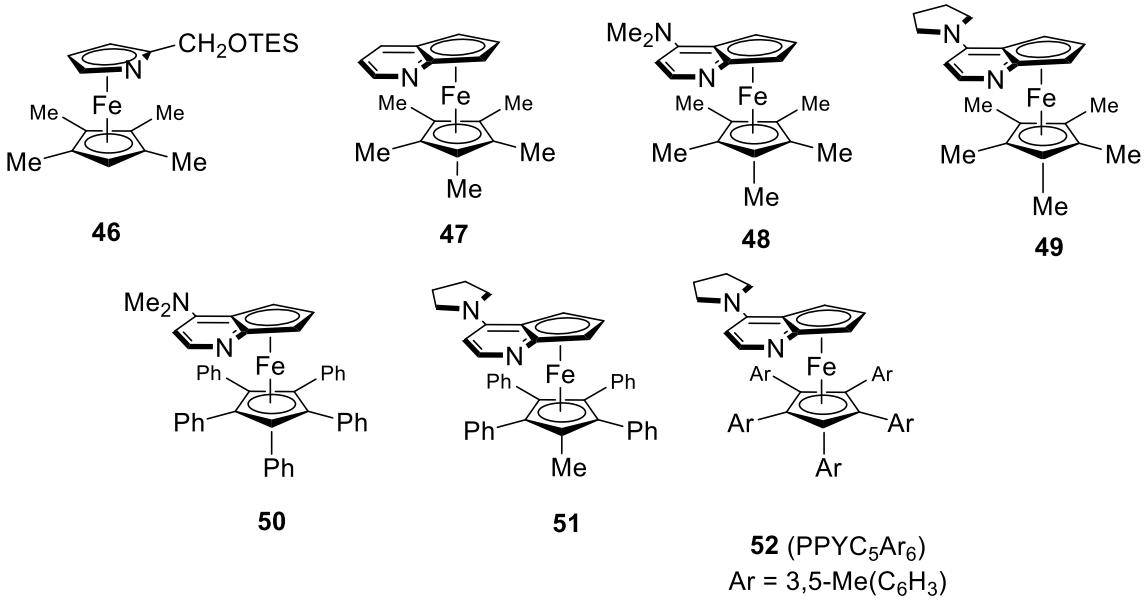

Figure 1.28. Fu's planar-chiral catalysts.[39]

Fu's initial tests yielded moderate selectivities (s-values up to 6.5) for the kinetic resolution of racemic 1-(1-naphthyl)ethanol with **46** as catalyst.[70] Optimization studies revealed the best catalyst to be **50**,[77] solvent (*t*-amyl alcohol),[78] and a temperature of 0 °C;[78] The kinetic resolution of the customary aryl alkyl carbinols produced some impressive s-values (Table 1.13). Catalyst **50** also showed activity in the kinetic resolution of chiral allylic alcohols (s-values up to 80),[79] as well as propargylic alcohols (s-values up to 20).[80] Fu noted that the high

stereoselectivity displayed by **50** is attributable to the η^5-C_5Ph_5 group, which effectively desymmetrizes one face of the catalyst.[77]

Table 1.13. Kinetic resolution of benzylic secondary alcohols with **50**.

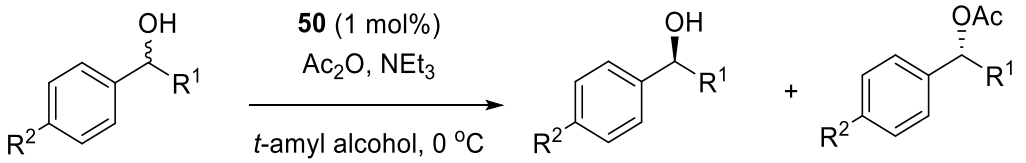

substrate	C	$ee_{(alcohol)}$	s-value
R^1 = Me; R^2 = H	55	99	43
R^1 = ^{t}Bu; R^2 = H	51	96	95
R^1 = CH_2Cl; R^2 = H	56	98	32
R^1 = Me; R^2 = F	54	99	68
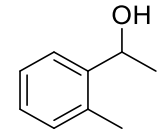	53	99	71
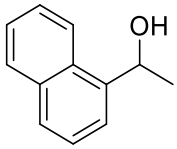	52	95	65

To demonstrate the potential of their catalysts in actual synthesis, the Fu group resolved two key intermediates in high ee,[79] as **54** from Brenna's total synthesis of (–)-baclofen,[81] and **55** from Sinha-Lerner's total synthesis of epothilone A (Fig. 1.29).[82]

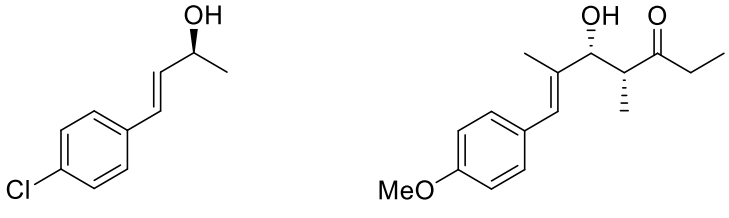

Figure 1.29. Structure of (–)-baclofen (**54**) and epothilone A (**55**).

In another example of the selectivity of **50**, Ley performed a kinetic resolution of **57** from racemic **56** (Fig. 1.30) in his total synthesis of iso- and bongkrekic acid.[83]

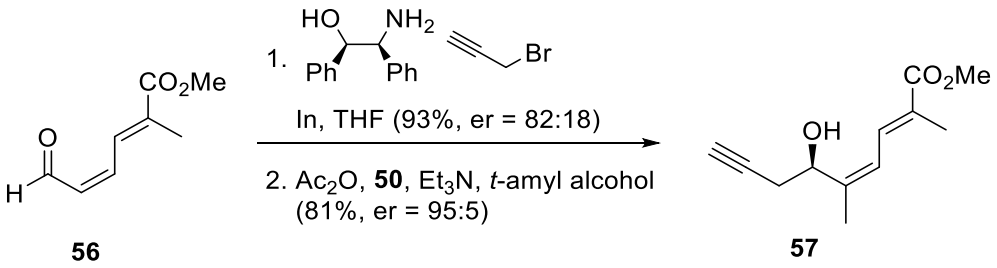

Figure 1.30. Kinetic resolution of **50** in the total synthesis of iso- and bongkrekic acid.

The concept of planar DMAP catalysis generated great interest in other research groups. In 2005 Johannsen *et al.* synthesised chiral DMAP derivatives with a planar-chiral ferroence substituent at the pyridine C-2 position **58** and at the C-3 position **59** (Fig. 1.31). Although **59** was more reactive than **58** (due to steric congestion at the 2-position in **58**), neither of the two catalysts showed any selectivity in the kinetic resolution of 1-phenylethanol, probably because, unlike Fu's catalyst, they are not able to provide effective discrimination of the two pyridine faces.[84,85]

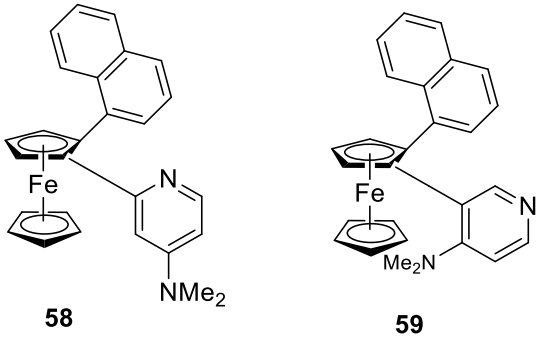

Figure 1.31. Johannsen's planar-chiral ferroence catalysts.

1.7.4 Helicenoidal DMAP

In 2011 Carbery and co-workers presented the first asymmetric DMAP organocatalyst **60** consisting of a DMAP moiety embedded into a helicenoidal framework.[86]

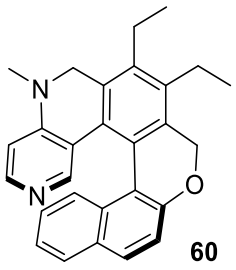

Figure 1.32. Carbery's helicenoidal DMAP.

Catalyst **60** resulted in excellent selectivities at a low catalyst loading of 0.5 mol % for the kinetic resolution of secondary aryl alkyl alcohols (Table 1.14).[86]

Table 1.14. Kinetic resolution of benzylic secondary alcohols with **60**.

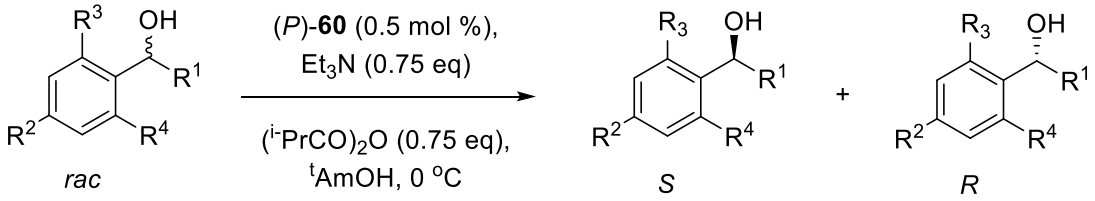

Substrate	C	s-value
R^1 = Me, R^2 = F, R^3 = H, R^4 = H	47	18
R^1 = Et, R^2,R^3 = H, R^4 = H	43	23
R^1 = t-Bu, R^2,R^3 = H, R^4 = H	46	26
R1 = Me, R^2 = H, R^3 = Br, R^4 = H	42	23
R^1 = Me, R^2 = H, R^3 = Me, R^4 = H	40	32
R^1 = Me, R^2 = H,R^3 = OMe, R^4 = H	47	43
R^1 = Me, R^2 = H, R^3 = Ph, R^4 = H	55	27
R^1,R^2,R^3,R^4 = Me	42	52
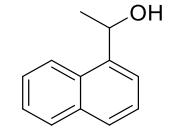	48	33
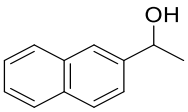	51	33
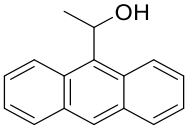	51	116

Molecular modelling revealed two factors responsible for the observed selectivity as: i) π–stacking between the substrate aryl group and the pyridinium ring of the catalyst – as in previous cases this discriminates the two pyridine faces; ii) minimization of steic clash between the methyl group (as "R_s") and the ^{i}Pr group of the acyl group – this assumes that the phenyl group of the alcohol (as R_L) points "away" towards the less hindered side away from the helix, while the methyl group (as R_S) points away from the isopropyl group of the acyl group being transferred, (Fig. 1.33).

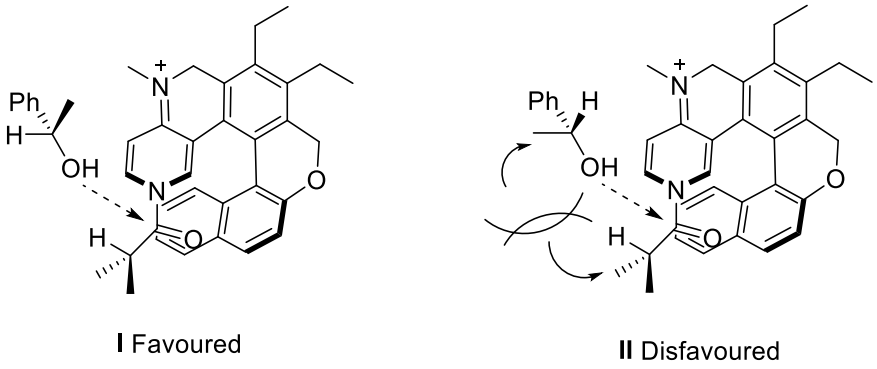

Figure 1.33. Proposed transition-state model for catalyst **60**.[86]

Catalyst **60** was demonstrated to be catalytically active at loadings as low as 0.05 mol % as shown in the preparative kinetic resolution of 1-(1-naphthyl)ethanol (Scheme 1.14).

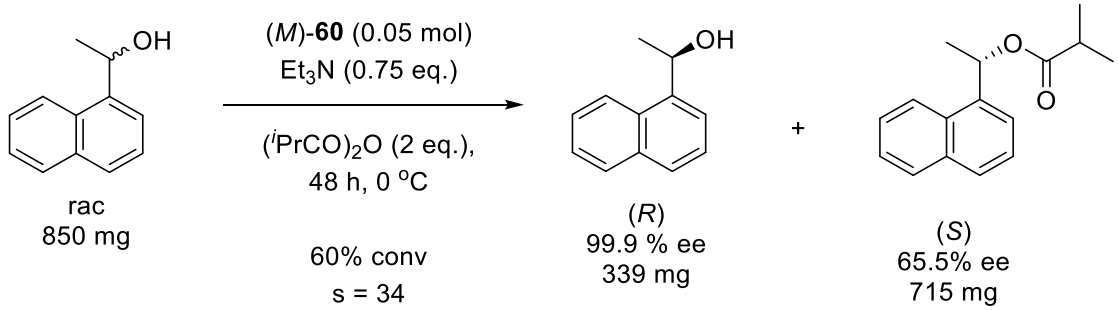

Scheme 1.14

Carbery's catalysts gave impressive selectivities, but the synthesis of **60** had two limitations:[87] 1) the catalyst was synthesised as a racemate and had to be resolved by chiral HPLC; 2) some of the intermediates in the synthesis were sensitive, which limited scalability; However, the researchers succeeded in synthesizing derivatives of **60** in the hope of improving the selectivity. Thus **62** was synthesised via a rhodium-catalysed [2+2+2] triyne cycloisomerization in a 95:5 dr (Scheme 1.15), with the major product being easily obtained following column chromatography. Catalyst **62** was obtained in a low yield of 33%, but the larger scale of the reaction enabled **62** to be formed in over 1 g. In a kinetic resolution of 1-(2-naphthyl)ethanol, **62** gave an s-value of 33 (similar to **60**).[87]

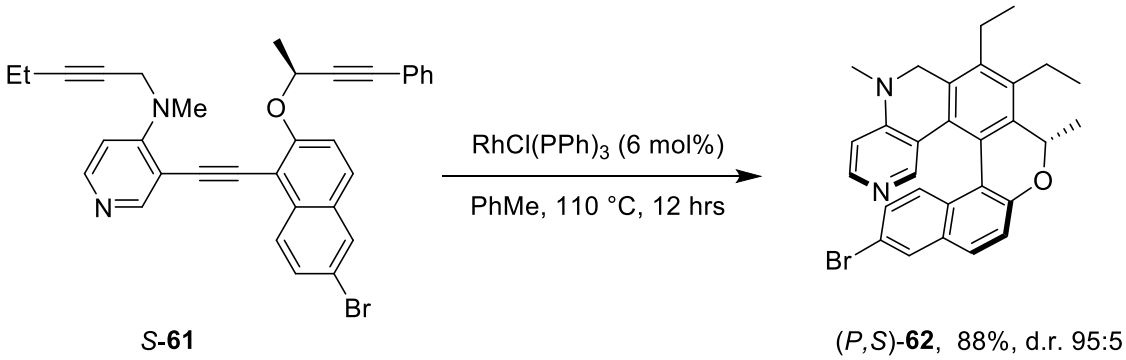

S-**61** (*P,S*)-**62**, 88%, d.r. 95:5

Scheme 1.15

1.7.5 Combination of Thiourea Derivatives with DMAP

During the previous decade the use of chiral ion-pairs has become a useful tool in organocatalysis.[88] The use of chiral ion-paring is well established in the field of phase-transfer catalysis, in which anionic intermediates form supramolecular interactions with chiral cations. List and co-workers expanded on this concept and introduced asymmetric counter-ion-directed catalysis (ACDC),[89, 90] in which enantioselectivity is achieved by ion pairing of a cationic intermediate with a chiral, enantiomerically-pure anion to form an asymmetric catalyst. Thiourea derivatives in particular have emerged as an important class of compounds for the development of new organocatalytic reactions, since they are especially valuable for their ability to recognize anions and negative charges.[91-93]

The Seidel group took a different and interesting approach in their design of a chiral acylation catalyst, in that they decided to introduce the chiral environment via the leaving group of the acylating agent. In this they combined achiral DMAP with a chiral thiourea anion binder in the expectation of H-bonding between the chiral thiourea and the anion leaving group from the acylating agent occurring to create a chiral ion-pair with the acyl-pyridinium cation, thus creating a local chiral environment for discrimination of the alcohol enantiomers, (Scheme 1.16).

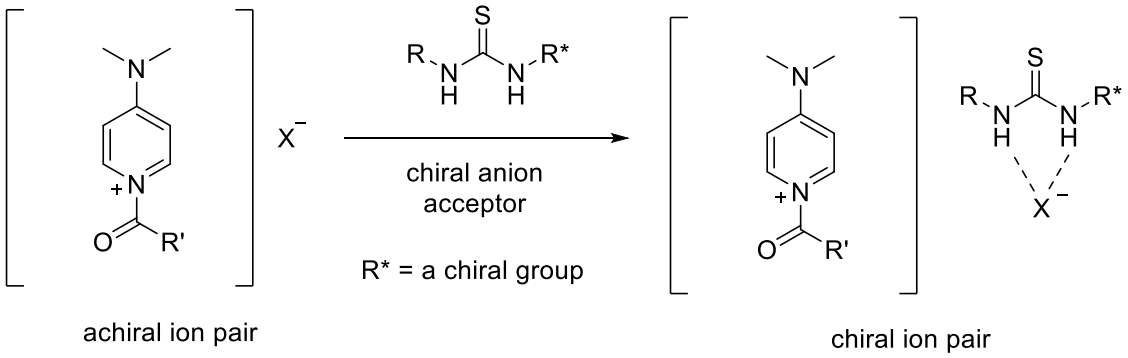

Scheme 1.16. In situ generation of chiral acyl pyridinium salt

Of the chiral H-bond donor ligands tested, bis-thiourea **63** gave good selectivities (s-values up to 24) in the kinetic resolution of racemic secondary amines (Table 1.15).[94,95] The kinetic resolution of amines poses challenges to small-molecule catalysts (e.g. the amine is usually just as nucleophilic as the catalyst) that the Seidel group hoped to address using their dual-catalysis strategy.[95,96]

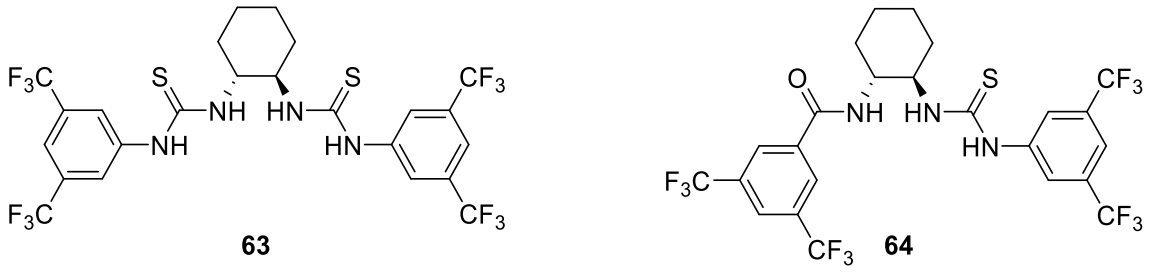

Figure 1.34. Chiral H-bond donor ligands.

The mixed amide-thiourea **64** gave even better results and was applied to the kinetic resolution of racemic propargylic amines,[96] allylic amines (with 4-PPY),[97] as well as the *meso*-desymmetrization of *meso*-diamines,[98] and other reactions.[99] Some results for aryl/alkyl secondary amines are shown in Table 1.15. More recently (2012), the Seidel group have used **64** in combination with 4-dipropylamino pyridine in the kinetic resolution of secondary amines to achieve s-values up to 65,[100] as well as 1,2-diaryl-1,2-diaminoethanes with s-values up to 65.[101]

Table 1.15. The kinetic resolution of secondary amines with **64**.

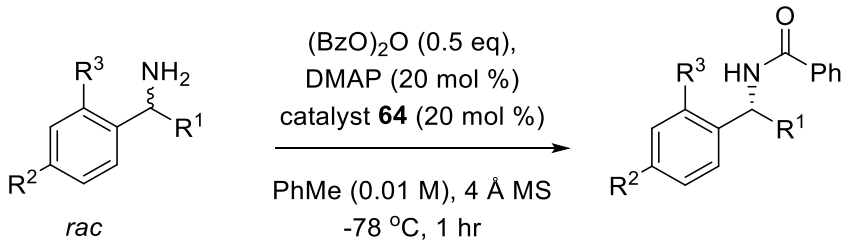

Substrate	C	s-value
R^1 = Me, R^2,R^3 = H	41	13
R^1, R^3 = Me, R^2 = H	44	17
R^1 = Me, R^2 =Cl, R^3 = H	48	38
R^1 = Et, R^2,R^3 = H	43	20
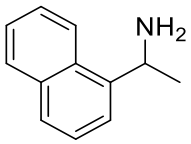	48	21

1.8 Amino Acids and Peptides as Asymmetric Catalysts

Amino acids are chiral pool molecules that are widely used in asymmetric synthesis as starting materials, auxiliaries, reagents, and catalysts. The range of structural and functional diversity in the amino acid side chains can exert a high degree of stereocontrol through steric effects (amino acids with bulky side chains have proven to be particularly useful), H-bonding effects, chelation, π–stacking, etc; these properties are also incorporated into peptides by easily coupling amino acids together.[2]

The use of amino acids and short peptides – or peptide-like molecules – as asymmetric catalysts is currently a subject of great interest in organic synthesis.[102-104] They provide several advantages over other catalysts such as enzymes and transition-metal catalysts, since they are inexpensive, readily available in high enantiomeric purity, and are available as both enantionmers. Peptides are also usually more stable than enzymes or other bioorganic molecules, and are more easily attached to a solid support than organometallic compounds or bioorganic compounds. Their smaller size, compared to enzymes, make mechanistic investigations much easier.[105]

Amino acids have been used as asymmetric catalysts in C-C bond formation, oxidation, brominations and many other reactions.[102] Some of the earliest examples of the use of peptides and amino acids in asymmetric catalysis date back to the early 1970's: Inoue and Oku showed that polyamino acids catalyse the conjugate addition of thiols to enones;[106,107] Juliá and Colonna demonstrated that poly-alanines and poly-leucines catalyse the oxidation of chalcones;[108,109] and Hajos, Parrish, Eder, Sauer, and Wiechert showed that proline catalyses the asymmetric Aldol reaction.[110,111] Despite these early examples of peptide catalysis, the field has only started to flourish in the last decade following the work of Miller (peptides),[112] and various researchers in the field of organocatalysis (List, Barbas, McMillan, Jørgensen,[25] and others).

1.8.1 Peptides as Acyl-Transfer Catalysts in Kinetic Resolution Reactions

1.8.1.1 *N*-Alkylimidazoles

Inspired by nature's acyl-transfer enzymes, in 1998 Miller and co-workers introduced a series of acyl-transfer catalysts, which were shown to catalyse reactions with high efficiency and specificity. Miller's catalysts contained an *N*-substituted imidazole **65** or an *N*-alkylated histidine (substituent at C-5) **66** (Fig. 1.35) residue embedded in a peptide chain.[112] These residues were chosen because of their ease of synthesis and the nucleophilicity of imidazole moieties.

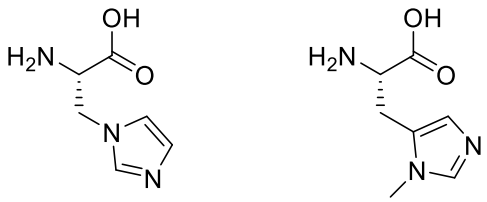

65 **66**

Figure 1.35. Miller's imidazole **65** and *N*-alkylated histidine **66** amino acid fragments.

The catalysts function in a similar way to DMAP, with the imidazole ring participating as the nucleophile in the acyl-transfer reaction. Scheme 1.17 shows the resonance structure of the imidazole group of histidine (substituent at C-4), indicating the nucleophilic nitrogen available for formation of an acyl-imidazolium ion intermediate for transfer.

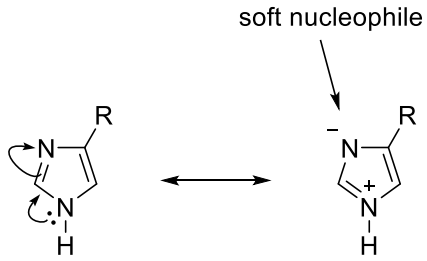

Scheme 1.17 Resonance structures of histidine

The first catalyst tested was **67**, in the kinetic resolution of acetamidocyclohexanol (Fig 1.36).[112]

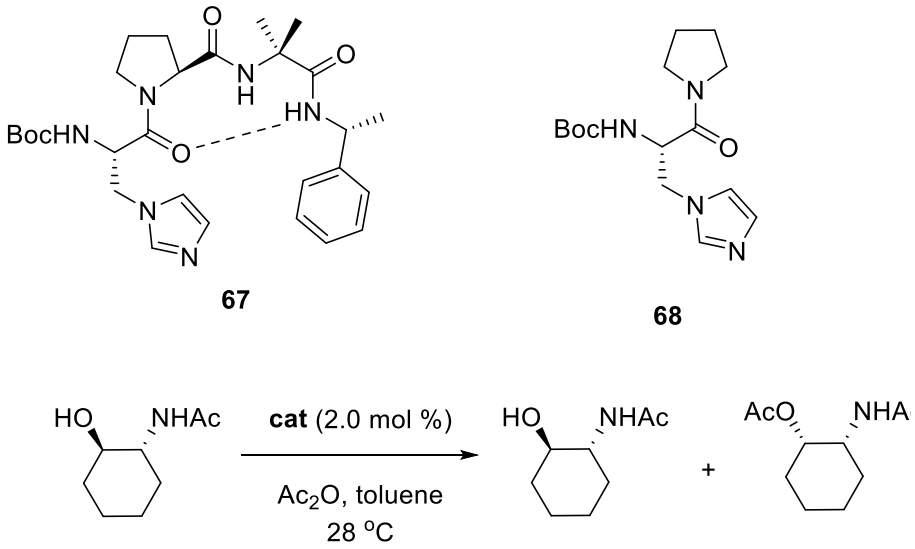

Figure 1.36

Catalyst **67**, which adopted a secondary structure through a β-turn – a region of a peptide involving four consecutive amino acid residues in which the polypeptide chain folds back on itself by almost 180 degrees[113] – gave a good s-value of 17, while the control, catalyst **68**, gave no selectivity, since the molecule can not form a secondary β-turn structure.

Miller's second set of β-turn catalysts, diastereomers **69** and **70** (Fig. 1.37), which differ only in the stereochemistry at the proline residue, both incorporated fragment **66** into the peptide backbone.[114] These two catalysts displayed dramatically different conformations and reactivities. Catalyst **69**, which forms one H-bond in its secondary structure, gave an s-value of 3, while catalyst **70**, which forms two H-bonds in its secondary structure, gave an s-value

of 28 for the same substrate. They rationalised that the extra H-bond in **70** promotes formation of a more rigid molecule, which promotes the enantioselectivity.

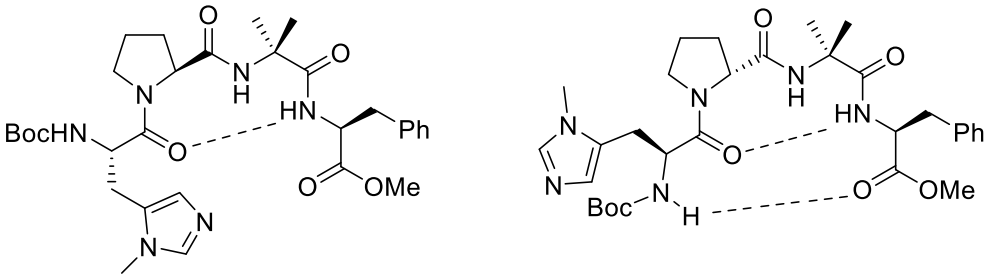

69 **70**

Figure 1.37

This hypothesis was tested with larger peptide catalyst **71**, which forms four intramolecular H-bonds (according to NMR studies) versus its diastereomer, catalyst **72**, which only forms one intramolecular H-bond. Catalyst **71** gave an s-value of 51, while catalyst **72** gave an s-value of 7.[115]

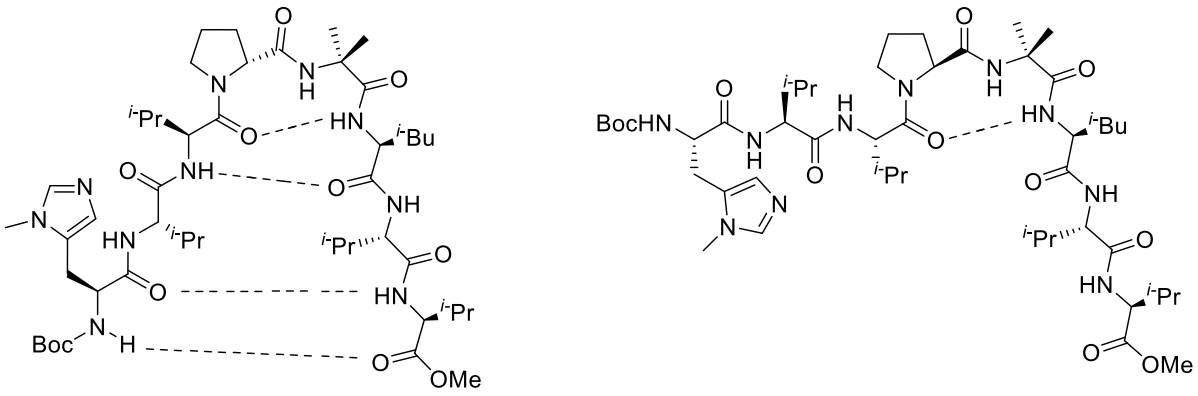

71 **72**

Figure 1.38

Compound **74 –** an analogue of **71**, which was synthesised via a Ru-catalysed cross-coupling metathesis (Scheme 1.18)[115] **–** was then tested and the results compared to its analogue **71**. Although **74** was designed to be more rigid than previous catalysts tested, s-values dropped to 12, suggesting that a subtle balance between flexibility and rigidity is important for attaining the preferred conformation in the stereoselective step.

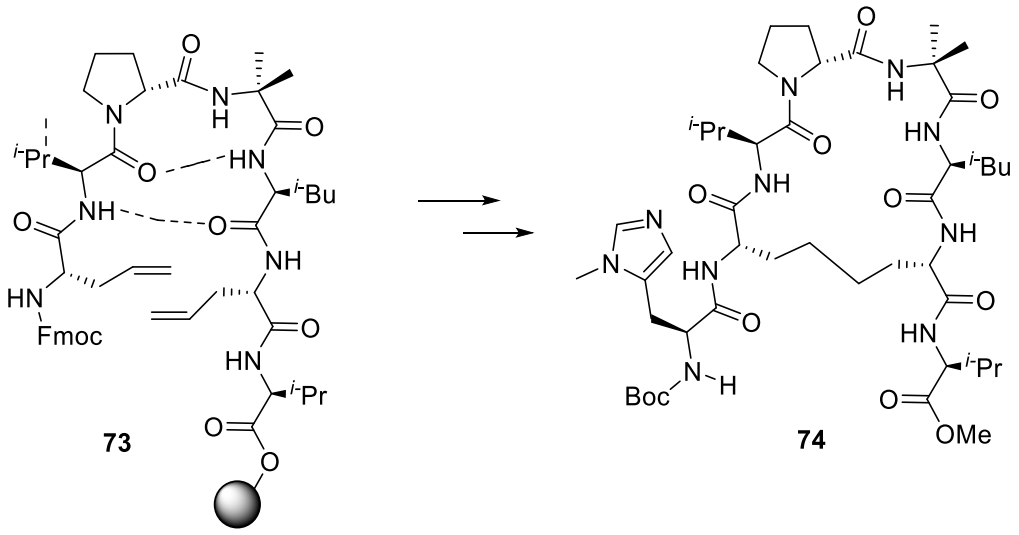

Scheme 1.18

Figure 1.39 shows the mechanistic model proposed by Miller, using NMR and IR techniques, to explain the enantioselectivity induced by peptide catalyst **70**.[114] In this model, one of the substrate enantiomers can preferentially H-bond to the catalyst, resulting in promotion of a faster acylation by the acylimidazolium moiety.

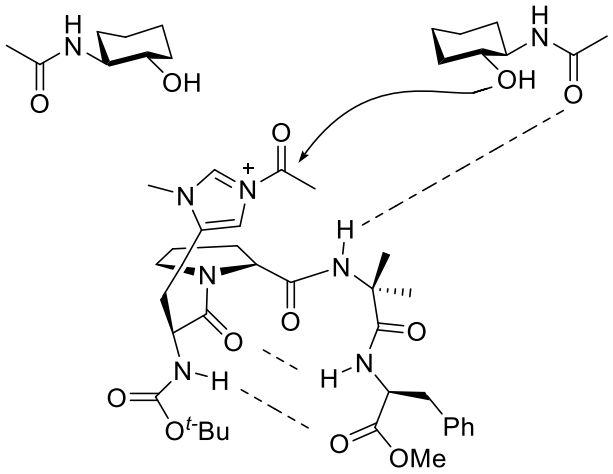

Figure 1.39

The acylation with catalyst **75**, which lacks the H-bond donor amide gave a low s-value of less than 1.5, consistent with Miller's model.[116a]

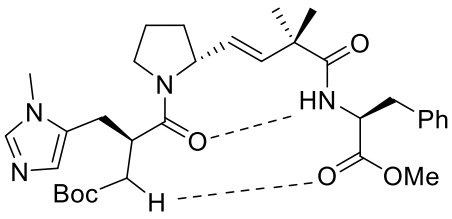

75

Figure 1.40

Miller then set out to screen a library of compounds in order to find a more reactive and selective peptide catalyst. The screening involved using a fluorescently labelled assay in which a resin-bound proton-activated fluorophore was used as a sensor during the acylation of racemic alcohols (Fig. 1.41).[117116b] The brightest beads under the fluorescence microscope allowed identification of the most active catalysts, based on the conjugate acid formed by scavenging the acetic acid by-product being fluorescent.

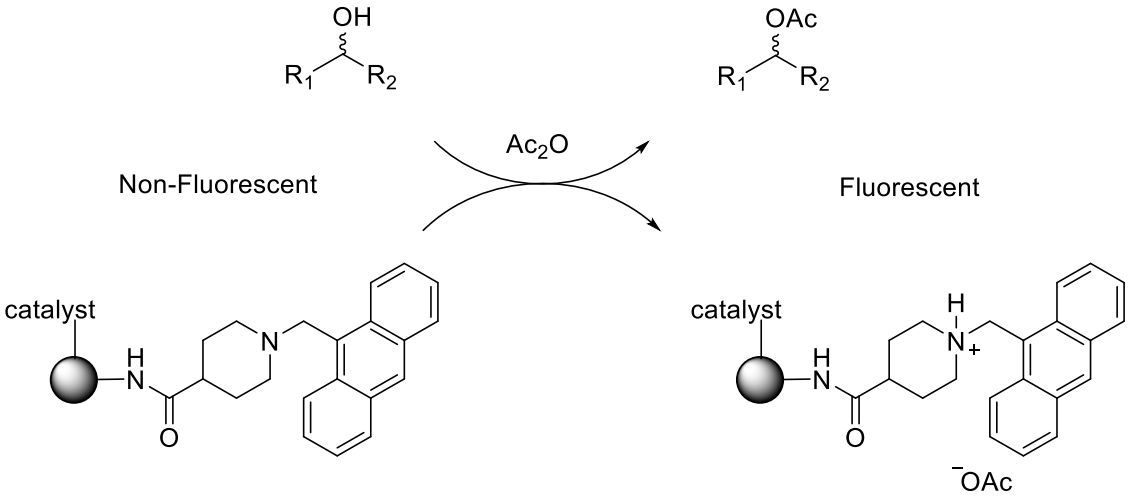

Figure 1.41

This screening (of approximately 10^5 proteins) led to identification of octapeptide **76** containing an alkylated histidine residue. Catalyst **76** proved to be an effective asymmetric acylation catalyst in the kinetic resolution of a variety of racemic secondary alcohol substrates, producing excellent (> 10) s-values for aromatic secondary alcohols (except for 1-phenyl-1-propanol), but much lower values for certain non-aromatic secondary alcohols (Fig. 1.42).

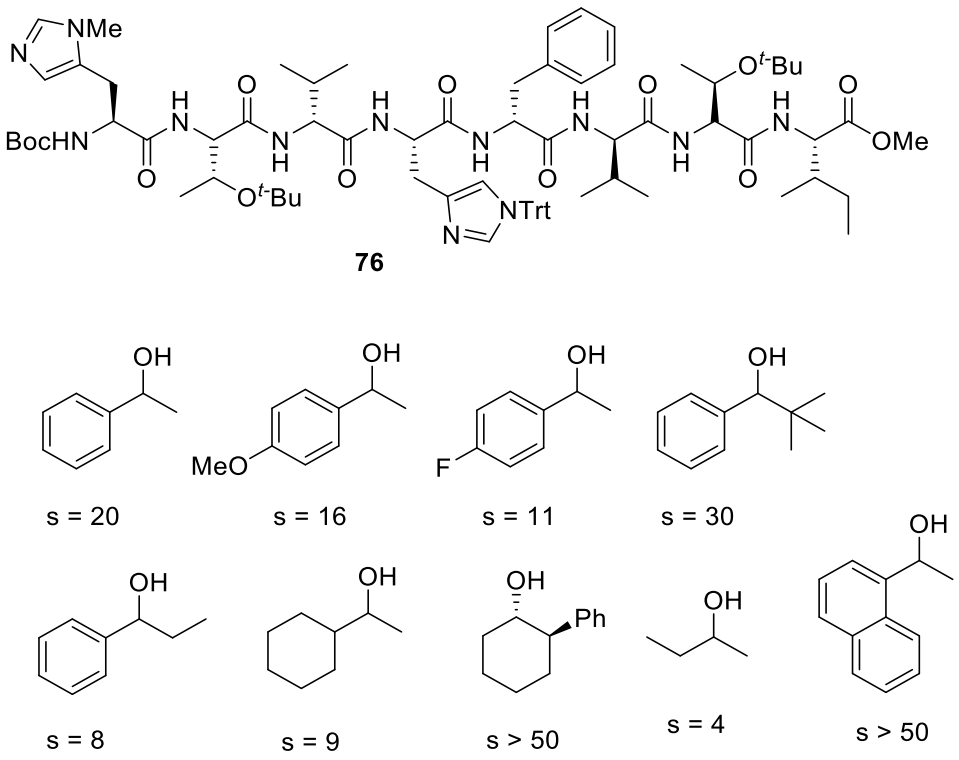

Figure 1.42

Miller tested the efficiency of another peptide catalyst **77** (found in the fluorescent screen and shown in Figure 1.43) in the kinetic resolution of substrate **78**, to form **79**, which was converted into mitosane, a key intermediate in the synthesis of mytomycin C (Fig. 1.44).[117a,117b]

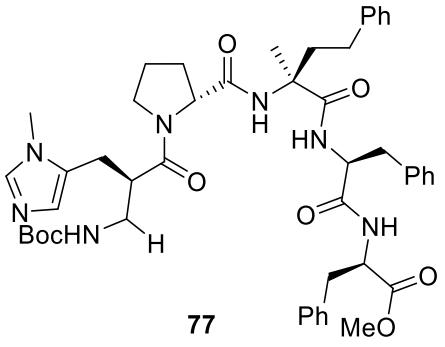

Figure 1.43

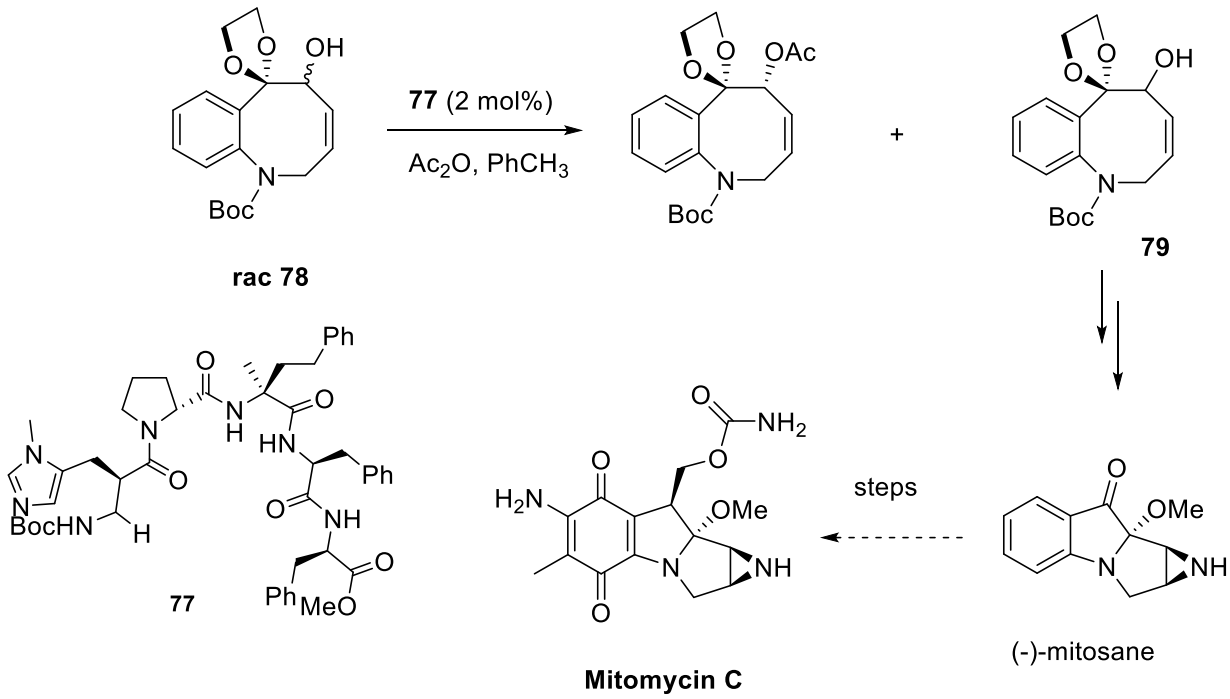

Figure 1.44

In 2008, Schreiner *et al*. synthesised and evaluated an *N*-methyl histidine peptide **80**. Unlike other groups, whose design concept focus on forming a catalytically active secondary structure via hydrogen bonding, **80** contained a γ-aminoadamantane carboxylic acid as well as natural and non-natural amino acids in the chain.[118a] The lipophilic character of the catalyst favoured the formation of the acyl-pyridinium ion in non-polar solvents like toluene.

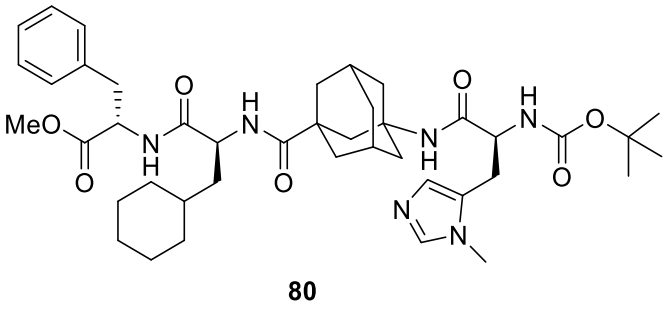

80

Figure 1.45

The catalyst was tested in the kinetic resolution of *trans*-cyclohexan-1,2-diol to produce excellent results (Table 1.16).

Table 1.16. Kinetic resolution of secondary alcohols using catalyst **80**.

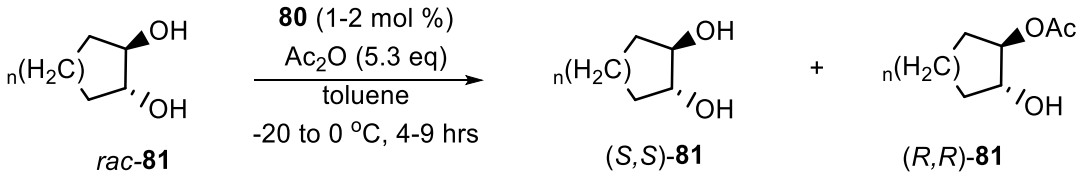

N	ee (*S*,*S*)-**81**	yield	s-value
1	> 85	37	> 8
2	> 99	37	> 50
3	> 99	41	> 50
4	> 99	41	> 50

The origin of the stereoselective step was determined by molecular modelling (Fig. 1.46), which revealed two C=O groups to likely provide the hydrogen-bonding contacts needed for chiral recognition of the diols. The model also showed that the adamantane building block provides a scaffold that holds the catalytic site and the centres governing recognition and stereochemistry into place.

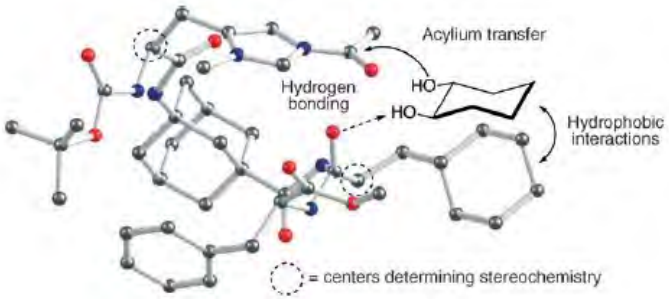

Figure 1.46[118b]

1.8.1.2 Amidine-based Catalysts (ABC's)

In 2004, Birman introduced a new class of acyl-transfer catalysts based on a 2,3-dihydroimidazo[1,2-*a*]pyridine (DHIP) core. Thus 2-phenyl-6-trifluoromethyl-dihydroimidazo[1,2-*a*]pyridine (**CF3-PIP**, Fig. 1.47) was tested in the kinetic resolution of secondary benzylic alcohols and gave selectivity factors up to 85.[119a] The π-system of the catalyst was expanded to include a 1,2-dihydroimidazo[1,2-*a*]quinoline (DHIQ) tricyclic core (**ClPIQ**, Fig. 1.47), which improved reaction rates and s-values compared to **CF3-PIP**.[119b]

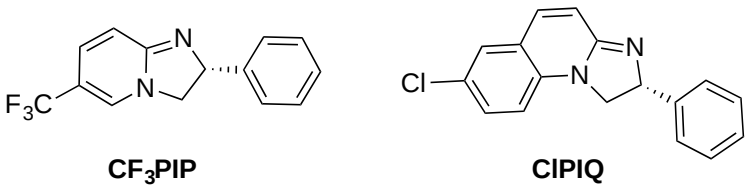

Figure 1.47. Birman's catalysts.

Birman proposed a trasnistion-state model in which the phenyl ring of the substrate stacks above the pyridinium ring of the *N*-acylated catalyst due to π-π and/or π-cation interactions (Fig. 1.48).[119a]

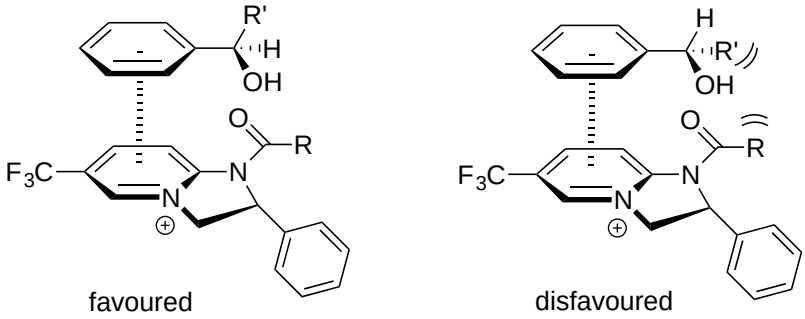

Figure 1.48[120c]

Birman and Houk performed computational studies to determine the origin of enantioselectivity, which supports a π-inteaction.[119c] They concluded that enantioselectivity depends on electrostatic attraction between the phenyl ring (substrate) and pyridinium ring (catalyst), and steric repulsion between the alkyl group of the substrate and the catalyst. The Birman group later extended the substrate scope to include propargylic and *β*-substituted cycloalkanols.[119d]

1.8.1.3 Amino Acids Attached to DMAP-Type Catalysts

In 2013 the Suga group introduced a chiral acyl-transfer catalyst containing a peptide as the chiral element into the C-3 position of DMAP.[120] These chiral DMAP catalysts were synthesised using an Ugi multicomponent reaction to attach amino acids at the C-3-position. After testing a range of peptides containing different amino acids, they found that catalyst **82** was the best catalyst.

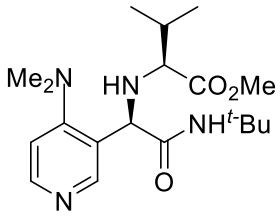

82

Figure 1.49

The catalyst was tested in the kinetic resolution of a range of secondary alcohols, but reactivity was modest (low conversion) and selectivity as seen by the s-values varied for a range of secondary alcohols (Table 1.17), with the exception of one substrate, which gave a high s-value of 12.4 (at a low conversion of 8%) (Table 1.17, entry 4).

Table 1.17 Kinetic resolution of secondary alcohols using catalyst **82**.

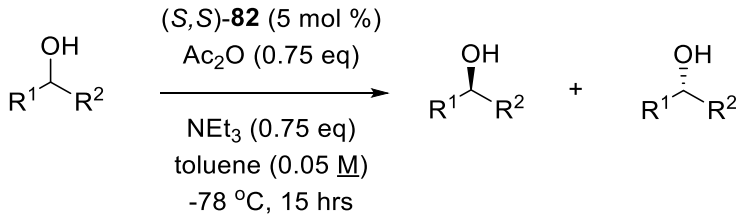

Entry	substrate	C	s-value
1.	R^1 = Ph, R^2 = CH_3	17	8.1
2.	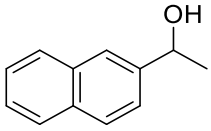	17	9.3
3.	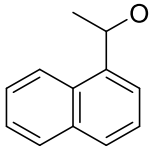	14	9.1
4.	R^1 = Ph, R^2 = ^{t}Bu	8	12.4
5.	R^1 = Ph, R^2 = CCH_3	18	2.8
6.	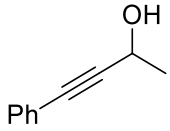	19	3.8
7.	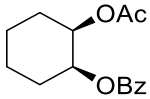	14	10.4
8.	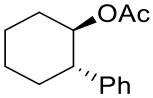	34	2.6

Kawabata reported on a range of 4-PPY-catalysts containing amino acids as the chiral element attached to the pyrrolidine ring (Scheme 1.50).[121a, 121b] The catalysts were tested in the kinetic resolution of amino alcohols,[121b] meso-desymmetrization of diols.[121c] C_2-symmetric catalyst **A** has also proven to be efficient in the chemo- and regioselective acylation of monosaccharides.[121d-121f]

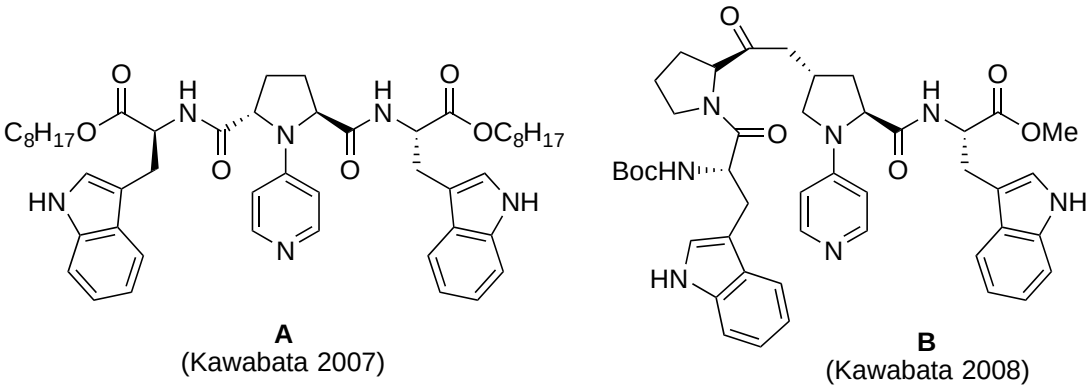

Figure 1.50. Kawabata's PPY-based catalysts.

Similarly, Campbell has demonstrated that chiral catalysts with the stereogenic centre in the 4-pyrrolidino moiety as *N*-4'-pyridinyl-α-methyl proline kinetically resolved a range of *N*-protected β-aminoalcohols with s values up to 10.[121g]

1.9 Objectives of the Study

This thesis discusses the use of amino acids and peptides in asymmetric catalysis. Chapter 2 discusses the epoxidation of *meso*-epoxides by chiral Lewis acids. Chapter 3 discusses the kinetic resolution of secondary alcohols. Thus, the overall objectives of the project were the following:

i. To synthesise and evaluate four chiral ligands that could coordinate to scandium(III) triflate for the *meso*-desymmetrization of epoxides (Chapter 2).
ii. To synthesise and evaluate three classes of DMAP-type acyl-transfer catalysts in which the peptide is attached α, β, and γ to the pyridine nitrogen (Chapter 3).
iii. To use computational modelling to determine a transition-state model for the stereo-discriminating step.

Chapter 2: Lewis Acid Catalysis

2.1 Desymmetrization of *Meso*-Epoxides

Epoxide ring opening is an important reaction in organic synthesis since it allows for the formation of chiral 1,2-difunctionalized chirons for fine chemicals in one step. The inherent ring-strain of three-membered heterocycles (approximately 113 kJ/mol) provides the driving force for this important reaction, which can occur via either nucleophilic S_N2 (**A**) or acid-catalysed S_N1 or S_N2 mechanisms (shown as S_N1 in **B**) (Fig. 2.1).[122] Strong nucleophiles (e.g. RSH, S^-, CN^-, RNH_2) can open at the less-hindered carbon atom, while weak nucleophiles (e.g. ROH) need acid catalysis, in which regioselectivity depends on the degree of epoxide opening in the transition-state.

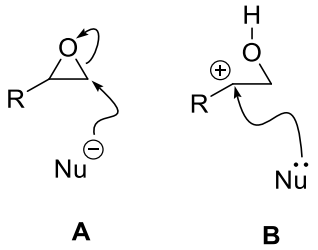

Figure 2.1. Mechanisms of epoxide ring opening: (**A**) Nucleophilic mechanism; (**B**) Acid-catalysed mechanism.

Epoxides can be opened by a wide range of nucleophiles such as alcohols (1,2-diol monoethers),[123] thiols (1,2-mercaptoalcohols),[124] halogens (1,2-halohydrins),[125] etc. Enantioselective ring-opening can occur using either racemic or *meso* achiral epoxides via kinetic resolution and *meso*-desymmetrization respectively (Scheme 2.1).

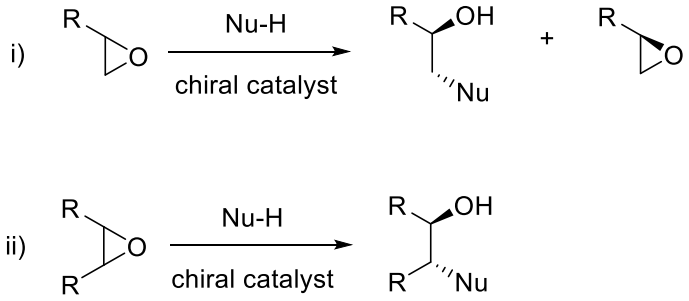

Scheme 2.1. Enantioselective ring-opening of i) a racemic epoxide (kinetic resolution), and ii) a *meso*-epoxide (*meso*-desymmetrization).[122]

In the kinetic resolution (discussed in Chapter 1), a chiral catalyst must distinguish between the two enantiomers in the racemic mixture, and selectively promote reaction of one enantiomer over the other to give the ring-opened product together with the unreacted epoxide in as close to a 50:50 ratio as possible. In a *meso*-desymmetrization, a chiral catalyst has to distinguish between the two enantiotopic carbons in promoting formation of the 1,2-disubstitued product. The advantage of the latter is that the desymmetrized compound (with two new contiguous stereogenic centres) can be formed in up to 100% yield.[122]

This study focused on the desymmetrization of *meso*-epoxides using chiral Lewis acid complexes formed from trifluoromethanesulfonate (scandium triflate, $Sc(OTf)_3$)[126-129] – a water- and organic-soluble as well as recoverable Lewis acid that has been shown to be useful for ring-opening reactions[127] – and chiral amino acid/peptide ligands. Benzyl alcohol was chosen as the nucleophile as a protected form of water, since chiral vicinal diols are important for the preparation of optically active compounds[130] that can be used as auxiliaries, building blocks for complex molecules, and chiral catalysts. Figure 2.2 shows the general idea behind desymmetrization involving a chiral Lewis promotor.[131]

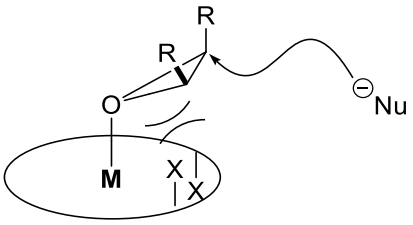

Figure 2.2. Basic idea behind epoxide desymmetrization using a C_2-symmetric Lewis acid.

2.1.1 Examples of *meso*-desymmetrization from the Literature

The first reported addition of an oxygen nucleophile desymmetrizing a *meso*-epoxide was that of Jacobsen *et al.* who used the C_2-symmetric cobalt(III)(salen) complex **83** as a chiral Lewis acid (Scheme 2.2). Carboxylic acids were used as nucleophiles under base catalysis to generate the more nucleophilic carboxylate ion in the formation of 1,2-monoesters ultimately, and in good yield and excellent enantioselectivity.[132]

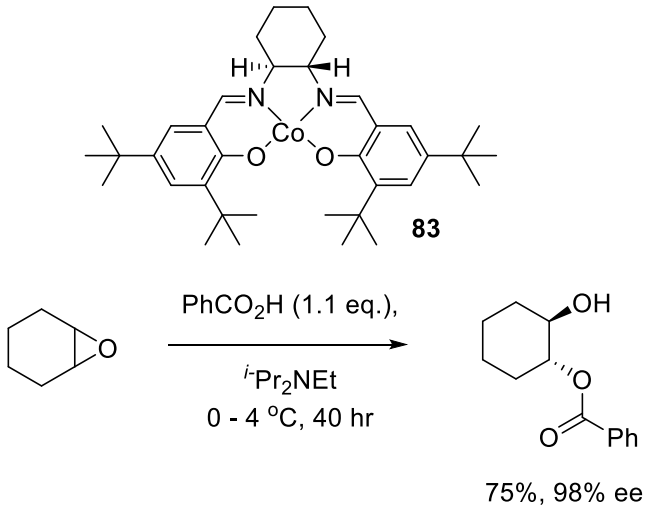

Scheme 2.2. *Meso*-desymmetrization using Jacobsen's C_2-symmetric cobalt(III)(salen) complex **83**.

Similarly, Shibasaki used a gallium-lithum bis(binaphthoxide) (GaLB) bifunctional complex **84** for the addition of phenols to *meso*-epoxides (Scheme 2.3).[133]

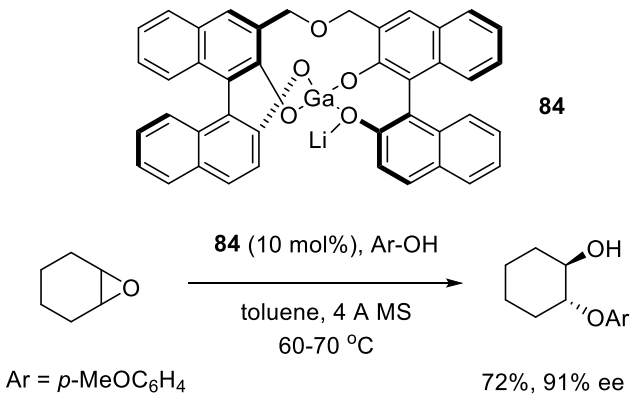

Scheme 2.3. Proposed structure of (*R*)-Ga-Li-bis(binaphthoxide) (GaLB, **84**).

They postulated that the bimetallic complex would overcome the low reactivity of oxygen nucleophiles towards epoxide ring opening, since the gallium centre could act as the Lewis acid to activate the epoxide, while the lithium alkoxide could act as a Brønsted base to activate the nucleophile. Epoxide-opened products were formed in good to high ee (67–93%), but yields were generally only modest (31–75%).[133]

The first addition of aliphatic alcohols to *meso*-epoxides was reported by Schneider *et.al* who used a scandium-bipyridine complex **85**.[134] According to the author, a chiral complex is formed via metal coordination to the pyridine nitrogen and hydroxyl donors.[134] *Meso*-vicinal diols were formed in good to high ee (up to 96%), but yields were generally modest (Scheme 2.4).

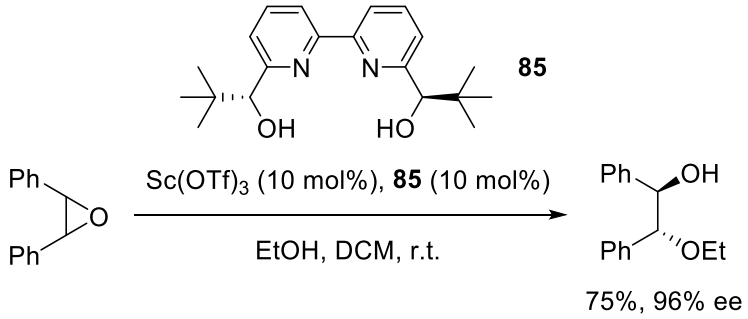

Scheme 2.4. *Meso*-desymmetrization using Schneider's scandium-bipyridine complex **85**.

Snapper and Hoveyda use a titanium dipeptide Schiff base to furnish β-cyanohydrins from a *meso*-epoxide in good yield and ee, using either trimethylsilyl cyanide or HCN as a nucleophilic cyanide source (Scheme 2.5). The most efficient chiral ligand was shown to be the *tert*-leucine-threonine-based dipeptide ligand **86**.[135]

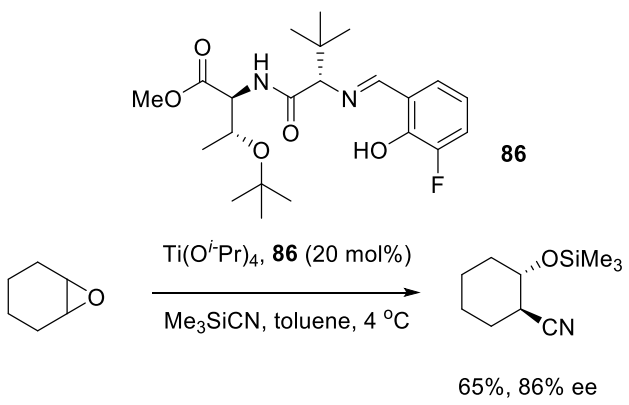

Scheme 2.5. *Meso*-desymmetrization using Snapper and Hoveyda's titanium dipeptide Schiff base ligand **86**.

2.2 Ligand Design in this Project

Our catalyst design was based on Trost's C_2-symmetric ligands, which consist of a phenolic template with two *ortho* side arms containing electron-donating groups that can coordinate to the Lewis acid. Trost's catalyst **87** used two chiral diphenylprolinol units as the side arms, while diethylzinc was used as the Lewis acid in a stoichiometry of Lewis acid: ligand = 2:1 and in which each equivalent of organometallic reacted in different ways. The first equivalent underwent two successive metal-hydrogen exchange reactions with the phenolic and one of the prolinol hydroxyl groups rendering a bonded zinc alkoxide, while the second zinc equivalent exchanged with the remaining prolinol hydroxyl group only, retaining one ethyl group as shown, albeit with extra coordination. This made for a highly Lewis acidic environment embedded within a C_2-symmetric framework (Fig. 2.3).[136,137] According to the researchers, the conformation of the diphenylprolinol moieties creates the chiral space responsible for the enantiodiscrimination.[138] These catalysts were shown to return high enantiomeric excesses in the asymmetric aldol and nitro-aldol (Henry) reactions (Scheme 2.6).[139]

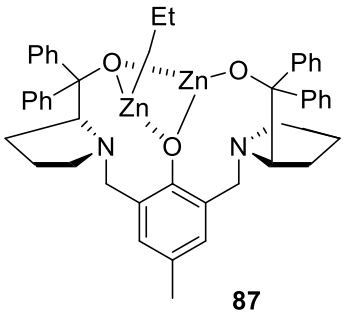

87

Figure 2.3. a) Trost's chiral dinuclear zinc catalyst.

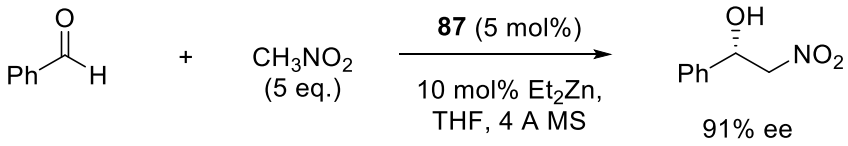

Scheme 2.6. Henry reaction using Trost's C_2-symmetric ligand **87**.

Figure 2.4 shows our catalyst design, in which the aim was to use a peptide as the chiral element. This would be attached to the template via an amide bond. It was hoped that the carbonyl group oxygen atoms and the phenolic oxygen would coordinate to the scandium to form a chiral complex **89** (Fig. 2.4). Template **88** was readily available via a short synthetic sequence.[140]

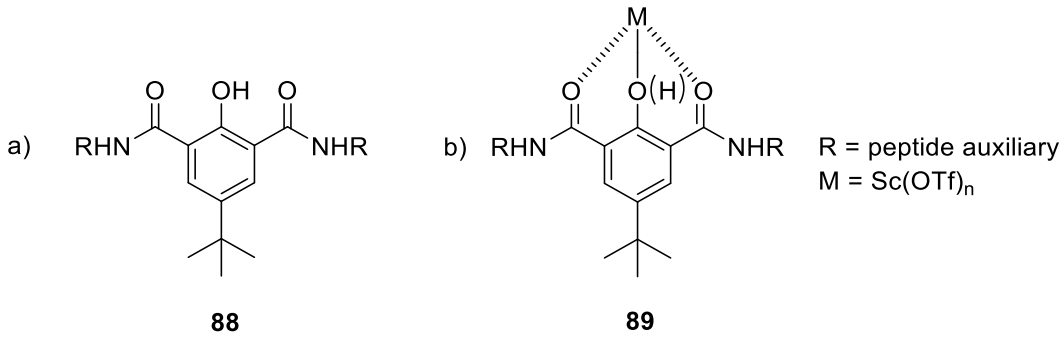

Figure 2.4. Catalyst design showing: a) the template pre-catalyst, and b) the template coordinated to the Lewis acid to form a chiral catalytic complex.

The next step was to decide on the nature of the amino acids used as chiral auxiliaries. The amino acid leucine was chosen to explore whether its bulky *iso*-butyl side chain might provide a chiral environment upon complexation with the Lewis acid. Tryptophan was also chosen because of its electron-rich indole ring, which might participate in π–stacking (the phenolic ring bears two carboxamides that might create a suitable acceptor for the indole) to create a tight chiral environment around the Lewis acid. Finally, cysteine was chosen because the bigger sulfur (compared to oxygen) might lead to better coordination with the $Sc(OTf)_3$.

2.3 Synthesis and Characterization of Peptide Ligands

Diacid template **94** was synthesised in four steps using Pfaltz' procedure, and is shown in Scheme 2.7.

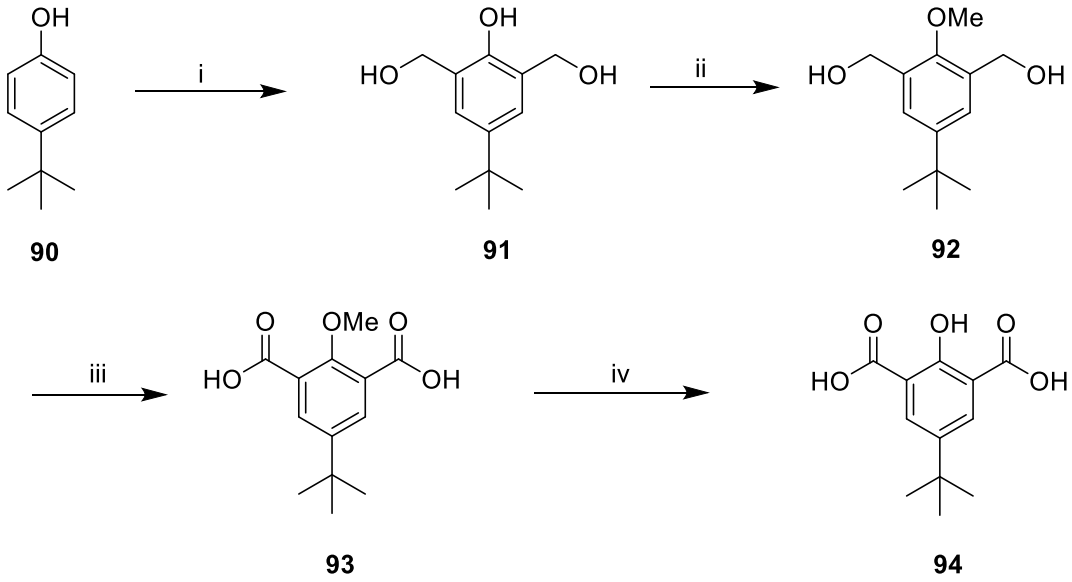

Scheme 2.7. *Reagents and conditions:* (i) Formaldehyde, aq. NaOH (10%), 48 hrs (33%); (ii) K_2CO_3, methyl iodide, CH_3CN, 48 hrs (70%); (iii) $KMnO_4$, adogen 464, 50 °C, aq. NaOH (5%), 2 hrs (72%); (iv) HBr/AcOH (33%), 120 °C, 30 min. (87%).

Thus, commercially available 4-*tert*-butyl phenol **90** was bis-*ortho* reacted with formaldehyde under basic conditions to give diol **91** in a yield of 33% after adjusting the pH with 1M HCl to protonate the phenoxide and extracting. The low yield was consistent with the literature value of 34%, while the ^{1}H NMR spectrum of **91** showed diagnostic peaks resonating at δ_H 4.91 ppm for the four methylene protons (singlet), and δ_H 3.29 ppm for the two hydroxyl groups (broad singlets). In order to perform the oxidation to the diacid **93**, the phenolic OH group of **91** first had to be protected as its methyl ether. This was achieved by exploiting the acidity of the phenolic proton in which **91** was refluxed with methyl iodide and K_2CO_3 in acetonitrile for 48 hours to give the phenoxy ether/diol **92** in 70% isolated yield. A new methoxy singlet resonated in the ^{1}H NMR spectrum at δ_H 3.78 ppm, while the two hydroxyl groups resonated at δ_H 2.49 ppm, indicating a chemoselective protection of the phenolic hydroxyl group, since K_2CO_3 is not a strong enough base to deprotonate aliphatic alcohols.

The next step involved oxidation with $KMnO_4$ in the presence of a phase-transfer catalyst. The excess $KMnO_4$ was quenched with ethanol, and the crude mixture filtered through Celite ®. The filtrate was acidified with 1M HCl and the pure diacid **93** precipitated as a colourless solid in 72% yield. Compound **93** could be crystallized making for an attractive procedure overall. Its ^{1}H NMR spectrum lacked the methylene signals of the starting material and showed the appearance of a broad singlet at δ_H 8.93 ppm corresponding to the two carboxylic OH protons. Scheme 2.8 shows the mechanism of the oxidation reaction involving a manganese ester intermediate.

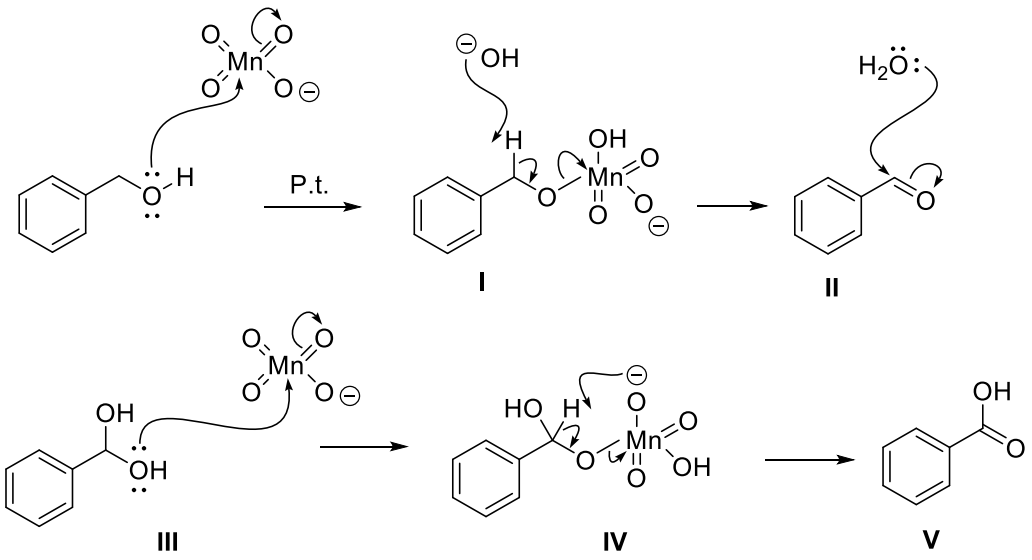

Scheme 2.8. General mechanism for the oxidation of an alcohol to a carboxylic acid with $KMnO_4$.

With the diacid in hand, the next step was to remove the methyl group of **93** with HBr/AcOH by heating to 120 °C for 30 minutes. This involves protonation of the poorly nucleophilic phenolic oxygen (hence the high temperature) followed by nucleophilic attack by bromide at the methyl carbon (S_N2) to effect demethylation. Following reaction, the mixture was cooled to room temperature and quenched with water resulting in precipitation of phenol **94** as a colourless solid in 87% yield. Its ^1H NMR spectrum revealed that the methoxy group had been removed. With the diacid **94** in hand, coupling with the amino acids to form the chiral ligands could proceed.

Fig. 2.5 shows the four molecules that were targeted for use as chiral peptide ligands for transition metal-based desymmetrization reactions, together with the structures of possible metal-ligand complexes.

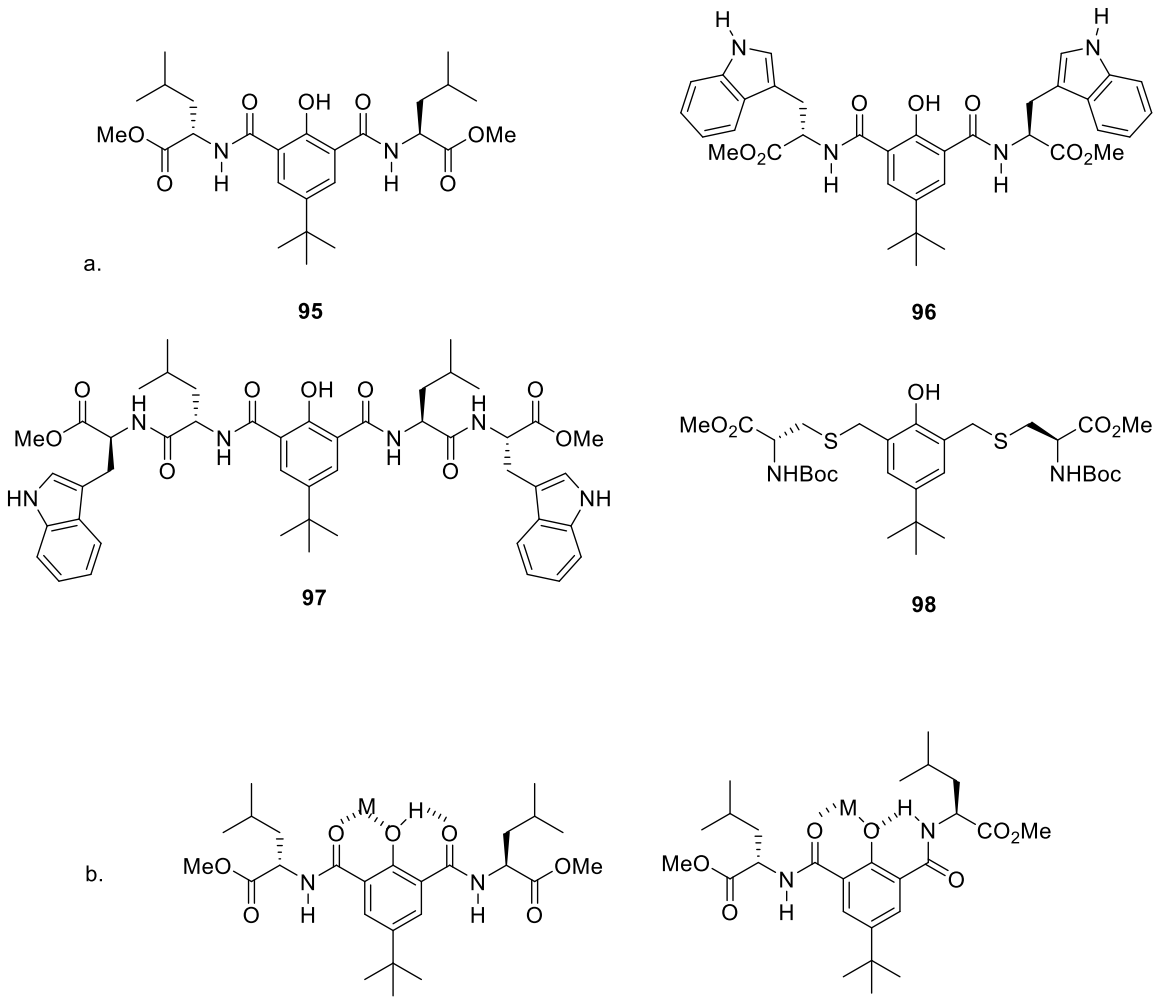

Figure 2.5. a. Structures of the target molecules. b. Possible metal-ligand complexes.

Compounds **95** and **96** were formed from diacid **94** (Scheme 2.7)[136] via double nucleophilic acyl substitution (S_NAc) of the acid dichloride of **94** (prepared with $SOCl_2$) by the requisite amino acid amines. Conversely, compound **97** was prepared by coupling NH_2-Leu-Trp-OMe to **94** using standard peptide coupling conditions. For compound **98**, the amino acid was added to the C_2-symmetric dibromide (Scheme 2.15) via an S_N2 reaction. The details of these reactions now follow.

For ligand **95** involving coupling via the diacid dichloride, thionyl chloride was used as chlorinating agent. This involved heating the diacid **94** in neat thionyl chloride to reflux temperature to give **99** as the crude diacid dichloride. Following $SOCl_2$ removal coupling was then carried out in dry DCM with commercially available HCl-Leu-OMe **100**, and triethylamine in DCM at 0 °C. The reaction was monitored by TLC to reveal a fluorescent spot after one hour. Following work-up and column chromatography using ethyl acetate\hexane the compound was isolated in a 33% yield (Scheme 2.9).

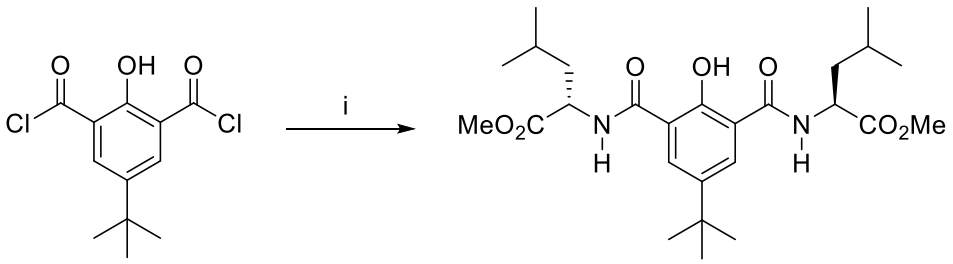

99 **95**

Scheme 2.9. *Reagents and conditions:* (i) HCl-Leu-OMe, NEt_3, DCM, r.t., 20 min (33%).

The ^1H NMR spectrum of **95** (Fig. 2.6) showed that two amino acids had coupled to the diacid, with diagnostic peaks appearing at δ_H 1.26 ppm, a singlet for *tert*-butyl group (9H integration), and at δ_H 4.81 ppm, a multiplet for the two α-protons of leucine (2H). The amide hydrogens resonated at δ_H 8.1 ppm. The two diastereotopic methyl groups of the *iso*-butyl side chain appeared as two doublets resonating at δ_H 0.97 ppm and δ_H 0.98 ppm. Similarly, the ^{13}C NMR spectrum showed two downfield singlets for the ester and the newly formed amide carbonyl carbons. Double substitution was confirmed by virtue of the presence of 14 singlets as 2:4:8 for carbonyl:aromatic:aliphatic resonances. Elemental analysis was in agreement with the calculated values.

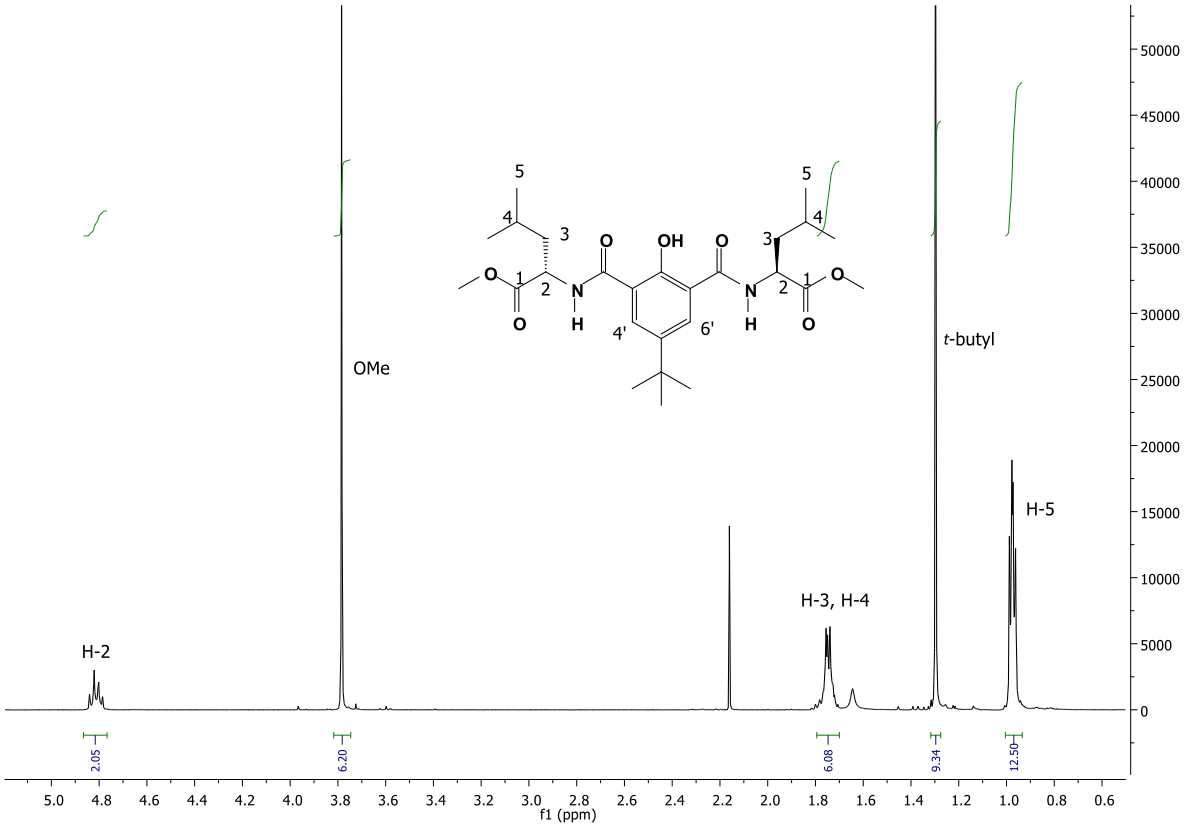

Figure 2.6. A portion of ^{1}H NMR ($CDCl_3$) spectrum of compound **95**.

The tryptophan ligand **96** was synthesised in the same way by coupling dichloride **99** to HCl-L-trp-OMe **101 (**formed via Fischer esterification of tryptophan) to give product **96** in 62% yield after column chromatography (Scheme 2.10). The presence of the new amide bond was again confirmed by the ^{1}H NMR spectrum with a diagnostic peak at δ_H 7.87 ppm for the NH (as 2H). The rest of the tryptophan signals were consistent with compound **101**, while the template aromatic protons resonated at δ_H 7.76 ppm as a singlet and the *tert*-butyl protons at δ_H 1.15 ppm.

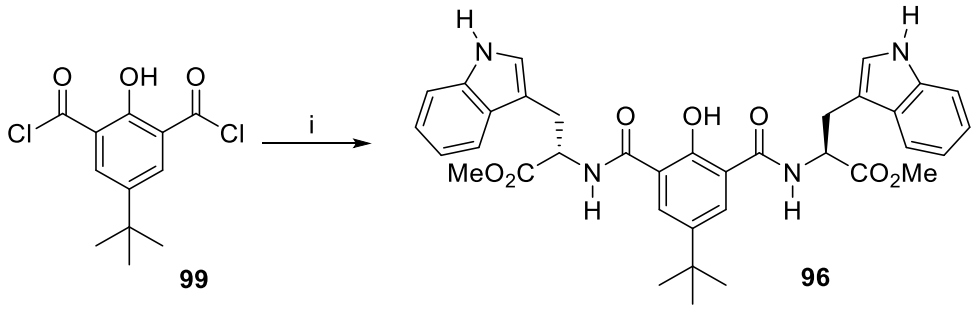

Scheme 2.10. *Reagents and conditions:* (i) HCl-Trp-OMe, NEt_3, DCM, r.t., 1 hr (62%).

For ligand **97**, dipeptide **104** had to be synthesised. This was achieved by following a typical peptide protection and deprotection sequence (Scheme 2.11).

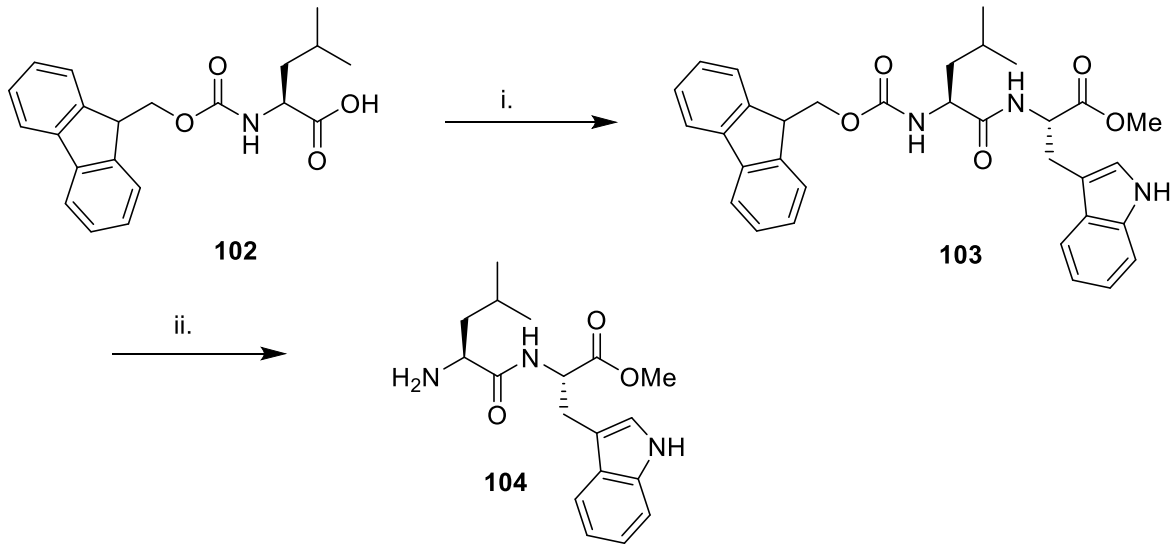

Scheme 2.11. *Reagents and conditions:* (i) **97**, EDC, HOBt, pyridine, r.t., 18 hrs (98%), (ii) piperidine, 0 °C, 2 hrs (68%).

Thus, commercially available Fmoc-L-Leucine **102** and HCl-trp-OMe **101** were reacted with EDC and HOBt in pyridine at room temperature. HOBt is a catalyst and was used in a pseudo-catalytic (30%) amount to prevent racemization during coupling.[141] Following an acidic workup (to remove the pyridine), and column chromatography product **103** was isolated as a colourless solid in 98% yield. The ^{1}H NMR spectrum of the product showed characteristic peaks at δ_H 5.10 ppm for the new amide NH and the two multiplets at δ_H 4.90 ppm and around δ_H 4.20 ppm for the α-protons of leucine and tryptophan respectively.

Scheme 2.12 shows the general mechanism for a peptide coupling reaction using a carbodiimide (usually DCC or EDC), and HOBt. In the first step, the carboxylic acid is deprotonated by the carbodiimide to form intermediate **I**. This is followed by nucleophilic addition of the carboxylate to the imino-iminium ion to form **II**. HOBt then attacks the carbonyl to form benzotriazolyl ester **III** with loss of a urea by-product (which is either soluble (for EDC) or insoluble (for DCC) in water). Intermediate **III** finally undergoes S_NAc with the amine to form the amide (peptide bond) with regeneration of the catalyst.

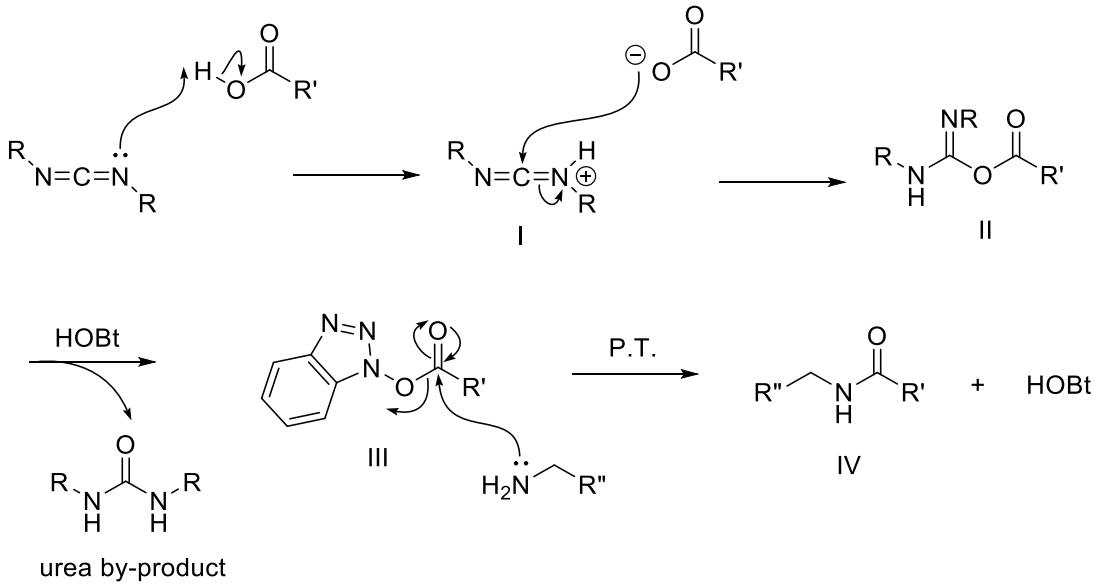

Scheme 2.12. Mechanism of carbodiimide/HOBt peptide coupling mechanism

The ^{13}C NMR spectrum of Fmoc-dipeptide **103** showed only one set of peaks, which suggested that epimerization had not occurred, but in order to confirm the enantiomeric purity, chiral HPLC was performed. Therefore, the four stereoisomers of **103** were synthesised as a racemic diastereoisomeric mixture.

Racemic HCl-Trp-OMe was synthesised by mixing equal amounts of L-tryptophan and D-tryptophan and forming the methyl ester as previously described. Racemic Fmoc-Leu-OH was prepared by mixing equal amounts of L-leucine and D-leucine together and reacting the mixture with Fmoc-choride under basic conditions.[142] The two racemic amino acids were then reacted under peptide coupling conditions according to Scheme 2.11. The diastereomeric mix of Fmoc-Leu-Trp-OMe and the supposed enantiomerically pure Fmoc-Leu-Trp-OMe (**103**) were evaluated using chiral HPLC, which revealed four peaks corresponding to the two diastereomers and their enantiomers (Fig. 2.7), and one peak for **103** (Fig. 2.8), confirming that epimerization had not occurred.

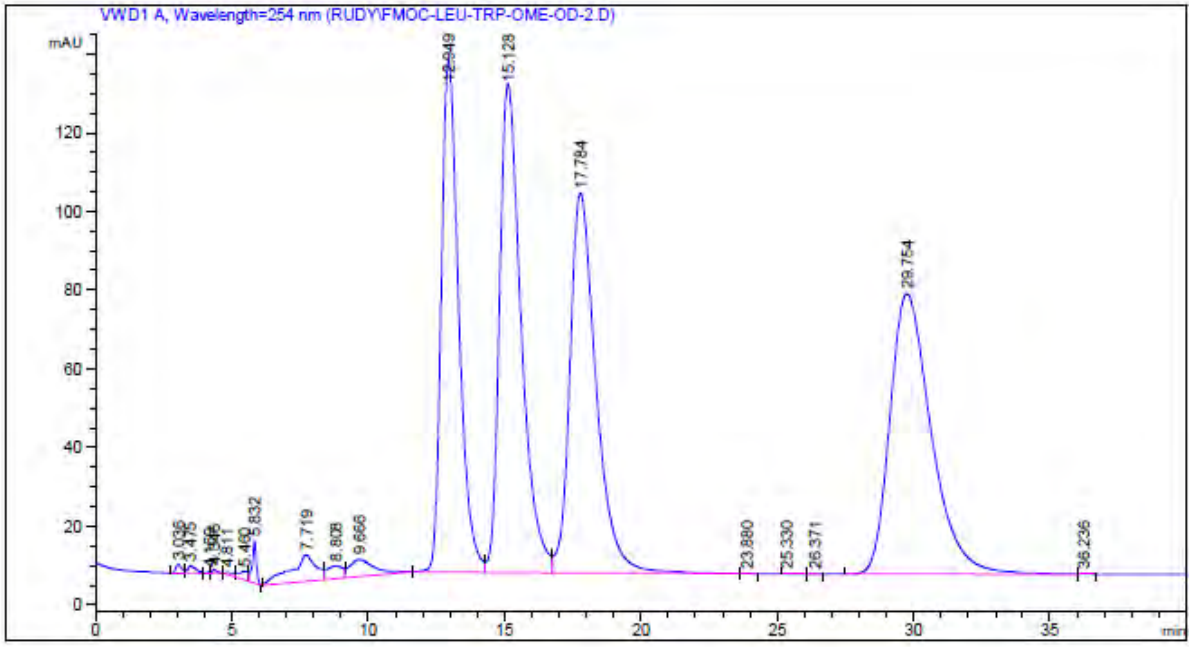

Figure 2.6. Chromatogram of the racemic diastereomeric mix of dipeptide **103**.

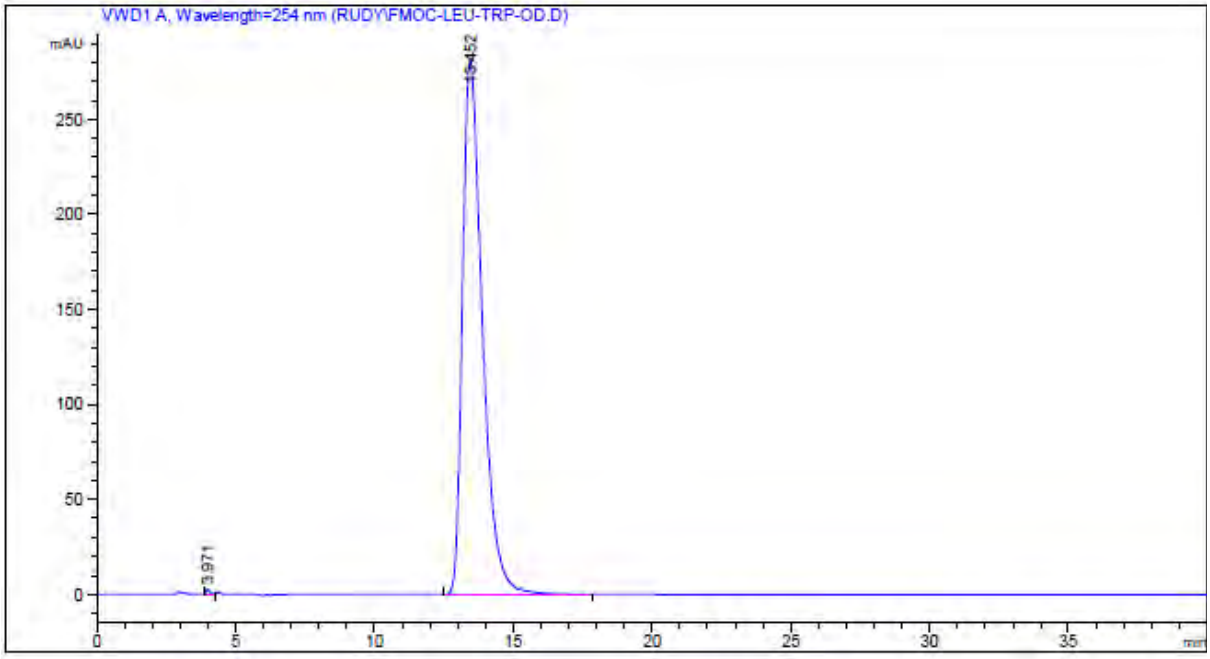

Figure 2.7. Chromatogram of enantiomerically pure **103**.

The next step was to remove the Fmoc protecting group of **103** under basic conditions using piperidine. The reaction was followed by TLC using a polar solvent system of 10% methanol in DCM, which revealed a polar amine spot of R_f 0.5. Compound **104** was isolated in 64% yield following column chromatography. Scheme 2.14 shows the mechanism for the

deprotection of the Fmoc group, which involves deprotonation of the acidic benzylic proton to form intermediate **I**, which fragments with elimination of CO_2 and 9-methylene-9H-fluorene to give the desired amine .

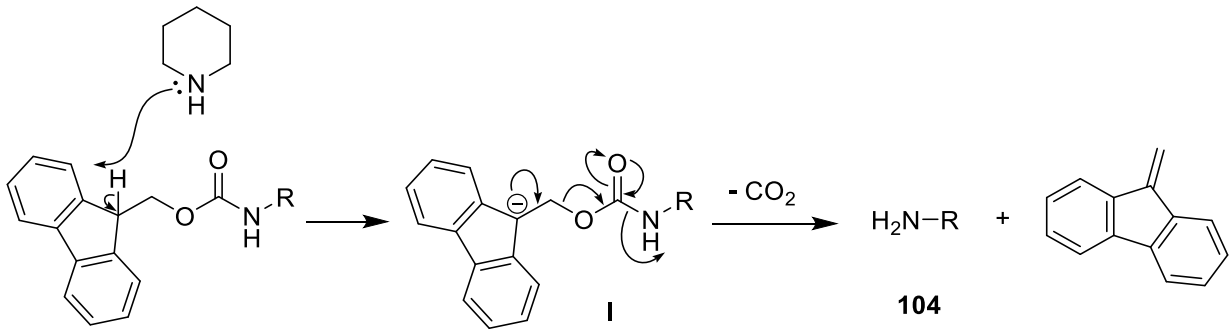

Scheme 2.14. Mechanism of the Fmoc deprotection

The coupling between the dipeptide **104** and the diacid **94** to form **97** was successfully achieved using EDC and HOBt in pyridine. The reaction gave the dipeptide catalyst **97** in a 60% yield, which was assigned using a combination of 1D, 2D, NMR spectroscopy as well as high resolution mass spectrometry and infra-red spectroscopy. Its ^{1}H NMR spectrum showed diagnostic peaks at δ_H 7.80 ppm for the amide and δ_H 4.93 ppm and δ_H 4.70 ppm for the two α-protons of the amino acids (Fig. 2.6), and once again ^{13}C NMR confirmed its C_2-symmetric character by the presence of 24 singlets (C-2” and OMe overlapping) as 3:12:9 for carbonyl:aromatic:aliphatic resonances.

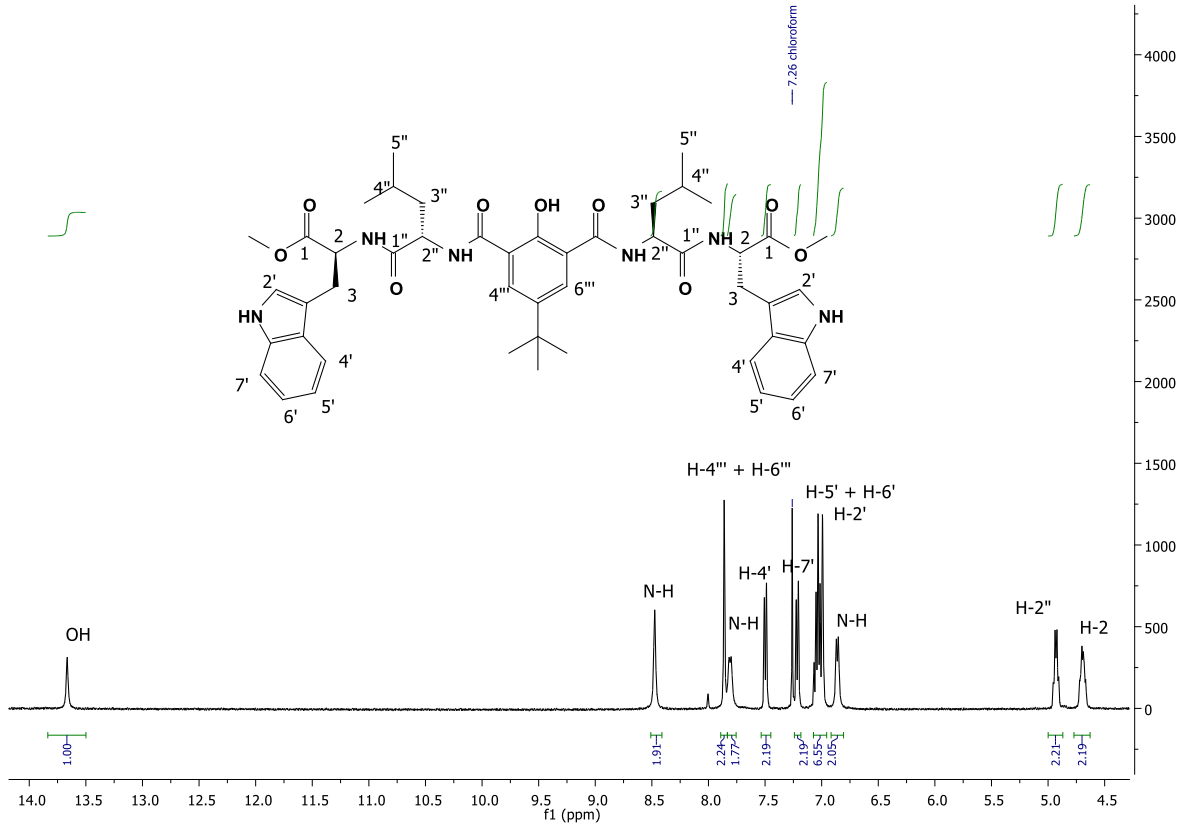

Figure 2.6. A portion of ^{1}H NMR ($CDCl_3$) spectrum of compound **97**.

Finally, the disulfide ligand **98** with sp^3 rather than sp^2 connecting atoms was synthesised using the dibrominated **105**, which was prepared using reaction of **91** with HBr/AcOH (33%) at reflux temperature for one hour in order to form dibromide **105** (Scheme 2.15).[143] However, the ^{1}H NMR spectrum showed the presence of two compounds as the expected product **105** as well as the acylated phenol **106**. These were not separated, but taken to the next step together.

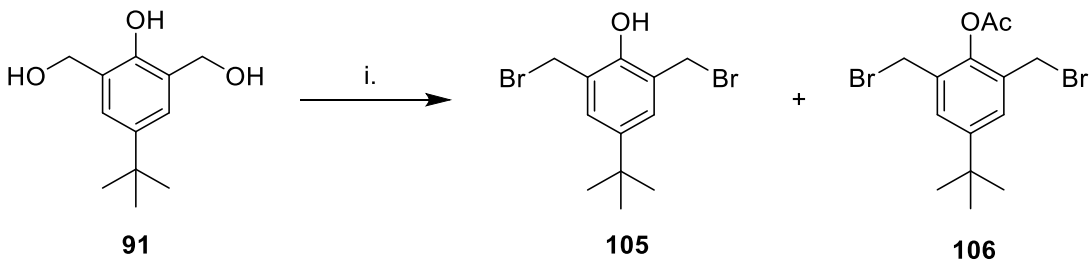

Scheme 2.15. *Reagents and Conditions:* (i) HBr/AcOH (33%), 120 °C, 30 min.

For the amino acid of ligand **98**, commercially available HCl-Cys-OMe was Boc-protected with di-*tert*-butyl dicarbonate to give the Boc-Cys-OMe **107** in 89% yield shown in Figure 2.8. Its ^{1}H NMR spectrum showed the diagnostic peaks for the *tert*-butyl group at δ_H 1.43 ppm, and the α-proton at δ_H 4.60 ppm.

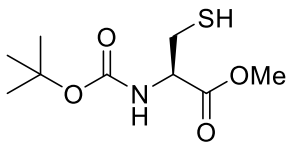

107

Figure 2.8

The thiol **107** (2 eq.) was then reacted with the mixture of dibromide compounds (**105** and **106**) and triethylamine in DCM at room temperature. TLC confirmed the presence of two compounds after one hour. The solvent was removed *in vacuo*, the residue redissolved in MeOH, and the temperature lowered to −5 °C. K_2CO_3 was added and after 30 minutes TLC revealed the disappearance of the top spot with retention of the lower (phenolic). Following a work-up followed by column chromatography, compound **98** was obtained as a clear oil in 66% yield. The structure of **98** was assigned on the basis of its spectroscopic data including 1D, 2D, ^{1}H (Fig. 2.9) and ^{13}C NMR as well as IR spectroscopy and high resolution mass spectrometry.

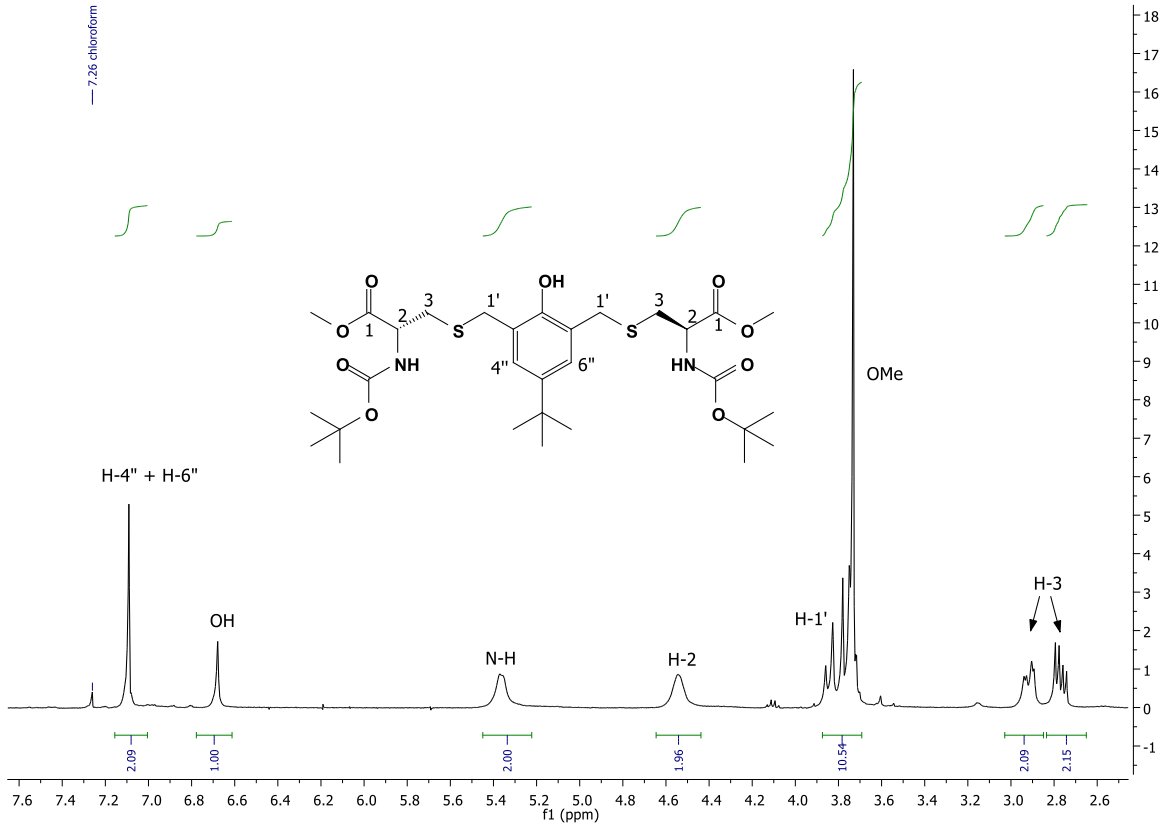

Figure 2.9. A portion of ^{1}H NMR ($CDCl_3$) spectrum of compound **98**.

The diastereotopic methylene protons (H-3) resonated at δ_H 2.84 ppm as two double doublets (due to coupling with the α-proton at H-2) in an ABX system. The benzylic methylene signals resonated further downfield at δ_H 3.76 ppm. Finally, a correct HRMS evaluation (*m/z* HRMS (ES) 645.2881 $[M + H]^+$, $C_{30}H_{49}N_2O_9S_2$ requires *m/z*, 645.28795 $[M + H]^+$), confirmed the structure of **98**. The four ligands were then tested in the desymmetrization of a *meso*-epoxide.

2.4 *Meso*-Desymmetrization Reactions

The ligands were screened in the *meso*-desymmetrization of cyclohexene oxide **108** as a model substrate and benzyl alcohol as a UV-active nucleophile (for HPLC evaluation) in the presence of a Sc(III)-ligand complex. The model reactions were studied with respect to ligand, temperature, and ligand/scandium ratio (Scheme 2.16). Catalyst formation between the scandium triflate and ligand was carried out with and without base (triethylamine or NaH via the phenoxide), as it was not clear to what extent triflic acid would be generated (coordination complex versus substitution), the acid being a danger for promoting a non-asymmetric opening.

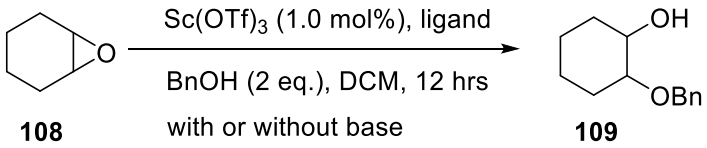

Scheme 2.16. Model reaction for the scandium-ligand-catalysed ring-opening of *meso*-cyclohexene oxide with benzyl alcohol.

Control experiments were performed in the absence of a chiral ligand, but with scandium triflate, to form racemic alcohol **109** in 16% yield (Scheme 2.17) following vacuum distillation to remove excess benzyl alcohol (residual BnOH could not be easily removed by column chromatography). The stereochemistry of the scandium-catalysed ring opening was determined by ^{1}H NMR analysis, which showed a multiplet for proton H-2 in the *trans*-configuration. This was compared to the *cis* stereoisomer **111** (Scheme 2.18) – formed from *cis*-1,2-cyclohexane diol, benzyl bromide, and base – in which H-2 appeared with different multiplicity as a doublet of triplets (Fig. 2.10), confirming a *cis* arrangement of H-1 and H-2 (in which H-2 is axial with just one large axial-axial coupling).

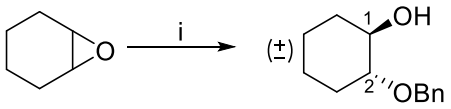

Scheme 2.17. *Reagents and conditions:* i. $Sc(OTf)_3$ (1 mol%), BnOH (2 eq.), DCM, 4 hrs, 0 °C (16%).

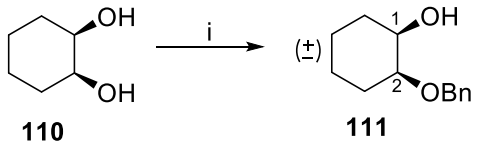

Scheme 2.18. *Reagents and conditions:* i. NaH (60%), BnBr, THF, 2 hrs, 0 °C (46%).

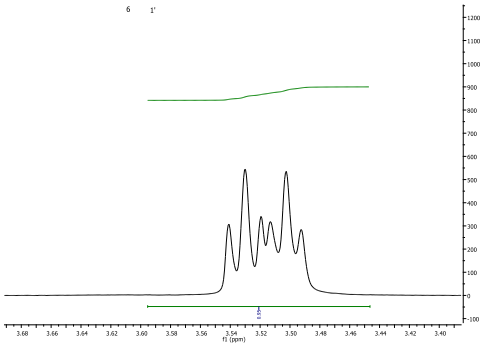

Figure 2.10. Doublet of triplets for H-2 of compound **111**.

2.4.1 General procedure

Thus, scandium triflate (1 mol%) was weighed in a glove box and suspended in dichloromethane. The chiral ligand (1.5 or 2.0 mol%, Table 2.1) was added to form the chiral complex *in situ*. In the cases where a base (NEt_3 or NaH/THF) was added, this was added at this point as a slight excess to the ligand. After twenty minutes at room temperature, the temperature was lowered to −78 °C before adding the benzyl alcohol (2 eq.) and the epoxide substrate (1 mol eq.). After twelve hours an aliquot of the solution was removed and a mini-work-up performed using ethyl acetate/1M HCl. The sample was dried and the solvent removed and the crude ee evaluated by chiral HPLC. This procedure was repeated continuously (i.e. every 12 hours) at −20 °C, 0 °C, and room temperature depending on the ligand; the ligand/scandium ratio was also varied.

Since no column chromatography was performed, conversions were calculated from the HPLC data. The yields were not calculated, but were generally moderate (~20% between −78 and 20 °C, ~70% between 0 °C and r.t.). In this, the reference had to be the benzyl alcohol, since the epoxide (limiting reagent) was not UV-active. Since the benzyl alcohol was present as two equivalents and 100% conversion only consumed one equivalent, the conversions were calculated according to the following equations in which A_R = area in the HPLC trace for residual benzyl alcohol as a percentage of the total (the remaining percentage reflecting products as a total percentage). Importantly, however, was that the two enantiomers separated by almost a minute on the HPLC trace (Chiralpak AD column), and an ee could thus be easily calculated. The results of the study are shown in the following three tables.

1. $C = 2(100 - A_R)$

2. $ee = \frac{E_{Major} - E_{Minor}}{E_{Major} + E_{Minor}}$

A_R = Area of benzyl alcohol (residual)

E_{Major} = Major Enantiomer

E_{Minor} = Minor Enantiomer

2.4.2 Results

i. Leucine-based Ligand

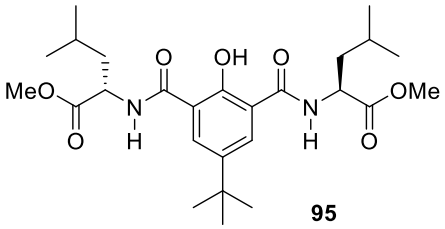

95

Table 2.2. Results of the *meso*-desymmetrization of cyclohexene oxide using chiral Lewis acid catalysis and ligand **95**.

entry	ligand	ligand (mol%)	*T* (°C)	C	ee (%)
1.	**95**	1.5	−20	8	17
2.	**95**	1.5	0	17	3
3.	**95**	2.0	–78	11	14
4.	**95**	2.0	r.t.	46	8

ii. Tryptophan-based Ligand

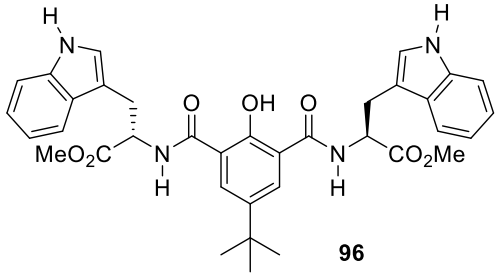

96

Table 2.2. Results of the *meso*-desymmetrization of cyclohexene oxide using chiral Lewis acid catalysis and ligand **96**.

entry	ligand	ligand (mol%)	*T* (°C)	C	ee (%)
1.	**96**	1.5	r.t.	24	25
2.	**96**	2.0	0	20	18
3.	**96**	2.0	r.t.	88	6

iii. Dipeptide- and Cysteine-based Ligands

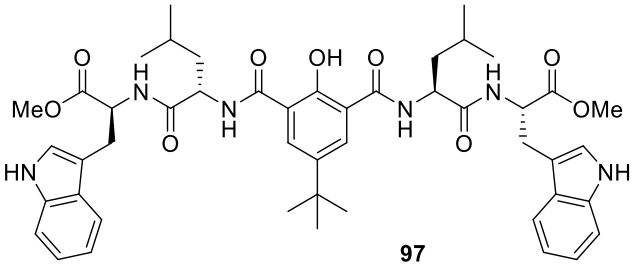

97

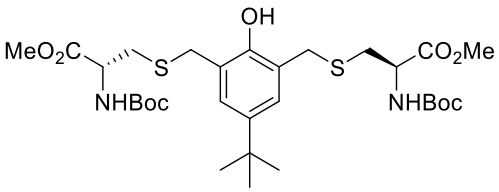

98

Table 2.3. Results of the *meso*-desymmetrization of cyclohexene oxide using chiral Lewis acid catalysis and ligand **97** and **98**.

entry	ligand	ligand (mol%)	*T* (°C)	C	ee (%)
1.	**97**	1.5	–20	100	39
2.	**98**	1.5	–20	15	41
3.	**98**	1.5	0	17	22
4.	**98**	1.5	r.t.	99	10
5.	**98**	2.0	−78	8	17
6.	**98**	2.0	0	33	9
7.	**98**	2.0	r.t.	97	11

2.4.3 Conclusions

This study attempted to develop an asymmetric alcoholysis of a *meso*-epoxide using a scandium Lewis acid bearing a chiral peptide ligand. Four different ligands were synthesised as **95**–**98**. The reaction was studied with respect to ligand, temperature and ligand/scandium ratio (loading). Unfortunately, the different catalysts all gave modest to low enantioselectivities. However, some observations were noteworthy in which conversions increased with increasing temperature as expected, but enantioselectivity decreased with increasing temperature in all cases. Furthermore, the ligand/scandium ratio also affected the results giving higher enantiomeric excesses but lower conversions for the lower loading (1.5 eq.). The optimal conditions appeared to occur at −20 °C for the cysteine ligand **98** (Table 2.3, entry 3), which gave an ee of 41% (the highest ee) at a 15% conversion with a 1.5 loading, while the dipeptide ligand **97** (Table 2.3, entry 1) also gave an encouraging ee of 39% at 100% conversion at a 1.5 loading. These results suggest that conformational restriction imposed by having amide connections between template and “arms” is less

optimal than an sp^3 connection as in the cysteine case, where flexibility presumably allows for a better involvement of the chiral part of the arm with the Lewis acid. Moreover, having two amino acids rather than one in the arm improved the ee. Although it looked attractive to pursue developing the cysteine system with longer peptides there was a concern about the lack of transition-state understanding, notably regarding the association constant of the complex and whether triflic acid could be generated for promoting a non-asymmetric process. In this regard attempts to induce a greater association constant using base catalysis on the phenol of the ligand (e.g. using triethylamine or NaH) failed to improve results.

In light of the low enantiomeric excesses and the difficulties in controlling the factors determining enantioselectivity (H-bonding, steric effects, π–stacking) the focus shifted to using amino acids and peptides in Lewis-base enantiocatalysis, specifically in the area of asymmetric DMAP catalysis. This is a field of asymmetric catalysis that is well established as far as transition-state models are concerned, and in which it was thus felt that predictive catalyst design involving developing and optimizing ligand structure and reaction conditions to yield a mature catalytic asymmetric method,[144] was likely to be more feasible. These endeavours will be discussed in the next chapter.

Chapter 3: Lewis Base Catalysis

This part of the study describes the shift away from using peptides in a Lewis acid context to one in which Lewis base catalysis was used as the theme of catalysis in the form of chiral DMAP-type catalysis for the kinetic resolution of secondary alcohols, a theme in current organocatalysis that was extensively reviewed in Chapter 1. In all cases the chiral element was either an amino acid or a short peptide (two or three amino acid residues long). It was natural to consider the influence of placing the chiral element (peptide) at the three possible positions on the pyridine ring (α, β, and γ), in which α was excluded based on the findings of Litvinenko and Kirichenko[48] regarding the imposition of a severe steric parameter, which prompted the inclusion of the 8-hydroxyquinoline template where a resonance effect was hoped would offset the steric issue. Figure 3.1 shows the structures of the target templates **A–C**, as well as the attachment sites for the chiral peptide groups **R***.

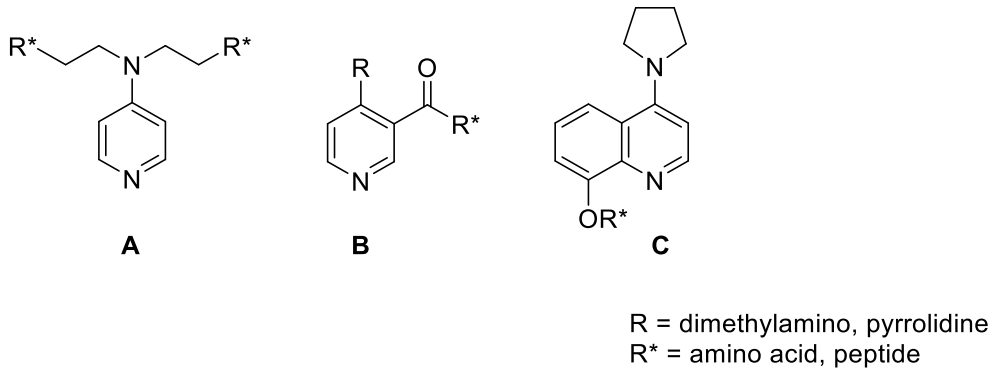

Figure 3.1

Of crucial importance in design was that **R*** include an electron-rich aromatic ring from the amino acids tryptophan or tyrosine that could potentially π–stack to the electron-deficient acyl-pyridinium cation (section 1.7) in a similar manner to Fuji's induced-fit model. The synthesis, characterisation, and activity of the three classes of catalysts are discussed in the following three sections.

3.1 γ-Substituted DMAP Catalysis

The *γ*-substituted DMAP catalysts were designed having the chiral group attached to alkyl chains on the nitrogen 4-substituent. Figure 3.2 shows the two target compounds belonging to this class of catalyst. A C-2 tether was selected as the minimum-length tether in which the idea was that the flexible alkyl chains might allow the electron-rich amino acids to π–stack to

the pyridine nitrogen. A C_2-symmetric design was chosen because it would render the two faces of the pyridine equivalent (Fig. 3.3). Such a strategy was used by Spivey in the design of his original catalysts involving a chiral 2,5-disubstituted pyrrolidino moiety.[50]

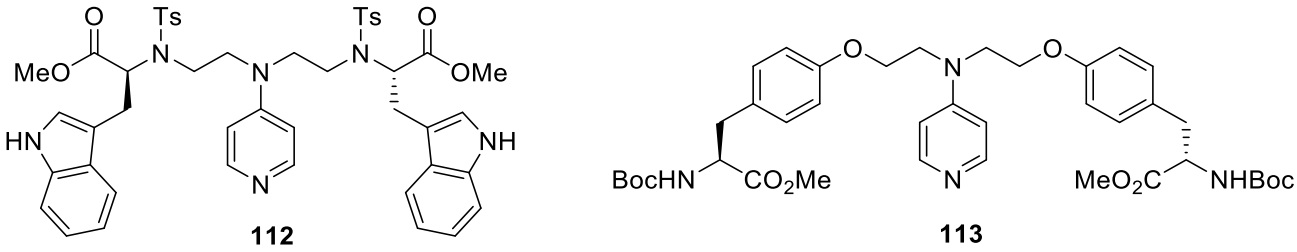

Figure 3.2

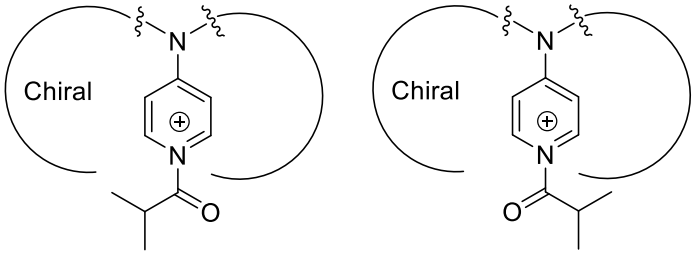

Figure 3.3. Two rotamers of the *iso*-propyl moiety in a. C_2-symmetric DMAP catalyst view from the top face. b. C_2-symmetric DMAP catalyst view from the bottom face.

Furthermore, the catalysts were designed to be synthetically easily accessible via Mitsunobu coupling to a 4-pyridine diol derivative. However, their inbuilt conformational flexibility, to allow π–stacking, was a concern regarding the possibility of incurring an entropic penalty in promoting a specific highly organised transition state. In this regards, encouragement was provided by the work of Kawabata who had shown that a C_2-symmetric acyl-transfer catalyst **114** could adopt a conformation containing two hydrogen bonds between the catalyst and a monosaccharide in the rate-determining step of the acylation reaction (Fig. 3.4), although he did have some preorganisation generated by the pyrrolidine scaffold.

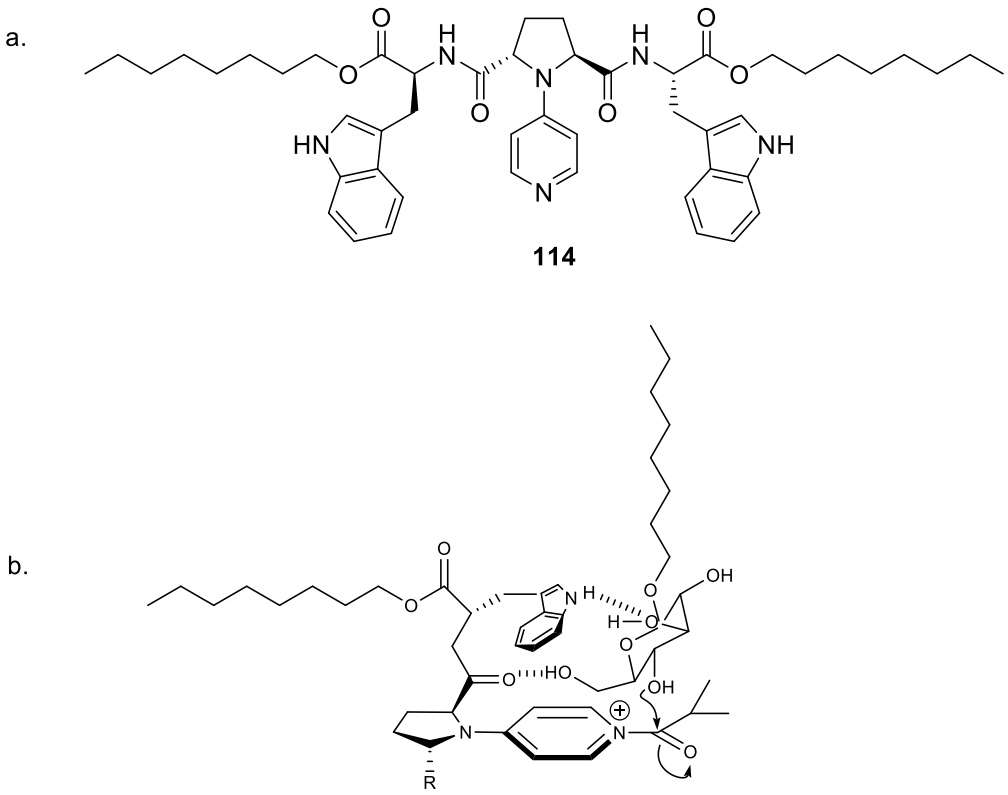

Figure 3.4. a) Kawabata's C_2-Symmetic acyl-transfer catalyst; b) Transition-state model for the regioselective and chemoselective acylation reaction of monosaccharides.

For the synthesis, commercially available 4-chloro-pyridine **115** was converted to the target diol **116** by heating it in excess diethanolamine as both reagent and solvent with sodium hydroxide as base at 180 °C, followed by purification by vacuum distillation to remove the excess diethanolamine, and then column chromatography.[145] The polar compound **116** was recovered as a viscous, brown oil in 55% yield (Scheme 3.1)

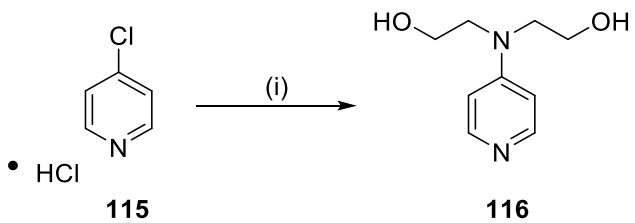

Scheme 3.1. *Reagents and conditions:* (i) 6M NaOH (aq.), diethanolamine, 180 °C, 5 hrs (55%).

Its ^{1}H NMR spectrum was fairly simple due to the C_2-symmetry revealing characteristic peaks for the four equivalent protons adjacent to the hydroxyl groups in the chain at δ_H 3.64 ppm, as well as the four protons adjacent to the 4-nitrogen atom at δ_H 3.76 ppm – this was

somewhat downfield due to deshielding by resonance of the 4-nitrogen lone pair into the heteroaromatic ring as well as the inductive effect of the hydroxyl groups. In the aromatic region of the spectrum the two protons β to the pyridine nitrogen resonated at δ_H 6.74 ppm due to resonance from N-4, while the two protons α to the pyridine nitrogen appeared deshielded at δ_H 8.04 ppm. With the template in hand, the next step was to couple to aromatic amino acids using a Mistunobu reaction.[146]

For the first catalyst based on the electron-rich indole ring, L-tryptophan was converted to its methyl ester **101** using thionyl chloride and methanol.[147] The ^{1}H NMR spectrum of the product obtained was consistent with published results as discussed earlier in section 2.3. The enantiomeric purity was determined by measuring the optical rotation, which gave a value of + 19° in methanol (lit.[147] + 18°). Since the NH proton of the amino acid was not acidic enough for carrying out a Mitsunobu reaction, the tryptophan methyl ester amino group was sulfonylated by reacting with tosyl chloride and triethylamine to form the sulfonamide **117** in 75% yield (Scheme 3.2).[148] Its ^{1}H NMR spectrum was consistent with published results, showing a peak for the methyl group of the tosyl moiety at δ_H 2.73 ppm and two new signals in the aromatic region for the new symmetrical aryl group. Its optical rotation was measured in THF and pleasingly agreed with the literature value (recorded as + 16°, lit.[148] + 17°).

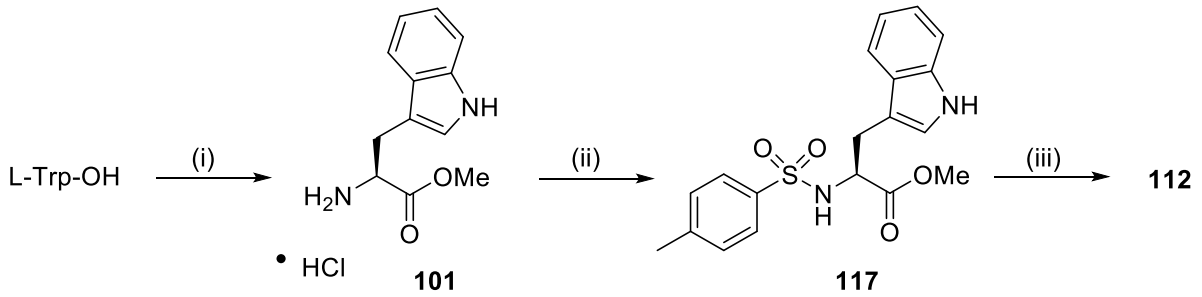

Scheme 3.2. *Reagents and conditions*: $SOCl_2$, MeOH, r.t., 18 hrs, 98%, (ii) TsCl, NEt_3, DCM, r.t., 3 hrs (75%), (iii) **116**, DIAD, PPh_3, DCM/DMF, r.t., 3 hrs (36%).

In the next step of the synthesis (Scheme 3.2), **117** (2 equivalents) was coupled to template **116** via a Mitsunobu reaction using triphenylphosphine and DIAD in a solution of THF and DMF (to dissolve the polar template). Compound **112** was obtained in 36% yield following column chromatography. The symmetrical nature of the ^{1}H NMR spectrum, e.g. in the aromatic region, suggested that a bis-coupling had been achieved. Specifically, the spectrum showed a characteristic singlet for the tosyl methyl group at δ_H 3.17 ppm integrating for six protons, while the eight alkyl protons of the tether now resonated collectively at δ_H 3.53 ppm

in view of oxygen having been substituted by nitrogen. Similarly, a single resonance was observed for amino acid α-protons at δ_H 4.92 ppm. In addition, the protons of the pyridine ring resonated as an AB doublet pair δ_H 8.19 ppm (α) and δ_H 6.64 ppm (β), while the protons of the indole ring could be seen in the aromatic region as two doublets, two triplets, and a singlet. The ^{13}C NMR spectrum for **112** displayed all the required signals as a 1:6:15 carbonyl:aliphatic:aromatic split, confirming the C_2-symmetry (Figure 3.4 shows an APT spectrum for compound **112**). For the amino acid, the carbonyl carbon resonated at δ_C 171.4 ppm, while the chiral carbon resonated at δ_C 59.5 ppm. The methoxy was present at δ_C 52.0 ppm (Fig. 3.5). Finally, a correct HRMS evaluation for the product (m/z HRMS (ES): *m/z* 891.3208 $[M + H]^+$, calculated for $C_{47}H_{51}N_6O_8S_2$, 891.3210 $[M + H]^+$), confirmed the structure of **112**.

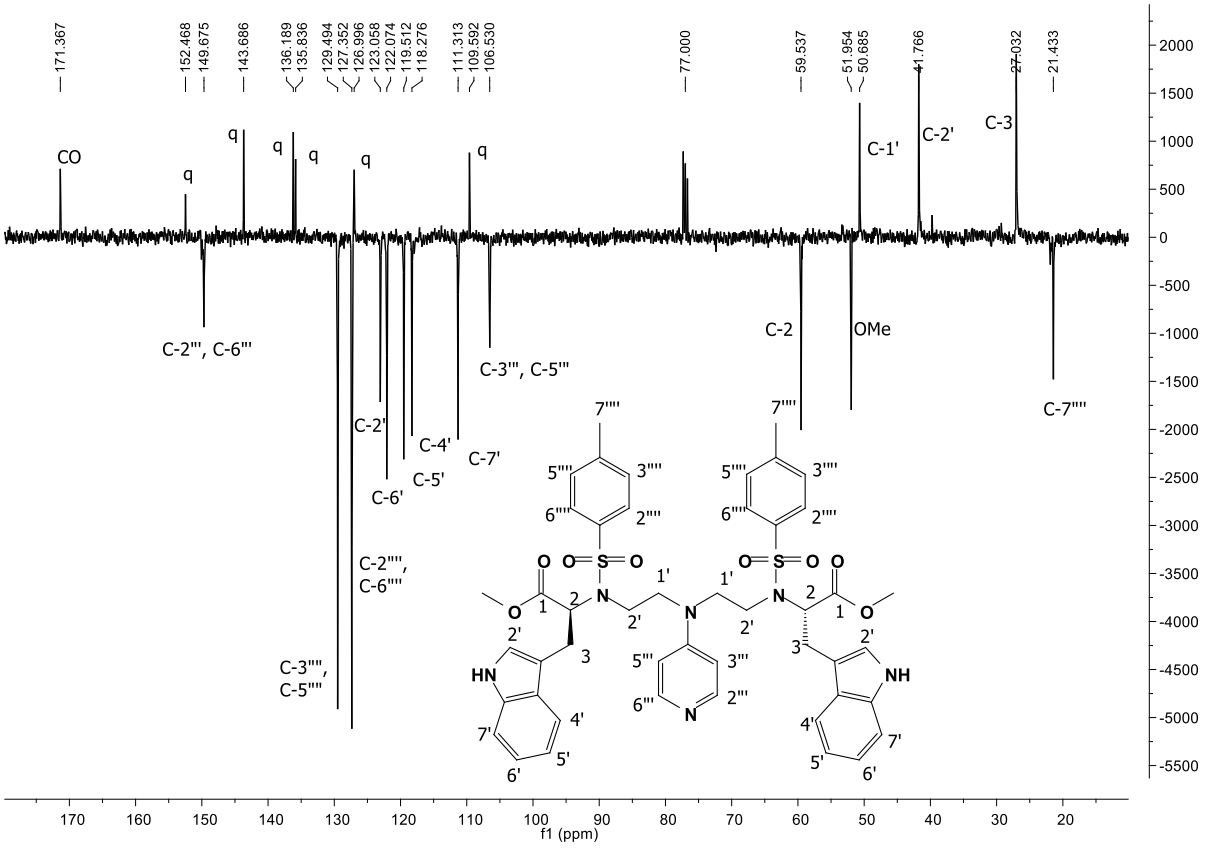

Figure 3.5. An APT spectrum of catalyst **112**.

Mechanistically, the Mitsunobu reaction starts with attack of the triphenylphosphine on DIAD to form zwitterion **I**, which deprotonates the acidic sulfonamide NH of **117** to form azaphosphonium cation **II**, which is rapidly intercepted by the hydroxyl group of diol **116** to form an activated oxyphosphonium ion of the reactant that rapidly undergoes S_N2 reaction

with the sulfonamide anion to render the product **112** together with triphenylphosphine oxide as by-product.

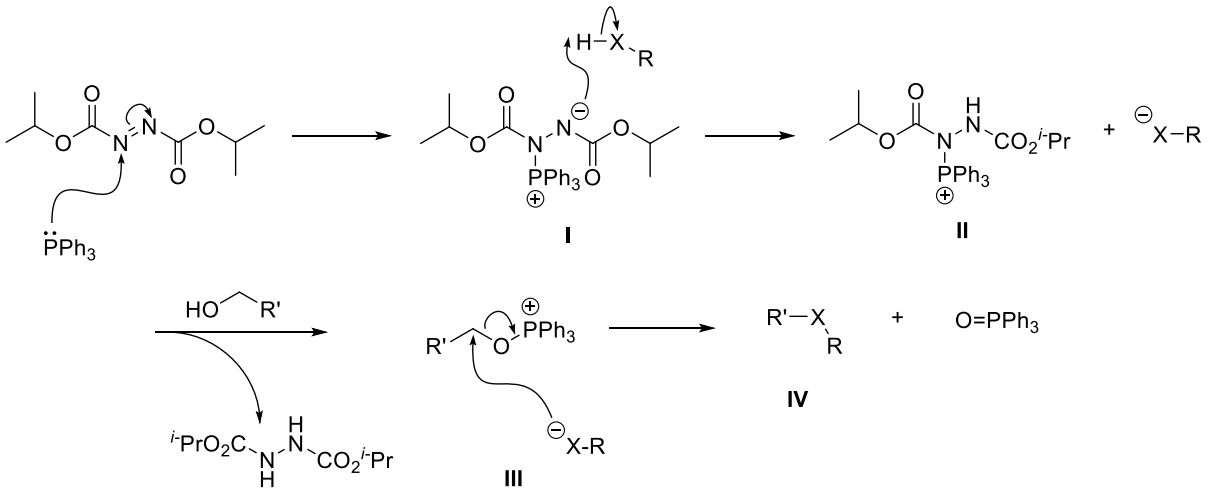

Scheme 3.3. Mechanism of the Mistunobu reaction

The second target for the *γ*-substitued DMAP was compound **113**, a tyrosine-containing compound that could also be synthesised by the Mitsunobu reaction, since tyrosine contains an acidic phenolic proton. For this purpose L-tyrosine was first protected at both *C*- and -*N* amino acid termini (Scheme 3.4).

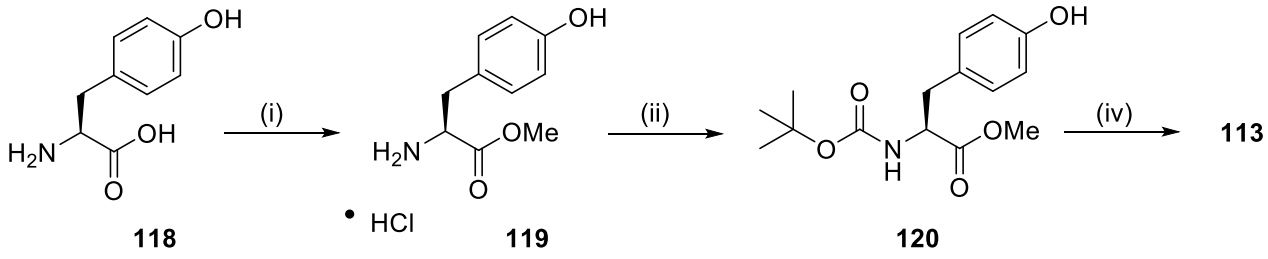

Scheme 3.4 *Reagents and conditions:* (i) AcCl, MeOH, r.t., 18 hrs (98%), (ii) $(Boc)_2O$, NaOH, EtOH, 18 hrs (92%), (iii) **116**, DIAD, PPh_3, DCM/DMF, r.t., 3 hrs (41%).

Thus, the complete synthesis involved first protection of L-tyrosine as its methyl ester **119** using acetyl chloride in MeOH at room temperature. The reaction could be monitored by TLC using ethyl acetate/water/*n*-butanol/acetic acid in a 1:1:1:1 ratio. The ^{1}H NMR spectrum of **119** revealed a characteristic peaks for the methoxy singlet at δ_H 3.80 ppm and the α-proton at δ_H 4.23 ppm. In the aromatic region the protons resonated between δ_H 7.08 ppm and δ_H 6.79 ppm. The optical rotation was measured in pyridine and gave a value of + 68.8°,

which agreed fairly well with that of the literature value of + 76°.[149] The next step was to chemoselectively protect the *N*-terminus using a Boc-group under basic conditions; the amine is selectively protected because the lone pairs of the phenolic OH are delocalised into the π system of the aromatic ring by resonance, which makes the oxygen less nucleophilic. TLC revealed a less polar spot, which following an acidic work-up gave compound **120** in 33% yield (the low yield was due to some Boc substitution) after column chromatography. Its ^{1}H NMR spectrum was consistent with published results in which the phenolic proton was observable and its optical rotation measured in chloroform gave excellent parity with that of the literature + 51.3° (lit.[150] + 52.8°).

Compound **120** was then reacted with **116** under Mitsunobu conditions as described previously to form catalyst **113** in 53% yield after column chromatography. Its ^{1}H NMR spectrum showed a large singlet integrating for 18 protons (for the *tert*-butyl groups of the amino acid moieties) at δ_H 1.40 ppm, as well as a multiplet for the two equivalent α-protons at δ_H 4.51 ppm. The eight alkyl protons that linked the amino acid to the pyridine ring now resonated in two sets at δ_H 3.88 ppm and δ_H 4.15 ppm, the latter for the protons close to oxygen. As with **112** the four protons of the pyridine ring resonated as two AB doublet pairs at δ_H 6.61 ppm and δ_H 8.23 ppm. The ^{13}C NMR showed all the required carbon atoms in a 2:7:7 carbonyl:aromatic:aliphatic split as shown in the APT spectrum in Fig. 3.5. Notably, characteristic peaks for two carbonyl carbons as downfield singlets at δ_C 172.3 ppm and 157.4 ppm were observed for ester and carbamate (N-resonance pushes value upfield) functionalities respectively. The chiral carbon resonated at δ_C 54.5 ppm, while the methoxy carbon resonated at δ_C 52.2 ppm. The carbons of the pyridine ring resonated at δ_C 149.4 ppm (β to the pyridine nitrogen), and at δ_C 106.7 ppm (α to the pyridine nitrogen) (Fig. 3.6). A correct HRMS evaluation (m/z HRMS (ES): *m/z* 737.3761 $[M + H]^+$, calculated for $C_{39}H_{53}N_4O_{10}$, 737.37617 $[M + H]^+$), confirmed the structure of **113**.

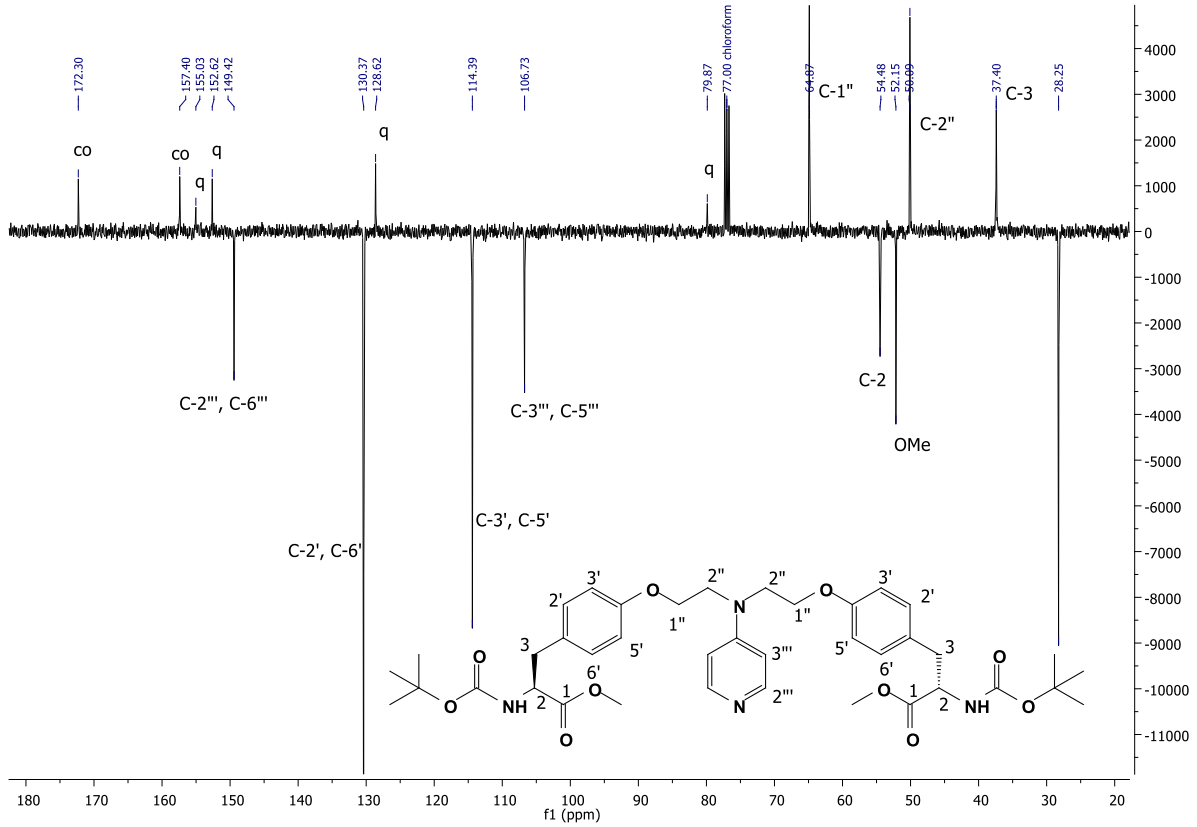

Figure 3.6. APT spectrum of catalyst **113**.

Catalysts **112** and **113** were then tested in the kinetic resolution of 1-(2-naphthyl)ethanol **121** as a model compound (Table 3.1).The acylation reaction was performed using isobutyric anhydride (0.7 eq.) in the presence of 5 mol% catalyst (**112** or **113**) in DCM at −78 °C, with triethylamine as an auxiliary base. The reaction could be monitored by TLC, and a less polar spot appeared at R_f = 0.8 in 20% ethyl acetate/hexane after three hours. The reaction was quenched with 1 mL methanol (at −78 °C), followed by a basic work-up using $NaHCO_3$ to give the product ester and the recovered starting material after separation by column chromatography using ethyl acetate and hexane. After purification, the ester was hydrolysed to the alcohol under basic conditions (1M NaOH) so that the both alcohols could be compared to the HPLC retention times of the racemic mixture.

Table 3.1. Kinetic resolution of 1-(2-naphthyl)ethanol **121** using catalyst **112**and **113**.

entry[a]	catalyst	C[b]	ee (alcohol)	ee (ester)[c]	s-value[d]
1.	**112**	13	0.2	1.6	1.0
2.	**113**	55	1.4	1.1	1.0

*a. All reactions were conducted in the presence of 5 mol% **catalyst**, 0.7 eq. of (^{i}PrCO)$_2$O, and 0.9 eq. of Et_3N at −78 °C for 3 hrs., unless otherwise noted. b. Conversion (%) = (ee of recovered alcohol)/(ee of recovered alcohol + ee of ester). c. hydrolysed (2M NaOH in MeOH/H_2O) and ee calculated. d. Selectivity factor* $s = \frac{ln(1-C)(1-ee)}{ln(1-C)(1+ee)}$.

The results of the study show that both catalysts gave no kinetic resolution (s-values = 1) revealing that the rate of the reaction was the same for both *R* and *S* alcohol reactants in each case. However, there was a notable difference in the conversions, i.e. the rate of each reaction in which catalyst **113** promoted a much faster reaction than that of **112**. Thus, attention was turned to molecular modelling to help assist with understanding conformational aspects of the transition state.

Molecular Modelling

Molecular modelling using the Spartan '10 molecular modelling programme was performed on the acyl-pyridinium ions of **112** and **113** (only one configuration around the *N*-acyl centre in each due to C_2-symmetry) in order to determine the lowest energy conformers (Fig. 3.7).

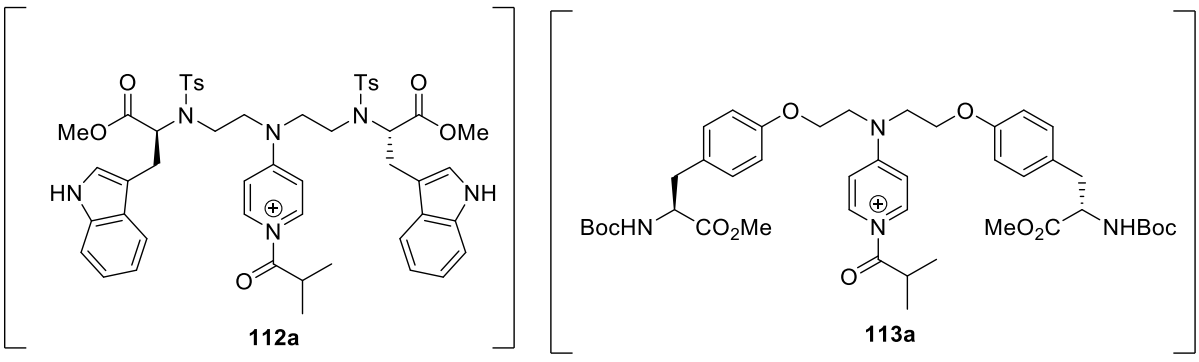

Figure 3.7. Acyl-pyridinium ions of catalysts **112** and **113**.

Thus, a conformer distribution was calculated using the MMFF94 force field,[151] in which 100000 conformers were analysed for the acylated cations (**112a** and **113a**) in the gas phase.

The energies of the ten lowest energy conformers were then compared in a Boltzmann distribution. Figure 3.8 shows the lowest energy conformers of **112a** with their relative energies. Catalyst **112a** had four low-energy conformers which appeared in a 41:28:25:6 ratio based on the energies and are shown in Fig. 3.8 as conformer **A**, **B**, **C**, and **D** respectively. None of the conformers showed any favourable π–stacking interactions, since the indole ring did not overlap appreciably with the pyridine ring (Fig. 3.8, and Table 3.2). One possible explanation for the lack of overlap could be due to the presence of the bulky sulfonamide groups, which prevent appropriate stacking in **112a** resulting in a lack of a suitable chiral environment being created for recognition. Additionally, it looks as though nucleophilic attack is possible from either *N*-acyl face meaning that the nucleophile was facing an "opposite" acyl configuration in each case – opposite, regarding which side (C=O or *iso*-propyl) of the acyl moiety was closest to the bulky chiral chain. This presumably would have communicated an inverted stereo-information to the positioning preference of the incoming nucleophile. However, the pictures in Figure 3.8 also suggest that the low conversion (13 % after 3 hr at −78 °C) was due to the tryptophan rings impeding the approach of the nucleophile.

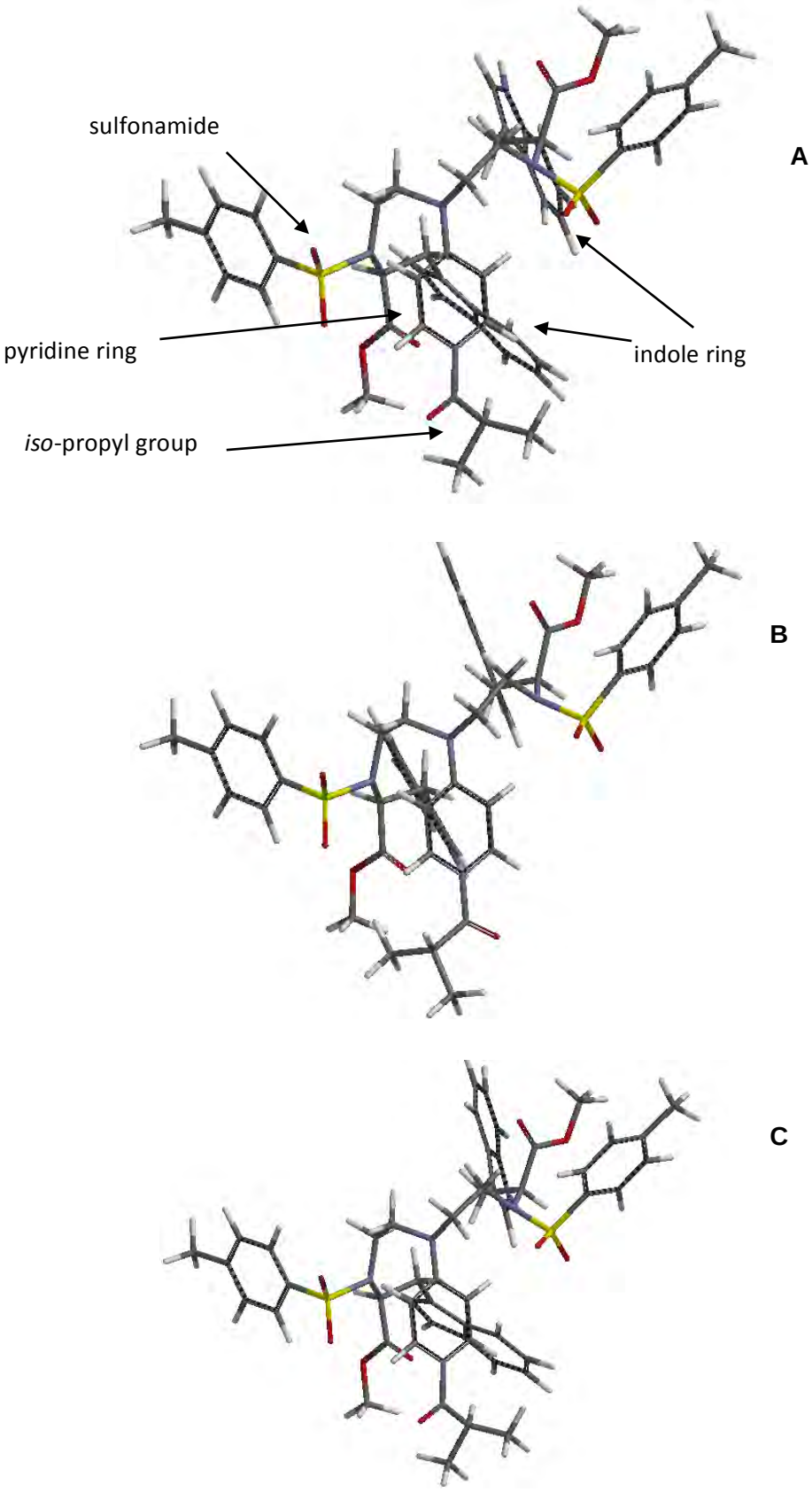
sulfonamide
pyridine ring
indole ring
iso-propyl group
A
B
C

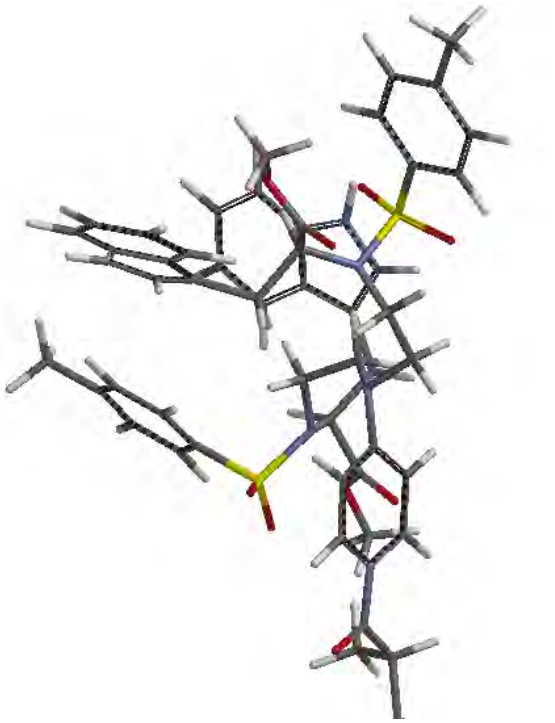

Figure 3.8. Four lowest energy conformers for the acyl-pyridinium ion (**112a**) of catalyst **112**.

Table 3.2. Relative energies of the four lowest energy conformers of **112a**.

conformer	relative energy (kJ/mol)
A	0.00
B	0.95
C	1.26
D	4.64

By comparison, for **113a** only two dominant low-energy conformers were present, in a ratio of 49.3:49.3, with no difference in energy between them (Fig. 3.9 and Fig. 3.10). Here the two tyrosine residues (no sulfonamide groups) do both appear to interact better with each pyridinium face but stacking is not optimal either. It does seem that attack from either face of the acyl group is possible resulting one again in a transfer of "inverted" stereo-information as before. The conversion was decent (55 % in 3 hrs at −78 °C) so access of the nucleophile does not appear to have been a problem in this case. Possibly a longer connection tether might have placed the tyrosine rings more optimally over the pyridinium ring, and certainly it looks as though future catalyst design with tyrosine, albeit contained in a non C_2-symmetric system might warrant further investigation.

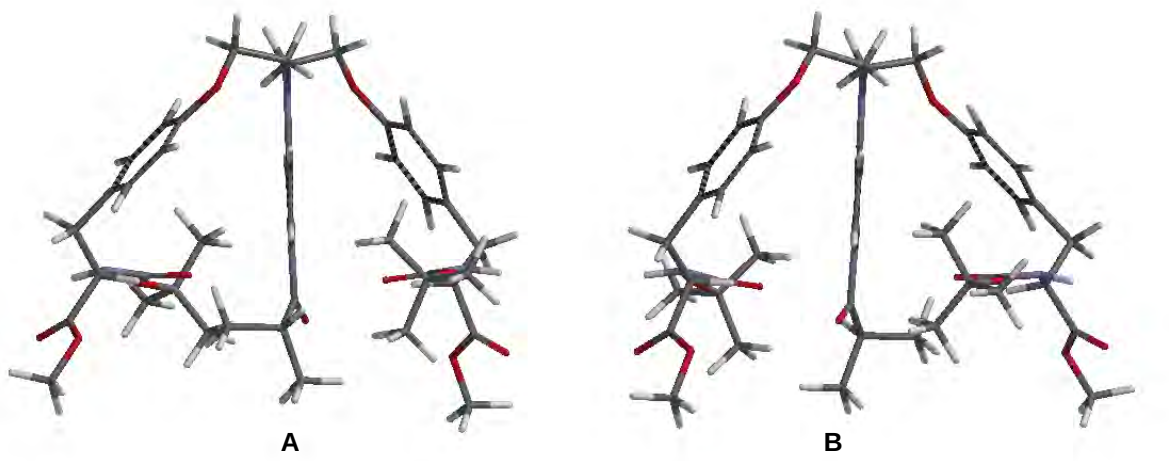

Figure 3.9. Two lowest energy conformers for the acyl-pyridinium ion (**113a**) of catalyst **113**.

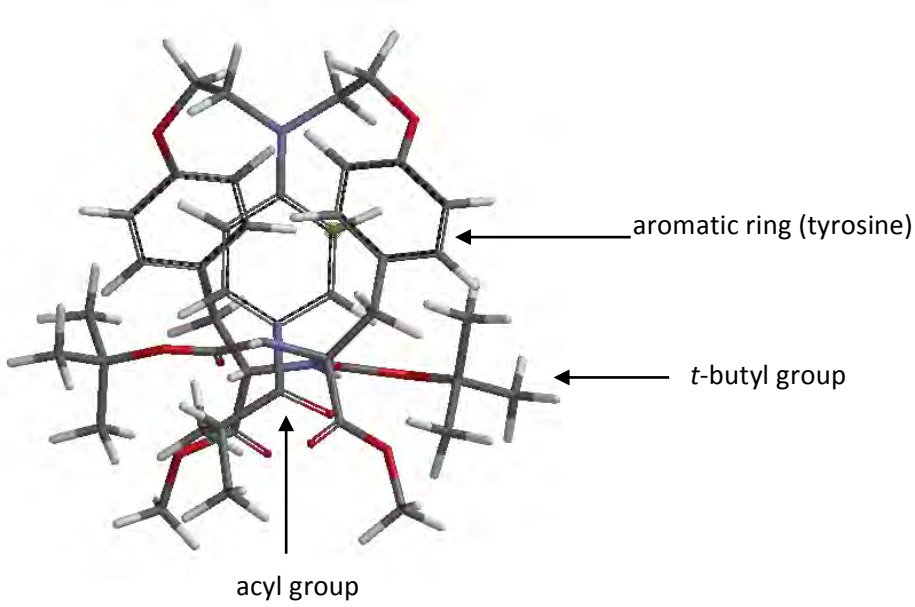

Figure 3.10. Front view of catalyst **113a** showing C_2-symmetry.

The inadequate s-values and the results of the modelling suggested that the catalyst design was not ideal for the purpose. Therefore, all things considered it was decided to bring the chiral element closer to the pyridinium centre by attaching it as a 3-carboxamide. In such a way it was hoped that in this non C_2-symmetric case one of the pyridinium faces would be preferentially blocked.

3.2 β-Substituted DMAP Catalysis

3.2.1 Monopeptide and Dipeptide

The decision to place the peptide in the β-position of the DMAP template was inspired by Connon and Yamada's catalysts (Chapter 1) in which the chiral directing group was attached β to the pyridine nitrogen via an acyl connection. Access to a DMAP template was thus required that would allow attachment of an amino acid or peptide to the β-position, preferably via an amide bond (Fig. 3.11). A β-substituted catalyst would also have the advantage of not having its pyridinium ion hindered by the presence of a substituent in the α position.

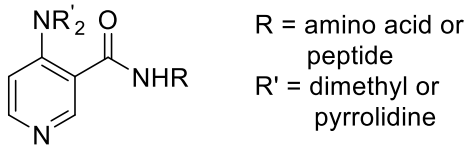

Figure 3.11. The template for the β-substituted DMAP catalysts.

The chemistry adopted for catalyst was that used by Yamada in which commercially available 4-chloronicotinic acid **123** was first reacted with dimethylamine (40 wt. % in H_2O) in toluene under reflux conditions (Scheme 3.5) via an S_NAr reaction. The product was isolated as the β-substituted carboxylate salt **124** by removing the toluene *in vacuo* and dissolving the crude salt in aqueous potassium carbonate. Following filtration, the potassium salt was dried and isolated in 90% yield. Its ^1H NMR spectrum in D_2O confirmed substitution by revealing a characteristic peak for the two new methyl groups as a singlet resonating at δ_H 3.06 ppm indicating free rotation around the N-C_{aryl} bond in spite of resonance. In the aromatic region the three pyridine protons resonated at δ_H 6.85 ppm for H-5 (a doublet with J = 6.3 Hz), δ_H 8.14 ppm for H-6 (a doublet with J = 6.3 Hz), which coupled to the β-pyridine proton, and δ_H 8.21 ppm for H-2 (a singlet), which was strongly deshielded by the pyridine nitrogen and the carbonyl group.

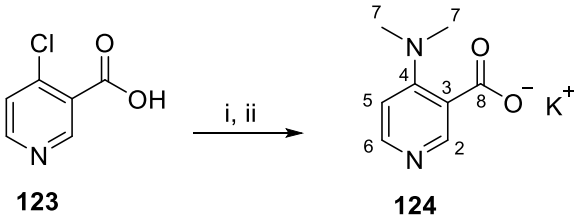

123 **124**

Scheme 3.5. *Reagents and conditions:* (i) dimethylamine, toluene, reflux, 2 hrs, (ii) K_2CO_3, 30 min (90%).

With the template **124** in hand, the first catalyst chosen to evaluate was one containing tryptophan in the hope of generating a π–stacking opportunity between the electron-rich indole and electron-deficient pyridinium rings. Scheme 3.6 shows the synthesis of the first catalyst.

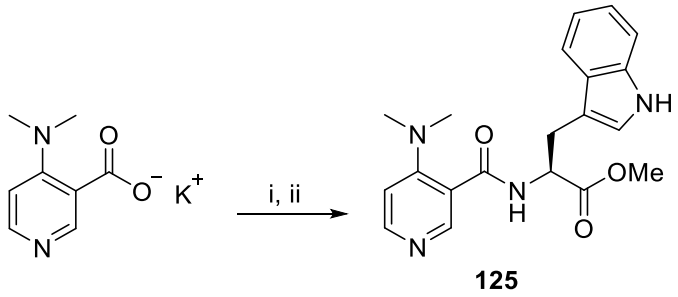

125

Scheme 3.6. *Reagents and conditions:* (i) $SOCl_2$, reflux, 1 hr, (ii) HCl-Trp-OMe, NEt_3, DCM, 0 °C, 30 min (25%).

Following Yamada's procedure for forming an amide via an acid chloride, compound **124** was dissolved in thionyl chloride and heated to reflux temperature. After one hour the solvent was removed and the crude acid chloride residue dried on the vacuum pump. Since the amino acid was prepared as a hydrochloride salt, it was first suspended in DCM at 0 °C and treated with triethylamine (dropwise) to form the free amine. The acid chloride was then dissolved in dry DCM and added to the tryptophan (free amine) at 0 °C. After two hours, TLC showed the formation of a new UV spot below the amine, which appeared as a bright spot under anisaldehyde spray. Following a basic work-up, the product was purified by chromatography using 10% MeOH/DCM as eluent in a low 25% yield. The ^{1}H NMR spectrum of **125** showed characteristic resonances for both pyridine and tryptophan moieties in a 1:1 ratio. Notably, a singlet for the two dimethylamino methyl groups at δ_H 2.68 ppm as well as the two diastereotopic benzylic methylene protons of the amino acid at δ_H 3.14 ppm (Fig. 3.12) were observed. The methoxy group resonated at δ_H 3.66 ppm while the α-proton resonated at δ_H

4.71 ppm. The protons of the pyridine ring appeared at chemical shifts that were consistent with the template (described previously). Similarly, the ^{13}C NMR spectrum showed 19 singlets corresponding to the 20 carbon atoms in the molecule (the two methyl group of the dimethylamino moiety resonated as one peak in accordance with the ^{1}H NMR data).

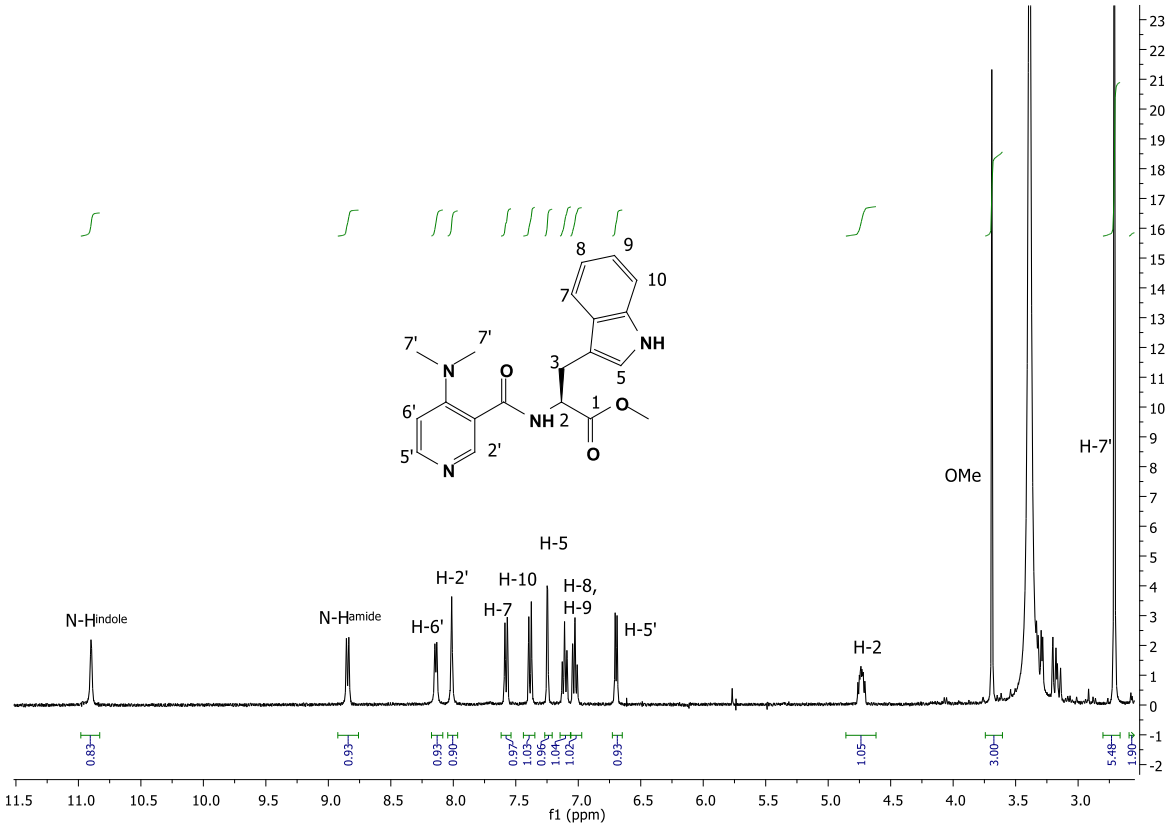

Figure 3.12. A portion of the ^{1}H NMR ($CDCl_3$) spectrum of **125**.

This result validated the methodology of coupling, and this was used in the synthesis of subsequent catalysts. Unfortunately, tryptophan catalyst **125** was only soluble in DMSO and could therefore not be reacted in solvents such as DCM, which was the solvent of choice for acyl-transfer reactions. The next challenge was thus to determine how to improve the solubility of the molecule.

One way perceived to increase the solubility was to replace the dimethylamino group with a pyrrolidino group containing two extra methylene groups. The use of a 4-PPY catalyst, instead of a 4-DMAP catalyst, also has the advantage of increased catalytic activity (Chapter 1) due to inductive effects. Scheme 3.7 shows synthesis of the next target template **126** in which dimethylamine was substituted by pyrrolidine using the same isolation methodology as with **124** involving the carboxylate salt.

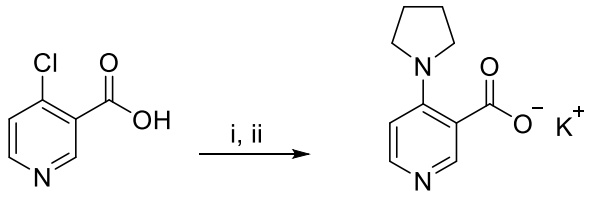

126

Scheme 3.7. *Reagents and conditions:* (i) pyrrolidine, toluene, reflux, 2 hrs, (ii) K_2CO_3, 30 min (95%).

The ^{1}H NMR spectrum of compound **126** showed characteristic peaks for the eight pyrrolidine protons: four at δ_H 1.68 ppm, and four at δ_H 3.09 ppm (deshielded by the pyrrolidine nitrogen). The three aromatic protons resonated at δ_H 6.37 ppm (doublet), δ_H 7.73 ppm (doublet), and δ_H 7.81 ppm (singlet). Coupling the amino acid to **126** (following the acid chloride methodology) was successful, but the yield was low (varying between 20% and 30%), so we decided to use the standard peptide coupling reagent EDC together with catalytic (30%) HOBt (Scheme 3.8). The advantage of this methodology was that the reaction could be done directly in a pyridine/water mix which easily solubilised the carboxylate salt. In such a way tryptophan catalyst **127** was obtained in 44% yield after a conventional work-up and column chromatography.

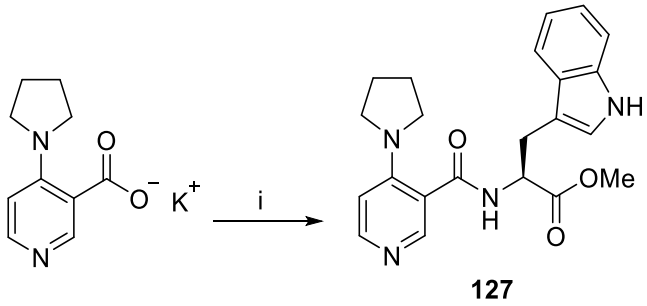

127

Scheme 3.8. *Reagents and conditions*: (i) **101**, EDC, HOBt, pyridine/water, r.t., 2hrs (44%).

Once again, the ^{1}H NMR spectrum of **127** showed that coupling of the two fragments had occurred in which a new amide proton was present, resonating at δ_H 6.32 ppm, as well as the characteristic peak for the α-proton at δ_H 5.12 ppm and the pyridine protons at δ_H 6.42 ppm, δ_H 8.15 ppm, and δ_H 8.16 ppm. The ^{13}C NMR for this compound showed that there were two singlets downfield at δ_C 171.4 ppm and δ_C 172.4 ppm for the ester and the amide carbonyl carbons along with all of the other carbon singlets expected. The IR spectrum showed a peak at 3289 cm^{-1} for the new secondary amide NH, while a C=O stretch typical of a secondary

amide was observed at 1617 cm^{-1}.The structure was further confirmed by mass spectrometry data, which gave a value of HRMS (ES): m/z found 393.1928 $[M + H]^+$, $C_{22}H_{25}N_4O_3$ requires *m/z* 393.1926 $[M + H]^+$.

The tryptophan-PPY catalyst **127**, with its two extra methylene groups, was less polar than the tryptophan-DMAP catalyst **125**, but it was still only partially soluble in DCM. Therefore it was decided to extend the chiral group by synthesizing a dipeptide also containing a non-polar side chain in addition to a π–stacking moiety. L-leucine was chosen, since the bulky *iso*-butyl side chain was thought might impose restrictions to conformational freedom of the chain, even to the extent of promoting a helical twist so as to achieve facial selection for π–stacking. As outlined in Chapter 2, the leucine-tryptophan dipeptide **104** (Fig. 3.13) was synthesised from commercially available Fmoc-Leu-OH and HCl-Trp-OMe using peptide coupling conditions, followed by deprotection with piperidine to form the amine dipeptide **104** in 64% yield.

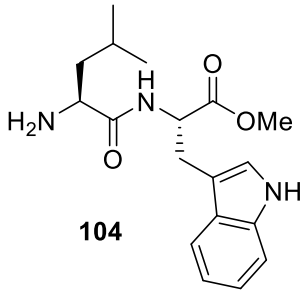

Figure 3.13. The structure of dipeptide **104**.

Subsequent coupling of peptide **104** to the PPY **126** salt using EDC and HOBt in pyridine and water as before successfully gave the desired product **128** in a 44% yield (Scheme 3.9).

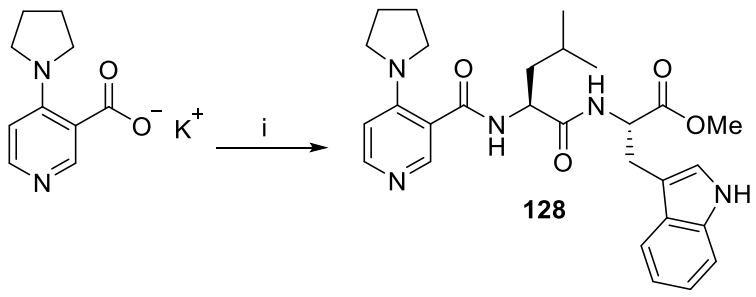

Scheme 3.9. *Reagents and conditions:* **104**, EDC, HOBt, pyridine, H_2O, 12 hrs (44%)

The ^{1}H NMR spectrum of compound **128** revealed resonances for both starting materials indicating that successful coupling had taken place. This was confirmed by the presence of the two α-protons at δ_H 4.57 ppm and δ_H 4.91 ppm of leucine and tryptophan respectively, while the pyridine protons resonated at δ_H 6.43 ppm, δ_H 8.12 ppm and δ_H 8.14 ppm (Fig. 3.14).

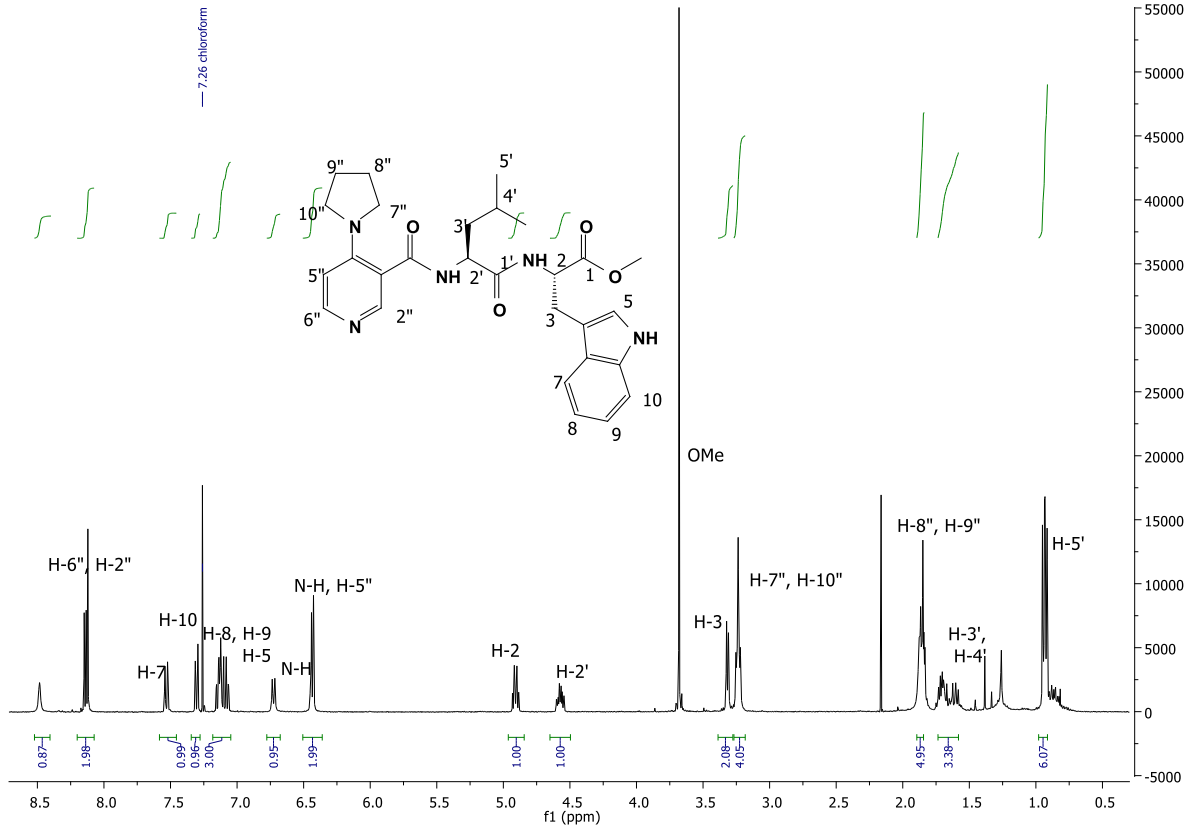

Figure 3.14. ^{1}H NMR ($CDCl_3$) spectrum of **128**.

The carbon atoms were assigned using ^{13}C NMR, HSQC, and APT. Figure 3.12 shows an APT spectrum for compound **128**. Three downfield singlets were present at δ_C 171.9 ppm, δ_C 171.4 ppm, and δ_C 169.0 ppm corresponding to the two amides and the one ester group. The CH carbons of the pyridine resonated at δ_C 150.1 ppm, δ_C 149.2 ppm, and δ_C 108.6 ppm, while the chiral carbons resonated at δ_C 52.9 ppm and δ_C 52.4 ppm (which overlapped with the carbon of the methoxy group), (Fig.3.15). The enantiomeric purity of the compound was evaluated using chiral HPLC which showed one peak present, indicating that epimerization had not occurred (Fig. 3.16).

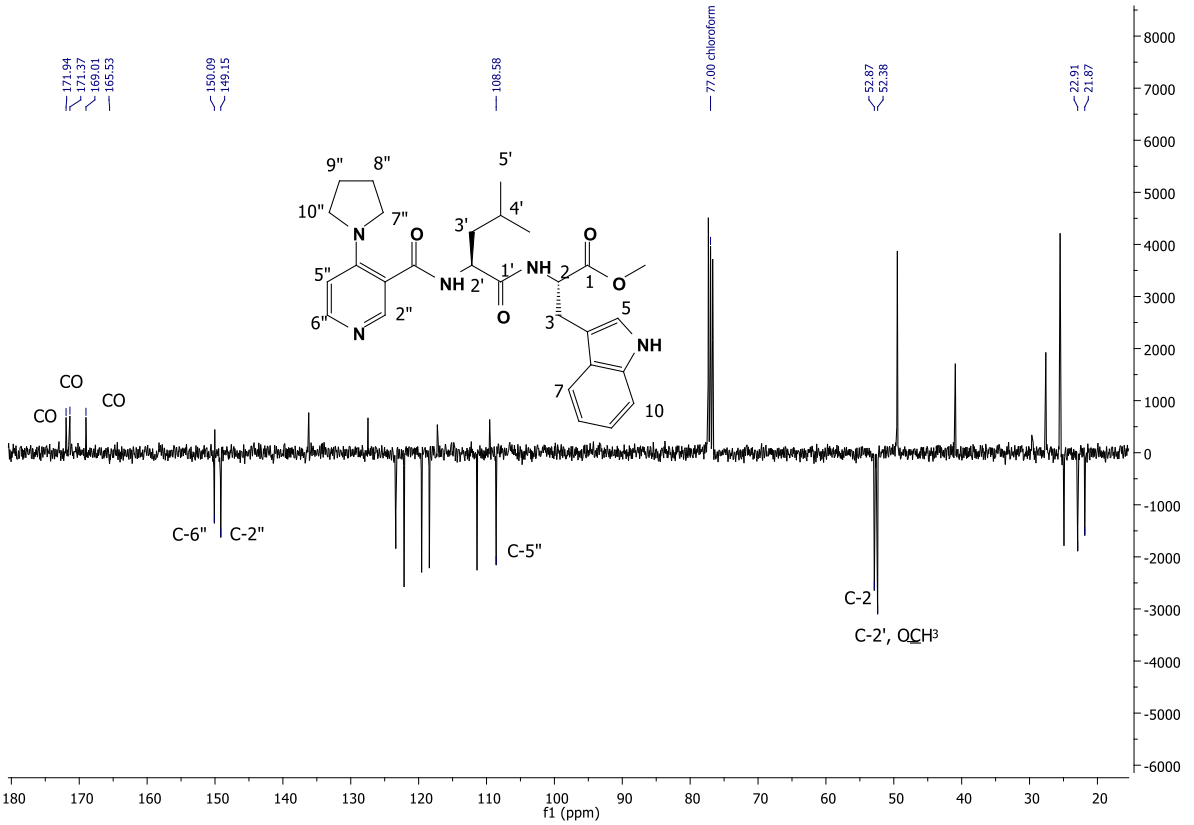

Figure 3.15. APT ($CDCl_3$) spectrum of **128**.

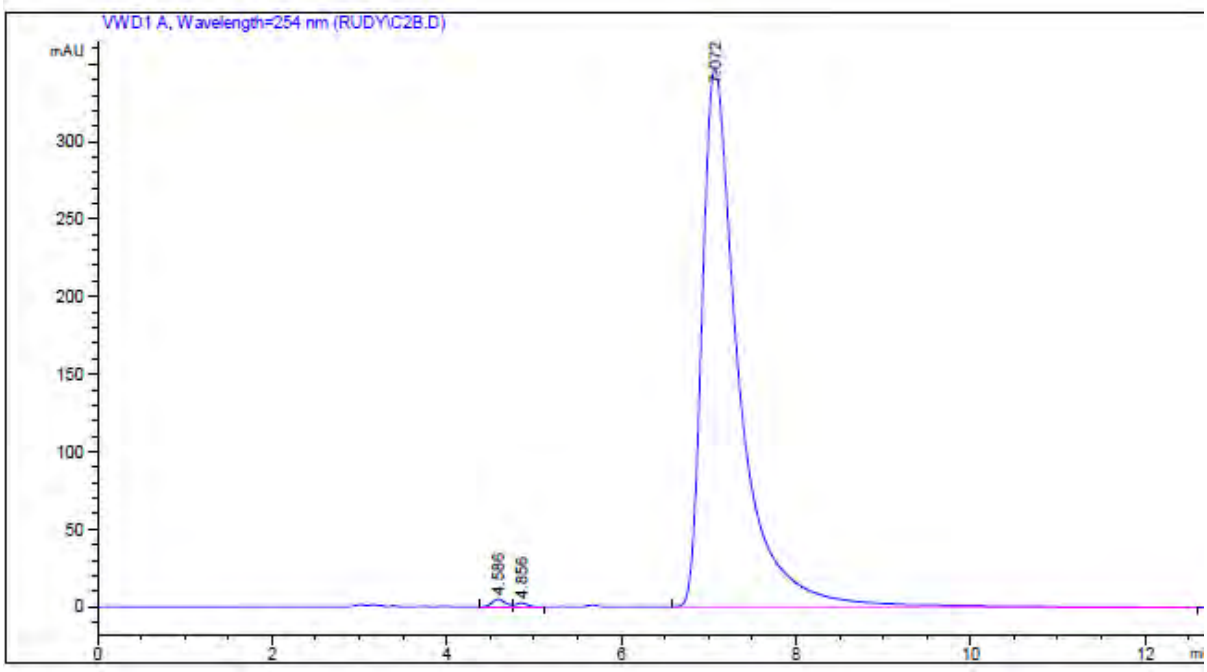

Figure 3.16. HPLC chromatogram of dipeptide catalyst **128**.

Kinetic resolution of 1-(2-naphthyl)ethanol

The two catalysts – **127** containing only tryptophan, and **128** containing both leucine and tryptophan – were then tested in the kinetic resolution of a secondary alcohol following the same procedure as before as shown in Table 3.3. TLC showed approximately 50% conversion of starting material to product after three hours without the need to warm the solution, boding well for catalysis having taken place

Table 3.3. The kinetic resolution of 1-(2-naphthyl)ethanol.

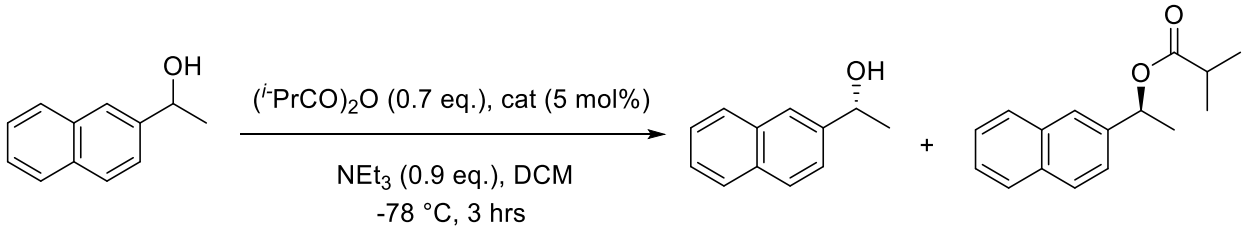

entry[a]	Catalyst	C[b]	ee (alcohol)	ee (ester)[c]	s-value[d]	configuration[d]
1.	**DMAP**	43	1.2	1.0	1.0	–
2.		no reaction	–	–	–	–
3.	**127**	42	21.9	30.3	2.3	S
4.	**128**	34	31.2	59.4	5.3	S

*a. All reactions were conducted in the presence of 5 mol% **catalyst**, 0.7 eq. of (^{i}PrCO)$_2$O, and 0.9 eq. of Et$_3$N at −78 °C for 3 hrs., unless otherwise noted. b. Conversion (%) = (ee of recovered alcohol)/(ee of recovered alcohol + ee of ester). c. hydrolysed (2M NaOH in MeOH/H$_2$O) and ee calculated. d. Selectivity factor* $s = \frac{ln(1-C)(1-ee)}{ln(1-C)(1+ee)}$. *e. The absolute configuration of the faster reacting enantiomer was determined by comparison of* $[\alpha]_D^{20}$ *values with those reported in the literature.*

Entry 1 shows the control reaction with DMAP used a catalyst. Although several studies have shown that the kinetics of the acylation DMAP catalysts is zero-order with respect to an auxiliary base such as triethylamine, a blank reaction was also performed (Table 3.3, entry 2), which showed no product on TLC under the reaction condition. The results for catalyst **127**

gave disappointing enantiomeric excesses and a low s-value of 2.3, while the dipeptide catalyst **128** gave an improved ee and thus a slightly higher s-value of 5.3. The fast reacting enantiomer for both catalyst **127** and **128** was the *S*-enantiomer as determined by comparing the sign of optical rotation to literature values. To test the generality of **128** as a catalyst for kinetic resolution, a range of secondary alcohols were used as substrates (Table 3.4).

Table 3.4. The kinetic resolution of various *sec*-alcohols catalysed by **128**.

entry[a]	substrate	C_{HPLC}[b]	ee (alcohol)	ee (ester)[c]	s-value[d]	configuration[e]
1.	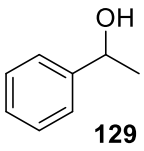 **129**	49	38.6	40.1	3.3	S
2.	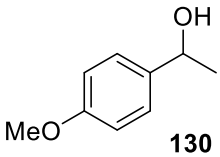 **130**	42	21.9	30.3	2.3	S
3.	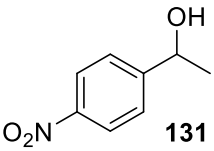 **131**	63	12.4	7.1	1.3	S
4.	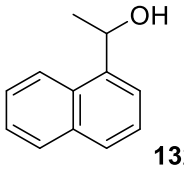 **132**	60	48.4	32.2	3.0	S
5.	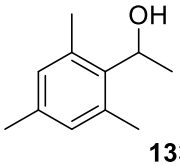 **133**	27	17.3	46.3	3.2	S

*a. All reactions were conducted in the presence of 5 mol% **128**, 0.7 eq. of (^{i}PrCO)$_2$O, and 0.9 eq. of Et_3N at −78 °C for 3 hrs., unless otherwise noted. b. Conversion (%) = (ee of recovered alcohol)/(ee of recovered alcohol + ee of ester. c. hydrolysed (2M NaOH in MeOH/H_2O) and ee calculated. d. Selectivity factor* $s = \frac{ln(1-C)(1-ee)}{ln(1-C)(1+ee)}$*. e. The absolute configuration of the faster reacting enantiomer was determined by comparison of* $[\alpha]_D^{20}$ *values with those reported in the literature.*

The results of this study gave generally low s-values, varying between 1.3–3.3, but the s-value of 5.3 (obtained from catalyst **128**) was encouraging, and we believed that it would be possible to improve the enantiomeric excess by making appropriate modifications to the catalyst. In order to help with insight into this, once again molecular modelling was carried out in order to determine the structure(s) of the low-energy conformer(s) and the possibility of π–stacking. In addition, the possibility of corroborating any π–stacking via observing chemical shift changes in the ^{1}H NMR spectrum of the pyridinium ion was also considered.

Computational Modelling

A conformer distribution was calculated using MMFF94 force field. 100000 conformations were analysed for the acyl-pyridinium cation (**128a** in Fig. 3.17) of **128** in the gas phase, which showed that the lowest energy conformer was dominant at 81%.

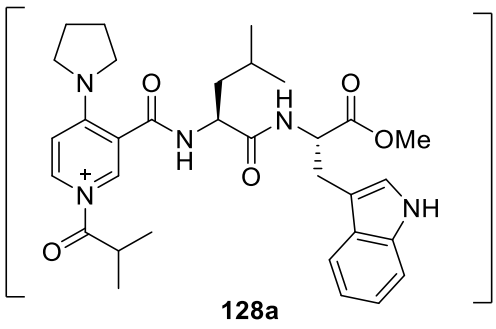

128a

Figure 3.17. Acyl-pyridinium cation of catalyst **128**.

The ten lowest energy conformers were then optimised at the M06/6-31G* level of theory. This resulted in minimum-enery conformers **A** and **B**, which were identified in a 93.8:6.2 ratio (Fig. 3.18) with a 6.75 kJ/mol energy difference.

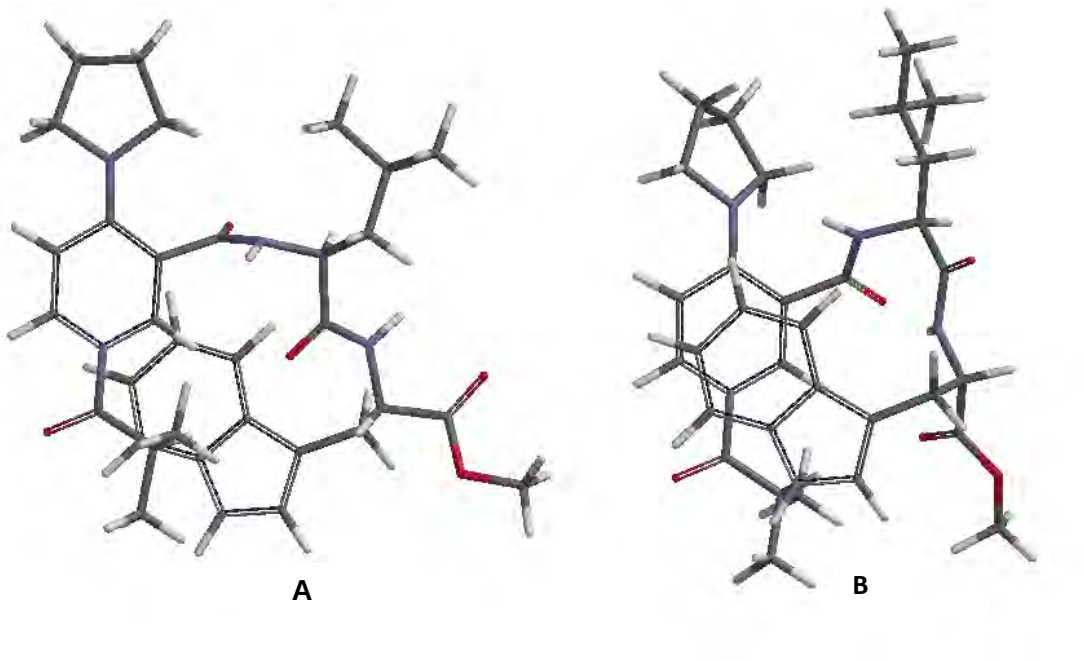

Figure 3.18. Lowest energy conformers of **128a**, showing the tryptophan moiety on the underneath face.

In both conformers (**A** and **B**) the peptide chain curves such that the indole ring is close to the acyl site and effectively blocks the *si* (underneath; O>N>C) face of the *N*-acyl carbonyl group which is in an s-*trans* conformation (C=O / C-2$_{pyridine}$ are *trans*) regarding the C(CO) to pyridine (N) bond, allowing the nucleophile to attack from the opposite exposed (top) face (*re* face) of the acyl carbonyl group. The s-*trans*$_{N(CO)}$ preference for the *N*-acyl group (i.e. one rotomer) is important in the context of facial discrimination as will be discussed later. While it may seem counterintuitive that the bulky *iso*-propyl group is on the same side as the peptide substituent at C-3, this is in agreement with reports by Spivey[67] and Connon.[55] Spivey has suggested that while the preferred orientation of the *N*-acyl group is not sterically driven, the orientation of the *iso*-propyl group may be due to a stereoelectronic stabilisation due to partial conjugation with the C-3 substituent.[67] At this stage it looked as though the π–stacking hoped for was responsible for the observed improvement in kinetic resolution selectivity.

^{1}H NMR Study

A ^{1}H NMR study was performed to investigate conformational changes (π–stacking) in the catalyst upon acylation. This required a reference compound that lacked the tryptophan moiety. A leucine residue was chosen since the *iso*-butyl group could not π–stack to the pyridine ring. Scheme 3.10 shows the synthesis.

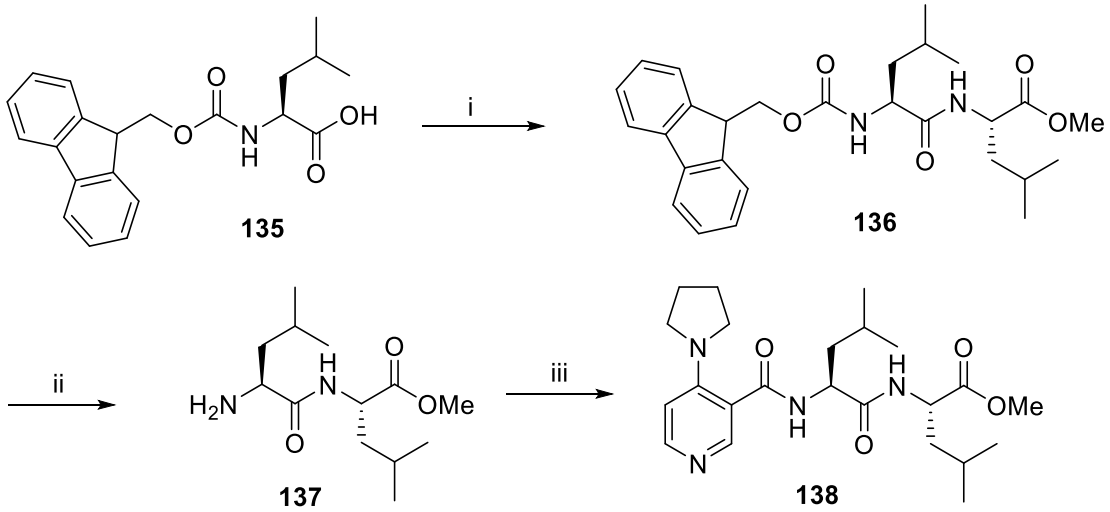

Scheme 3.10. *Reagents and conditions*: HCl-Leu-OMe, EDC, HOBt, pyridine, H_2O, 12 hrs (80%), (ii) anisole, piperidine, DCM, 0 °C, 18 hrs, (67%), (iii) **126**, EDC, HOBt, pyridine, H_2O, 12 hrs (27%).

Thus commercially available (*S*)-Fmoc-leucine was reacted with HCl-leu-OMe under peptide coupling conditions, and after 18 hours, TLC revealed that the reaction was complete. Following an acidic work-up to remove the pyridine, the *N*-protected dipeptide **136** was isolated in an 80% yield. The compound was characterised using a combination of 1D and 2D ^{1}H NMR (shown in Fig. 3.19), as well as ^{13}C NMR.

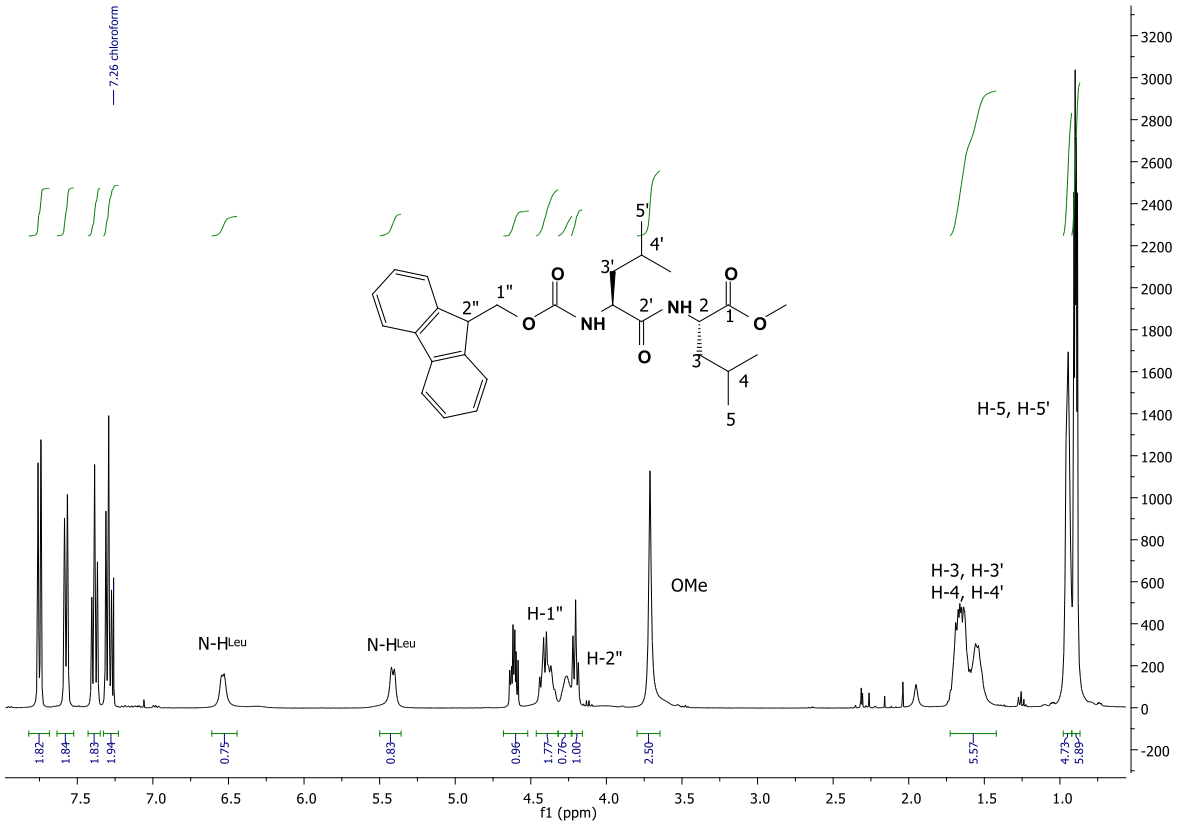

Figure 3.19. Partial ^{1}H NMR spectrum ($CDCl_3$) of dipeptide **136**.

In the aromatic region, the Fmoc protons resonated between δ_H 7.75 ppm and 7.29 ppm. The two α-protons of the leucine residues resonated at δ_H 4.61 ppm and 4.26 ppm, while the acidic proton of the Fmoc group resonated at δ_H 4.20 ppm. Downfield at δ_H 0.90 ppm and 0.89 ppm two doublets indicated the presence of the four methyl groups as two diastereotopic sets for the two *iso*-butyl residues. The ^{13}C NMR spectrum revealed three carbonyl peaks at δ_C 173.1 ppm, δ_C 172.0 ppm, and δ_C 156.2 ppm, while the two chiral carbons resonated at δ_C 53.4 ppm and δ_C 50.7 ppm. Finally, an elemental combustion analysis of the compound corresponded well with the calculated values for C, H and N. The next step was to remove the Fmoc group under basic conditions (using piperidine at r.t.), which following flash chromatography afforded the amine **137** in 54% yield. Its ^{1}H and ^{13}C NMR spectra closely matched that of the starting material, but lacked the signals in the aromatic regions indicating that the Fmoc had indeed been removed.

Coupling of the free amine **137** with the PPY template **126** via the EDC/HOBt coupling conditions from before successfully furnished **138** after 18 hours as a polar spot on TLC, which was isolated in 27% yield following column chromatography. The ^{1}H NMR spectrum of **138** displayed aromatic protons for the pyridine ring resonating at δ_H 8.26 ppm, δ_H 8.13

ppm, and δ_H 6.47 ppm (Fig. 3.20). The two α-protons overlapped at δ_H 4.61 ppm, while the pyrrolidine ring protons resonated as two multiplets at δ_H 3.30 ppm and δ_H 1.94 ppm. Its ^{13}C NMR spectrum revealed peaks for the carbonyl carbons at δ_C 173.1 ppm, δ_C 171.6 ppm, and δ_C 168.8 ppm, while the three pyridine carbons resonated at δ_C 149.3 ppm, δ_C 148.7 ppm, and δ_C 108.6 ppm. In the IR spectrum, the new amide NH stretch appeared at 3420 cm^{-1}. Finally, a correct HRMS evaluation (m/z HRMS (ES) 433.2810 $[M + H]^+$, $C_{23}H_{37}N_4O_4$ requires m/z 433.28148 $[M + H]^+$) confirmed the structure of **138**.

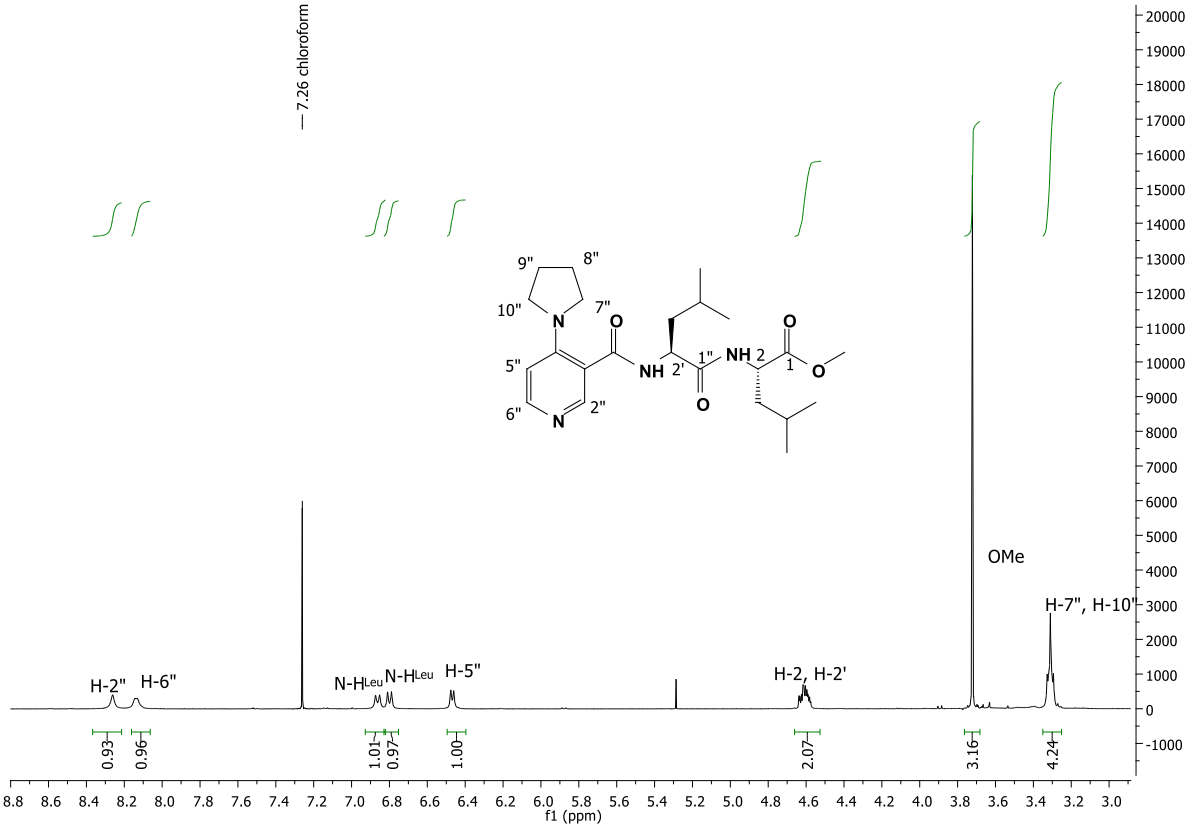

Figure 3.20. A partial ^1H NMR spectrum ($CDCl_3$) of dipeptide **138**.

With the reference compound in hand, the next step was to alkylate both **128** and **138** by reacting with methyl iodide. This was achieved by dissolving the compounds in DCM, followed by the addition of methyl iodide at room temperature. The reactions were monitored by TLC which showed a more polar spot in the case of **128** (= **128a**) and a spot with an identical R_f to the starting material for **138** (= **138a**) after sixteen hours at room temperature. Intermediate **128a** precipitated and was filtered, dried and dissolved in $CDCl_3$, while catalyst **138a** was soluble in DCM and was isolated as a solid following solvent removal. The structures of the alkylated catalysts were confirmed by 1D and 2D NMR, which indicated that the new methyl groups were present for both **128a** and **138a**.

Table 3.5 shows the chemical shifts of the three pyridine ring protons in the ^{1}H NMR spectra of **128, 138** and their corresponding methylated derivatives **128a** and **138a**. The chemical shift difference between each proton of the pyridine ring (H-2, H-5, and H-6) for the unmethylated and methylated compounds are given by Δδ and Δδa respectively for each series (**128** to **138** and **128a** to **138a**)

Table 3.5. Selected ^{1}H NMR chemical shifts (ppm) for **128**, **138,** and their methylated analogues.

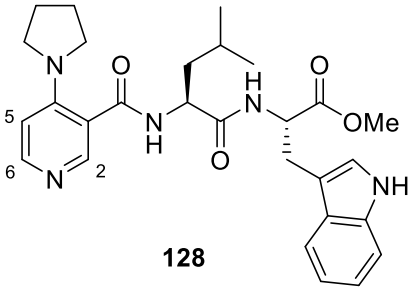

128

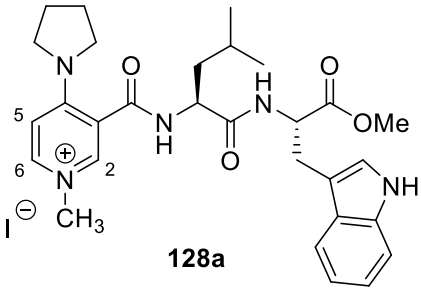

128a

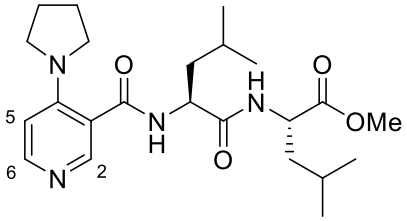

138

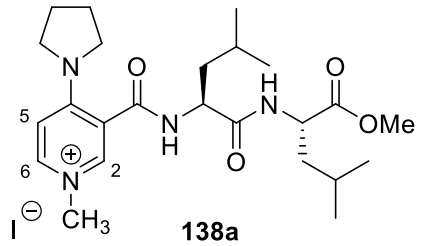

138a

Proton	δ**128**	δ**138**	Δδ [c]	δ**128a**	δ**138a**	Δδa[c]
H-2 [a,b]	8.08	8.26	–0.18	8.30	8.87	–0.57
H-5 [a,b]	6.35	6.47	–0.12	6.50	6.66	–0.16
H-6 [a,b]	8.05	8.13	–0.08	8.77	9.01	–0.24

a. Measured using $CDCl_3$ as solvent. *b.* All pyridine protons where unambiguously assigned by NMR spectroscopy (^{1}H, ^{13}C, HSQC, and COSY). *c.* The Δδ values were calculated using the equations, Δδ = δ128 − δ138, and Δδa = δ128a − δ138a.

For reference catalyst **138**, all the protons of the pyridine ring were upfield form the corresponding ones of catalyst **128**, which may indicate an interaction of the pyridine ring with the indole ring even in the unmethylated state. There was also a significant difference between H-2 in the unmethylated series (0.18) compared to H-5 and H-6 (0.12 and 0.08 respectively), further indicating structural differences in the unmethylated compounds. Upon methylation, further deshielding of all three protons in each compound **128a** and **138a** was observed in accordance with the positive charge on the pyridine ring. However, the relative

degree of deshielding, proton for proton in the two methylated compounds was much more pronounced with H-2 and H-6. Here, going from unmethylated to methylated caused a three-fold increase in chemical shift difference for H-2 and H-6 (0.57/0.18; 0.24/0.08 respectively) compared to only a 1.3 increase for H-5 (0.12/0.16). These results suggest a strong extra deshielding for H-2 and H-6 which suggests a π–stacking by the indole via its deshielding zone. This would involve interaction with the sides rather than the face (shielding zone) as suggested by conformation **A** in Fig. 3.18. These results are similar to Yamada's previously reported cation–π complex (Chapter 1), and suggest that **128a** has a fixed conformation in which there is interaction of the indole ring with the pyridinium face. This interaction is absent or less pronounced than in **128**.

3.2.2 Tripeptides and Derivatives of the Dipeptide Catalyst

The results of the kinetic resolution using dipeptide catalyst **128** were promising enough to justify further investigation on the influence of structural changes in **128** on activity. The two sites on **128** that were chosen for potential development were the C-terminus of the peptide, and the nitrogen of the indole moiety (Fig. 3.21).

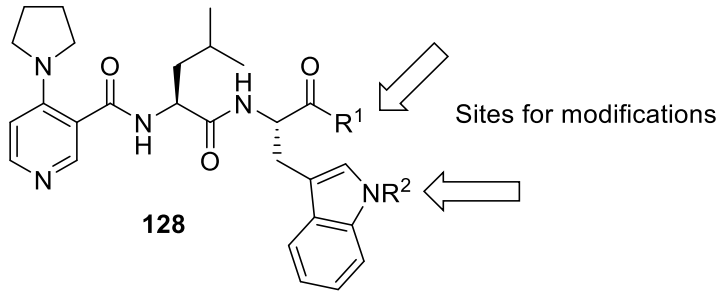

Figure 3.21. Possible sites for modification for catalyst **128**.

Extending the peptide at the C-terminus to form a tripeptide raised the question of which amino acid to use and it was decided to compare the effect of incorporating tryptophan (target **139**) as a potential π–stacking group against leucine as a provider of a steric influence only (catalyst **140**). For extension at the indole nitrogen a Boc substitution was chosen (target **141)** in view of its anticipated ease of synthesis, as well as its potential to provide both steric and H-bonding effects (Fig. 3.22). The synthesis and evaluation of tripeptides **139** and **140** will be described first.

Tripeptides

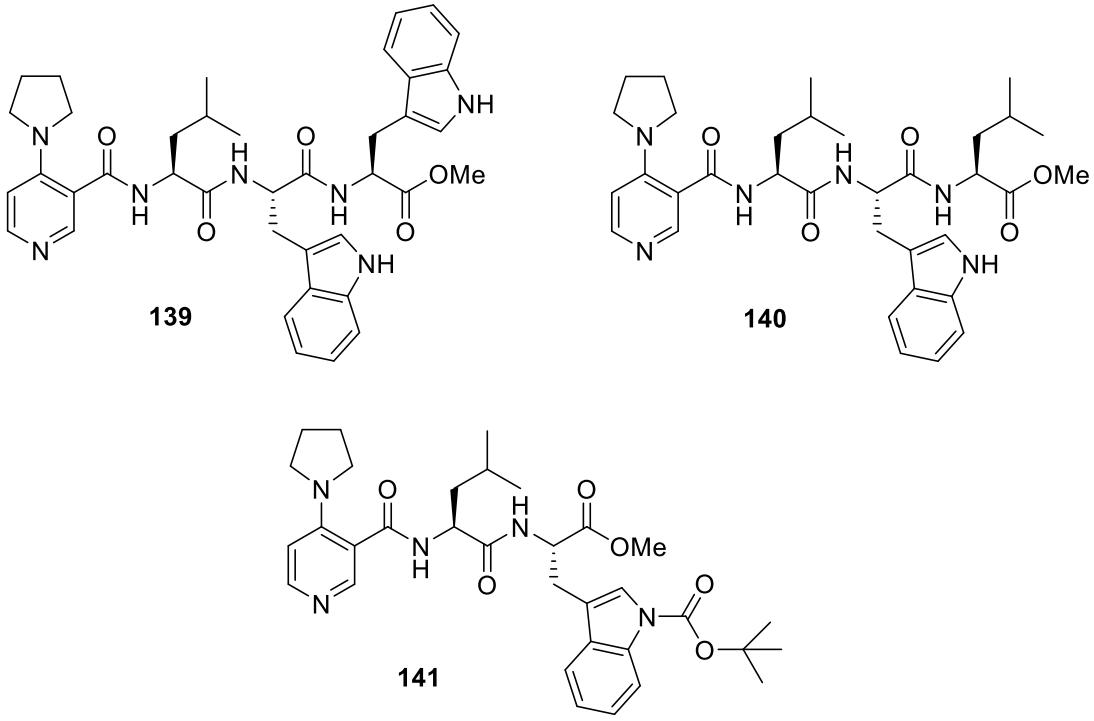

Figure 3.22

Tripeptide **139** was synthesised first (Scheme 3.11) by initially reacting commercially available Boc-Trp-OH with HCl-Trp-OMe **101** using standard peptide coupling conditions used in this project to form dipeptide **142** (Scheme 3.11). Its ^{1}H NMR spectrum showed a doubling of peaks in the aromatic region between δ_H 7.88 ppm and δ_H 6.65 ppm, indicating that two indole rings were present. The two α-protons of the dipeptide resonated at δ_H 4.43 ppm and δ_H 4.82 ppm, while the *tert*-butyl group appeared as a singlet at δ_H 1.40 ppm. The enantiomeric purity of **142** was determined by measuring the optical rotation, which gave a value of − 20.5° (lit.[152] − 15°).

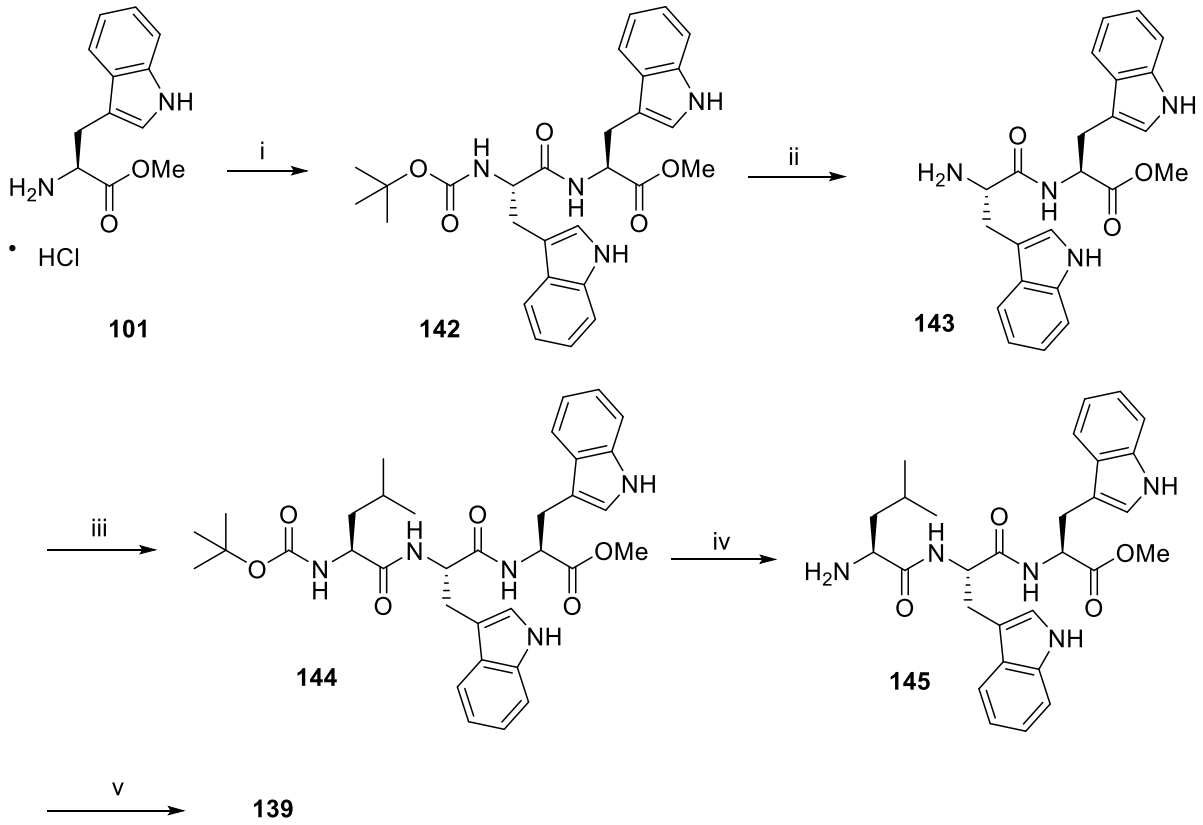

Scheme 3.11. *Reagents and conditions:* (i) Boc-Trp-OH, EDC, HOBt, pyridine, r.t., 18 hrs (81%); (ii) TFA/DCM (20%), anisole, 0 °C, 2 hrs (99%); (iii) Boc-Leu-OH, EDC, HOBt, pyridine, r.t., 18 hrs (61%); (iv) TFA/DCM (20%), anisole, 0 °C, 2 hrs (99%); (v) **107**, EDC, HOBt, pyridine, r.t., 18 hrs (53%).

The next step was to remove the Boc-protecting group under acidic conditions with TFA at 0 °C, followed by a basic work-up using saturated $NaHCO_3$, and then column chromatography with MeOH/DCM. In such a way, free amine **143** was isolated in an excellent yield of 99%. Its ^{1}H NMR spectrum lacked the *tert*-butyl signal of the Boc group, and the α-proton adjacent to the free amine shifted upfield to δ_H 3.64 ppm, indicating removal of the Boc group. The enantiomeric purity was determined by measuring the optical rotation, which gave a value of −15.2° (lit.[153] −11°). Dipeptide **143** was then extended to a tripeptide by coupling to Boc-Leu-OH using EDC/HOBt to form tripeptide **144** in 61% yield. Its ^{1}H NMR spectrum showed the two diastereotopic methyl groups of the *iso*-butyl moiety of leucine as two doublets resonating at δ_H 0.94 ppm and δ_H 0.85 ppm, and the *tert*-butyl group as a singlet resonating at δ_H 1.43 ppm, while the NH of the carbamate resonated at δ_H 4.65 ppm. The three α-protons resonated at δ_H 4.05 ppm, δ_H 4.70 ppm, and δ_H 4.77 ppm for one leucine and two tryptophans respectively (Fig. 3.23).

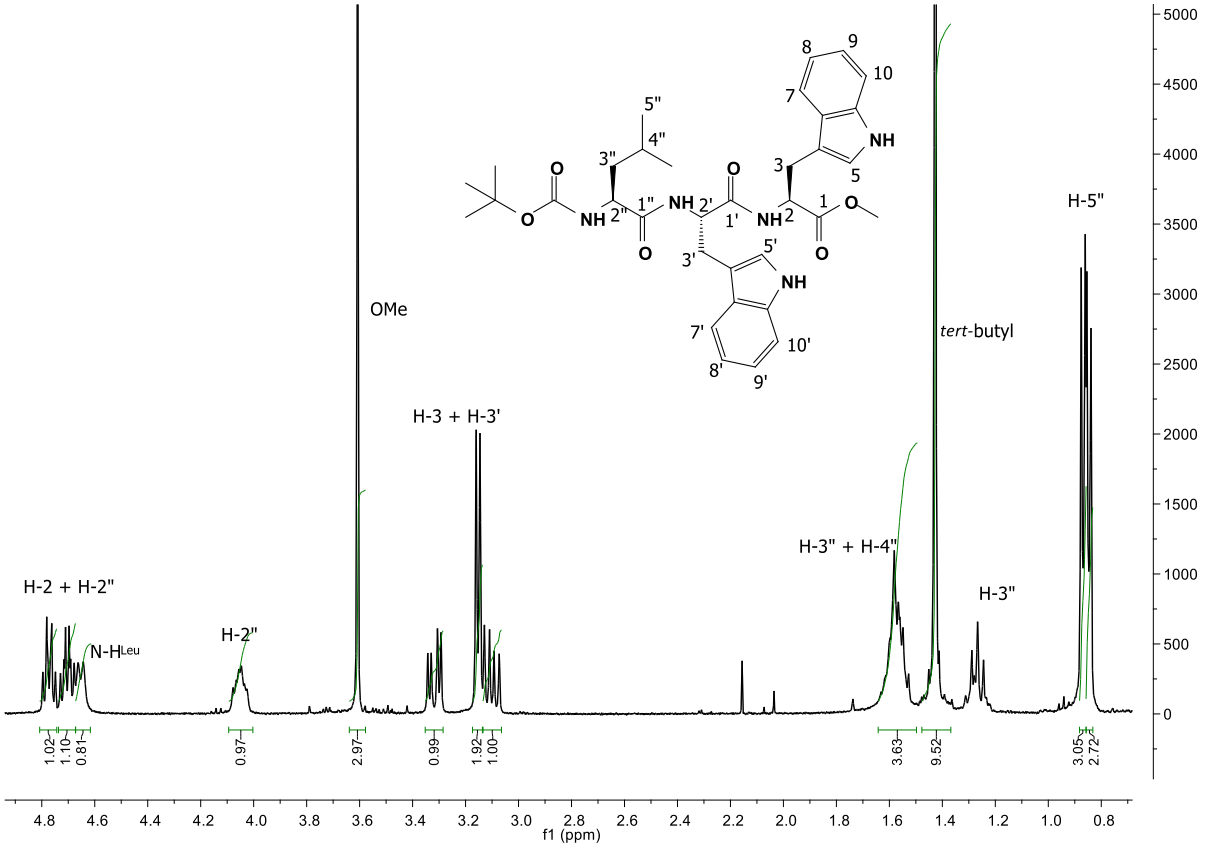

Figure 3.23. A portion of ^{1}H NMR ($CDCl_3$) spectrum of **144**.

The ^{13}C NMR spectrum revealed four carbonyl signals (one for the carbamate, two for the amides, and one for the ester) between δ_C 172.4 ppm and δ_C 155.6 ppm. The aromatic carbons of the two indole rings resonated between δ_C 136.4 ppm and δ_C 109.8 ppm, while the three chiral carbons resonated at δ_C 53.8 ppm, δ_C 52.8 ppm, and δ_C 52.1 ppm.The rest of the ^{13}C NMR spectrum of **144** was assigned using 2D NMR and APT spectroscopy. Elemental combustion analysis confirmed the correct molecular formula of $C_{34}H_{43}N_5O_6$ for compound **144**. Deprotection of the Boc group of **144** again using TFA was carried out to give the target molecule **145** in 99% yield, after isolation by column chromatography using 10% MeOH/DCM. The structure of **145** was assigned on the basis of its spectroscopic data using a combination of 1D, 2D, and APT, as well as IR spectropcopy. The ^{1}H NMR spectrum of **145** lacked the signals for the Boc group, and revealed an upfield shift (due to a lack of deshielding by the carbamate compared to the free amine) for the α-proton of leucine from δ_H 4.05 ppm in **144** to between δ_H 3.32–3.06 ppm (a multiplet, together with the four methylene protons of the tryptophan moieties). The appearance of a broad singlet at δ_H 1.62 ppm for the two amine protons also supported the absence of the carbamate. The APT and ^{13}C NMR spectrum was consistent with **144**, but lacked the signals for the Boc-protecting group.

The final step was to couple the free amine **145** to the PPY-salt **126** using EDC/HOBt, which gave catalyst **139** in a 53% yield, following a work-up and column chromatography using 8% MeOH/DCM. Its ^{1}H NMR spectrum confirmed that the coupling had occurred, since resonances for both starting materials were present. The pyridine protons resonated at δ_H 8.03 ppm, δ_H 7.98 ppm, and δ_H 6.37 ppm, and the pyrrolidine protons at δ_H 3.19 ppm and δ_H 1.81 ppm. A new amide peak was present at δ_H 6.80 ppm, and the leucine α-proton shifted downfield to δ_H 4.55 ppm. The structure of the molecule was confirmed using a combination of 2D, APT, and IR spectroscopy. The ^{13}C NMR spectrum of **139** revealed the presence of four carbonyl singlets (including the newly formed amide carbonyl) between δ_C 171.9 ppm and δ_C 168.8 ppm. Three chiral carbons corresponding to three amino acids were present at δ_H 53.5 ppm, δ_H 52.9 ppm, and δ_H 52.8 ppm.

Similarly Scheme 3.12 shows the synthesis of the second tripeptide that was synthesised. In the first step, commercially available Boc-Trp-OH was coupled with HCl-Leu-OMe to form dipeptide **147** in a good yield of 85%. Its ^{1}H NMR spectrum showed a characteristic singlet peak for the *tert*-butyl group of tryptophan at δ_H 1.54 ppm, while the methoxy protons of the newly introduced leucine resonated at δ_H 3.64 ppm indicating that the coupling had occurred. The aromatic region revealed the protons of the indole ring; the α-protons resonated at δ_H 4.52 ppm and δ_H 4.42 ppm for tryptophan and leucine respectively.

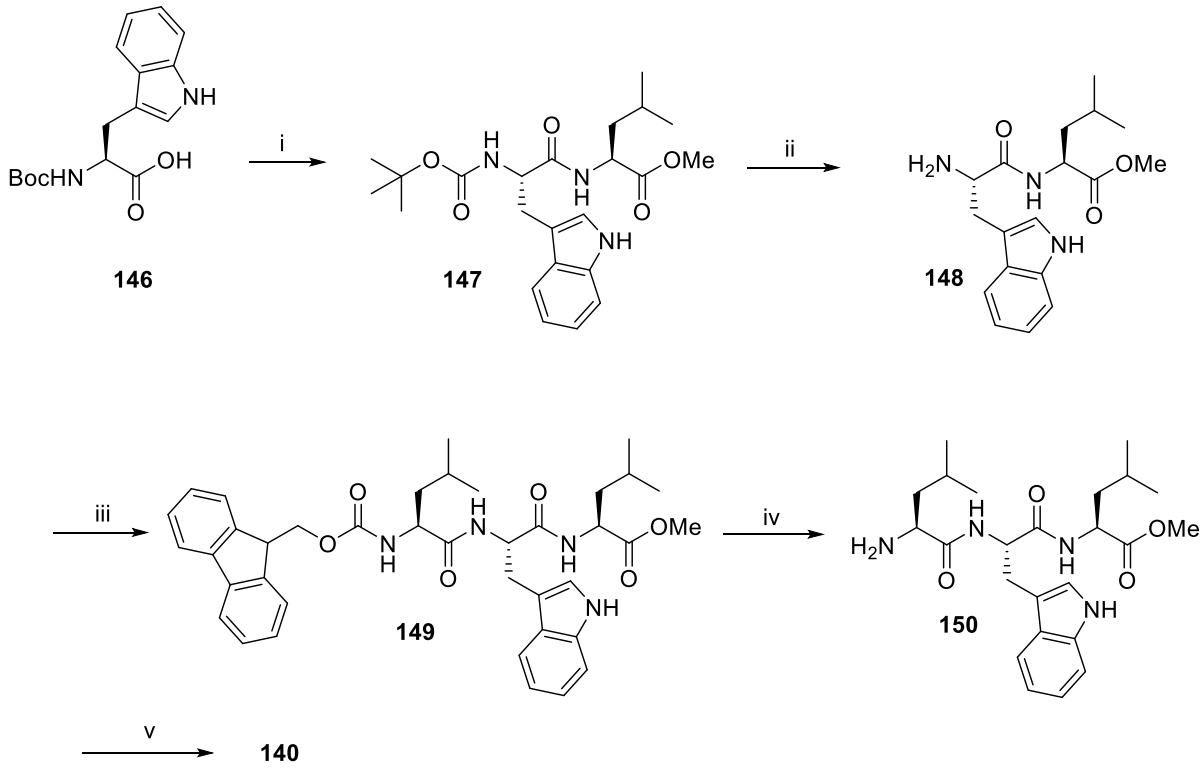

Scheme 3.12. *Reagents and conditions:* (i) HCl-Leu-OH, EDC, HOBt, pyridine, r.t., 18 hrs (85%); (ii) TFA/DCM (20%), anisole, 0 °C, 2 hrs (58%); (iii) Fmoc-Leu-OH, EDC, HOBt, pyridine, r.t., 18 hrs (60%); (iv) piperidine, DCM, 0 °C, 6 hrs (61%); (v) **126**, EDC, HOBt, pyridine, r.t., 18 hrs (44%).

The next step was to remove the Boc-protecting group of **147** using acidic conditions to form amine **148** in a 58% yield. Its ^{1}H NMR spectrum revealed that the *tert*-butyl group was absent and the α-proton adjacent to the amine had shifted upfield to δ_H 3.71 ppm. The optical rotation of **148** measured in MeOH (−6.0°) (lit.[154] −1.2°). The free amine was then reacted with commercially available Fmoc-Leu-OH to form tripeptide **149** in 60% yield – we decided to switch to the Fmoc protectiong group, since the amino peptides would not be subjected to a strongly acidic medium in the deprotection step. Fmoc deprotection also did not require workup, and the solvent could be removed *in vacuo* and the crude product could be directly purified by column chromatography. Its ^{1}H NMR spectrum (Figure 3.24) confirmed that the coupling had occurred, as three NH protons were present; the carbamate resonating at δ_H 6.20 ppm, and the two amides resonating at δ_H 6.62 ppm and δ_H 4.98 ppm. In the aromatic region, the protons of the Fmoc-protecting group and the indole ring resonated between δ_H 7.78 ppm and δ_H 7.04 ppm.The two sets of multiplets as diastereotopic pairs for the four methyl groups

of the two *iso*-butyl moieties resonated at δ_H 0.82 ppm and δ_H 0.89 ppm, while the three α-protons of the tripeptide resonated at, δ_H 4.72 ppm, δ_H 4.48 ppm, and δ_H 4.13 ppm.

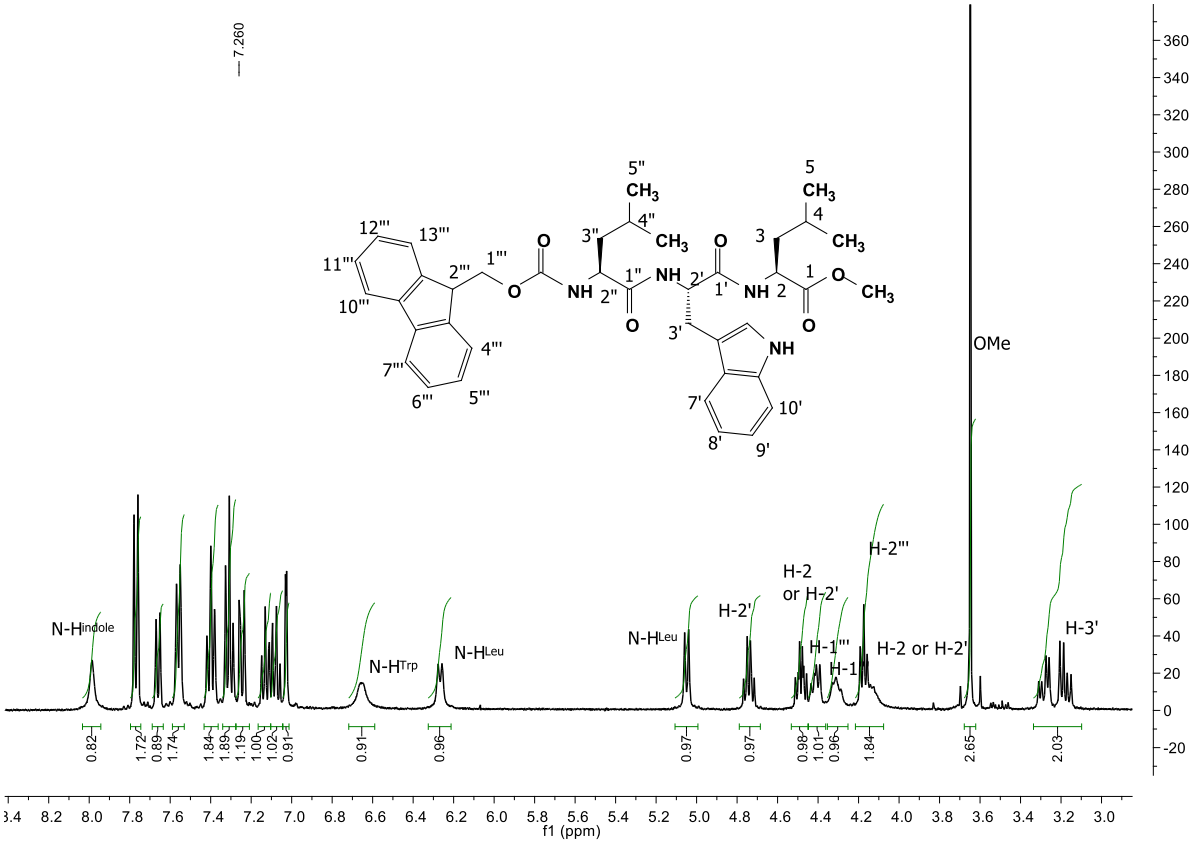

Figure 3.24. A portion of ^{1}H NMR ($CDCl_3$) spectrum of **149**.

The ^{13}C NMR spectrum was assigned using a combination of 2D and APT spectroscopy. Four carbonyls were present corresponding to the carbamate, the amides and the ester. The aromatic carbons and the quaternary carbons of the Fmoc-protecting group and the indole ring resonated between δ_C 143.9 ppm and δ_C 110.7 ppm. The three chiral carbons resonated at δ_C 53.9 ppm, δ_C 53.9 ppm, and δ_C 51.1 ppm, while the acidic proton of the Fmoc-protecting group appeared at δ_C 47.1 ppm. Chiral HPLC was performed on compound **149**, and gave one peak corresponding to one diastereomer of the compound.

The Fmoc group was then removed using piperidine. The reaction could be monitored by TLC, which showed the Fmoc-protected tripeptide **149** as a purple spot in 50% ethyl acetate/hexane with an R_f of 0.5. After 18 hours the starting material was gone and a new polar spot was present at R_f 0.5 in 10% MeOH/DCM. Following flash chromatography, compound **150** was obtained in 61% yield. Its ^{1}H NMR spectrum revealed that the aromatic region lacked the signals corresponding to the Fmoc group and the NH of the carbamate. The

resonances of the indole ring were still present. An upfield shift for the α-proton of leucine to δ_H 3.34 ppm also confirmed the removal of the the Fmoc group (and the presence of the free amine); the two amides resonated at δ_H 7.83 ppm and δ_H 6.39 ppm. The ^{13}C NMR spectrum was consistent with that of compound **149**, but lacked the carbonyl singlet for the carbamate group, as well as the peaks for the Fmoc group in the aromatic region. No doubling of the peaks was observed, which indicated that epimerization had likely not occurred; this was confirmed by chiral HPLC, which only showed one peak corresponding to a single diastereomer of **150** (in our experience diastereomers (epimers) were always well separated on the Chiralcel OD and Chiralpak AD columns). In the IR spectrum a broad peak at 3020 cm^{-1} indicated the presence of an amine group, further confirming the absence of the Fmoc group. For HRMS (ES), the parent ion was found to be 445.2815 (M^+ + H) correlating to the correct molecular formula of $C_{24}H_{37}N_4O_4$ (requires (M^+ + H) 445.2815), thus confirming the formation of **150**.

The free amine **150** was then coupled to the PPY-salt **126** in pyridine using the peptide coupling conditions from before to form the tripeptide-catalyst **140** in 44% yield after work-up and chromatography (Scheme 3.13). Its ^1H NMR spectrum confirmed that the coupling occurred based on signals for both partners, in which a new amide NH was observed resonating at δ_H 6.84 ppm. The protons of the pyridine ring resonated at δ_H 8.11 ppm, δ_H 8.05 ppm, and δ_H 7.09 ppm, the α-protons of the tryptophan residue resonated at δ_H 4.81 ppm, and the α-protons of the leucine residues resonated further upfield at δ_H 4.60 ppm and δ_H 4.47 ppm (Fig. 3.25).

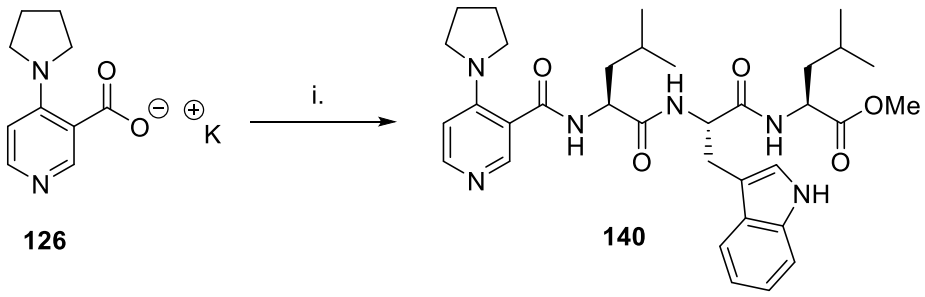

126 **140**

Scheme 3.13. *Reagents and conditions:* (i) **150**, EDC, HOBt, pyridine, DCM, r.t., 12 hrs (44%).

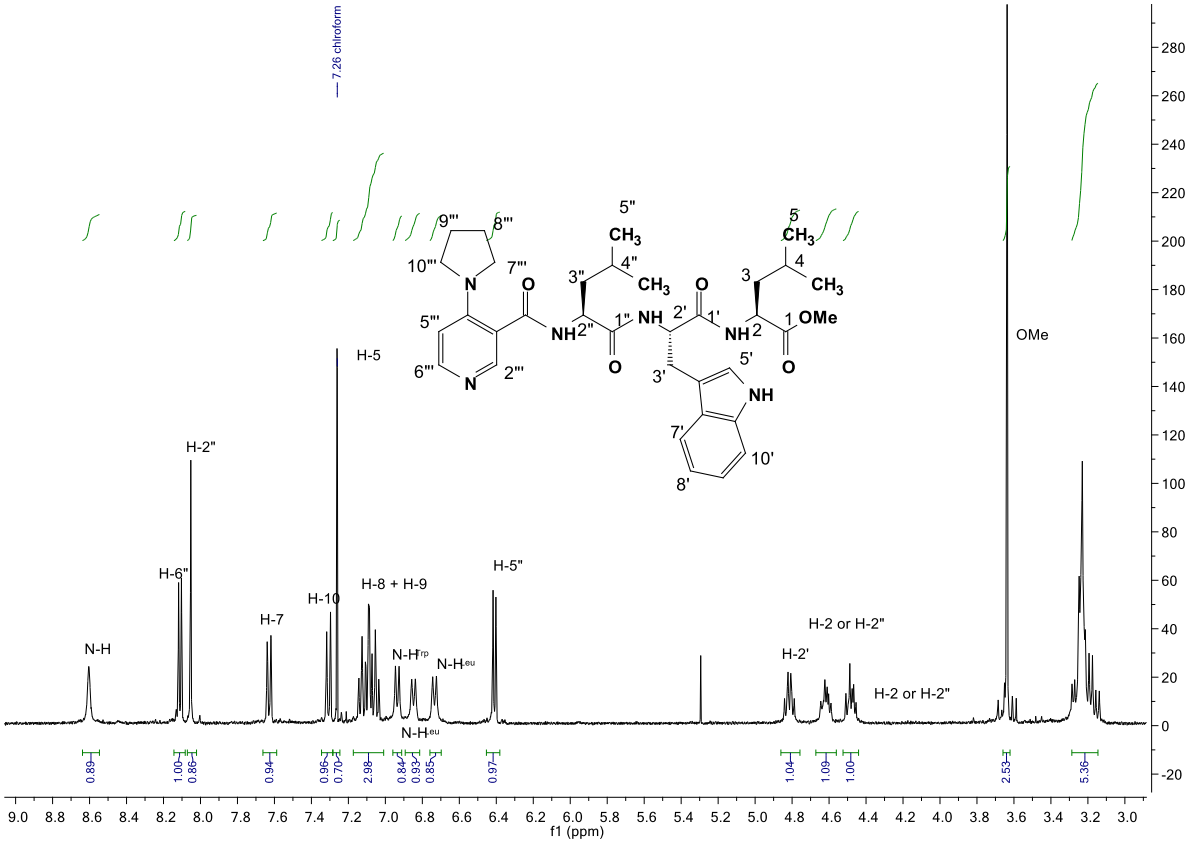

Figure 3.25. A portion of ^{1}H NMR ($CDCl_3$) spectrum of compound **140**.

The ^{13}C NMR spectrum was assigned using 2D NMR and APT spectroscopy. The amide and ester carbonyls resonated downfield between δ_C 172.9 ppm and δ_C 168.8 ppm. The carbons of the pyridine ring resonated at δ_C 149.4 ppm, δ_C 148.7 ppm, and δ_C 108.5 ppm, while the carbons of the indole ring resonated further upfield in the aromatic region. The three chiral carbons resonated at δ_C 52.5 ppm, δ_C 53.4 ppm, and δ_C 51.0 ppm, and the pyrroldine protons resonated at δ_C 49.5 ppm and δ_C 25.5 ppm. Finally, a correct HRMS evaluation (*m/z* HRMS (ES) 619.3606 $[M + H]^+$, $C_{34}H_{47}N_6O_5$ requires *m/z* 619.3608 $[M + H]^+$), confirmed the structure of **140**. The enantiomeric purity of the compound was determined by chiral HPLC, which corresponded to a purity of 97% (Fig.3.26).

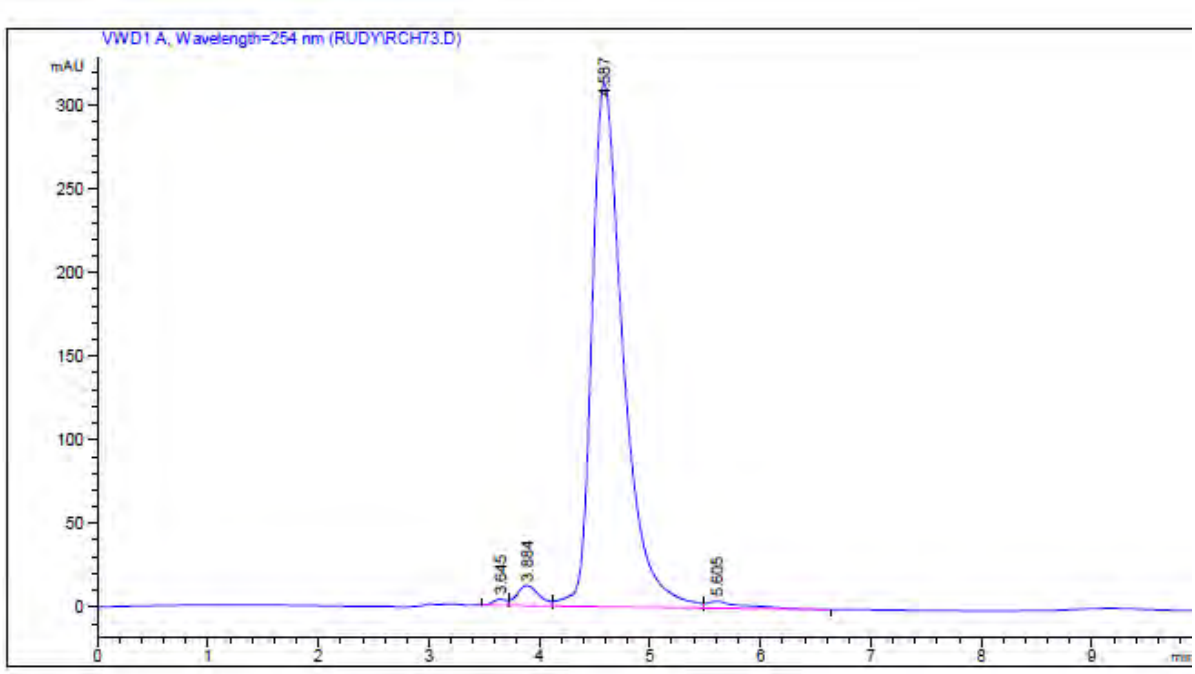

Figure 3.26. Chiral HPLC of compound **140**.

Tripeptide catalysts **139** and **140** were then evaluated as asymmetric acylation catalysts in order to establish the effect on activity of having the extra amino acids in the chain compared to results for the current lead catalyst, dipeptide **128** Table 3.6 compares some results for the two tripeptide catalysts in the kinetic resolution of some standard secondary alcohols. Results of the equivalent reactions with dipeptide lead **128** are given in brackets for comparison purposes.

Table 3.6. Kinetic resolution of various *sec*-alcohols using tripeptides **139** and **140**.

entry[a]	catalyst	substrate	C_{HPLC}[b]	ee (alcohol)	ee (ester)[c]	s-value[d]	configuration[f]
1.	**139**	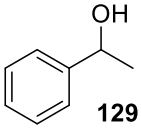 **129**	28	10.7	28.2	2.0	S
			(49)	(38.6)	(40.1)	(3.3)	(S)
2.	**139**	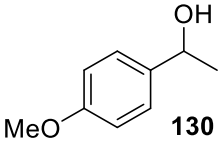 **130**	35	12.1	22.3	1.8	S
			(42)	(21.9)	(30.3)	(2.3)	(S)

3.	**139**	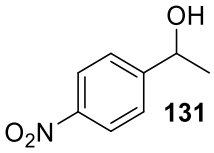 **131**	53 (63)	7.6 (12.4)	6.7 (7.14)	1.2 (1.3)	S (S)
4.	**139**	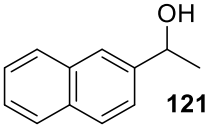 **121**	51	21.6	21.1	1.9	S
5.	**140**	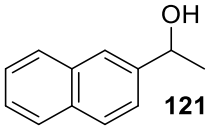 **121**	5.8	3.2	52.5	3.3	S
6.[e]	**140**	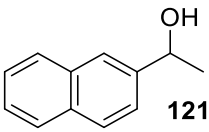 **121**	46	26.4	30.4	2.4	S

*a. All reactions were conducted in the presence of 5 mol% **catalyst**, 0.7 eq. of (^{i}PrCO)$_2$O, and 0.9 eq. of Et$_3$N at -78 °C for 3 hrs., unless otherwise noted. b. Conversion (%) = (ee of recovered alcohol)/(ee of recovered alcohol + ee of ester. c. hydrolysed (2M NaOH in MeOH/H$_2$O) and ee calculated. d. Selectivity factor* $s = \frac{ln(1-C)(1-ee)}{ln(1-C)(1+ee)}$. *e. T = 12 hr. f. The absolute configuration of the faster reacting enantiomer was determined by comparison of* $[\alpha]_D^{20}$ *values with those reported in the literature.*

Disappointingly, the study gave low enantiomeric excesses and s-values for both tripeptide catalysts. Interestingly, catalyst **139** having two tryptophan units gave poorer results than the Trp/Leu combination in **140**, suggesting that it is favourable to have just one π–stacking unit to avoid conflicting conformations. Furthermore, catalyst **140** with the extra bulky Leucine fragment required a longer time (increase from 3 hrs to 12 hrs) to achieve 50% conversion as with catalyst **139**, at least suggesting that the chain was reaching over to the acylation site. Overall, selectivity factors ranged between 1.8 and 3.3, which is much lower than the generally accepted threshold of s = 10 required for a synthetically useful kinetic resolution reaction. Importantly, though, the results suggested that "bigger" was not necessarily "better" and at this stage we resorted to modelling to assist in the direction of the project. Additionally, and this would be important for developing a transition-state model later, the configuration of the fast- reacting enantiomer as determined by measuring the optical rotations and comparing them to literature values was always determined to be the *S*-enantiomer.

N-Boc-indole Dipeptide: Computational Modelling

Having demonstrated varying degrees of enantioselectivity for catalyst **128** in the kinetic resolution of secondary alcohols, attention was turned to computational modelling in an attempt to elucidate the origin of the enantioselectivity, and determine whether π–stacking played a role in the enantiodiscriminating step. As stated earlier, the Boc-substituted dipeptide **141** was thought might provide steric and H-bonding effects, and on paper looked straightforward to synthesise. Once again, a conformer distribution was calculated for its acyl-pyridinium cation (Fig. 3.27) using MMFF94 force field.[151] The ten lowest energy conformers (out of 100 0000 conformations) were optimised at the M06/6-31G* level of theory. This resulted in minimum-energy conformers, which were present in a 91:8.9 ratio (Fig. 3.28, as **A** and **B** respectively).

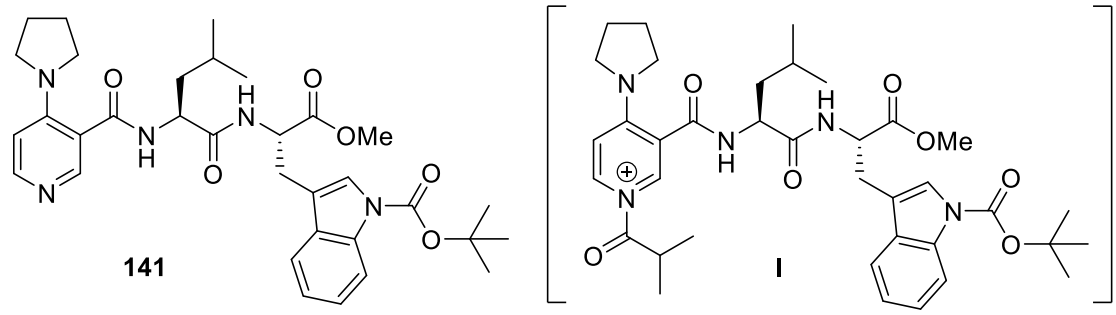

Figure 3.27. Target **141** and its *N*-acyl-pyridinium cation.

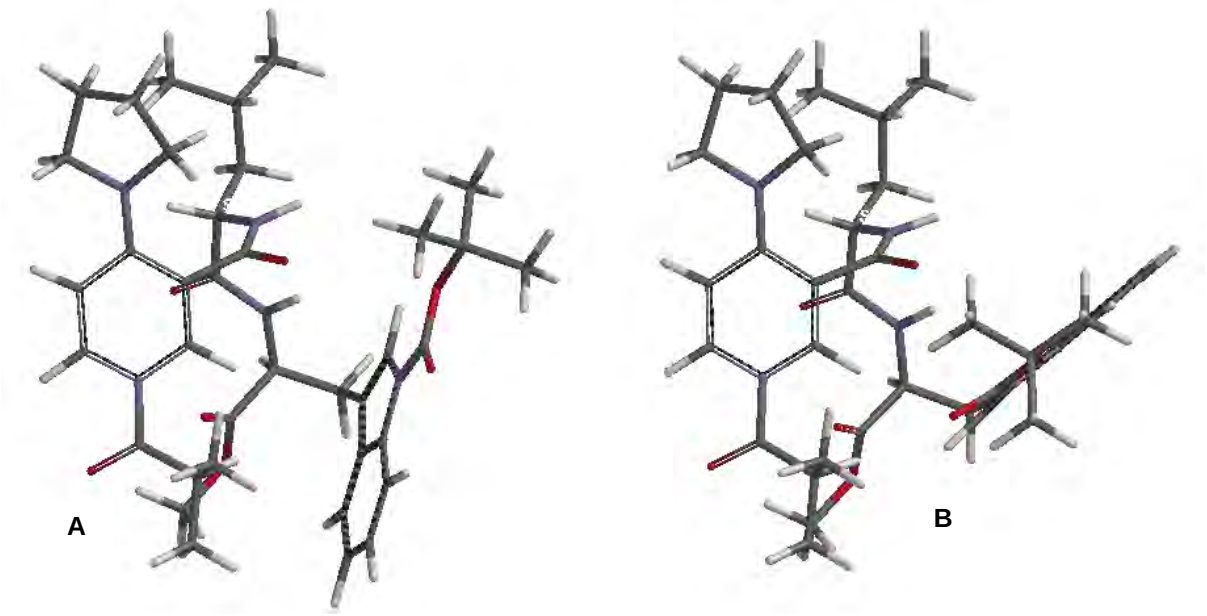

Figure 3.28. Results of the M06/6-31G*level.

The dominant conformer did not indicate a π–stacking interaction, because the indole ring did not overlap with the pyridine ring, and so the ten conformers were subjected to geometry optimization using density functional theory calculations, performed at the B3LYP/6-31G* level of theory followed by a single-point energy calculation using the ωB97X-D/6-31G* level of theory– a functional that is significantly superior for non-bonded interactions like π–π stacking, compared to other empirical-dispersion density functionals.[155] This time the conformers were distributed in a 96:2:1 ratio, shown in Fig. 3.29 as **A**, **B** and **C** respectively together with their relative energies. In conformer **A**, the lowest energy conformer, once again the *N*-acyl moiety was contained in an s-*trans* configuration as before and blocked on its *si*-face by the indole ring of the tryptophan. The bulky *tert*-butyl group of the Boc was now on the "left side" of the molecule on the side of C-5 and C-6. In conformer **B**, the same apply but now the *tert*-butyl group pointed to the other side (right) of the molecule. In conformer **C** the *si* face was blocked, but to a lesser extent. The population for the three conformers, **A**, **B,** and **C** supports the preference of conformer **A**. A more accurate calculation was not further pursued, due to lack of computational power.

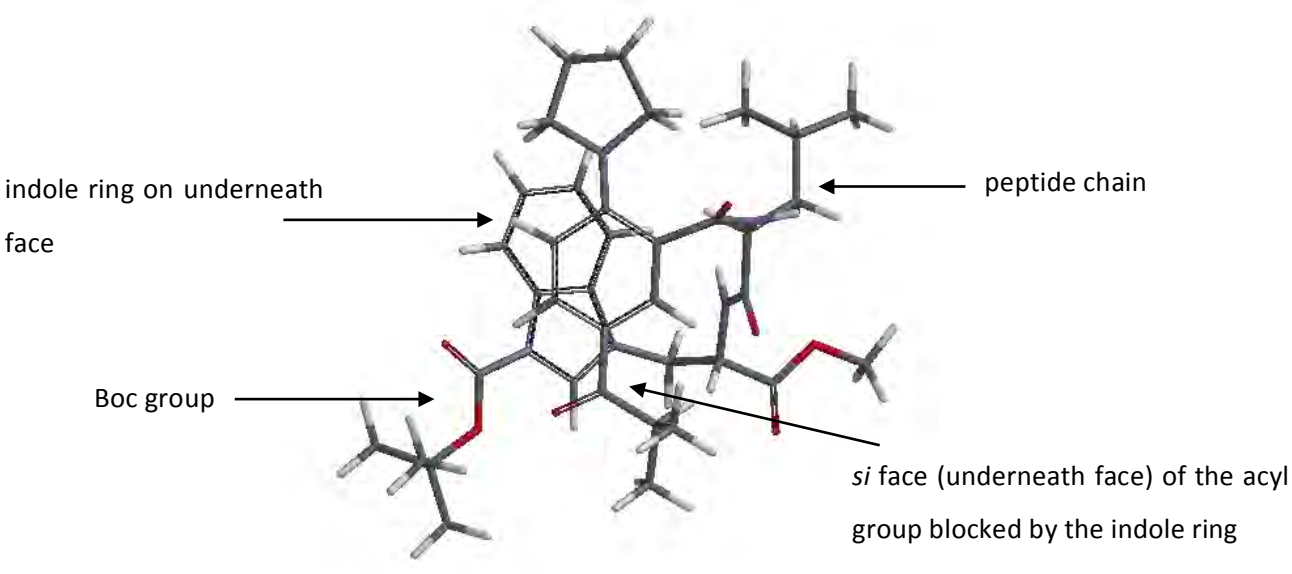

A Rel. Energy = -12.65 kJ/mol

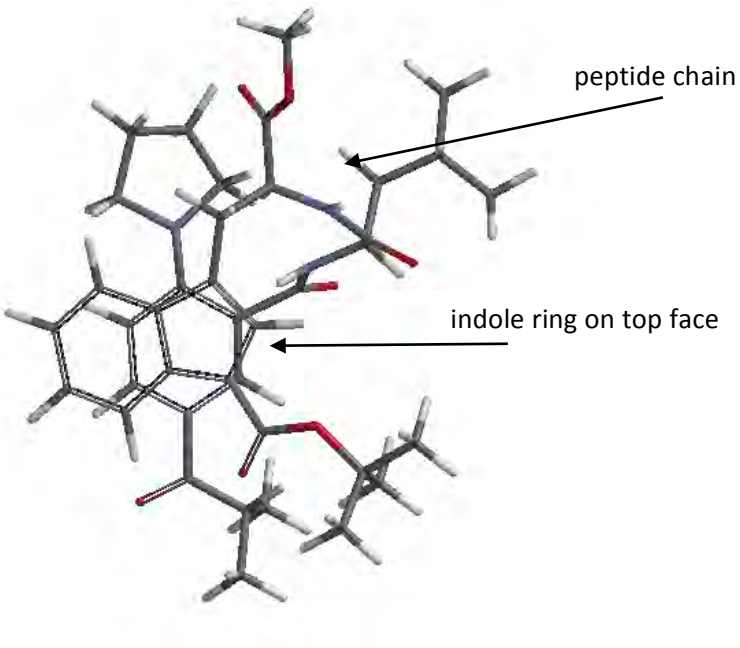

B Rel. Energy = -2.81 kJ/mol

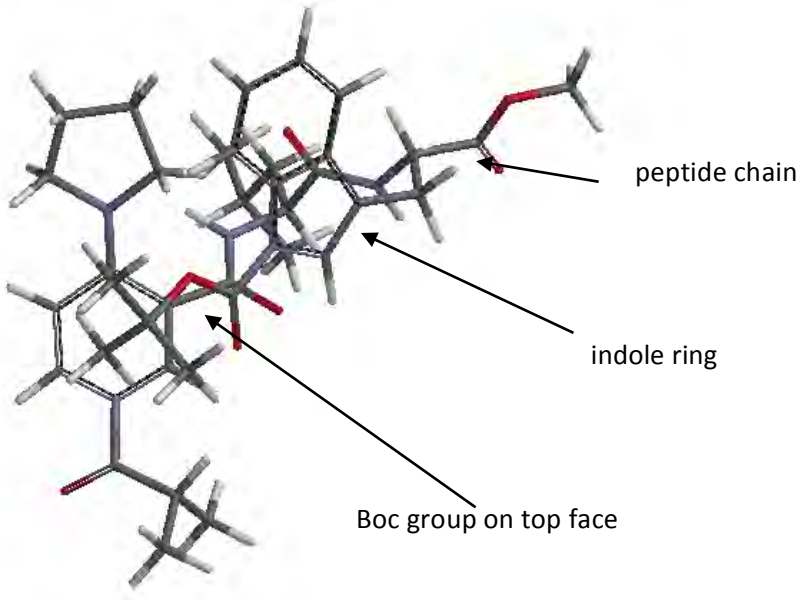

C Rel. Energy = 5.16 kJ/mol

Figure 3.29. Geometry optimized structures of **141** obtained at the ωB97X-D/6-31G* level.

The results of the geometry optimization shown in Figure 3.29 lent support to our original hypothesis that the electron-deficient pyridine ring π–stacks to the electron-rich indole ring. Salient conformational features follow:

1. The dipeptide chain coils such that the indole moiety blocks the underneath face of the pyridinium ion with C-3 on the "right". This is the pyridine *re*-face w.r.t. the pyridine N (C of acyl C=O = priority 1; C-2 = priority 2; C-6 = priority 3.
2. The catalyst adopts the conformation shown in Fig. 3.30, in which an intramolecular π–cation interaction exists between the indole ring and the pyridinium ion.
3. The indole ring ends up on the *si* face of the *N*-acyl group, which is in an s-*trans* conformation. Hence, only the *re* face for approach of the alcohol onto the acyl group looks as though it is available.

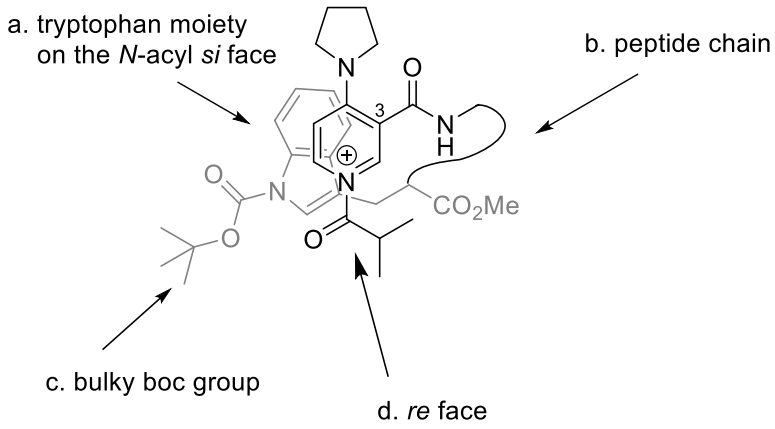

Figure 3.30. Top face of the catalyst, showing (a) indole ring covering the *N*-acyl underneath (*si*) face, (b) coiling of the peptide chain, (c) Boc group blocking one side (left) of the molecule, (d) *re* (top) face of the acyl group.

4. The orientation of the *iso*-propyl group is in the direction of the C-3 substituent, similar to catalyst **128**, and in agreement with Spivey and Connon's observations. Only the *N*-acyl *re* face is available for attack by the nucleophile.

5. Finally, the Boc provides a buttress on the opposite side to the *iso*-propyl group to ensure that the bulk of the alcohol is denied the open space.

Encouraged by these results we set out to synthesise compound **141** and test it as an acyl-transfer catalyst in kinetic resolution reactions.

Catalyst **128** was reacted with di-*tert*-butyl dicarbonate in THF at 0 °C in which it was hoped that the relatively low temperature would avoid any epimerisation. The reaction did not go completion after four hours, according to TLC, even after the addition of a catalytic amount of DMAP and two equivalents of Boc-anhydride. Following a basic work-up, the crude product was purified by column chromatography using 10% MeOH/DCM, and catalyst **141**

was isolated in 51% yield as a pale-yellow solid (Scheme 3.14). The low yield was because the starting material was so close to the product on TLC that only a few fractions of clean product could be isolated.

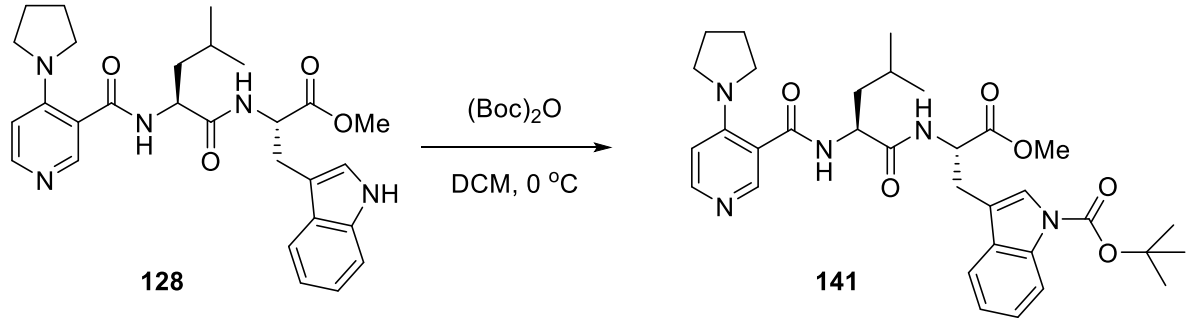

Scheme 3.14. Synthesis of catalyst **141**

Mechanistically, the reaction proceeds via the same Lewis base catalysis as that in this project in which dipeptide **128** is perceived to react with di-*tert*-butyl dicarbonate to form the acyl-pyridinium ion (**I**) with elimination of *tert*-butoxide, which acts as a base to deprotonate the indole NH. THF is crucial as solvent to stabilise the ion-pair. The resulting anion then attacks the pyridinium ion to form the acylated peptide-catalyst **141** (Scheme 3.15).

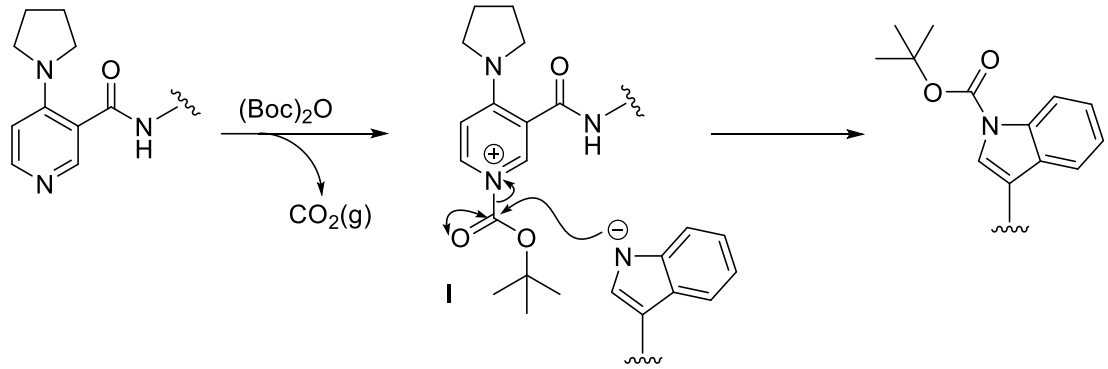

Scheme 3.15. Mechanism of catalyst acylation

The structure of compound **141** was unequivocally assigned on the basis of its spectroscopic data using a combination of 1D, 2D ^{1}H and ^{13}C NMR as well as IR and high resolution mass spectrometry. The ^{1}H NMR spectrum of **141** (Fig. 3.31) lacked the singlet at δ_H 8.48 ppm for the indole NH and a new singlet was present downfield at δ_H 1.64 ppm integrating for nine protons corresponding to the *tert*-butyl protons of the Boc group, which together indicated that a successful reaction had occurred. The protons of the pyridine ring and the indole ring resonated between δ_H 8.25 ppm and δ_H 6.44 ppm; the rest of the spectrum was consistent with

dipeptide catalyst **128**. A small amount of ethyl acetate could be observed (quartet at ~4.1 ppm) that was not removed on the vacuum pump but this was not considered to be limiting.

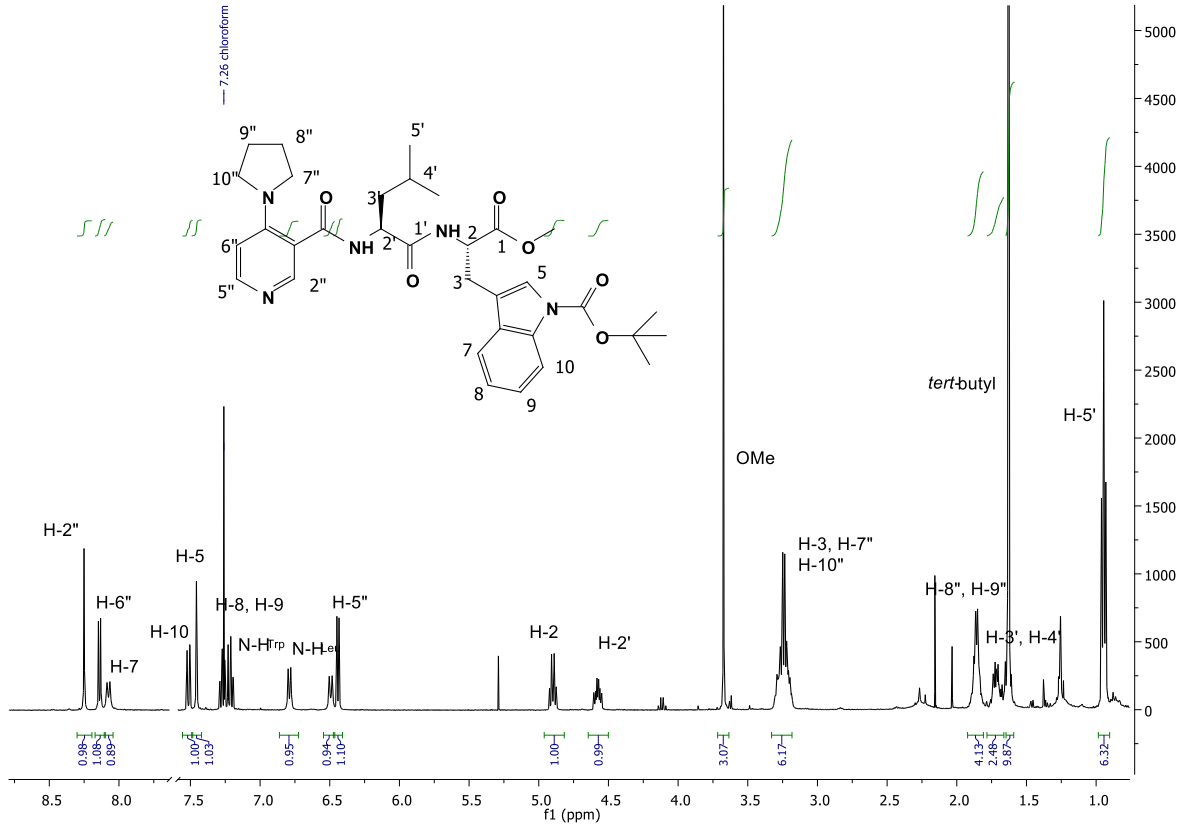

Figure 3.31. ^{1}H NMR spectrum ($CDCl_3$) of compound **141**.

Figure 3.32 shows an APT spectrum for compound **141**, which shows the four carbonyl groups, including that of the new carbamate group resonating at δ_C 150.1 ppm. The presence of the new Boc group was further confirmed by the appearance of resonances for the *t*-butyl group at δ_C 83.8 ppm for the quaternary carbon and at δ_C 28.2 ppm for the homotopic methyl groups. Finally, a correct HRMS evaluation (*m/z* HRMS (ES) 606.3290 $[M + H]^+$, $C_{33}H_{44}N_5O_6$ requires *m/z* 606.3292 $[M + H]^+$), confirmed the structure of **141**. The purity was determined to be 92% by chiral HPLC.

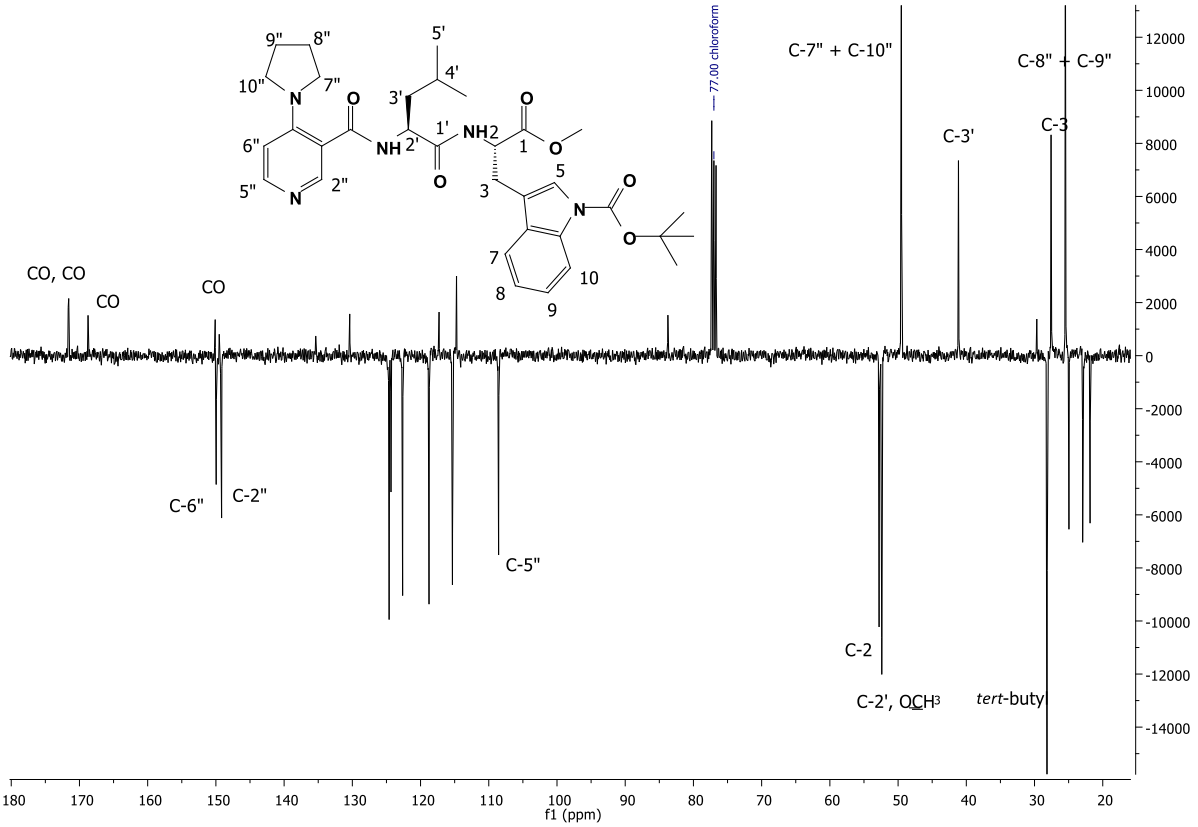

Figure 3.32. APT spectrum ($CDCl_3$) of compound **141**.

Catalyst **141** was tested in the kinetic resolution of a range of secondary alcohols under the same conditions described previously (Table 3.7). The s-values of six substrates (entries 1–6) are compared to dipeptide [§]**128,** and tripeptides ***139** and [‡]**140**.

Table 3.7. The kinetic resolution of various alcohols catalysed by **141**.

entry[a]	substrate	C_{HPLC}[b]	ee (alcohol)[c]	ee (ester)	s-value[d]	configuration[e]
1.	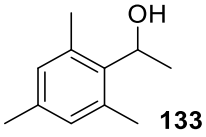 **133**	44 (27)[§]	57.1 (17.3)	72.0 (46.3)	10.8 (3.2)	S (S)
2.	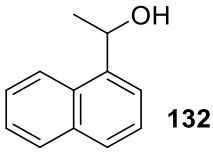 **132**	45 (60)[§]	59.3 (48.4)	71.1 (32.2)	10.7 (3.0)	S (S)
3.	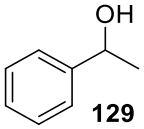 **129**	42 (49)[§]	50.2 (38.6)	69.1 (40.1)	8.9 (3.3)	S (S)
4.	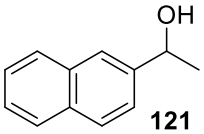 **121**	50 (34)[§] (51) * (46)[‡]	63.2 (31.1) (21.6) (26.4)	62.4 (59.4) (21.1) (30.4)	8.1 (5.3) (1.9) (2.3)	S (S) (S) (S)
5.	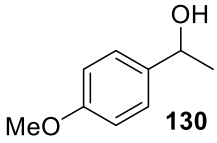 **130**	30 (42)[§] (35) *	29.4 (21.9) (12.1)	68.0 (30.3) (22.3)	7.0 (2.3) (1.8)	S (S) (S)
6.	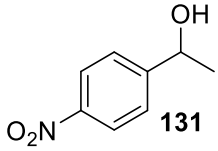 **131**	36 (63)[§] (53)*	13.9 (12.4) (7.6)	24.6 (7.1) (6.7)	1.9 (1.3) (1.2)	S (S) (S)
7.	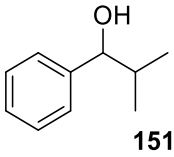 **151**	50	68.5	68.8	10.9	S
8.	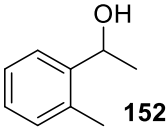 **152**	44	53.8	69.9	9.6	S
9.	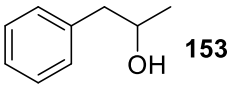 **153**	20	16.2	65.3	5.6	S

10.	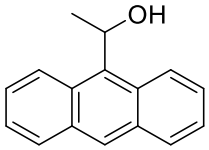 **154**	56	50.6	39.8 [f]	3.7	S
11.	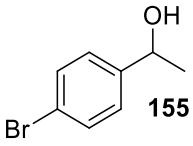 **155**	45	35.7	43.1	3.5	S
12.	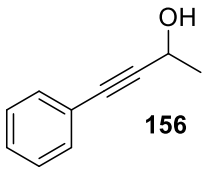 **156**	11	3.6	30.6	1.9	S

*a. All reactions were conducted in the presence of 5 mol% **141**, 0.7 eq. of (^{i}PrCO)$_2$O, and 0.9 eq. of Et$_3$N at −78 °C for 3 hrs., unless otherwise noted. b. Conversion (%) C = (ee of recovered alcohol)/(ee of recovered alcohol + ee of ester. c. hydrolysed (2M NaOH in MeOH/H$_2$O) and ee calculated. d. Selectivity factor* $s = \frac{ln(1-C)(1-ee)}{ln(1-C)(1+ee)}$. *e. The absolute configuration was determined by comparison of* $[\alpha]_D^{20}$ *values with those reported in the literature. f. ee of ester (not hydrolysed) measured by chiral HPLC.* [§]**128**, *__139__, and [‡]**140**.

The results of this study indicated that the presence of a bulky *tert*-butyl group of **141** greatly enhances the selectivity, since higher s-values were obtained compared to dipeptide **128**, and tripeptides **139** and (Table 3.7, entries 1–6); we were especially pleased to observe s-values exceeding 10 (Table 3.7, entries 1 and 2). Entries 7–12 are new substrates that were only tested using **141**, and s-values varied between 9.7 and 1.9, with two results approaching an s-value of 10 (Table 3.7, entries 7 and 8). In all cases, the fast reacting enantiomer was the *S*-enantiomer as determined by measuring the sign of the optical rotations and comparing them to literature values.

Figure 3.33 shows one example of the chromatograms for the kinetic resolution of alcohol **132** which was catalysed by **141** (Table 3.7, entry 2).

a.

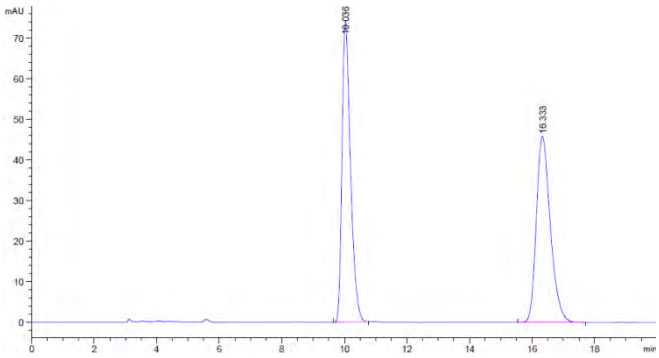

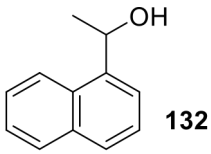

retention time (min)	area %
10.036	49.5602
16.333	50.4398

b.

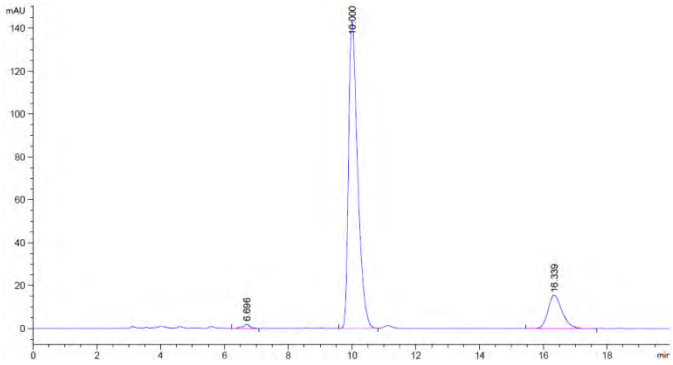

retention time (min)	area %
10.000	84.8175
16.339	14.3188

c.

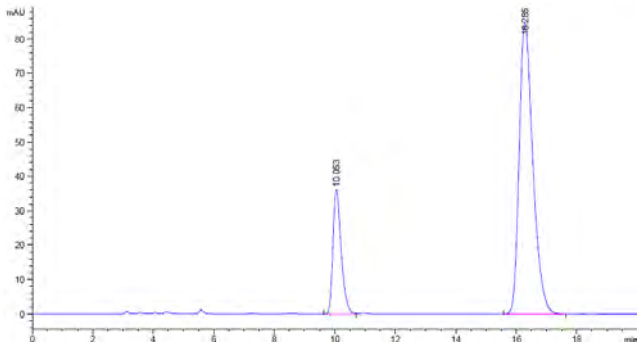

retention time (min)	area %
10.053	20.3230
16.285	79.6770

Figure 3.33. Chiral HPLC chromatograms of the kinetic resolution of 1-(1-naphthyl)ethanol **132**; a. Racemic **132**. b. **132** after ester hydrolysis. c. Recovered starting material.

Figure 3.34 outlines transition-state models for the two enantiomers, which involves a stereoelectronic effect between one of the lone pairs of the nucleophile and the *N*-acyl-pyridinium carbonyl carbon. One of the enantiomers of racemic *sec*-alcohol preferentially attacks the *N*-acyl-pyridinium cation from one side to give the corresponding ester. The *S* selectivity in the kinetic resolution can be explained by comparing the two possible transition-state models, TS-I and TS-II, for the acylation of (*S*)- and (*R*)-2-phenylethanol, respectively.

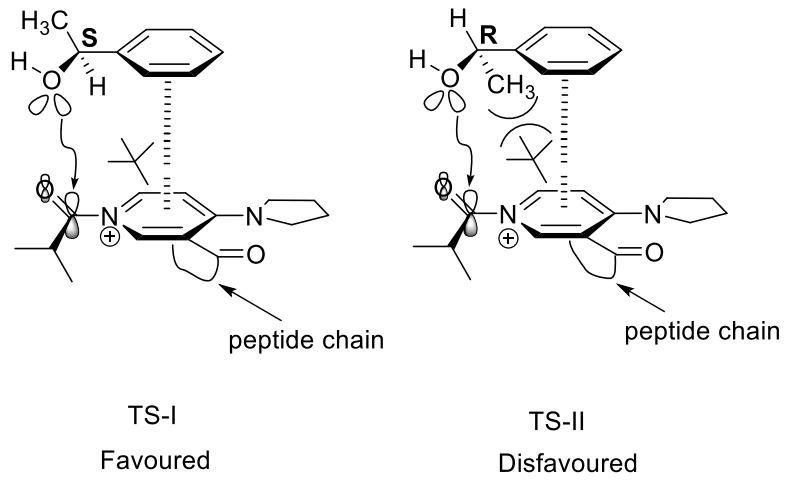

Figure 3.34. Proposed transition-state models.

The alcohols would approach the pyridinium ion in a face-to-face manner due to an intermolecular π–cation interaction between the pyridinium cation and the aromatic ring of each.[3,4] The (*S*)-alcohol can effectively attack the *re* face of the *N*-acyl group, such that one of the lone pairs of the oxygen atom (sp^3 hybridised, with a tetrahedral arrangement of two bonds and two lone pairs) is colinear to the p-orbital of the carbonyl group ($n–\pi^*_{C=O}$). This interaction is possible for both TS-I and TS-II, however, the (*R*)-alcohol experiences a steric repulsion between the benzylic methyl group and the *tert*-butyl group attached to the chiral element; therefore, the acylation would preferentially proceed through TS-I to give predominately the (*S*)-ester. The lower selectivities in the cases where the aromatic ring is further away from the hydroxyl group (Table 3.7 entries 9 and 12) may be attributable to a decrease in the intermolecular π–cation interactions between the aromatic ring and the pyridinium-cation.

Figure 3.35 shows four alternate transition-state structures with different orientations of the groups at the chiral carbon and illustrates why these interactions are not as favourable as the TS-I model in Fig. 3.34.

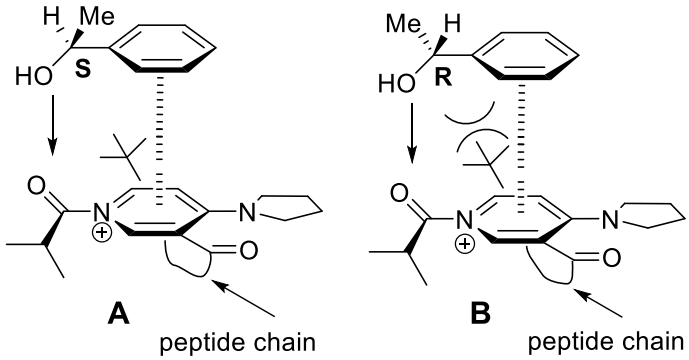

interaction	**A** (*S*-enantiomer)	**B** (*R*-enantiomer)
methyl group/*tert*-butyl interaction	• No interaction, since methyl and *tert*-butyl are on opposite "sides" of the molecule	• Unfavourable steric hindrance between methyl group and bulky *tert*-butyl group
lone pair/carbonyl-C interaction	• Unfavourable interaction, due to orientation of the C-O bond.	• Unfavourable interaction, due to orientation of the C-O bond.

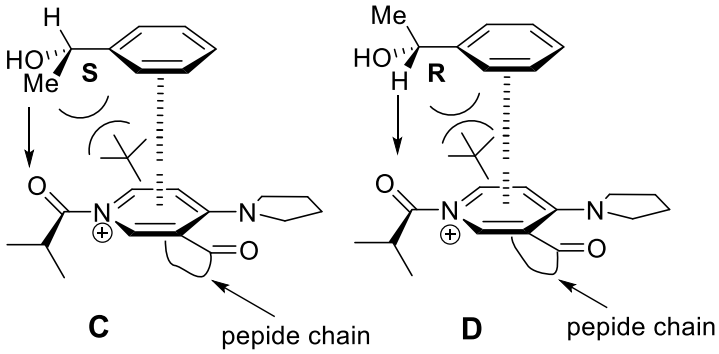

interaction	**C** (*S*-enantiomer)	**D** (*R*-enantiomer)
methyl group/*tert*-butyl interaction	• No interaction, since methyl and *tert*-butyl are on opposite "sides" of the molecule • OH group is on the same "side" of the *tert*-butyl group and may experience a steric affect.	• No interaction, since methyl and *tert*-butyl are on opposite "sides" of the molecule • OH group is on the same "side" of the terbutyl group and may experience a steric affect.
lone pair/carbonyl-C interaction	• Unfavourable interaction, due to orientation of the C-O bond.	• Unfavourable interaction, due to orientation of the C-O bond.

Figure 3.35. Four alternate transition-state interactions.

Derivatives of Dipeptide Catalyst

The introduction of the Boc substituent clearly had a favourable effect on the enantioselectivity of catalyst **141**. Our transition-state model (TS-I) showed that one explanation for the higher selectivity values displayed by **141** compared to **128** was the effect of the bulky *tert*-butyl group, which restricted the approach of the alcohol in the enantiodiscriminating step. Therefore, it was thought a good idea to extend this finding to synthesising derivatives of **141** varying the carbamate group. Figure 3.36 shows targets identified based on computational modelling performed at the MMFF94 Force Field level.

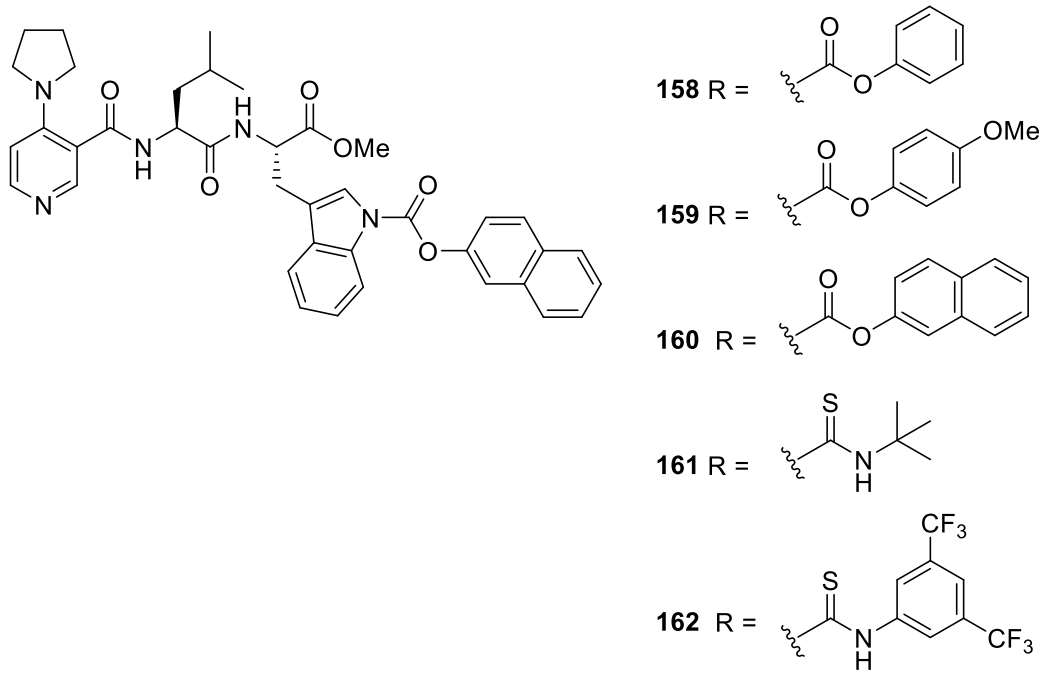

Figure 3.36. Carbamate derivative modifications for catalyst **141**.

Results of the modelling indicated an interaction between the oxygen of the carbamate and the carbonyl carbon of the *N*-acyl-pyridinium ion for catalysts **158**, **159**, and **160**; and the sulfur of the thiourea and the carbonyl of the *N*-acyl-pyridinium ion for catalysts **161** and **162** in addition to the steric effect of the substituents. The carbamates **158-162** were synthesised by deprotonating the indole NH using a strong base (NaH), and reacting with an electrophile, either as a chloroformate or an isothiocyanate. DMF was found to be the preferred solvent, since no reaction occurred in THF (Scheme 3.16).

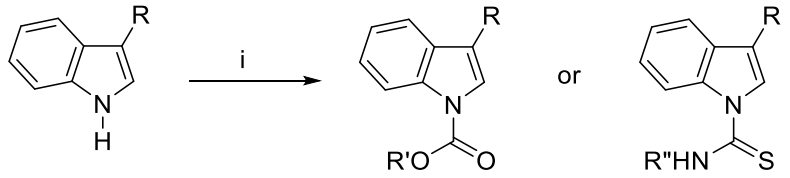

Scheme 3.16. *Reagents and conditions:* (i) NaH, R'CO_2Cl (or S=C=N-R"), DMF, 0 °C, 2hrs.

All the reactions were performed with 0.9 equivalents of NaH to prevent potential epimerizaton at the α-positions of the amino acids. As a result, some starting material was always present in the reaction. This hampered isolation of the catalysts, since the product was very close to the starting material on TLC, and only a few clean fractions were obtained. Therefore the yields for these reactions were generally low.

Compound **158** was isolated in a 30% yield following a work-up and column chromatography, and characterized using a combination of 1D, 2D ^{1}H NMR and ^{13}C NMR. Its ^{1}H NMR spectrum lacked the singlet for the indole proton, which suggested that the reaction had taken place, and showed the appearance of a multiplet integrating for five protons between δ_H 7.38 ppm and δ_H 7.29 ppm corresponding to the new phenyl group. The rest of the spectrum was consistent with the ^{1}H NMR spectrum of the dipeptide starting material **128**. The ^{13}C NMR spectrum confirmed the presence of the carbamate group. The new carbonyl carbon resonated at δ_C 157.7 ppm while the carbons of the phenyl group resonated in the aromatic region. Finally, a correct HRMS evaluation (*m/z* HRMS (ES) 626.2973 $[M + H]^+$, $C_{35}H_{40}N_5O_6$ requires *m/z* , 626.2979 $[M + H]^+$), confirmed the structure of **158**. Similarly, compound **159** was isolated in a 31% yield and characterized using a combination of 1D, 2D ^{1}H NMR and ^{13}C NMR. Its ^{1}H NMR spectrum also lacked the indole peak, and showed two doublets in the aromatic region at δ_H 6.91 ppm and δ_H 7.18 ppm corresponding to the protons of the new 1,4-disubstituted phenyl group. The protons of the additional methoxy group resonated at δ_H 3.67 ppm upfield to those of the methyl ester at δ_H 3.82 ppm (Fig. 3.37 displays a portion of the spectrum).

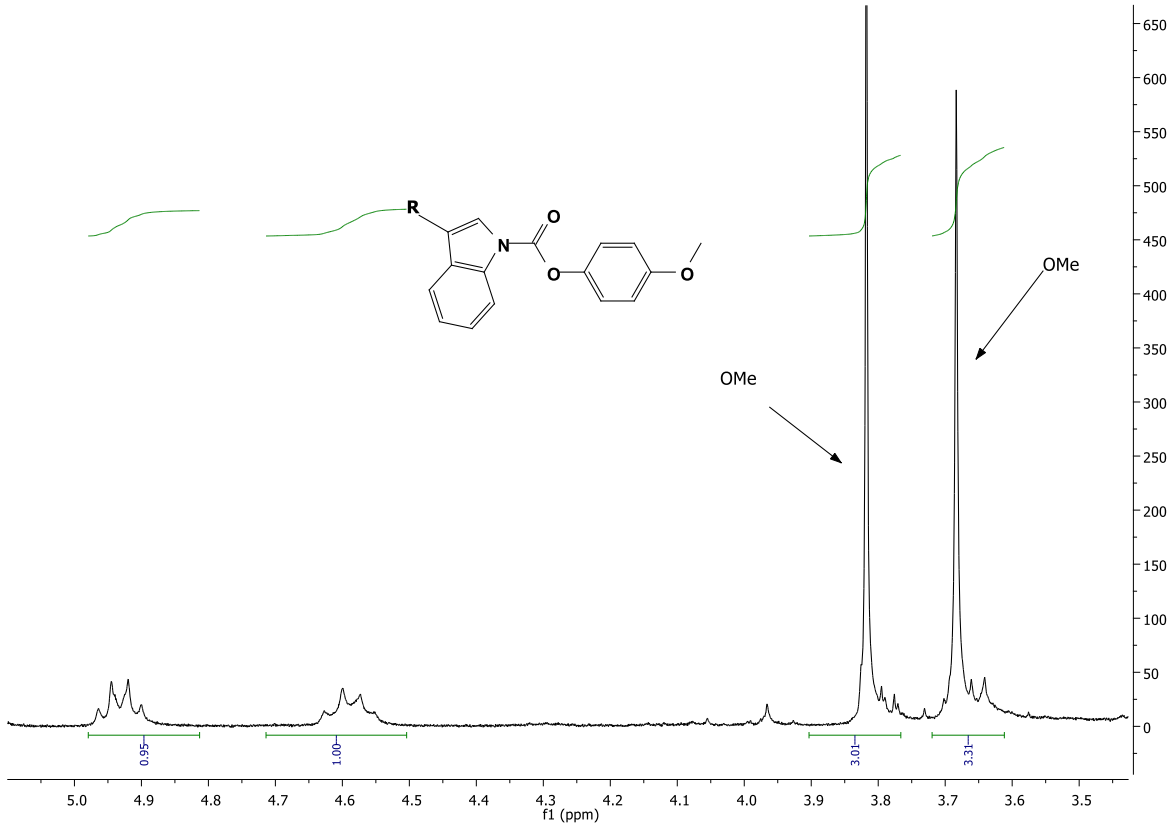

Figure 3.37. Partial ^{1}H NMR spectrum of **159** showing the two methoxy peaks at δ_H 3.67 ppm and δ_H 3.82 ppm.

Finally, compound **160** was isolated in 40% yield following work-up and column chromatogrpahy. Its ^{1}H NMR spectrum also confirmed a successful reaction by virtue of the absence of the indole proton and the appearance of seven new protons of the naphthyl group resonating in the aromatic region. The ^{13}C NMR spectrum showed a new singlet resonating at δ_C 150.2 ppm for the carbamate carbonyl group, while the carbons of the naphthyl ring appeared in the aromatic region. Finally, a correct HRMS evaluation (*m/z* HRMS (ES) 676.3142 $[M + H]^+$, ($C_{39}H_{42}N_5O_6$ requires *m/z* 676.31351 $[M + H]^+$), confirmed the structure of **160**.

Synthesis and Characterisation of 161 and 162

Compound 161 was isolated in a 24% yield and characterised by a combination of 1D and 2D NMR. Its ^{1}H NMR spectrum showed the *tert*-butyl group resonating at δ_H 1.65 ppm, which indicated that the reaction was likely successful. The indole NH proton was absent, while the new NH proton of the thiourea appeared at δ_H 8.83 ppm. The ^{13}C NMR spectrum showed a downfield singlet at δ_C 178.0 ppm for the thiourea thiocarbonyl carbon (C=S), while the carbons of the *tert*-butyl group resonated at δ_C 28.1 ppm. The infra-red spectrum revealed a

sharp peak at 1266 for the carbon sulfur double bond. Finally, a correct HRMS evaluation (*m/z* HRMS (ES) 621.3219 $[M + H]^+$, $C_{33}H_{45}N_6O_4S$ requires *m/z* 621.32230 $[M + H]^+$), confirmed the structure of **161**.

In order to synthesise catalyst **162**, isothiocyanate **164** first had to be synthesised from commercially available 3,5-bis(trifluoromethyl)aniline **163** and thiophosgene under basic conditions. Following workup and column chromatography, compound **164** was isolated in 71% yield (Scheme 3.17).

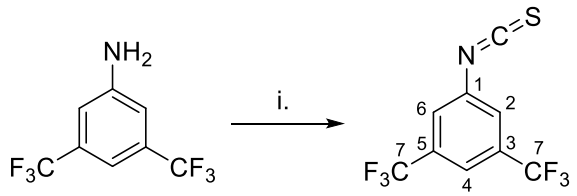

163 **164**

Scheme 3.17. *Reagents and conditions:* (i) thiophosgene (1.2 eq.), Hünig's base (2 eq), DCM, r.t., 5 hrs (71%).

The ^{1}H NMR spectrum of **164** lacked the protons of the amine in the starting material and showed two singlets for the three aromatic protons. The ^{13}C NMR spectrum was more instructive, showing the C=S singlet resonating at δ_C 141.0 ppm, while the quaternary proton (C-1) resonated at δ_C 134.1 ppm. The CF_3 groups (C-7) resonated as a quartet between δ_C 118.4 ppm and δ_C 126.6 ppm with a C-F coupling constant of 273 Hz. Quaternary carbons C-3 and C-5 appeared as a smaller quartet resonating at δ_C 133.4 ppm with a coupling constant of 34 Hz, also due to C-F (^{2}J) coupling. The rest of the spectrum is shown in Fig. 3.38.

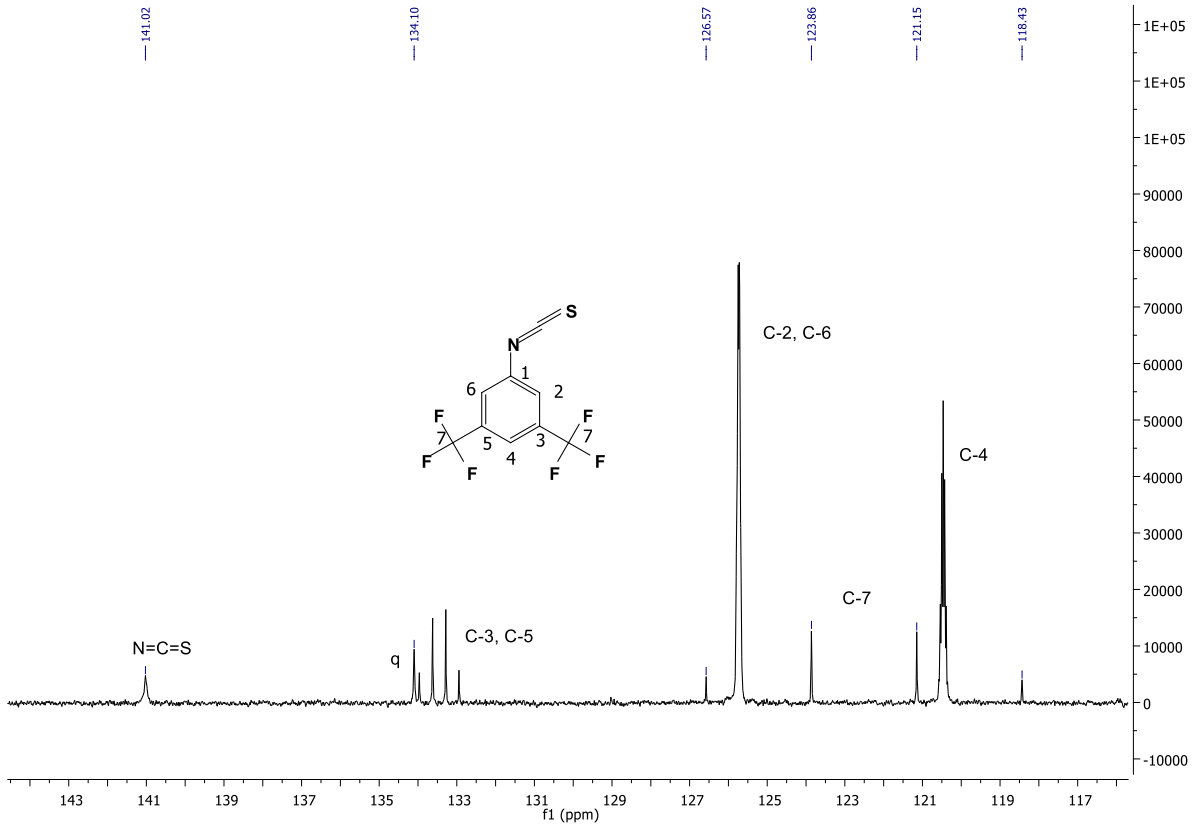

Figure 3.38. ^{13}C NMR ($CDCl_3$) spectrum of isothiocyanate **164**.

The next step was to couple isothiocyanate **164** to dipeptide catalyst **128** under basic conditions, following workup and column chromatography, **162** was isolated in a 17% yield. Figure 3.39 shows a partial ^{1}H NMR spectrum of compound **162**. The three protons of the 3,5-disubstituted aromatic ring resonated at δ_H 8.17 ppm (H-2”’ and H-6”), and δ_H 7.71 ppm (H-4”’). The proton *α* to the pyridine nitrogen, H-2”, shifted upfield to δ_H 6.94 ppm while the rest of the aromatic region contained the aromatic protons of the indole ring and the pyridine ring. The ^{13}C NMR spectrum showed a downfield singlet at δ_C 179.4 ppm for the thiocarbonyl carbon, which further confirmed the presence of the thiourea group. The quartet corresponding to the two CF_3 group could not be assigned (too small), but the quartet corresponding to C-3”’ and C-5”’ could be assigned and had a C-F coupling of 33.0 Hz. The IR spectrum which showed a peak at 1266 cm^{-1} corresponding to the C=S group.

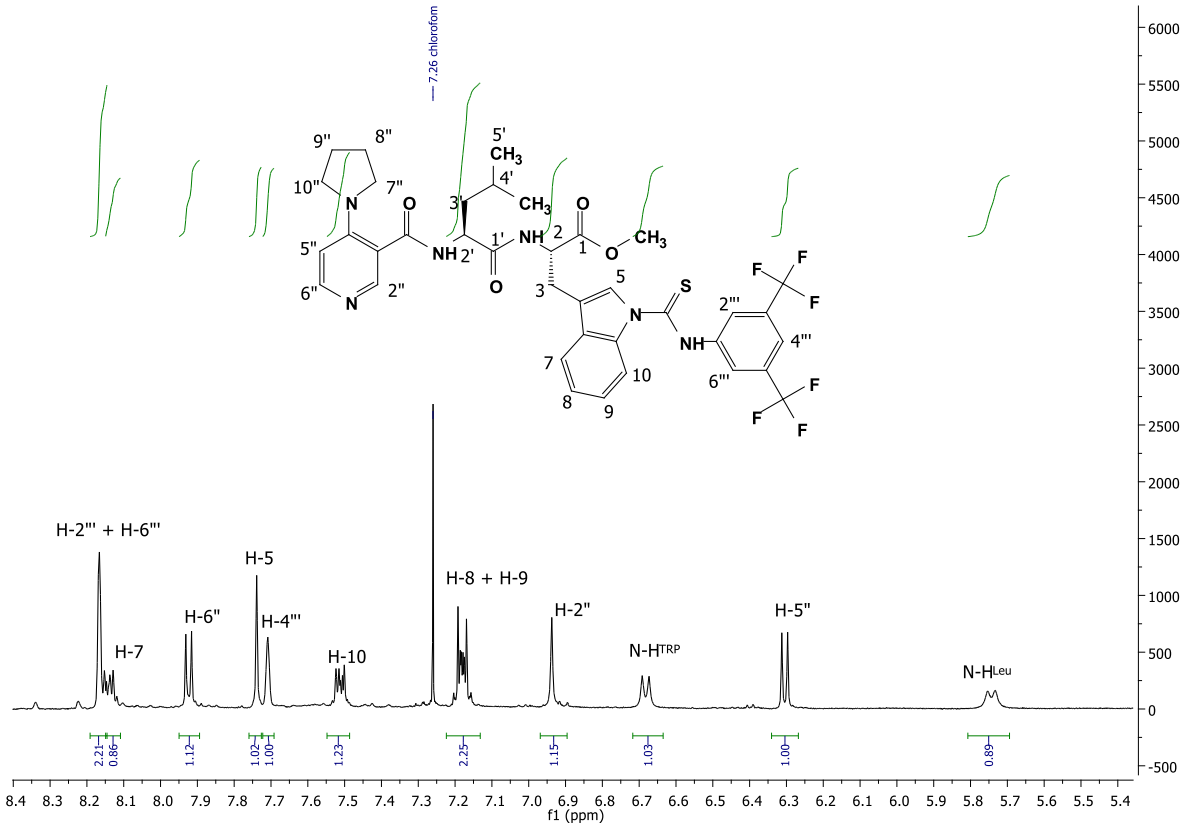

Figure 3.39. A portion (aromatic region) of the ^{1}H NMR spectrum of compound **162**.

The purity of the five derivatives was evaluated using chiral HPLC, which unfortunately indicated varying degrees of what was assumed to be epimerization at the α-stereogenic centres for all five catalysts (Table 3.8). Therefore the strategy of lowering the amount of sodium hydride to prevent epimerization was unsuccessful.

Table 3.8. Purity evaluation of catalysts **158**–**162**.

entry	derivative	ee (%)
1.	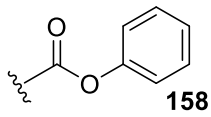 **158**	45
2.	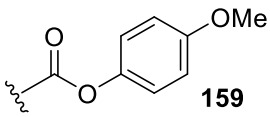 **159**	85
3.	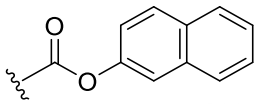 **160**	44
4.	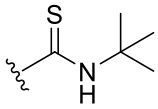 **161**	50
5.	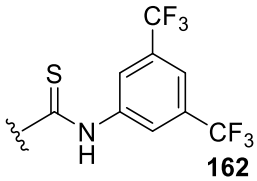 **162**	53

However, having synthesised the five compounds, screening of the catalysts in the kinetic resolution of 1-(2-naphthyl)ethanol went ahead (Table 3.9). Selectivity factors varied between 1.1 (for the *tert*-butyl thiourea derivative **161**) and 7.0 (for the phenyl carbamate derivative **158**). However, the *tert*-butyl carbamate substituted catalyst **141** still remained the most selective catalyst for this substrate (s-value = 8.1). The rest of the carbamates gave higher s-values (Table 3.9, entries 3, 4, and 5) than the free amine catalyst **128** (Table 3.9, entry 1) though, further suggesting that the presence of a carbamate substituent on the indole nitrogen plays an important role in the enantiodescriminating step in which steric aspects predominate. However, the thiocarbamate catalysts **161** and **162** both gave lower s-values than the free amine (Table 3.9, entries 7 and 8) indicating that the oxygen of the carbamate must play a role in the orientation of the *tert*-butyl group (and/ or other) groups**.**

Table 3.9. Kinetic resolution of 1-(2-naphthyl)ethanol with various catalysts.

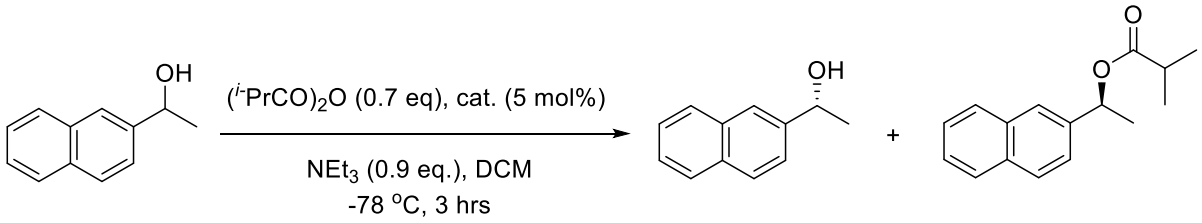

entry[a]	**R**	catalyst	C_{HPLC} [b]	ee (alcohol)	ee (ester)[c]	s-value[d]
1.	H	**128**	34	31.2	9.4	5.3
2.	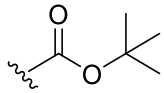	**141**	50	63.2	62.4	8.1
4.	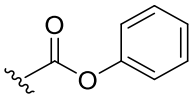	**158**	48	54.4	59.1	6.6
3.	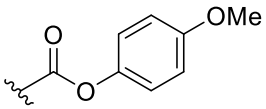	**159**	48	55.5	60.5	7.0
5.	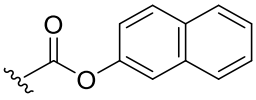	**160**	52	60.5	54.3	6.1
6.	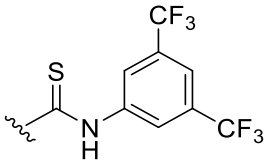	**161**	19	11.0	47.2	3.1
7.	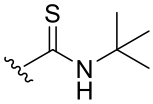	**162**	49	2.1	2.2	1.1

*All reactions were conducted in the presence of 5 mol% **catalyst**, 0.7 eq. of (^{i}PrCO)$_2$O, and 0.9 eq. of Et$_3$N at −78 °C for 3 hrs., unless otherwise noted. b. Conversion (%) = (ee of recovered alcohol)/(ee of recovered alcohol + ee of ester. c. hydrolysed (2M NaOH in MeOH/H$_2$O) and ee calculated. d. Selectivity factor* $s = \frac{ln(1-C)(1-ee)}{ln(1-C)(1+ee)}$.

3.3 α-Substituted Acylation Catalysts

The final part of this thesis involved the development of two quinoline-based catalysts, which were inspired by Fu's quinolone-based ferrocene complexes (section 1.7.3). Even though quinoline is known to be an inefficient acyl-transfer catalyst itself due to an α-steric effect, the iron atom in Fu's catalyt increases the nucleophilicity of the quinoline nitrogen, and also provides a scaffold for a quinoline moiety. Therefore, it was rationalised that a chiral oxy-substituent attached to C-8 of a 4-aminoquinoline template might present a catalytic effect in which extra mesomeric donation to the ring nitrogen from the oxygen might compensate for the well-known α-steric effect established by Litvinenko and Kirichenko. To test our hypothesis, catalysts **165** and **166** were synthesised by coupling an 8-hydroxy-4-pyrrolidinoquinoline template to two different modified amino acids (Fig. 3.40). Catalyst **165** was chosen because of success with the leucine/tryptohan dipeptide motif in π–stacking. Catalyst **166** was chosen based on work done by Connon et.al. who found that for 4-pyrrolidinopyridine-based catalysts (e.g. **32**, Chapter 1), the pyrrolidine substituents with a hydroxyl group were more active than those lacking the hydroxyl group. The observed enantioselectivity was affected by substrate H-bonding interaction during the enantiodiscriminating step, as determined by computational modelling calculations.

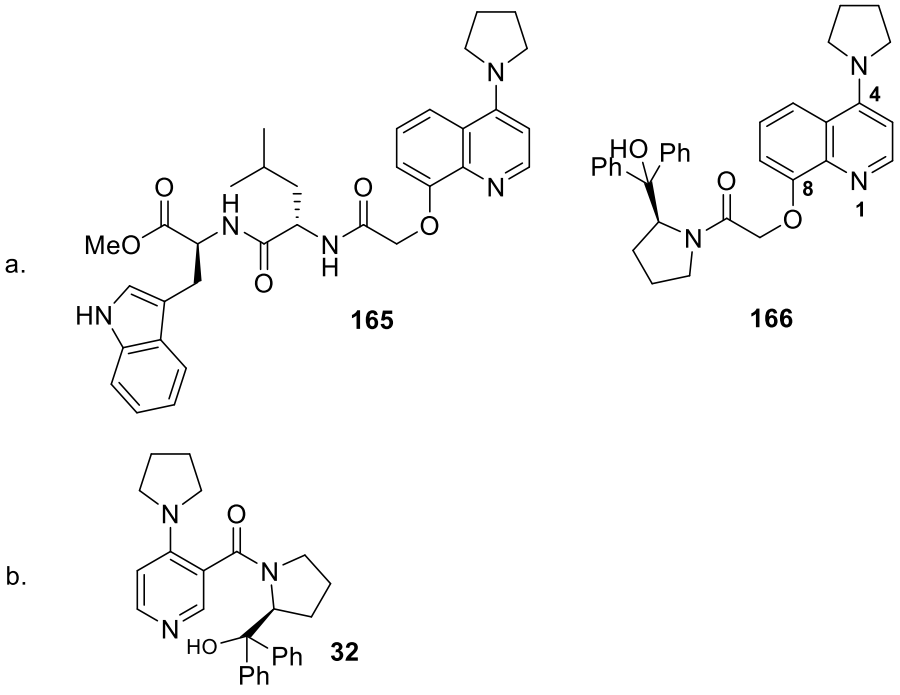

Figure 3.40. a. Structure of target quinoline catalysts. b. Connon's PPY-based catalyst.

Scheme 3.18 shows the five step synthesis of the quinoline template **172**, which was based on recent literature. Thus, commercially available xanthurenic acid was decarboxylated by refluxing in diphenyl ether, to afford **168** in 92% yield following filtration.[156] Its ^{1}H NMR spectrum lacked the acidic proton of the carboxylic acid, indicating that a successful decarboxylation had occurred, and also revealed broad singlets at δ_H 11.21 ppm and δ_H 10.61 ppm for the protons of the two hydroxyl groups. In addition a characteristic AB doublet pair for H-2 and H-3 was noted. The next step was to chemoselectively protect the C-8 phenoxide as a tosylate. This was possible because the C-4 phenoxide is less reactive than its C-8 counterpart due to resonance stabilization of the former directly onto nitrogen. Thus, **168** was reacted with *p*-toluenesulfonyl chloride in water with sodium hydroxide as base, and after twelve hours a grey compound precipitated, which was filtered and isolated in 96% yield. Its ^{1}H NMR spectrum showed the diagnostic singlet peak at δ_H 2.36 ppm corresponding to the methyl group of the tosylate **169**.

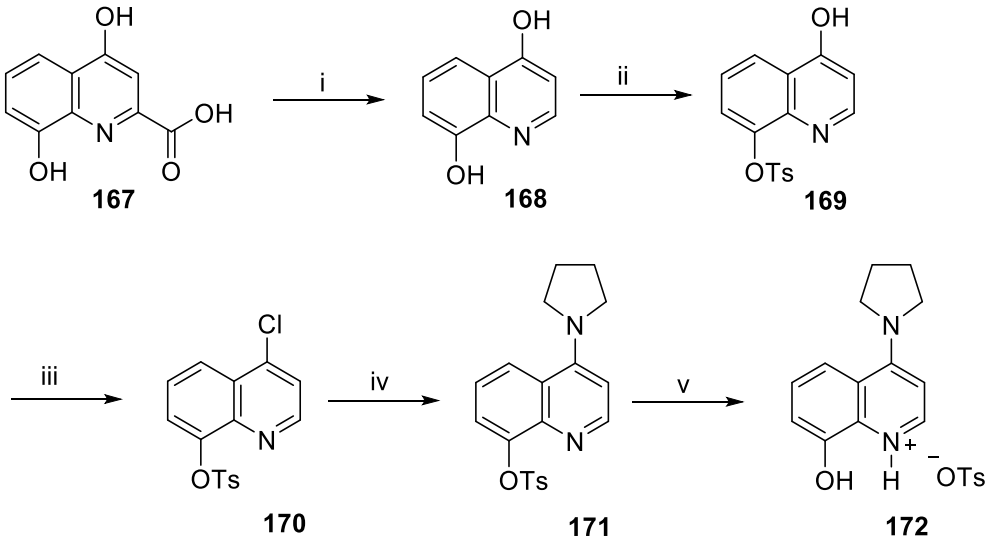

Scheme 3.18. *Reagents and condtions:* (i) diphenyl ether, reflux, 3 hrs, 92%; (ii) TsCl, 1M NaOH, r.t., 18 hrs, 96%; (iii) $POCl_3$, reflux, 3 hrs, 74%; (iv) pyrrolidine, K_2CO_3, toluene, 100 °C, 18 hrs, 67%; (v) 2M NaOH, ethanol, reflux, 3 hrs, 96%.

As expected, the hydroxyl group at C-4 did not react and resonated as a broad singlet at δ_H 11.43 ppm. The C-4 hydroxyl group was then substituted for a chloride in a nucleophilic aromatic substitution by refluxing **169** in phosphoryl chloride for three hours. Following a basic work-up, chloride **170** was isolated in 74% yield. Its ^{1}H NMR lacked the singlet for the hydroxyl group, the rest of the spectrum was consistent with published results. The chloride was then substituted in a further S_NAr reaction using pyrrolidine and K_2CO_3 in toluene. After

18 hours the mixture was filtered and then purified by column chromatography to give compound **171** in a 67% yield. Its ^{1}H NMR spectrum confirmed that the reaction was successful by the appearance of two multiplets at δ_H 3.90 ppm and δ_H 2.01 ppm corresponding to the eight protons of the pyrrolidine ring. Finally, the tosylate was removed under basic conditions using sodium hydroxide. The reaction was quenched with hydrochloric acid and compound **172** was isolated as a tosylate salt in a 96% yield, which could be used as the nucleophilic template in the coupling to follow on the understanding that the tosic acid moiety would be taken care of by the base (in excess). With the template in hand, the next step was to synthesise the peptide to be attached to the template (Scheme 3.19). Here, it was envisaged that a bis-electrophilic coupling tether based on chloroacetate could be used to join the two nucleophilic sites of the peptide and template respectively.

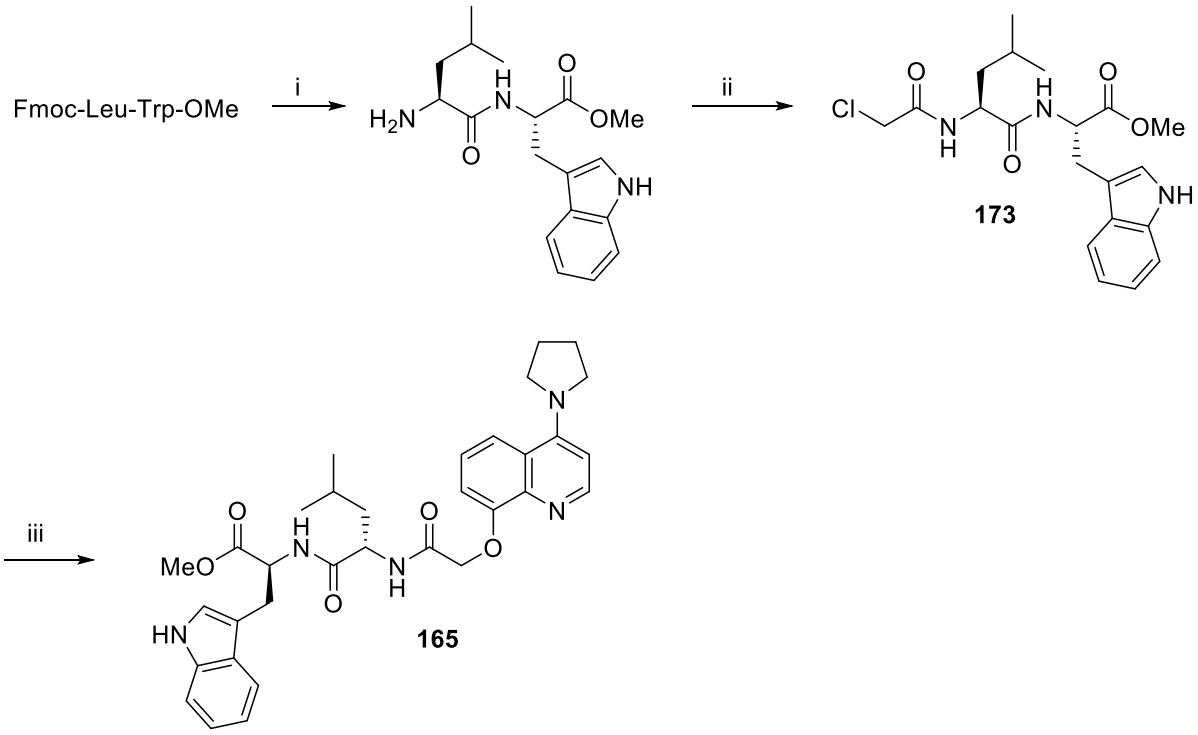

Scheme 3.19. *Reagents and conditions:* (i) piperidine, DCM, 0 °C, 12 hrs, 67%; (ii) chloroacetic acid, DCC, HOBt, DCM, 0 °C, 18 hrs, 92%; (iii) **172**, $CsCO_3$, CH_3CN, r.t., 60 °C, 7 hrs, 60%.

The synthesis of the dipeptides, Fmoc-Leu-Trp-OH and NH_2-Leu-Trp-OH, have been previously discussed (Chapter 2). The free amine was reacted with chloroacetic acid under peptide coupling conditions used in this project. Following a work-up and column chromatography, the chloride **173** was isolated in 92% yield. Its ^{1}H NMR spectrum in $CDCl_2$

revealed a new amide NH singlet at δ_H 6.86 ppm, while the α-proton of the leucine moiety shifted downfield to δ_H 4.52 ppm, indicating that the coupling was successful. The presence of the new methylene protons where confirmed by the appearance of two doublets at δ_H 3.87 ppm and δ_H 3.65 ppm (Fig. 3.41). The ^{13}C NMR spectrum of **173** revealed three carbonyl singlets including the carbonyl of the amide group. The methylene carbon resonated at δ_C 42.2 ppm. The rest of the ^{13}C NMR spectrum was consistent with that of the starting material. Further evidence was given by mass spectrometry data, HRMS (ES): *m/z* 408.1691, which correlated with the calculated value 408.16901 for the molecular formula of $C_{20}H_{27}ClN_3O_4$.

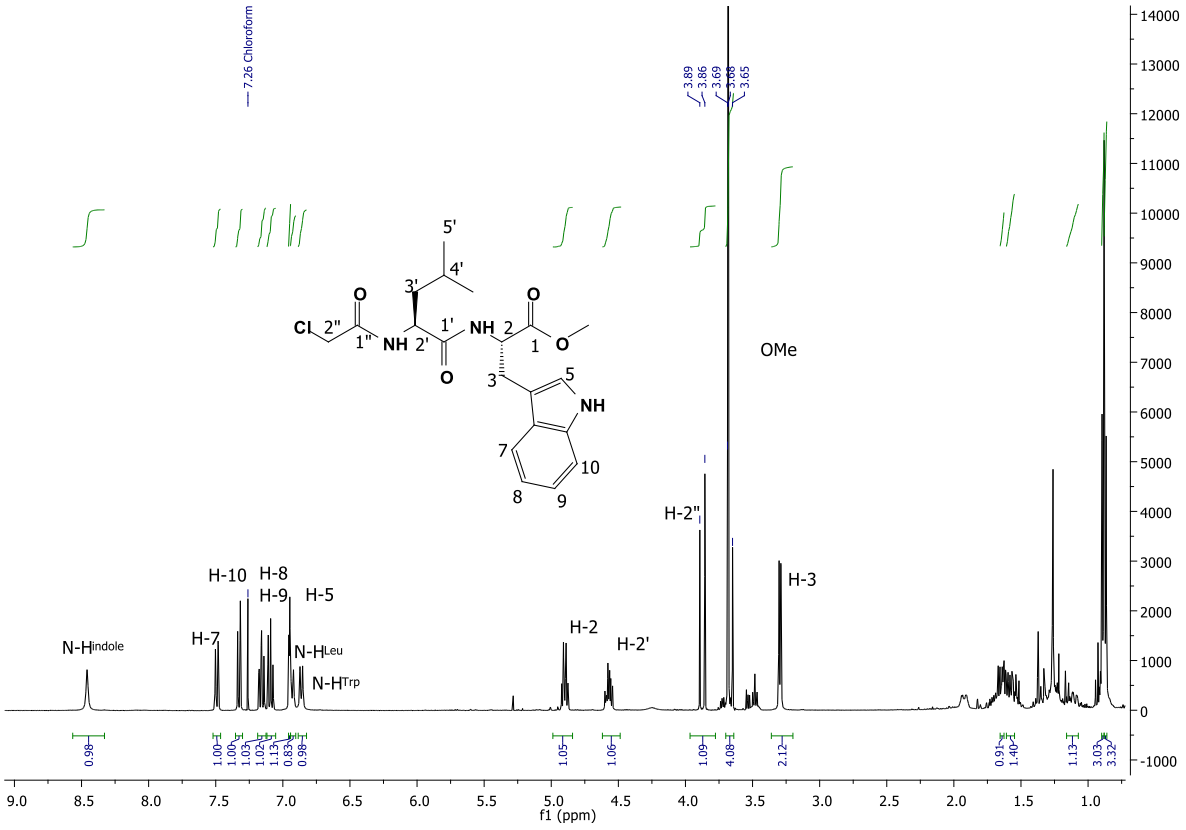

Figure 3.41. ^{1}H NMR spectrum of compound **173**.

Finally, the dipeptide was coupled to the template **172** in an S_N2 reaction onto its chloride by refluxing in acetonitrile with caesium carbonate as base, and following work-up target catalyst **165** was isolated in 60% yield. Its ^{1}H NMR spectrum indicated that the reaction was successful, since the protons for both starting materials were present in the product, and the protons of the tosylate group were absent. In the aromatic region, the protons of the quinoline ring and the indole ring were both present. The amino acid α-protons resonated distinctively at δ_H 4.80 ppm and δ_H 4.65 ppm, while the methylene protons, which were now adjacent to

an oxygen, shifted downfield and appeared as two doublets at δ_H 4.63 ppm and δ_H 4.53 ppm. In the ^{13}C NMR of **165** the carbonyls (the ester and the two amides) were present at δ_C 172.4 ppm, δ_C 172.1 ppm and δ_C 167.8 ppm. The methylene carbon also shifted upfield to δ_C 69.0 ppm. For HRMS (ES), the parent ion was found to be 586.3038 $[M + H]^+$ correlating to the calculated molecular formula of $C_{33}H_{40}N_5O_5$ (requires $(M^+ + H)$ 586.3029), thus confirming the formation of **165**.

The next catalyst to be synthesised was compound **166**. The first step was to couple commercially available (*S*)-(-)-α,α-diphenyl-2-pyrrolidinemethanol **174** with chloroacetyl chloride and triethylamine as base, again with the intention of installing a tether. Following work-up and column chromatography, **175** was isolated in 90% yield (Scheme 3.20).

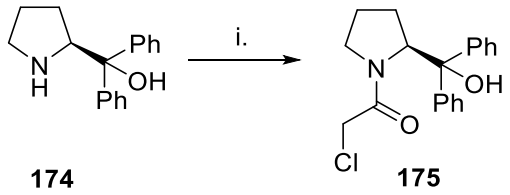

174 **175**

Scheme 3.20. *Reagents and conditions:* (i) chloroacetyl chloride, NEt_3, DCM, 0 °C, 1 hr (90%).

Its ^1H NMR spectrum indicated that the reaction was successful. Figure 3.42 reveals a fully assigned ^1H spectrum showing the ten protons of the two phenyl rings resonated in the aromatic region as two multiplets (integrating for four and six protons), while the hydroxyl group resonated as a singlet at δ_H 6.13 ppm. The α-proton at the chiral centre resonated at δ_H 5.21 ppm, while the methylene protons of the pyrrolidine ring resonated between δ_H 3.45 ppm and δ_H 1.09 ppm. The ^{13}C NMR spectrum of **175** displayed a new peak at δ_C 168.6 ppm corresponding to the carbonyl carbon of the amide group. The carbon corresponding to the methylene group between the carbonyl and the chloride resonated at δ_C 42.1 ppm.

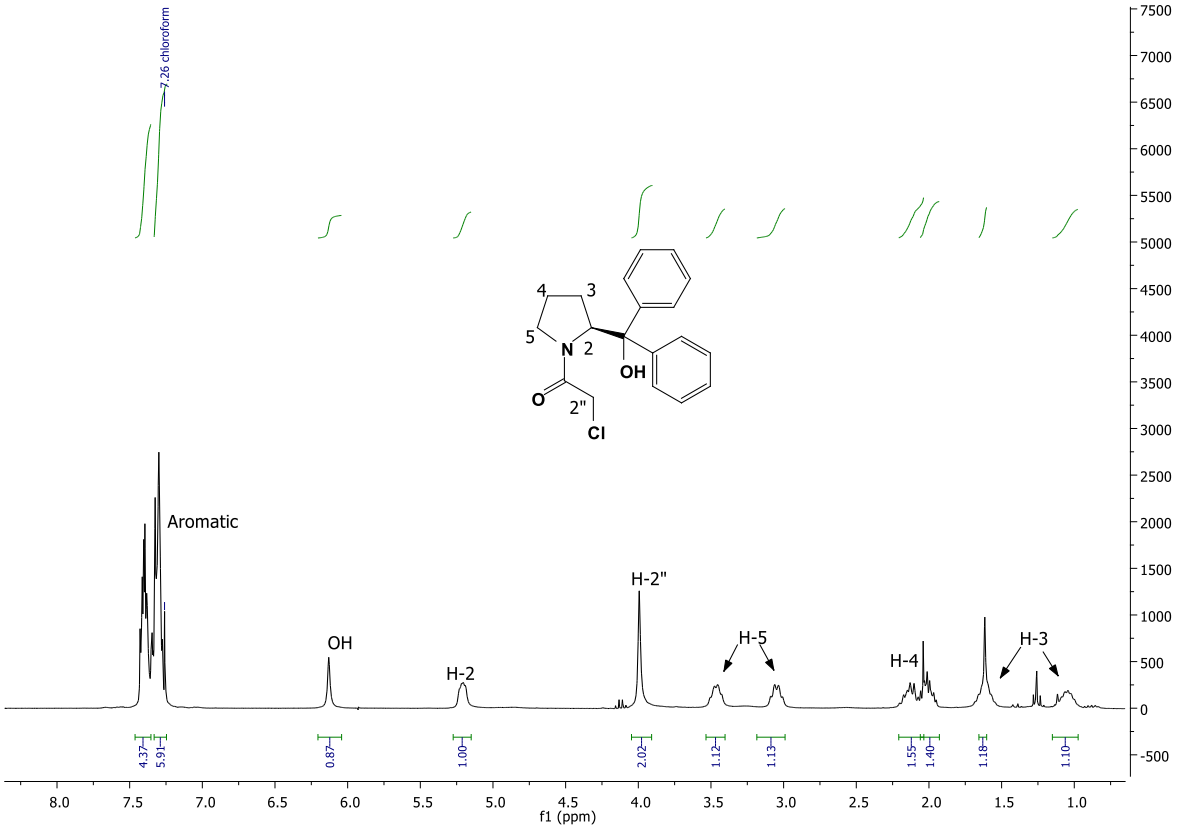

Figure 3.42. ^{1}H NMR spectrum of compound **175**.

The next step was to couple chloride **175** to the template using the S_N2 conditions**.** However, unfortunately the reaction produced several spots on TLC, so it was decided to substitute the chloride with an iodide in the hope of facilitating the substitution. Thus compound **175** was reacted with potassium iodide in CH_3CN at reflux temperature. TLC revealed a new, slightly less polar spot just above the starting material. Following basic work-up and column chromatography, compound **176** was isolated in 83% yield. Its ^{1}H NMR was consistent with that of **176**, in which the methylene hydrogens adjacent to iodide had shifted upfield to δ_H 3.63 ppm. Its ^{13}C NMR spectrum was also consistent with that of an iodide based on a significant upfield shielding of the same methylene (carbon) to δ_C −2.1 ppm, consistent with the presence of an iodide. Finally, a correct HRMS evaluation (*m/z* HRMS (ES) of 422.0614 $[M + H]^+$, agreed favourably with the calculated value of 422.0617 for $C_{19}H_{21}INO_2$.

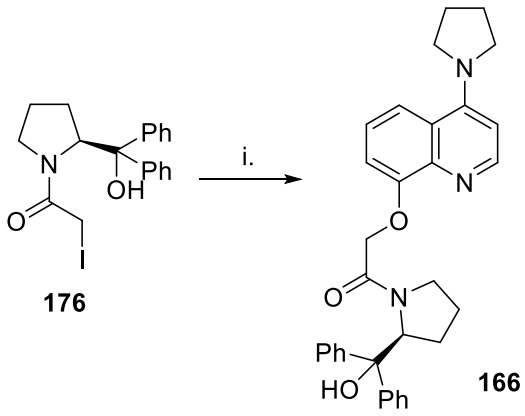

Scheme 3.21. *Reagents and conditions:* (i) **172**, $CsCO_3$, CH_3CN, reflux, 7 days (44%).

With the compound in hand the final step was to couple the template **172** to the iodide **176** under basic conditions using cesium carbonate in acetonitrile. Following work-up and extraction compound **166** was isolated in 44% yield. Its ^1H NMR spectrum indicated that the reaction was successful since protons of the starting material and product were present. The two phenyl rings and the quinoline protons resonated in the aromatic region. The hydroxyl group appeared as a singlet at δ_H 6.49 ppm. The methylene protons resonated at δ_H 5.30 ppm and δ_H 4.86 ppm, while the protons of the pyrrolidine ring resonate at δ_H 3.84 ppm and δ_H 2.12 ppm. The ^{13}C NMR spectrum of the **166** revealed singlets for both starting materials, with diagnostic peaks at δ_C 169.5 ppm corresponding to the carbonyl of the amide and a peak at δ_C 68.6 ppm corresponding to the methyl group of the tether. Finally, a correct HRMS evaluation (*m/z* HRMS (ES) of 508.2600 $[M + H]^+$, agreed favourably with the calculated value of 508.2607 for $C_{33}H_{34}N_3O_3$.

The two quinoline catalysts **165** and **166** were tested in the kinetic resolution of 1-(2-naphthyl)ethanol with *iso*-butyric anhydride as acylating agent (Table 3.10). The quinoline compounds were less reactive as acyl-transfer catalysts than the β-substituted pyridine-based catalysts, based on no reaction occurring at −78 °C. Therefore the temperature was increased to −20 °C, but even at this temperature TLC monitoring indicated that 10 days were needed to achieve a reasonable conversion for the peptide catalyst **165** while virtually no conversion was achieved for **166**. A higher temperature was not investigated as it was felt that there would be no enantioselectivity.

Table 3.10. The kinetic resolution of acylation of 1-(2-naphthyl)ethanol catalysed by **165** and **166**.

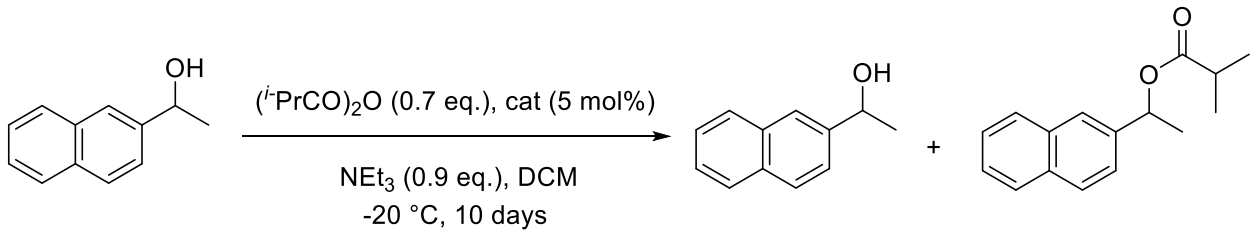

entry[a]	catalyst	C_{HPLC}[b]	ee (alcohol)	ee (ester)[c]	s-value[d]
1.	**165**	31	0.6	1.3	1.0
2.	**166**	3	0.06	2.15	1.0

*a. All reactions were conducted in the presence of 5 mol% **catalyst**, 0.7 eq. of (^{i}PrCO)$_2$O, and 0.9 eq. of Et$_3$N at −20 °C for 10 days, unless otherwise noted. b. Conversion (%) = (ee of recovered alcohol)/(ee of recovered alcohol + ee of ester. c. hydrolysed (2M NaOH in MeOH/H$_2$O) and ee calculated. d. Selectivity factor* $s = \frac{ln(1-C)(1-ee)}{ln(1-C)(1+ee)}$.

Table 3.10 shows that the dipeptide catalyst **165** gave a conversion of 31% compared to the pyrroldine catalyst **166**, which only gave a conversion of 3%. Enantioselectivities for both catalysts were non-existent with reactions giving s-values of only 1 – meaning the rates of the reaction for the two enantiomers were essentially identical. Hence, unfortunately, the concept pursued failed to bear fruit.

Molecular Modelling

Molecular modelling was performed using Spartan ’10 on the acyl-pyridinium ions of **165** and **166** in order to determine the lowest energy conformers (Fig. 3.43). A conformer distribution was calculated using MMFF94 force field[151] for the acylated cations (**165a** and **166a**), as previously described.

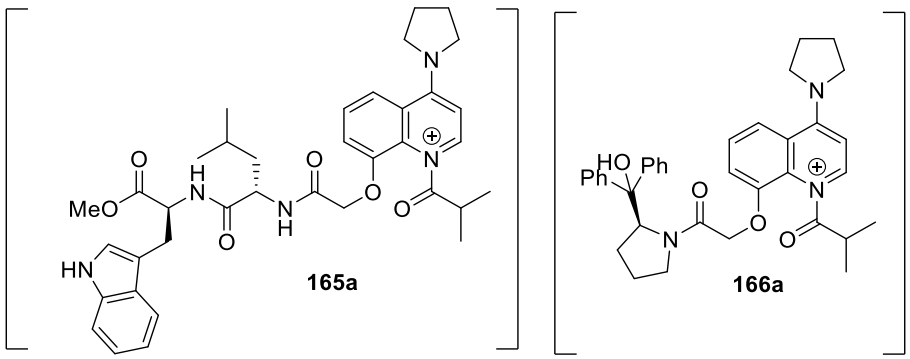

Figure 3.43. Acyl-pyridinium ions of catalysts **165** and **166**.

Figure 3.44 shows the three lowest energy conformers of **165a** in a 63:18:17 ratio and their relative energies as **A**, **B**, and **C** respectively. None of the conformers showed any favourable π–stacking interaction between the indole of the tryptophan and the pyridine ring of the quinoline; however, in each case the quinoline *si* face (w.r.t. the quinoline N; C of C=O of N-acyl group = priority 1, C-8a = priority 2, C-2 = priority 3) was blocked by the peptide chain, although probably too far away from the *N*-acyl group. In the major conformer, **A**, the bulky *iso*-propyl group of the *N*-acyl substituent (in an s-*cis* conformation – priority change compared to the pyridine 3-carboxamide catalysts), points away from the chiral substituent probably due to steric hindrance, while in the minor conformers, **B** and **C**, the *iso*-propyl group points towards the chiral substituent. This could explain the low selectivity, based, as explained previously, on an inversion of stereo-information transfer. However, the low conversion at a higher temperature suggests that several unfavourable factors are operating compared to reaction with catalyst **141**.

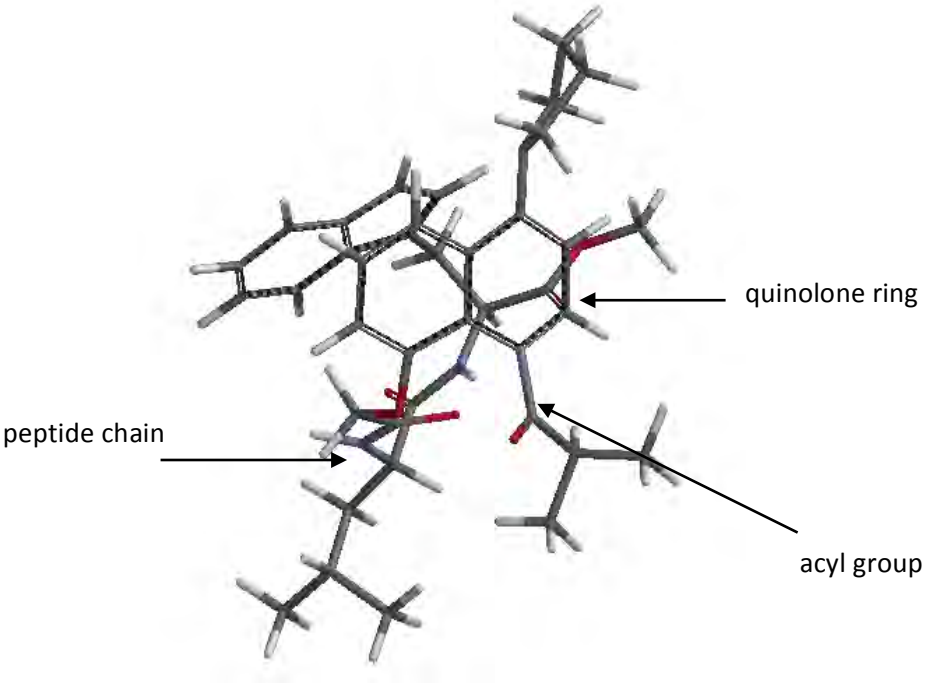

A Rel. energy = 0.00 kJ/mol

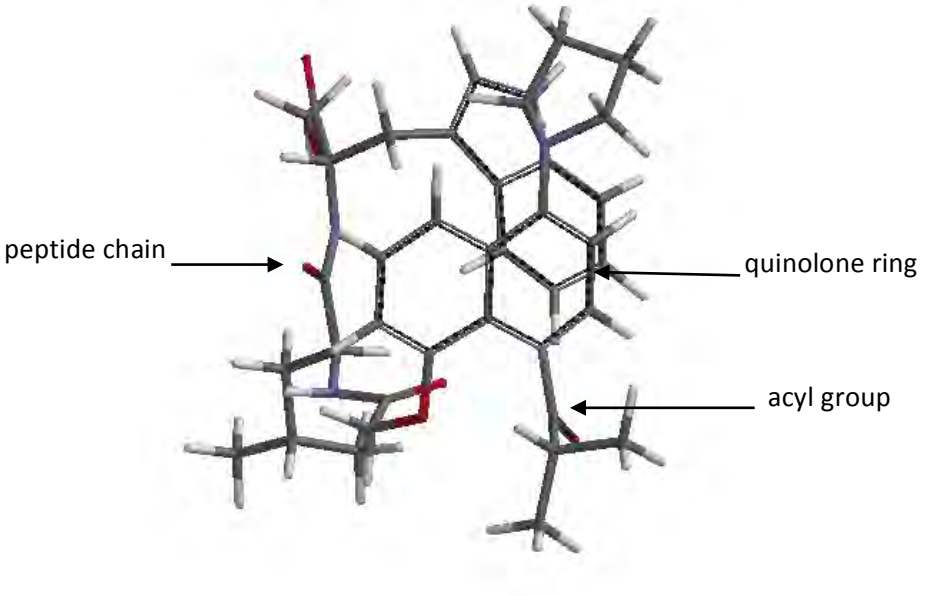

B Rel. energy = 3.10 kJ/mol

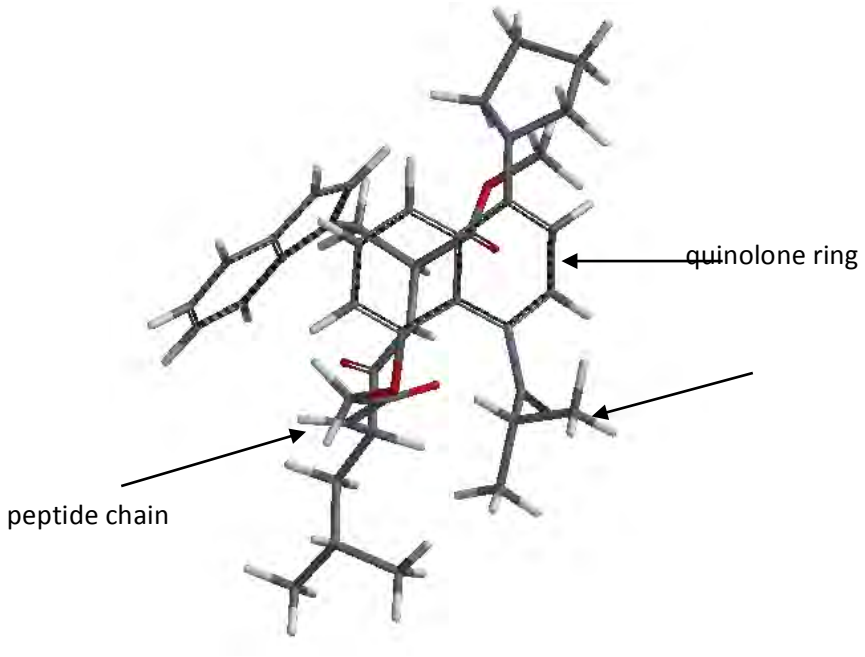

C Rel. energy = 3.12 kJ/mol

Figure 3.44. Lowest energy conformers pyridinium cation **165a**.

Turning to the other quinoline-based catalyst, the three lowest energy conformers of **166a** appeared in a 90:8:1 ratio (**A**, **B**, and **C** respectively, Fig. 3.45). As with **165a** in all three conformers, the quinolone *si* face was blocked by the chiral group, in which H-bonding between the hydroxyl group of the pyrrolidino moiety and the oxygen at C-8 of the quinoline ring may be important (Fig. 3.45). Furthermore, in contrast to **165a** all three conformers preferred placing the *N*-acyl group into an s-*trans* conformation with the carbonyl group pointing away from the quinoline benzene ring. It is unclear why the selectivity was low, since conformer **A** is present in 90% and the chiral chain appears to effectively block one face. However, once again the chiral chain does lie more over the benzene ring quite far away from the carbonyl site, and there is no buttressing on the other (C=O) side. The very low conversion (Table 3.9, entry 2) suggests that the alcohol reagent is associating with the hydroxyl group of the bulky chain through H-bonding (cf. Connon[55] discussed mentioned previously), rather than approaching from the more exposed face. Future studies could study the influence of protecting the tertiary hydroxyl group (as in Jørgensen's organocatalyst)[157] to block such an interaction.

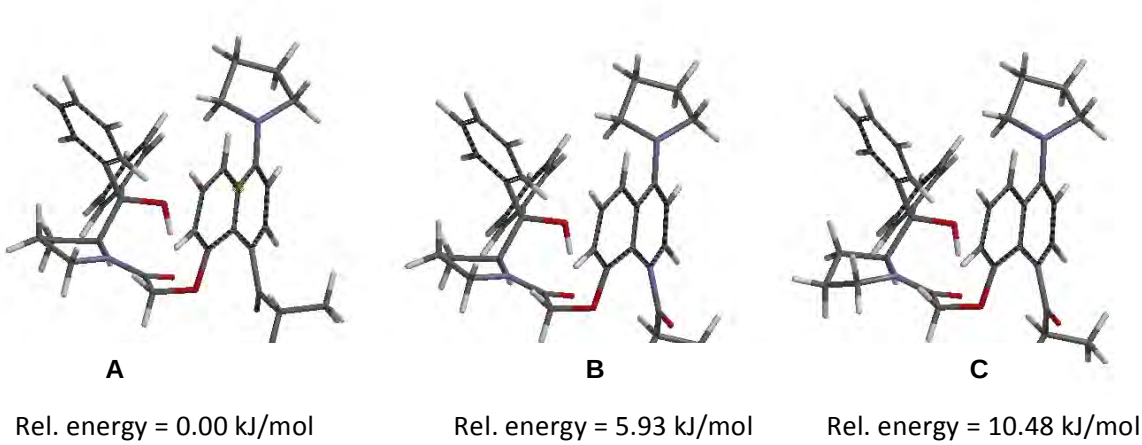

Figure 3.45. Lowest energy conformers pyridinium cation **166a**.

Chapter 4: Conclusion

This part of the thesis has described the synthesis of three classes of asymmetric acyl-transfer catalyst based on DMAP and 4-PPY substituted at the α, β, and γ positions of the pyridine, and in which the chiral directing group was either an amino acid or peptide. The catalysts were designed to explore possible π–stacking effects between the tryptophan and the *N*-acylpyridinium ion. The catalysts were tested in the kinetic resolution of secondary alcohols. γ- and α-substituted catalysts gave no selectivity. A leu-trp β-substituted dipeptide catalyst **128** gave moderate to good selectivity (s = 5.3) with 1-(2-naphthyl)ethanol **121**. Further development of the system culminated in the synthesis of two tripeptide catalysts, which did not improve the s-values, while the Boc-protected dipeptide catalyst of **128** as **141** did lead to an improvement, with the highest s-value of 10.7 with 1-(1-naphthyl)ethanol **132**. Throughout the study computational modelling using Spartan '10 (using molecular mechanics and quantum mechanics) was instrumental in assisting with explanations on selectivity via the generation of putative transition-state (TS) models. The TS model for the successful catalyst **141** suggests a tight π–cation interaction between the pyridinium cation and the indole ring of a tryptophan moiety during the stereodifferentiation step**.**

Future work could include varying the pyridine alkyl substituent of the 4-amino group, since it is known to influence the selectivity.[66,69] The catalyst could also be modified by changing the ester substituent (e.g. from methyl to hexyl) in order to decrease its polarity to make the catalyst more soluble in non-polar solvents. This would allow a study of solvent effects. Finally, the catalysts could be tested in different substrates and reactions: for example, in the kinetic resolution of azlactones, or diamines, the desymmetrization of *meso*-diols, the asymmetric Baylis-Hillman reaction, or the regioselective protection of monosaccharides.

Chapter 5: Experimental

5.1 General procedures

All reactions were performed in oven-dried glassware under an inert atmosphere of dry nitrogen. All starting materials were purchased from either Sigma-Aldrich (South Africa) or Abbliss Chemicals (USA), except for solvents, acids, and common salts. The following reaction solvents were distilled from the indicated drying agents: DCM (P_2O_5), diethyl ether (P_2O_5), THF (Na, benzophenone), acetonitrile (CaH_2), NEt_3 (CaH_2), toluene (CaH_2). Nuclear Magnetic Resonance spectra were recorded on a Varian Mercury 300 MHz (75.5 MHz for ^{13}C) or a Bruker 400 MHz (101 MHz for ^{13}C) instrument. The spectra were recorded in $CDCl_3$, Acetone-d6, CD_3OD-d4, or DMSO-d6 with tetramethylsilane as the internal standard. Chemical shifts are reported in ppm (δ). Coupling constants, *J*, are reported in Hertz. Mass spectra were recorded on a JEOL GCmatell and were recorded in Electron Ionisation mode. Infrared spectra were recorded on Perkin-Elmer Paragon 1000 FT-IR spectrophotometer on NaCl plates. Melting points/decomposition temperatures were determined using a Reichert-Jung Thermovar hot-stage microscope and are uncorrected. Elemental analyses were performed using a Fisons EA 1108 CHNS elemental analyser. Optical rotations were obtained using a Perkin Elmer 343 polarimeter at λ = 589 nm and 20 °C. The concentration *c* refers to g/100mL. Chiral HPLC was performed on an Agilent 1220 Infinity LC system. Analytical chiral HPLC was performed on Chiralpak AD 4.6 mm × 25 cm column, Chiralpak IC 4.6 mm × 25 cm column, or Chiralcel OD 4.6 mm × 25 cm column, using HPLC grade solvent purchased from Merck. The reaction progress was monitored by TLC using Merck silica-gel 60 F254. Visualisation was accomplished with UV light or spraying with anisaldehyde or cerium ammonium sulfate spray reagents and then heating at 150 °C. Column chromatography was performed with Merk silica-gel 60 (70-230 mesh). Flash chromatography: Chrom Tech Flash 150 pump; Foxy R1 fraction collector; Biotage® SNAP cartridge KP-Sil 10 g, 25 g, 50g, 100g.

5.2 Phenolic Ligands

4-*tert*-butyl-2,6-bis(hydroxymethyl)phenol (91)[136]

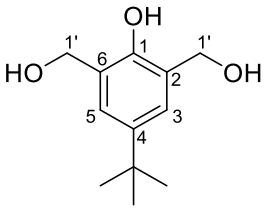

To a stirred mixture of aq. formaldehyde (37%, 16 mL) and aq. NaOH (10%, 40 mL) at r.t., was added 4-(*tert*-butyl)phenol (15 g, 100 mmol) in one portion. After 48 hrs the white precipitate was filtered off, washed with H_2O and treated with aq. HCl (1M, 100 mL). After stirring for 30 minutes the product was filtered off, washed with water, and dissolved in DCM and dried with $MgSO_4$ to give a colourless solid (6.9 g, 33%), ^{1}H NMR (300 MHz, $CDCl_3$) δ 8.11 (br. s, 1H, OH_{phenol}), 7.09 (s, 2H, *H-3, H-5*), 4.91 (s, 4H, *H-1'*), 3.29 (s, 2H, 2 x *OH*), 1.27 (s, 9H, *t*-Bu).

(4-(*tert*-butyl)-1-methoxy-2,6-phenylene) (92)[136]

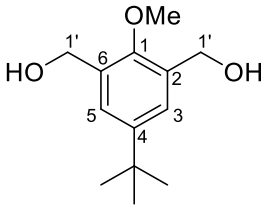

To a stirred suspension of **91** (2.78 g, 13.2 mmol) and K_2CO_3 (909 mg, 6.58 mmol) at r.t., in acetonitrile (50 mL), was added methyl iodide (1.65 mL, 26.5 mmol) in one portion. After 48 hrs at 65 °C, the mixture was cooled to r.t. and filtered. The solvent was removed under reduced pressure and the residue dissolved in DCM, washed with aq. (sat.) $NaHCO_3$ followed by aq. (sat.) NaCl, dried over $MgSO_4$, and the solvent removed to give a colourless solid (2.04 g, 70%), ^{1}H NMR (300 MHz, $CDCl_3$) δ 7.32 (s, 2H, *H-3, H-5*), 4.67 (s, 4H, *H-1'*), 3.78 (s, 3H, *OMe*), 2.49 (s, 2H, 2 x *OH*), 1.27 (s, 9H, *t*-Bu).

5-*tert*-butyl-2-methoxybenzene-1,3-dioic acid (93)[136]

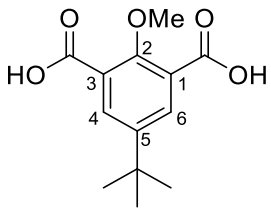

To a stirred solution of **92** (2.83 g, 12.6 mmol), NaOH (2.02 g, 122 mmol) and Adogen 464 (5 drops) at 50 °C in H_2O (50 mL), was added $KMnO_4$ (19.3 g, 122 mmol) in one portion. After 2 hrs, the reaction mixture was heated to reflux temperature for 10 minutes, after which it was cooled to r.t., filtered through Celite ®, washed with 5% aq. NaOH and cooled to 0 °C. The resulting solution was acidified with 1M HCl to pH 1 to give a white precipitate (2.29 g, 72%), which was dried under vacuum at 50 °C, ^{1}H NMR (400 MHz, $CDCl_3$) δ 8.93 (br. s, 2H, 2 x *COOH*), 8.33 (s, 2H, *H-4, H-6*), 4.09 (s, 3H, *OMe*), 1.36 (s, 9H, *t*-Bu).

5-*tert*-butyl-2-hydroxybenze-1,3-dioic acid (94)[136]

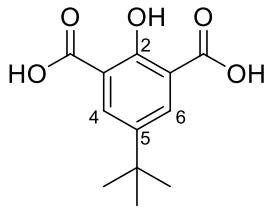

Compound **93** (1.00 g, 3.69 mmol) as added to 33% HBr/AcOH (5 mL) and the resulting suspension was heated at 120 °C for 30 minutes. The resulting orange mixture was cooled to r.t. and diluted with ice cold water (25 mL), to give a pale-yellow precipitate. The product was filtered, washed with water and dried under vacuum to give a white powder (822 mg, 87%) that was used in the next step without further purification, ^{1}H NMR (400 MHz, $(CD_3)_2CO$) δ 8.91 (s, 1H, $OH_{phenolic}$), 8.19 (s, 2H, *H-4, H-6*), 1.32 (s, 9H, *t*-Bu).

2,6-bis(bromomethyl)-4-(*tert*-butyl)phenol (105) and 2,6-bis(bromomethyl)-4-(*tert*-butyl)phenyl acetate (106)

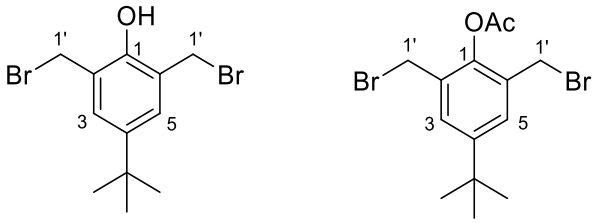

Compound **91** (1.013 g, 4.818 mmol) was dissolved in 33% HBr/AcOH (7 mL) and stirred at r.t. After 24 hrs, ice (20 g) was added followed by petroleum ether (30 mL). The aqueous layer was washed twice more with petroleum ether (30 mL). The combined organic layer was washed with water and dried over $MgSO_4$, and the solvent removed to give a brown solid, which was used in the next step without further purification (1.66 g), **105**: ^{1}H NMR (300 MHz, $CDCl_3$) δ 7.27 (s, 2H, *H-3, H-5)*, 5.49 (s, 1H, *OH*), 4.57 (s, 4H, *H-1'*), 1.29 (s, 9H, *t*-Bu); **106**: ^{1}H NMR (300 MHz, $CDCl_3$) δ 7.39 (s, 2H, *H-3*, *H-5)*, 4.38 (s, 4H, *H-1'*), 2.44 (s, 3H, *CH_3*), 1.32 (s, 9H, *t*-Bu).

L-Tryptophan methyl ester (101)[147]

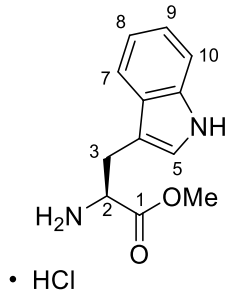

Thionyl chloride (7.2 mL, 99 mmol) was added dropwise to MeOH (120 mL) at 0 °C over 5 minutes. After 20 minutes L-tryptophan (10.0 g, 49.0 mmol) was added and the resulting solution stirred at r.t. After 10 hrs, the solvent was removed at reduced pressure to afford a crude solid that purified by recrystallization using MeOH/diethyl ether to give **101** as a colourless solid (8.4 g, 67% mmol), $[\alpha]_D^{20}$ + 19.0 (*c* 5.0, MeOH) (+ 18 Sigma-Aldrich); ^{1}H NMR (400 MHz, CD_3OD) δ 10.57 (s, 1H, *N-H_{indole}*), 7.54 (d, *J* = 8.0 Hz, *H-7*), 7.40 (d, *J* = 8.0 Hz, 1H, m, *H-10*), 7.21 (s, 1H, *H-5*), 7.14 (m, 1H, *H-9*), 7.07 (m, 1H, *H-8*), 4.33 (m, 1H, *H-2*), 3.78 (s, 3H, *OMe*), 3.47 (dd, *J* = 15.1, 6.3 Hz, 1H, *H-3*), 3.37 (dd, *J* = 15.1, 6.3 Hz, 1H, *H-3*).

Fmoc-Leu-Trp-OMe (103)[158]

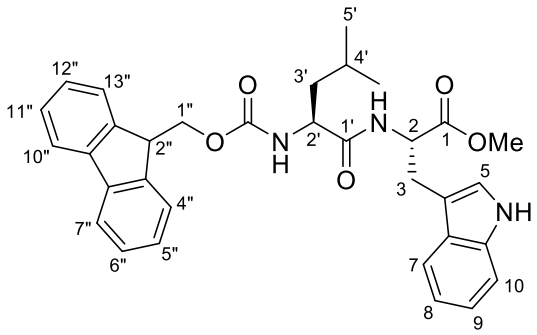

To a stirred solution of Fmoc-Leu-OH (606 mg, 1.72 mmol) and HCl-Trp-OMe (524 mg, 2.06 mmol) in pyridine (10 mL) at r.t., was added EDC (349 mg, 2.06 mmol) followed by HOBt (28 mg, 0.21 mmol). After 18 hrs 1M HCl (15 mL) was added followed by ethyl acetate (3 x 25 mL). The combined organic extracts was washed with 1 M HCl (3 x 50 mL) and dried over anhydrous $MgSO_4$. The solvent was removed to give a yellow residue that was purified by ethyl acetate/hexane (40/60) to afford Fmoc-Leu-Trp-OMe as a colourless solid (927 mg, 97%), mp 146–148 °C; $[\alpha]_D^{20}$ − 4.5 (*c* 0.5, MeOH); IR (DCM) 3055, 2989, 2309, 1422, 1266 cm^{-1}; ^1H NMR (400 MHz, $CDCl_3$) δ 7.97 (s, 1H, *N-H*$_{indole}$), 7.77 (d, *J* = 7.5 Hz, 2H, *H-7”*, *10”*), 7.55 (m, 2H, *H-4”*, *H-13”*), 7.50 (m, 1H, *H-7*), 7.41 (m, 2H, *H-5”*, *H-12”* or *H-6”*, *H-11”*), 7.31 (m, 2H, *H-5”*, *H-12”* or *H-6”*, *H-11”*), 7.26 (m, 1H, *H-10*), 7.13 (ddd, *J* = 8.1, 7.1, 1.2 Hz, 1H, *H-9*), 7.07 (ddd, *J* = 8.1, 7.1, 1.2 Hz, 1H, *H-8*), 6.95 (br. s, 1H, *H-5*), 6.51 (d, *J* = 7.9 Hz, 1H, *N-H*$_{Trp}$), 5.10 (d, *J* = 8.6 Hz, 1H, *N-H*$_{Leu}$), 4.90 (m, 1H, *H-2*), 4.39 (m, 1H, *H-1”*), 4.26 (m, 1H, *H-1”*), 4.22 –4.13 (m, 2H, *H-2’*, *H-2”*), 3.66 (s, 3H, *OMe*), 3.30 (d, *J* = 5.5 Hz, 2H, *H-3*), 1.60 (m, 2H, *H-3’*, *H-4’*), 1.44 (m, 1H, *H-3’*), 0.89 (br. s, 6H, *H-5’*); ^{13}C NMR (101 MHz, $CDCl_3$) δ 172.0 (CO), 171.9 (CO), 171.8 (CO), 143.8 (q), 141.3 (q), 136.1 (q), 127.8 (C-5”, C-12” or C-6”, C-11”), 127.1 (C-5”, C-12” or C-6”, C-11”), 125.1 (C-4” or C-13”), 125.0 (C-4” or C-13”), 123.0 (C-5), 122.2 (C-9), 120.0 (C-7”, C-10”), 119.6 (C-7), 118.5 (C-8), 111.7 (q), 111.7 (C-10), 109.7 (q), 67.0 (C-1”), 53.5 (C-3), 52.8 (C-2), 52.4 (O$\underline{C}H_3$), 47.1 (C-2”), 41.5 (C-3’), 27.6 (C-3), 24.6 (C-4’), 22.9 (C-5’), 21.9 (C-5’); Anal. Found C, 70.67; H, 6.67; N, 7.75 $C_{33}H_{35}N_3O_5$ requires C, 71.59; H, 6.37; N, 7.59; Chiralcel OD 20% isopropyl alcohol/hexane, 1.0 mL/min, 254 nm, 13.452 min.

NH_2-Leu-Trp-OMe (104)

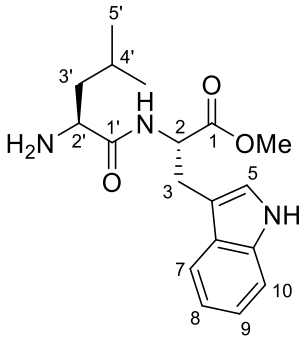

To a stirred solution of **103** (150.3 mg, 0.2715 mmol) in DCM (2 mL) at 0 °C, was added piperidine (0.05 mL, 0.5 mmol). After 18 hrs, the solvent was removed *in vacuo* to give a crude product that was purified by column chromatography using MeOH/DCM (10/90) to afford **104** as a clear oil (58.0 mg, 64%), $[\alpha]_D^{20}$ + 39.8 (*c* 1.0, DCM, 91% ee); IR (DCM) 3412 (NH), 2958, 1740 (CO_2Me), 1659 $(CO)_{amide}$, 1514, 1216 cm−1;^{1}H NMR (400 MHz, $CDCl_3$) δ 8.27 (br. s, 1H, *N-H_{indole}*), 7.71 (d, *J* = 8.3 Hz, 1H, *N-H_{Trp}*), 7.55 (m, 1H, *H-7*), 7.34 (m, 1H, *H-10*), 7.17 (m, 1H, *H-9*), 7.10 (m, 1H, *H-8*), 6.99 (s, 1H, *H-5*), 4.92 (m, 1H, *H-2*), 3.69 (s, 3H, *OMe*), 3.31 (m, 3H, *H-3, H-2'*), 1.63 (m, 2H, *H-4', H-3'*), 1.18 (m, 1H, *H-3'*), 0.91 (d, *J* = 6.4 Hz, 3H, *H-5'*), 0.87 (d, *J* = 6.4 Hz, 3H, *H-5'*); ^{13}C NMR (101 MHz, $CDCl_3$) δ 175.4 (CO),172.6 (CO), 136.1 (q), 127.7 (q), 122.6 (C-5), 122.1 (C-9), 119.5 (C-8), 118.7 (C-7), 111.2 (C-10), 110.4 (q), 53.4 (C-2), 52.7 (C-2'), 52.2 ($O\underline{C}H_3$), 43.9 (C-3'), 27.8 (C-3), 24.8 (C-4'), 23.4 (C-5'), 21.3 (C-5'); HRMS (ES): *m/z* 332.1962 $[M + H]^+$. Calculated for $C_{18}H_{26}N_3O_3$, 332.1974 $[M + H]^+$; Chiralpak AD 30% isopropyl alcohol/hexane, 1.0 mL/min, 254 nm, 6.628 min.

Methyl (*tert*-butoxycarbonyl)-L-cysteinate (107)

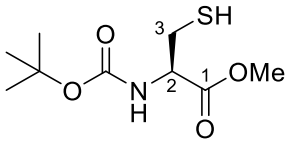

To a stirred suspension of HCl-cys-OMe (1.000 g, 5.827 mmol) in DCM (30 mL) at 0 °C was added Boc_2O (1.304 g, 5.975 mmol) and $NaHCO_3$ (1.477 g, 17.58 mmol). After 18 hrs water (30 mL) was added followed by DCM (3 x 30 mL). The combined organic extracts were washed with brine (3 x 90 mL) and dried over anhydrous $MgSO_4$. The solvent was removed under reduced pressure to afford **107** as a clear oil, which was used in the next step without

further purification (1.347 g, 98%), ^{1}H NMR (400 MHz, $CDCl_3$) δ 5.38 (br. s, 1H, *N-H*), 4.60 (br. s, 1H, *H-2*), 3.75 (s, 3H, *OMe*), 2.99 (m, 2H, *H-3*), 1.43 (s, 9H, *t*-Bu).

Dimethyl 2,2'-((5-(*tert*-butyl)-2-hydroxyisophthaloyl)bis(azanediyl))(2*S*,2'*S*)-bis(4-methylpentanoate) (95)

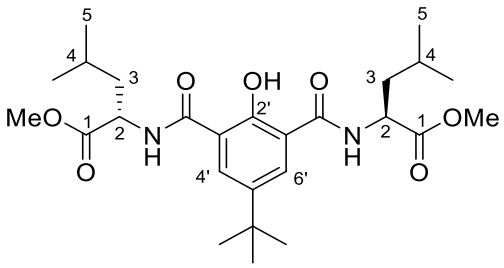

Compound **94** (2.004 g, 8.412 mmol) was dissolved in thionyl chloride (10 mL, 137 mmol) and the resulting solution stirred at reflux temperature. After 45 minutes, the thionyl chloride was removed under reduced pfressure to give the crude acid chloride that was dissolved in DCM (25 mL). Triethylamine (4.5 mL, 33 mmol) was added dropwise to a suspension of HCl-L-leucine-OMe (4.583 g, 19.425.25 mmol) in DCM (25 mL) at 0 °C. After 20 minutes the solution of free amine was added dropwise to the crude acid chloride, and the resulting mixture stirred at r.t. After 1 hour 1M HCl (50 mL) was added and the aqueous layer extracted with DCM (3 x 50 mL). The combined organic extracts were dried over anhydrous $MgSO_4$ and the solvent evaporated to afford a yellow residue that was purified by column chromatography using ethyl acetate/hexane (20/80), to provide **97** as a pale-yellow solid (1.352 g, 33%), mp 63–66 °C; $[\alpha]_D^{20}$ + 19.3 (*c* 1.0, DCM); IR (DCM) 3386 (OH), 3055, 2963, 1744 (CO_2Me), 1660, 1527, 1422, 1266 cm^{-1}; ^{1}H NMR (300 MHz, $CDCl_3$) δ 13.90 (s, 1H, *OH*), 8.11 (d, *J* = 7.7 Hz, 2H, *N-H*), 7.92 (s, 2H, *H-4', H-6'*), 4.81 (m, 2H, *H-2*), 3.79 (s, 3H, *OMe*), 1.75 (m, 6H, *H-3, H-4*), 1.26 (s, 9H, *t-Bu*), 0.98 (d, *J* = 4.7 Hz, 6H, *H-5*), 0.97 (d, *J* = 4.7 Hz, 6H, *H-5*); ^{13}C NMR (75 MHz, $CDCl_3$) δ 173.8 (CO), 167.6 (CO), 158.3 (q), 141.2 (q), 130.3 (C-4', C-6'), 116.8 (q), 52.3 ($O\underline{C}H_3$), 51.3 (C-2,), 41.1 (C-3), 34.3 (q), 31.2 ($C(\underline{C}H_3)_3$), 25.0 (C-4), 22.8 (C-5), 21.8 (C-5); Anal. Found C, 63.77; H, 8.19; N, 5.37 $C_{26}H_{40}N_2O_7$ requires C, 63.39; H, 8.18; N, 5.69.

Dimethyl 2,2'-((5-(*tert*-butyl)-2-hydroxyisophthaloyl)bis(azanediyl))(2*S*,2'*S*)-bis(3-(1*H*-indol-3-yl)propanoate) (96)

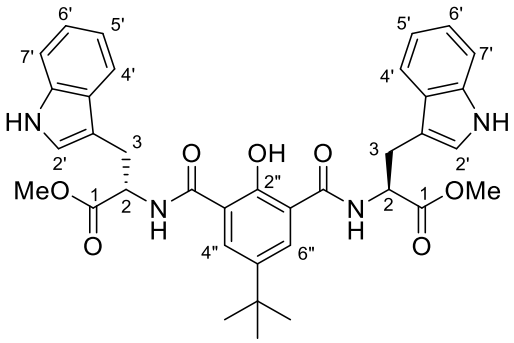

Compound **94** (600 mg, 2.52 mmol) was dissolved in thionyl chloride (3 mL, 41 mmol) and the resulting solution was stirred at reflux temperature. After 45 minutes, the thionyl chloride was removed under reduced pressure to give the crude acid chloride that was dissolved in DCM (10 mL). Triethyl amine (1.6 ml, 11 mmol) was added dropwise to a suspension of HCl-L-tryptophan-OMe (1.935 g, 7.600 mmol) in DCM (10 mL) at 0 °C. After 20 minutes the free amine was added dropwise to the crude acid chloride, and the resulting mixture stirred at r.t. After 1 hour 1 M HCl (20 mL) was added and the aqueous layer extracted with DCM (3 x 20 mL). The combined organic extracts were dried over anhydrous $MgSO_4$ and the solvent evaporated to afford a yellow residue that was purified by column chromatography using ethyl acetate/hexane (50:50), to provide **96** as a pale- yellow solid (992 mg, 62%), mp 121–124 °C; $[\alpha]_D^{20}$ + 13.5 (*c* 1.0, $CHCl_3$); IR (DCM) 3413 (OH), 2104, 1729 (CO_2Me), 1653, 1525, 1265 cm^{-1}; ^1H NMR (400 MHz, $CDCl_3$) δ 8.22 (s, *2*H, *N-H*$_{indole}$), 7.87 (d, *J* = 6.9 Hz, 2H, *N-H*$_{amide}$), 7.76 (s, 2H, *H-4", H-6"*), 7.57 (d, *J* = 8.0 Hz, 2H, *H-4'*), 7.34 (d, *J* = 8.0 Hz, 2H, *H-7'*), 7.17 (td, *J* = 7.6 Hz, 1.2 Hz, 2H, *H-6'*), 7.09 (td, *J* = 7.6 Hz, 1.2 Hz, 2H, *H-5'*), 7.06, (d, *J* = 2.4 Hz, 2H, *H-2'*), 5.08, (m, 2H, *H-2*) 3.71 (s, 6H, *OMe*), 3.43 (d, *J* = 5.7 Hz, 4H, *H-3*), 1.15 (s, 9H, *t-Bu*); ^{13}C NMR (101 MHz, $CDCl_3$) δ 172.2 (CO), 167.4 (CO), 158.3 (q), 141.4 (q), 136.2 (q), 130.2 (C-4", C-6"), 127.5 (q), 122.9 (C-2'), 122.3 (C-6'), 119.9 (C-5'), 118.4 (C-4'), 117.0 (q), 111.3 (C-7'), 109.9 (q), 53.6 (C-2), 53.6 ($O\underline{C}H_3$), 34.1 (q), 31.1 ($C(\underline{C}H_3)_3$), 27.5 (C-3); HRMS (ES): *m/z* 639.2817 $[M + H]^+$. Calculated for $C_{36}H_{39}N_4O_7$, 639.2819 $[M + H]^+$.

Dimethyl 2,2'-(((2*S*,2'*S*)-2,2'-((5-(*tert*-butyl)-2-hydroxyisophthaloyl)bis(azanediyl))bis(4-methylpentanoyl))bis(azanediyl))(2*S*,2'*S*)-bis(3-(1*H*-indol-3-yl)propanoate) (97)

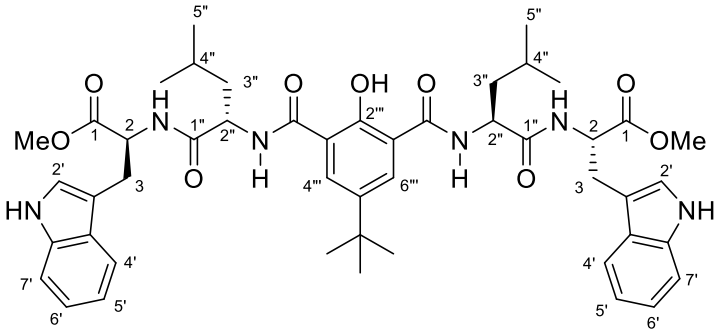

To a stirred solution of **94** (154.4 mg, 0.6481 mmol) and NH_2-Leu-Trp-OMe (493.0 mg, 1.488 mmol) in pyridine (10 mL), at r.t., was added EDC (311.0 mg, 1.622 mmol) followed by HOBt (174.8 mg, 1.293 mmol). After 18 hrs 1M HCl (15 mL) was added followed by extraction with ethyl acetate (3 x 30 mL). The combined organic extracts were washed with 1M HCl (3 x 100 mL) and dried over anhydrous $MgSO_4$. The solvent was removed to give a yellow residue that was purified by ethyl acetate/hexane (40/60) to afford **97** as a colourless solid (377 mg, 60%), mp 124–127 ^{o}C; $[\alpha]_D^{20}$ − 9.1 (*c* 0.28, MeOH); IR (DCM) 3290, 3052, 1738, 1664, 1368 cm^{-1}; ^{1}H NMR (400 MHz, $CDCl_3$) δ 13.76 (s, 1H, *OH$_{phenolic}$*), 8.42 (s, 2H, *N-H$_{indole}$*), 7.89 (s, 2H, *H-4"', H-6"'*), 7.80 (d, *J* = 7.8 Hz, 2H, *N-H$_{Leu}$*), 7.50 (d, *J* = 7.7 Hz, 2H, *H-4'*), 7.21 (d, *J* = 7.7 Hz, 2H, *H-7'*), 7.03 (m, 4H, *H-5', H-6'*), 6.98 (s, 2H, *H-2'*), 6.82 (d, *J* = 7.5 Hz, 2H, *N-H$_{Trp}$*), 4.93 (m, 2H, *H-2*), 4.70 (m, 2H, *H-2"*), 3.68 (s, 6H, *OMe*), 3.34 (m, 4H, *H-3*), 1.73 (m, 6H, *H-3", H-4"*), 1.30 (s, 9H, *t-Bu*), 0.93 (br. s, 6H, *H-5"*), 0.92 (br. s, 6H, *H-5"*); ^{13}C NMR (101 MHz, $CDCl_3$) δ 172.3 (CO), 171.8 (CO), 167.7 (CO), 158.1 (q), 141.7 (q), 136.4 (q), 130.2 (C-4"', C-6"'), 127.6 (q), 123.2 (C-2'), 122.1 (C-5' or C-6'), 119.5 (C-5' or C-6'), 118.4 (C-4'), 117.2 (q), 111.4 (C-7'), 109.5 (q), 53.2 (C-2), 52.3 (C-2", O$\underline{C}H_3$), 41.0 (C-3"), 34.4 (q), 31.3 (C($\underline{C}H_3$)$_3$), 27.6 (C-3'), 25.0 (C-4"), 22.9 (C-5"), 22.1 (C-5"); HRMS (ES): *m/z* 865.4491 $[M + H]^+$, Calculated for $C_{48}H_{61}N_6O_9$, 865.4500 $[M + H]^+$.

Dimethyl 3,3'-(((5-(*tert*-butyl)-2-hydroxy-1,3-phenylene)bis(methylene)) bis(sulfanediyl))(2*R*,2'*R*)-bis(2-((*tert*-butoxycarbonyl)amino)propanoate) (98)

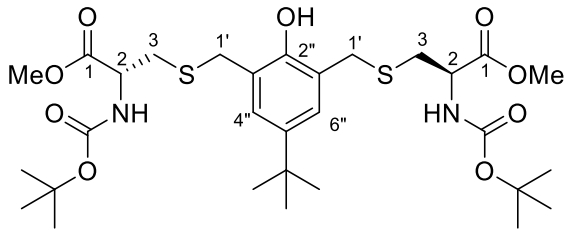

Triethylamine (0.52 mL, 3.7 mmol) was added dropwise to stirred solution of Boc-Cys-OMe (622 mg, 2.64 mmol), **105** and **106** (320 mg), in DCM (5 mL). After 30 minutes, the solvent was removed at reduced pressure to afford a yellow residue that was dissolved in dry MeOH (5 mL). To this mixture, K_2CO_3 (171 mg, 1.24 mmol) was added, and the resulting suspension stirred for 30 minutes at −5 °C. The K_2CO_3 was filtered off and following solvent removal the residue purified by column chromatography (ethyl acetate/hexane) (30:70) to afford a yellow oil that solidified after drying under vacuum (528 mg, 66%), $[\alpha]_D^{20}$ − 15 (*c* 1.0, DCM); IR (DCM) 3423 (OH), 2958, 1745 (CO_2Me), 1713 (Boc), 1504, 1367, 1266 cm^{-1}; ^1H NMR (400 MHz, $CDCl_3$) δ 7.08 (s, 2H, *H-4”, H-6”*), 6.67 (s, 1H, *OH*), 5.37 (br. s, 2H, *N-H*), 4.54 (m, 2H, *H-2*), 3.84 (d, *J* = 12.9 Hz, 2H, *H-1’*), 3.79–3.69 (m, 6H, *H-1’, OMe*), 2.91 (dd, *J* = 14.0, 4.6 Hz, 2H, *H-3*), 2.76 (dd, *J* = 14.0, 6.8 Hz, 2H, *H-3*), 1.44 (s, 18H, 2 x *t*-Bu), 1.27 (s, 9H, *t*-Bu); ^{13}C NMR (101 MHz, $CDCl_3$) δ 171.6 (CO), 155.4 (q), 150.8 (CO), 143.2 (q), 127.1 (C-4”, C-6”), 123.5 (q), 80.3 (q), 52.9 (C-2), 52.8 ($O\underline{C}H_3$), 34.2 (C-3), 32.3 (C-1’), 31.4 ($C(\underline{C}H_3)_3$), 28.3 ($C(\underline{C}H_3)_3$); HRMS (ES): *m/z* 645.2881 $[M + H]^+$. Calculated for $C_{30}H_{49}N_2O_9S_2$, 645.2880 $[M + H]^+$.

General Prodedure for the Scandium-ligand-catalysed alcoholysis of cyclohexne oxide: To a stirred suspension of $Sc(OTf)_3$ (0.01 mmol) and ligand (0.015 mmol or 0.020 mmol) in DCM (5 mL) at −78 °C – and in the cases where a base was used (NEt_3 (0.016 mmol) or NaH (0.016 mmol)/THF (5 mL)) – was added BnOH (4.1 mmol) followed by cyclohexene oxide (1.0 mmol). After 12 hrs an aliquot of the solution was removed and a mini-work-up performed using EtOAc (1 mL)/1M HCl (1 mL). This was repeated at −20 °C, 0 °C, and r.t. The sample was dried ($MgSO_4$) and the solvent removed and the crude ee evaluated by chiral HPLC, Chiralpak AD (4.6 mm x 25 cm), isopropyl alcohol/hexane (10/90), 1.0 mL/min, 254 nm, 8.52 min (BnOH), 9.07 min, 9.89 min.

trans-2-(benzyloxy)cyclohexan-1-ol (109)

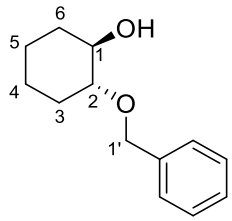

To a stirred solution of cyclohexene oxide (210 mg, 2.14 mmol) and BnOH (441 mg, 4.09 mmol) at 0 °C in DCM (5 mL), was added $Sc(OTf)_3$ (11 mg, 0.022 mmol). After 4 hrs, (sat.) $NaHCO_3$ (5 mL) was added followed by DCM (3 x 5 mL). The combined organic layer was dried over anhydrous $MgSO_4$ and the solvent removed under reduced pressure to give a crude oil that was purified by vacuum distillation to afford the **109** as a pale-yellow oil (71 mg, 16%), ^{1}H NMR (300 MHz, $CDCl_3$) δ 7.35 (s, 5H, *H-Ar*), 4.68 (d, *J* = 12 Hz, 1H, *H-1'*), 4.48 (d, *J* = 12 Hz, 1H, *H-1'*), 3.56–3.41 (m, 1H, *H-1*), 3.31–3.12 (m, 1H, *H-2*), 2.71 (s, 1H, *OH*), 2.20–2.08 (m, 1H, *H-6*), 2.08–1.94 (m, 1H, *H-6*), 1.79–1.61 (m, 2H, *H-3*), 1.40–1.10 (m, 4H, *H-4*, *H-5*).

cis-2-(benzyloxy)cyclohexan-1-ol (111)

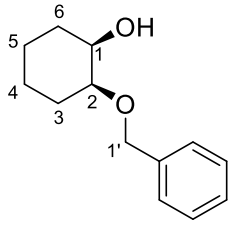

To a stirred solution of *cis*-1,2-cyclohexanediol (100.5 mg, 0.865 mmol) in THF (3.5 mL) at 0 °C was added NaH (60%) (27.6 mg, 1.15 mmol). After 20 minutes, BnBr (0.082 mL, 0.69 mmol) was added. After 2 hrs, water (10 mL) was added, followed by EtOAc (3 x 10 mL). The combined organic layer was dried over anhydrous $MgSO_4$, and the solvent removed under reduced pressure to give a crude compound that was purified by column chromatography suing ethyl acetate/hexane (30/70) to afford **111** as a clear oil (82 mg, 46%), ^{1}H NMR (300 MHz, $CDCl_3$) δ 7.33 (m, 5H, *H-Ar*), 4.63 (d, *J* = 11.8 Hz, 1H, *H-1'*), 4.52 (d, *J* = 11.8 Hz, 1H, *H-1'*), 3.87 (m, 1H, *H-1*), 3.52 (dt, *J* = 8.1, 3.2 Hz, 2H, *H-2*), 2.33 (s, 1H, *OH*), 1.93–1.75 (m, 2H, *H-3*), 1.72–1.46 (m, 4H, *H-3, H-4 or H-5*), 1.42–1.20 (m, 2H, *H-4 or H-5*).

5.3 γ-Sustituted Catalysts

4-(bis-2-hydroxyethyl) aminopyridine (116)[145]

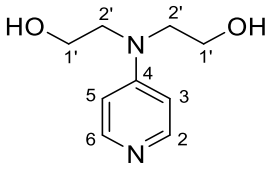

4-Chloropyridine-HCl (10 g, 0.067 mmol) was dissolved in water (50 mL). NaOH 6M (20 mL) was added until the pH rose to 14. The free amine was extracted with ethyl acetate (3 x 70 mL) and the combined organic layers dried over anhydrous $MgSO_4$ to give a brown oil that was used in the next step without further purification. 4-Chloropyridine and diethanolamine (25 mL, 0.23 mmol) were heated to 180 °C. After 5 hrs the mixture was added to a slurry of Na_2CO_3 (10 g) in 2-propanol (150 mL) and refluxed for 30 minutes. The mixture was filtered, washed with 2-propanol, and the solvent removed under reduced pressure to give a viscous oil that was purified by vacuum distillation followed by column chromatography using MeOH/DCM (10/90) to provide **116** as an orange solid (3.9 g, 32%), ^{1}H NMR (400 MHz, CD_3OD) δ 8.04 (m, *H-2, H-6*), 6.79 (m, 2H, *H-3, H-5*), 3.76 (m, 4H, *H-1', H-1'*), 3.64 (m, *4*H, *H-2, H-2'*).

Methyl tosyl-L-tryptophanate (117)[148]

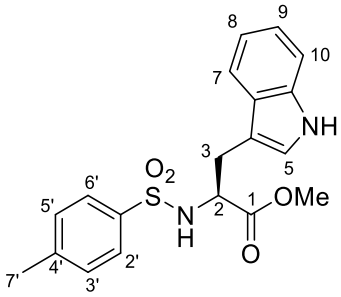

To a stirred suspension of **101** (3.26 g, 12.8 mmol) in DCM (50 mL), at 0 °C, was added triethylamine (5.35 mL, 38.8 mmol) dropwise over 2 minutes. After 10 minutes, toluenesulfonyl chloride (3.67 g, 19.2 mmol) was added. After 90 minutes, water (50 mL) was added, the organic layer was separated and washed with brine (50 mL), dried over $MgSO_4$ and the solvent removed to give a crude oil that was purified by chromatography using ethyl acetate/hexane 30/70 to afford **117** as a pale-orange solid (3.97 g, 83%), $[\alpha]_D^{20}$ +

16.3 (*c* 1.7, THF) (lit.[148] + 17); ^{1}H NMR (400 MHz, $CDCl_3$) δ 8.08 (s, 1H, *N-H$_{indole}$)*, 7.61 (m, 2H, *H-2’*, *H-6’*), 7.43 (m, *J* = 8.0 Hz, 1H, *H-7*), 7.32 (m, 1H, *H-10*), 7.16 (m, 3H, *H-3’*, *H-5’*, *H-9*), 7.07 (ddd, 1H, *J* = 8.0, 7.0, 1.0 Hz, *H-8*), 7.02 (d, 1H, *J* = 2.3, *H-5*), 5.15 (d, 1H, *J* = 8.8 Hz, *N-H*), 4.26 (m, 1H, *H-2*), 3.44 (s, 3H, *OMe*), 3.23 (m, 2H, *H-3*), 2.37 (s, 3H, *H-7’*).

Dimethyl 2,2'-(((pyridin-4-ylazanediyl)bis(ethane-2,1-diyl))bis(tosylazanediyl))(2S,2'S)-bis(3-(1*H*-indol-3-yl)propanoate) (112)

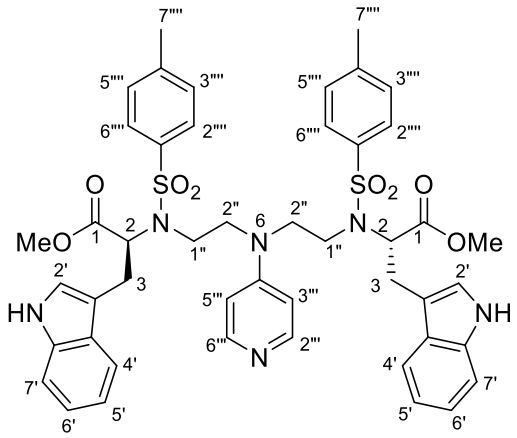

To a stirred solution of **116** (772.3 mg, 4.241 mmol), triphenylphosphine (2.785 g, 10.62 mmol) and **117** (3.636 g, 9.761 mmol) in DMF (7.0 mL) and THF (1.5 mL), at r.t. was added DIAD (2.1 mg, 11 mmol). After 3 hrs, the solvent was removed *in vacuo* to yield a crude residue that was purified by column chromatophraphy using ethyl acetate/hexane (80/20), followed by MeOH/DCM (5/95) to afford **112** as a pale-yellow solid (1.325 g, 36%), mp 106–109 °C; $[\alpha]_D^{20}$ − 30.8 (*c* 0.51, $CHCl_3$); IR (DCM) 1740, 1642, 1342, 1162 cm^{-1}; ^{1}H NMR (400 MHz, $CDCl_3$) δ 8.59 (s, 2H, *N-H$_{indole}$*), 8.19 (d, *J* = 5.6 Hz, 2H, *H-2’”*, *H-6’”*), 7.62 (d, *J* = 8.3 Hz, 4H, *H-2””*, *H-6””*), 7.51 (d, *J* = 8.1 Hz, 2H, *H-4’*), 7.31 (d, *J* = 8.1 Hz, 2H, *H-7’*), 7.16 (m, 6H, *H-6’*, *H-3””*, *H-5””*), 7.07 (m, 4H, *H-2’*, *H-5’*), 6.64 (d, *J* = 5.6 Hz, 2H, m, *H-3’”*, *H-5’”*), 4.92 (m, 2H, *H-2*), 3.53 (m, 15H, *H-1”*, *H-2”*, *H-3*, *OMe*), 3.17 (m, 1H, m, *H-3*), 2.36 (s, 6H, *H-7””*); ^{13}C NMR (101 MHz, $CDCl_3$) δ 171.4 (CO), 152.5 (q), 149.7 (C-2”’, C-6’”), 143.7 (q), 136.2 (q), 135.8 (q), 129.5 (C-3””, C-5””), 127.4 (C-2””, C-6””), 127.0 (q), 123.1 (C-2’), 122.1 (C-6), 119.5 (C-5), 118.3 (C-4), 111.3 (C-7), 109.6 (q), 106.5 (C-3”’, C-5”’), 59.5 (C-2), 52.0 (O$\underline{C}$H$_3$) 50.7 (C-1’) 41.8 (C-2’), 27.0 (C-3), 21.9 (C-7””); HRMS (ES): *m/z* 891.3208 $[M + H]^+$, Calculated for $C_{45}H_{51}N_6O_8S_2$, 891.3210 $[M + H]^+$.

L-Tryrosine methyl ester hydrochloride (119)[149]

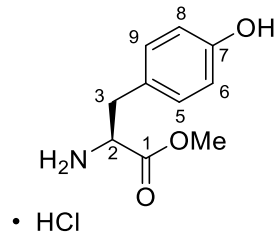

Acetyl chloride (28.0 mL, 329 mmol) was added dropwise to MeOH (220 mL) at 0 °C over 5 minutes. After 20 minutes L-tyrosine (10.0 g, 55.2 mmol) was added and the resulting solution stirred at reflux temperature. After 12 hrs, the solvent was removed at reduced pressure to afford a colourless solid (12.3 g, 96%) that was used in the next step without further purification, $[\alpha]_D^{20}$ + 68.8 (*c* 3.0, pyridine) (lit.[150] +76); ^{1}H NMR (400 MHz, CD_3OD) δ 7.08 (m, 2H, *H-6, H-8*), 6.79 (m, 2H, *H-5, H-9*), 4.23 (m, 1H, *H-2*), 3.80 (d, *J* = 2.9 Hz, 3H, *OMe*), 3.14 (dd, *J* = 14.5, 6.7 Hz, 2H, *H-3*).

Methyl (*tert*-butoxycarbonyl)-L-tyrosinate (120)[149]

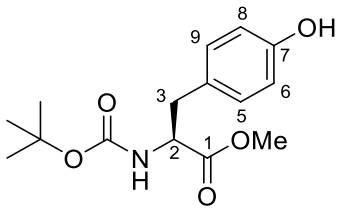

Di-*tert*-butyl dicarbonate (5.6 g, 26 mmol) was added to a stirred slurry of **119** (5.0 g, 22 mmol) and $NaHCO_3$ (2.2 g, 26 mmol) in ethanol (102 mL) at r.t. After 18 hrs the solution was filtered and the solvent evaporated to give a crude solid that was purified by column chromatography using ethyl acetate/hexane (20/80) to afford **120** as a colourless solid (2.2 g, 33%), $[\alpha]_D^{20}$ + 51.3 (*c* 1.0, $CHCl_3$) (lit.[159] + 52.8); ^{1}H NMR (300 MHz, $CDCl_3$) δ 6.96 (m, 2H, *H-6, H-8*), 6.72 (d, *J* = 8.3 Hz, 2H, *H-5, H-9*), 5.85 (s, 1H, *OH*), 5.01 (d, *J* = 7.5 Hz, 1H, *N-H*), 4.53 (m, 1H, *H-2*), 3.71 (s, 1H, *OMe*), 3.02 (m, 2H, *H-3*), 1.42 (s. 9H, *t*-Bu).

Dimethyl 3,3'-((((pyridin-4-ylazanediyl)bis(ethane-2,1-diyl))bis(oxy))bis(4,1-phenylene))(2*S*,2'*S*)-bis(2-((*tert*-butoxycarbonyl)amino)propanoate) (113)

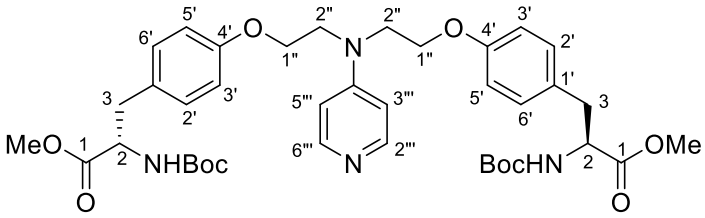

To a stirred solution of **116** (400.0 mg, 2.195 mmol) in DMF (1 mL) and THF (8 mL), were added triphenylphosphine (1.444 g, 5.505 mmol), **120** (1.640 g, 5.534 mmol) and DIAD (1.08 mL, 5.49 mmol). The resulting mixture heated in a microwave reactor to 100 °C. After 30 minutes, the solvent was removed *in vacuo* to yield a crude residue that was purified by column chromatography using ethyl acetate/hexane (80/20), followed by MeOH/(5/95) to afford **113** as a pale-yellow solid (844 mg, 53%), mp 72–74 °C; $[\alpha]_D^{20}$ + 46.4 (*c* 0.10, $CHCl_3$); IR ($CHCl_3$) 2978, 1847, 1739 (CO_2CH_3), 1711 $(CO)_{amide}$, 1597, 1512, 1366 cm^{-1}; ^1H NMR (400 MHz, $CDCl_3$) δ 8.23 (d, *J* = 5.8 Hz, 2H, *H-2"', H-6"'*), 7.01 (d, *J* = 8.5 Hz, 4H, *H-2', H-6'*), 6.78 (d, *J* = 8.6 Hz, 4H, *H-3', H-5'*), 6.61 (d, *J* = 5.8 Hz, 2H, *H-3"', H-5"'*), 4.96 (br. s, 2H, *N-H*), 4.51 (br. s, 2H, *H-2*), 4.15 (t, *J* = 5.7 Hz, 4H, *H-1")*, 3.88 (t, *J* = 5.7 Hz, 4H, *H-2"*), 3.69 (s, 6H, *OMe*), 3.11–2.89 (m, 4H, *H-3*), 1.40 (s, 18H, *t*-Bu); ^{13}C NMR (400 MHz, $CDCl_3$) δ 172.3 (CO), 157.5 (CO), 155.7 (q), 152.7 (q), 149.5 (C-2"', C-6"'), 130.4 (C-3', C-5'), 128.7 (q), 114.5 (C-2', C-6'), 106.8 (C-3"', C-5"'), 79.9 ($\underline{C}(CH_3)_3$), 65.0 (C-1"), 54.6 (C-2), 52.2 ($O\underline{C}H_3$), 50.2 (C-2"), 37.5 (C-3), 28.3 ($C(\underline{C}H_3)_3$); HRMS (ES): *m/z* 737.3761 $[M + H]^+$, Calculated for $C_{39}H_{53}N_4O_{10}$, 737.3762 $[M + H]^+$.

5.4 β-Substituted Catalysts

Potassium 4-(pyrrolidino) nicotinate (126)[160]

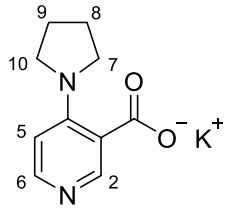

To as stirred suspension of 4-chloropyridine-3-carboxylic acid (153 mg, 0.97 mmol) in toluene (4 mL), was added pyrrolidine (0.35 mL, 4.2 mmol) and the resulting solution stirred at reflux temperature, After 2 hour, the temperature was lowered to r.t. and the reaction

mixture concentrated on the rotary evaporator. Saturated K_2CO_3 (10 mL) was added and the mixture stirred for 30 minutes and concentrated. Ethanol was added to the residue, and the solution was filtered through Celite ® to remove potassium salts. The ethanol was removed and the residue was dissolved in ethanol and filtered through Celite ® again. The solvent was removed under reduced pressure to give **126** as a brown solid (211 mg, 95%). The salt was used in the next step without further purification. ^{1}H HMR (400 MHz, D_2O) δ 7.81 (s, 1H, *H-2*), 7.73 (d, *J* = 6.2 Hz, 1H, *H-6*), 6.37 (d, *J* = 6.2 Hz, 1H, *H-5*), 3.09 (s, 4H, *H-7*, *H-10*), 1.68 (s, 4H, *H-8*, *H-9*).

_N_-4-Pyrrolidinyl Nicotinamido-L-tryptophan methyl ester (127)

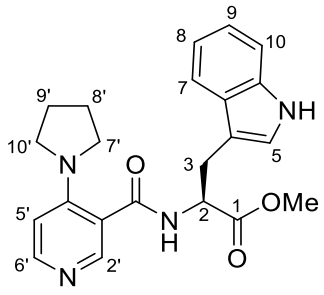

To a stirred solution of salt **126** (65.0 mg, 0.282 mmol) and HCl-Trp-OMe (107.8 mg, 0.423 mmol), at r.t. in pyridine (1.5 mL) and water (3 drops), were added EDC (108.1 mg, 0.564 mmol) and HOBt (15.2 mg, 0.112 mmol). After 18 hrs, (sat.) aq. $NaHCO_3$ (10 mL) was added and the aqueous layer extracted with ethyl acetate (3 x 15 mL). The combined organic extracts were dried over anhydrous $MgSO_4$, and the solvent evaporated to afford a yellow oil that was purified by column chromatography using ethyl acetate/hexane (80/20) followed by MeOH/DCM (5/95) to provide **127** as a colourless solid (49.0 mg, 44%), mp 214–217 °C; $[\alpha]_D^{20}$ − 29.0 (*c* = 0.13, DCM); IR (DCM) 3289, 2957, 1740 (CO_2Me), 1617, 1588 cm^{-1}; ^{1}H NMR (400 MHz, $CDCl_3$) δ 8.16 (s, 1H, *H-2'*), 8.15 (d, *J* = 6.1 Hz, 1H, *H-6'*), 8.09 (s, 1H, *N-H*$_{indole}$), 7.59 (d, *J* = 8.0 Hz, 1H, *H-7*), 7.35 (d, *J* = 8.0 Hz, 1H, *H-10*), 7.20 (t, *J* = 7.2 Hz, 1H, *H-9*), 7.13 (t, *J* = 7.2 Hz, 1H, *H-8*), 7.06 (d, *J* = 2.3 Hz, 1H, *H-5*), 6.42 (d, *J* = 6.1 Hz, 1H, *H-5'*), 6.32 (d, *J* = 7.4 Hz, 1H, *N-H*$_{Trp}$), 5.12 (d, *J* = 6.5 Hz, 1H, *H-2*), 3.76 (s, 3H, OMe), 3.46 (dd, *J* = 15.0, 6.0 Hz, 1H, *H-3*), 3.38 (dd, *J* = 15.0, 6.0 Hz, 1H, *H-3*), 3.29–3.14 (m, 4H, *H-7'*, *H-10'*), 1.91–1.78 (m, 4H, *H-8'*, *H-9')*; ^{13}C NMR (400 MHz, $CDCl_3$) δ 172.4 (CO), 171.4 (CO), 168.6 (q), 150.4 (C-2'),149.6 (C-6'),136.5 (q), 127.6 (q), 122.7 (C-5), 122.6 (C-9), 120.0 (C-8), 118.6 (C-7), 117.7 (q), 111.3 (C-10), 110.4 (q), 108.5 (C-5'), 53.1 (C-2), 52.3

(O<u>C</u>H$_3$), 49.4 (C-7', C-10'), 27.8 (C-3), 25.6 (C-8', C-9'); HRMS (ES): *m/z* 393.1928 [M + H]$^+$. Calculated for $C_{22}H_{25}N_4O_3$, 393.1927 [M + H]$^+$.

_N_-4-Pyrrolidinyl Nicotinamido-L-leucine-L-tryptophan methyl ester (128)

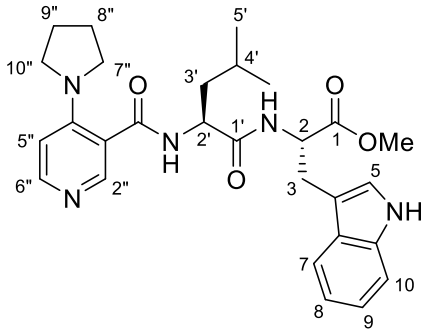

Salt **126** (98 mg, 0.426 mmol) and NH_2-Leu-Trp-OMe **103** (127 mg, 0.384 mmol) were dissolved in pyridine (2.0 mL) and water (3 drops) at r.t. EDC (as its hydrochloride) (112 mg, 0.587 mmol) and HOBt (21 mg, 0.16 mmol) were then added. After 12 hrs, (sat.) aq. $NaHCO_3$ (10 mL) was added and the aqueous layer extracted with ethyl acetate (3 x 15 mL). The combined organic extracts were dried over anhydrous $MgSO_4$ and the solvent evaporated to afford a yellow oil that was purified by column chromatography using ethyl acetate/hexane (80/20) followed by MeOH/DCM (5/95) to provide **128** as a pale-yellow solid (85 mg, 44%), mp 102–105 °C; $[\alpha]_D^{20}$ − 5.8 (*c* 0.12, DCM); IR (DCM) 3289, 2957, 1742 (CO_2Me), 1640, 1593, 1510 cm^{-1}; ^{1}H NMR (400 MHz, $CDCl_3$) δ 8.48 (s, 1H, *N-H$_{indole}$*), 8.14 (d, *J* = 6.1 Hz, 1H, *H-6"*), 8.12 (s, 1H, *H-2"*), 7.53 (d, *J* = 7.9 Hz, 1H, *H-7*), 7.30 (d, *J* = 7.9 Hz, 1H, *H-10*), 7.20–7.02 (m, 3H, *H-5, H-8, H-9*), 6.73 (d, *J* = 7.8 Hz, 1H, *N-H$_{Trp}$*), 6.45 (s, 1H, *N-H$_{Leu}$*), 6.43 (d, *J* = 6.1 Hz, 1H, *H-5"*), 4.91 (m, 1H, *H-2*), 4.57 (m, 1H, *H-2'*), 3.68 (s, 3H, *OMe*), 3.32 (d, *J* = 5.6 Hz, 2H, *H-3*), 3.25 (m, 4H, *H-7"*, *H-10"*), 1.85 (m, 4H, *H-8"*, *H-9"*), 1.77–1.54 (m, 3H, *H-3'*, *H-4'*), 0.93 (m, 6H, *H-5'*); ^{13}C NMR (400 MHz, $CDCl_3$) δ ; 171.9 (CO), 171.4 (CO), 169.0 (CO), 150.5 (C-6"), 150.0 (q), 149.1 (C-2"), 136.2 (q), 127.5 (q), 123.4 (C-5 or C-9), 122.1 (C-5 or C-9), 119.6 (C-8), 118.4 (C-7), 117.2 (q), 111.4 (C-10), 109.5 (q), 108.6 (C-5"), 52.9 (C-2), 52.4 (C-2', O<u>C</u>H$_3$), 49.5 (C-7", C-10"), 40.9 (C-3'), 27.6 (C-3), 25.5 (C-8", C-9"), 24.9 (C-4'), 22.9 (C-5'), 21.9 (C-5'); HRMS (ES); *m/z* 506.2767 [M + H]+. Calculated for $C_{28}H_{36}N_5O_4$, 506.2767 [M + H]+; Chiralpak AD 30% isopropyl alcohol/hexane, 1.0 mL/min, 254 nm, 7.072 min.

Fmoc-Leu-Leu-OMe (136)

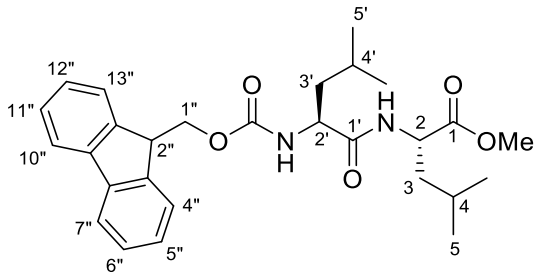

To a stirred solution of Fmoc-Leu-OH (748.6 mg, 2.118 mmol) and HCl-Leu-OMe **100** (577.0 mg, 3.160 mmol) in pyridine (10 mL), at r.t., was added DCC (570.0 mg, 2.796 mmol) followed by HOBt (288.1 mg, 2.132 mmol). After 18 hrs, 1M HCl (20 mL) was added followed by an extraction with ethyl acetate (3 x 20 mL). The combined organic extracts were washed with 1M HCl (3 x 60 mL), dried over anhydrous $MgSO_4$ and the solvent removed to give a yellow residue that was purified by ethyl acetate/hexane (40/60) to afford **136** as a colourless oily solid (818.2 mg, 80%), mp 111–113 °C; $[\alpha]_D^{20}$ − 39.2 (*c* 0.52, MeOH); IR ($CHCl_3$) 3321 (NH), 1742 (CO_2Me), 1674 $(CO)_{amide}$ cm^{-1}; ^1H NMR (400 MHz, $CDCl_3$) δ 7.75 (dd, *J* = 7.6, 0.6 Hz, 2H, *H-7”, H-13”, or H-4”, H-10”*), 7.58 (d, *J* = 7.5 Hz, 2H, *H-7”, H-13”, or H-4”, H-10”*), 7.39 (t, *J* = 7.5 Hz, 2H, *H-5”, H-12”, or H-6”, H-11”*), 7.29 (m, *J* = 7.4, 1.3 Hz, 2H, *H-5”, H-12”, or H-6”, H-11”*), 6.54 (d, *J* = 6.7 Hz, 1H, *N-H*$_{Leu}$), 5.41 (d, *J* = 7.9 Hz, 1H, *N-H*$_{Leu}$), 4.61 (td, *J* = 8.6, 5.2 Hz, 1H, *H-2 or H-2’*), 4.41 (m, 2H, *H-1”*), 4.26 (m, 1H, *H-2 or H-2’*), 4.20 (m, 1H, *H-2”*), 3.71 (s, 3H, *OMe*), 1.63 (m, 6H, *H-3, H-3’, H-4, H-4’*), 0.95 (m, 6H, *H-5 or H-5’*), 0.90 (d, *J* = 3.1 Hz, 3H, *H-5 or H-5’*), 0.89 (d, *J* = 3.3 Hz, 3H, *H-5 or H-5’*); ^{13}C NMR (101 MHz, $CDCl_3$) δ 173.1 (CO), 172.0 (CO), 156.2 (CO), 143.8 (q), 143.7 (q), 127.7 (C-10”, C-7” or C-4, C-13”), 127.0 (C-10”, C-7” or C-4”, C-13”), 125.0 (C-5”, C-12” or C-6”, C-11”), 119.9 (C-5”, C-12” or C-6”, C-11”), 67.1 (C-1”), 53.4 (C-2 or C-2’), 52.2 ($O\underline{C}H_3$), 50.7 (C-2 or C-2’), 47.1 (C-2”), 41.5 (C-3, C-3’), 41.4 (C-3, C-3’), 24.8 (C-4 or C-4’), 24.6 (C-4, C-4’), 22.8 (C-5 or C-5’), 22.7 (C-5 or C-5’), 22.0 (C-5 or C-5’), 21.9 (C-5 or C-5’); Anal. Found C, 69.58; H, 7.40; N, 5.53 $C_{28}H_{36}N_2O_5$ requires C, 69.98; H, 7.55; N, 5.83; Chiralpak AD 30% isopropyl alcohol/hexane, 1.0 mL/min, 254 nm, 3.78 min;

NH_2-Leu-Leu (137)

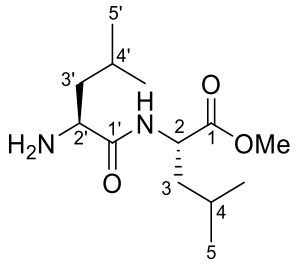

To a stirred solution of **136** (1.163 g, 2.421 mol) in DCM (10 mL) was added piperidine (0.5 mL, 5.0 mmol) at 0 °C. After 18 hrs the solvent and piperidine were removed to give a crude residue that was purified column chromatography using MeOH/DCM (5/95) to afford the title compound as a clear oil (337.7 mg, 54%), ^{1}H NMR (400 MHz, $CDCl_3$) δ 7.61 (d, *J* = 8.1 Hz, 1H, *N-H*$_{Leu}$), 4.61 (m, 1H, *H-2*), 3.73 (s, 3H, *OMe*), 3.43 (m, 1H, *H-2'*), 1.79–1.54 (m, 5H, *H-3, H-4, H-3', H-4'*), 1.39–1.28 (m, 1H, *H-3'*), 0.98–0.90 (m, 12H, *H-5, H-5'*); ^{13}C NMR (101 MHz, $CDCl_3$) δ 175.4 (CO), 173.6 (CO), 53.5 (C-2'), 52.1 ($O\underline{C}H_3$), 50.3 (C-2), 44.1 (C-3'), 41.5 (C-3), 24.9 (C-4 or C-4'), 24.8 (C-4 or C-4'), 23.3 (C-5 or C-5'), 22.8 (C-5 or C-5'), 21.9 (C-5 or C-5'), 21.4 (C-5 or C-5').

***N*-4-Pyrrolidinyl nicotinamido-L-leucine-L-leucine methyl ester (138)**

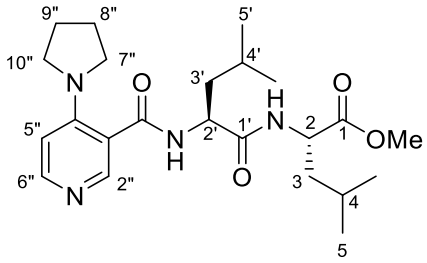

To a stirred solution of salt **126** (451.6 mg, 1.961 mmol) and **137** (337.7 mg, 1.307 mmol) in pyridine (5 mL) and water (0.5 mL), at r.t., was added EDC (326.0 mg, 1.700 mmol) followed by HOBt (212.0 mg, 1.569 mmol). After 18 hrs $NaHCO_3$ (10 mL) was added followed by ethyl acetate (3 x 15 mL). The combined organic extracts dried over anhydrous $MgSO_4$ and the solvent removed to give a yellow residue that was purified by column chromatography using MeOH/DCM (8/92) to afford **138** as a pale-yellow oil (151.2 mg, 27%), $[\alpha]_D^{20}$ − 25.3 (*c* 0.51, $CHCl_3$); IR ($CHCl_3$) 3420 (NH), 3022 (NH), 1742 (CO)$_{ester}$, 1644 (CO)$_{amide}$ cm^{-1}; ^{1}H NMR (400 MHz, $CDCl_3$) δ 8.26 (s, 1H, *H-2"*), 8.13 (s, 1H, *H-6"*), 6.86 (d, *J* = 8.3 Hz, 1H, *N-H*$_{Leu}$), 6.80 (d, *J* = 8.3 Hz, 1H), 6.47 (d, *J* = 6.0 Hz, 1H, *H-5"*), 4.61 (m,

2H, *H-2, H-2'*), 3.72 (s, 3H, *OMe*), 3.30 (m, 4H, *H-7", H-10"*), 1.94 (m, 4H, *H-8", H-9"*), 1.52–1.80 (m, 6H, *H-3, H-4, H-3', H-4'*), 0.97 (d, *J* = 6.2 Hz, 3H, *H-5 or H-5'*), 0.95 (d, *J* = 6.2 Hz, 3H, *H-5 or H-5'*), 0.92 (d, *J* = 2.5 Hz, 3H, *H-5 or H-5'*), 0.91 (d, *J* = 2.5 Hz, 3H, *H-5 or H-5'*); ^{13}C NMR (101 MHz, $CDCl_3$) 173.1 (CO), 171.6 (CO), 168.8 (CO), 150.2 (q), 149.3 (C-2"), 148.7 (C-6"), 117.4 (q), 108.6 (C-5"), 52.4 (C-2 or C-2'), 52.2 ($O\underline{C}H_3$), 50.8 (C-2 or C-2'), 49.5 (C-7", C-10"), 41.5 (C-3 or C-3'), 41.0 (C-3 or C-3'), 25.5 (C-8", C-9"), 24.9 (C-4 or C-4'), 24.8 (C-4 or C-4'), 22.9 (C-5 or C-5'), 22.8 (C-5 or C-5'), 22.0 (C-5 or C-5'), 21.9 (C-5 or C-5'); HRMS (ES): *m/z* 433.2810 $[M + H]^+$. Calculated for $C_{23}H_{37}N_4O_4$, 433.2814 $[M + H]^+$; Chiralpak AD 30% isopropyl alcohol/hexane, 1.0 mL/min, 254 nm, 7.651 min;.

Boc-Trp-Trp-OMe (142)[161]

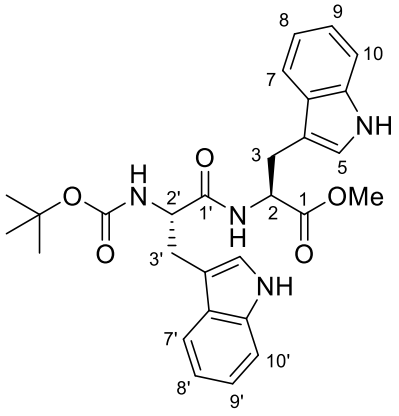

To a stirred solution of **101** (460.1 mg, 1.807 mmol) and *N*-Boc-Trp-OH (500.3 mg, 1.664 mmol) in pyridine (6.5 mL), at r.t., was added EDC (347.6 mg, 1.813 mmol) followed by HOBt (91.0 mg, 0.673 mmol). After 18 hrs 1M HCl (15 mL) was added followed by ethyl acetate (3 x 15 mL). The combined organic extracts were washed with 1M HCl (3 x 45 mL) and dried over anhydrous $MgSO_4$. The solvent was removed to give a yellow residue that was purified by ethyl acetate/hexane (40/60) to afford **142** as a colourless solid (674 mg, 81%), $[\alpha]_D^{20}$ − 20.5 (*c* 1.0, MeOH) (lit.[161] $[\alpha]_D^{25}$ − 15 (*c* 0.9, MeOH); ^{1}H NMR (400 MHz, $CDCl_3$) δ 7.88 (s, 1H, *N-H*$_{indole}$), 7.86 (s, 1H, *N-H*$_{indole}$), 7.65 (d, *J* = 7.8 Hz, 1H, *H-7 or H-7'*), 7.30 (m, 3H, *Ar-H*), 7.22–7.09 (m, 3H, *Ar-H*), 6.97 (t, *J* = 7.5 Hz, 1H, *Ar-H*), 6.90 (s, 1H, *H-5 or H-5'*), 6.65 (s, 1H, *H-5 or H-5'*), 6.24 (d, *J* = 7.6 Hz, 1H, *N-H*), 5.01 (s, 1H, *N-H*), 4.82 (dd, *J* = 13.4, 5.6 Hz, 1H, *H-2 or H-2'*), 4.43 (dd, *J* = 12.8, 7.4 Hz, 1H, *H-2 or H-2'*), 3.60 (s, 3H, *OMe*), 3.32–3.08 (m, 4H, *H-3, H-3'*), 1.40 (s, 9H, *t*-Bu).

NH_2-Trp-Trp-OMe (143)[153]

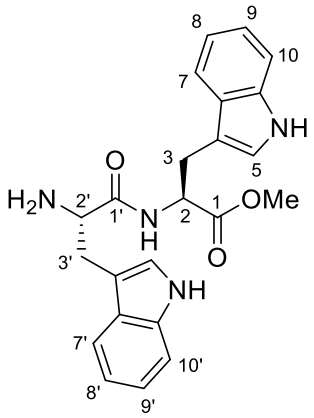

To a stirred suspension of **142** (358 mg, 0.710 mmol) and anisole (0.23 mL, 2.1 mmol) in DCM (5.5 mL), at 0 °C was added TFA (1.4 mL). After 2 hrs aqueous $NaHCO_3$ (15 mL) was added with cooling until a pH of 8 was reached. The organic layer was separated and the aqueous layer was washed with DCM (2 x 15 mL). The combined organic extracts were dried over anhydrous $MgSO_4$ and the solvent was removed to give a yellow residue that was purified by MeOH/DCM (10/90) to afford **143** as a colourless solid (286 mg, 99%), $[\alpha]_D^{20}$ − 15.2 (*c* 0.5, MeOH) (lit.[153] $[\alpha]_D^{25}$ − 11.0 (*c* 0.75, MeOH); ^{1}H NMR (400 MHz, $CDCl_3$) δ 8.37 (s, 1H, *N-H*$_{indole}$), 8.25 (s, 1H, *N-H*$_{indole}$), 7.79 (d, *J* = 8.3 Hz, 1H, *Ar-H*), 7.58 (d, *J* = 7.9 Hz, 1H, *Ar-H*), 7.39 (d, *J* = 7.9 Hz, 1H, *Ar-H*), 7.31 (d, *J* = 4.3 Hz, 1H, *Ar-H*), 7.16 (m, 2H, *Ar-H*), 7.09 (m, 1H, *Ar-H*), 7.01 (m, 1H, *Ar-H*), 6.79 (m, 1H, *H-5 or H-5'*), 6.69 (d, 1H, *J* = 2.3 Hz, *H-5 or H-5'*), 4.95 (m, 1H, *H-2*), 3.64 (m, 4H, *H-2'*, *OMe*), 3.30–2.85 (m, 4H, *H-3*, *H-3'*).

Boc-Leu-Trp-Trp-OMe (144)

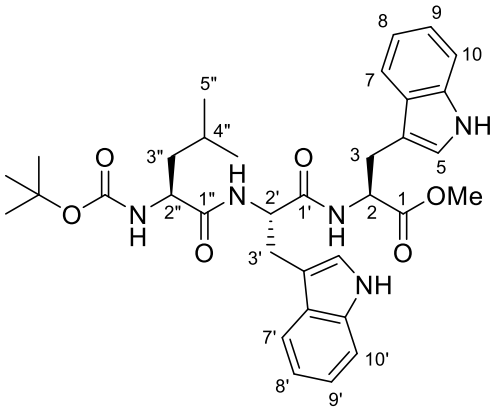

To a stirred solution of **143** (233.5 mg, 0.5773 mmol) and *N*-Boc-Leu-OMe (200.1 mg, 0.8651 mmol) in pyridine (3.0 mL), at r.t., were added EDC (168.7 mg, 0.8800 mmol) and HOBt (36.0 mg, 0.266 mmol). After 18 hrs, 1M HCl (15 mL) was added and the aqueous layer extracted with ethyl acetate (3 x 15 mL). The combined organic extracts were washed with 1M HCl (3 x 50 mL), dried over anhydrous $MgSO_4$, and the solvent evaporated to afford a yellow oil that was purified by column chromatography using ethyl acetate/hexane (50/50) to provide **144** as a colourless solid (218 mg, 61%), mp 107–109 °C; $[\alpha]_D^{20}$ − 23.2 (*c* 1.0, MeOH); IR (DCM) 3313 (NH), 1741 (CO_2Me), 1649 $(CO)_{amide}$, 1169 (C-N) cm^{-1}; ^1H NMR (400 MHz, $CDCl_3$) δ 8.07 (s, 1H, *N-H*$_{indole}$), 7.90 (s, 1H, *N-H*$_{indole}$), 7.70 (d, *J* = 7.8 Hz, 1H, *H-7 or H-7'*), 7.31 (m, 3H), 7.19 (m, 1H), 7.13 (m, 2H), 7.01 (t, *J* = 7.5 Hz, 1H), 6.96 (s, 1H, *H-5 or H-5'*), 6.68 (d, *J* = 7.7 Hz, 1H, *N-H*$_{Trp}$), 6.66 (s, 1H, *H-5 or H-5'*), 6.26 (d, *J* = 7.4 Hz, 1H, *N-H*$_{Trp}$), 4.77 (m, 1H, *H-2 or H-2'*), 4.70 (m, 1H, *H-2 or H-2'*), 4.65 (d, *J* = 8.0 Hz, 1H, *N-H*$_{Leu}$), 4.05 (m, 1H, *H-2"*), 3.61 (s, 3H, *OMe*), 3.32 (dd, *J* = 14.6, 6.6 Hz, 1H, *H-3 or H-3'*), 3.15 (d, *J* = 5.7 Hz, 2H, *H-3 or H-3'*), 3.10 (dd, *J* = 14.6, 6.6 Hz, 1H, *H-3 or H-3'*), 1.55 (m, 2H, *H-3", H-4"*), 1.43 (s, 9H, *t-Bu*), 1.27 (m, 1H, *H-3"*), 0.86 (d, *J* = 6.3 Hz, 3H, *H-5"*), 0.85 (d, *J* = 6.3 Hz, 3H, *H-5"*); ^{13}C NMR (400 MHz, $CDCl_3$) δ 172.4 (CO), 171.7 (CO), 170.6 (CO), 155.6 (CO), 136.4 (q), 136.3 (q), 127.7 (q), 127.5 (q), 123.6 (C-5 or C-5'), 123.2 (C-5 or C-5'), 122.3, 122.2, 119.9 (C-7 or C-7'), 119.6, 119.1, 118.6, 111.2 (q), 109.8 (q), 80.3 (q), 53.8 (C-2 or C-2', C-2"), 52.8 (C-2 or C-2'), 52.1 ($O\underline{C}H_3$), 41.5 (C-3"), 28.4 ($C(\underline{C}H_3)_3$), 28.0 (C-3 or C-3'), 27.6 (C-3 or C-3'), 24.9 (C-4"), 22.9 (C-5"), 21.8 (C-5"); Chiralpak AD 30% isopropyl alcohol/hexane, 1.0 mL/min, 254 nm, 6.185 min; Anal. Found C, 65.94; H, 7.06; N, 11.01 $C_{34}H_{43}N_5O_6$ requires C, 66.11; H, 7.02; N, 11.34.

NH_2-Leu-Trp-Trp-OMe (145)

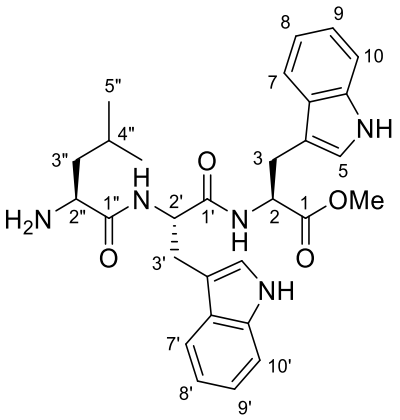

To a stirred suspension of **144** (216 mg, 0.350 mmol) and anisole (0.11 mg, 1.0 mmol) in DCM (2.8 mL), at 0 °C, was added TFA (0.7 mL) dropwise over 1 minute. After 2 hrs, (sat.) $NaHCO_3$ (10 mL) was added, with cooling, until a pH of 8 was reached. The aqueous layer was extracted with DCM (3 x 10 mL), the combined organic extracts dried over anhydrous $MgSO_4$, and the solvent evaporated to afford an orange oil that was purified by column chromatography using ethyl acetate/hexane (50/50) followed by MeOH/DCM (10/90), to give **145** as a pale-yellow oily-solid (180 mg, 99%), $[\alpha]_D^{20}$ + 3 (*c* 0.10, $CHCl_3$); IR 3308, 2956, 1739 (CO_2CH_3), 1657 $(CO)_{amide}$,1458, 1343, 1216; ^{1}H NMR (400 MHz, $CDCl_3$) δ 8.09 (s, 1H, *N-H*$_{indole}$), 7.98 (s, 1H, *N-H*$_{indole}$), 7.72 (d, *J* = 8.0 Hz, 1H, *N-H*$_{Trp}$), 7.68 (d, *J* = 7.9 Hz, 1H, *Ar-H*), 7.30 (t, *J* = 7.9 Hz, 3H, *Ar-H*), 7.21–7.05 (m, 3H, *Ar-H*), 6.96 (m, 2H, *Ar-H*), 6.68 (d, *J* = 1.9 Hz, 1H, *Ar-H*), 6.43(d, *J* = 7.5 Hz, H, *N-H*$_{Trp}$), 4.80 (m, *1*H, *H-2 or H-2'*), 4.73 (m, *1*H, *H-2 or H-2'*), 3.62 (s, 3H, *OMe*), 3.32–3.06 (m, *5*H, *H-3, H-3', H-2"*), 1.62 (br. s, 3H, *NH_2, H-4"*), 1.49(m, *1*H, *H-3"*), 1.11(m, *1*H, *H-3"*), 0.85 (d, *J* = 6.4 Hz, 3H, *H-5*), 0.80 (d, *J* = 6.4 Hz, 3H, *H-5*); ^{13}C NMR (400 MHz, $CDCl_3$) δ 175.6 (CO), 171.9 (CO), 171.2 (CO), 136.2 (q), 136.0 (q), 127.6 (q), 127.4 (q), 123.4 (C-5 or C-5'), 123.2 (C-5 or C-5'), 122.1, 122.0, 119.6, 119.5, 119.1, 118.5, 111.2, 111.1, 110.8 (q), 109.6 (q), 53.4 (C-2"), 52.7 (C-2, C-2'), 52.3 ($O\underline{C}H_3$), 43.6 (C-3"), 27.9 (C-3 or C-3'), 27.4 (C-3 or C-3'), 24.7 (C-4"), 23.3 (C-5") 21.3 (C-5"); Chiralpak AD 30% isopropyl alcohol/hexane, 1.0 mL/min, 254 nm, 7.856 min.

_N_-((4-Pyrrolidinyl)-nicotinamido)-Leu-Trp-Trp-OMe (139)

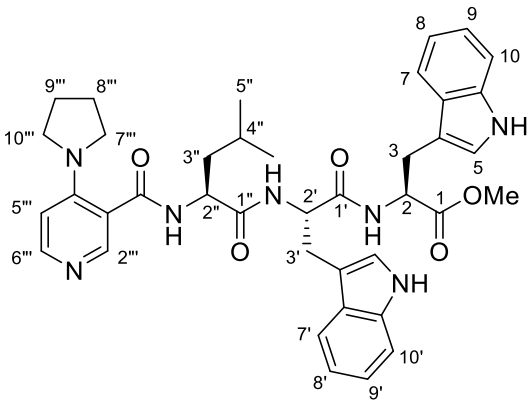

To a stirred solution of **126** (78 mg, 0.339 mmol), and **145** (160 mg, 0.309 mmol) in pyridine (5 mL) and water (5 drops), at r.t., were added EDC (71 mg, 0.37 mmol) and HOBt (20 mg, 0.15 mmol). After 12 hrs, (sat.) $NaHCO_3$ (20 mL) was added and the aqueous layer extracted with DCM (3 x 20 mL). The combined organic extracts were dried over anhydrous $MgSO_4$ and the solvent evaporated to afford a yellow oil that was purified by column chromatography using ethyl acetate/hexane (20/80) followed by MeOH/DCM (8/92) to provide **139** as a pale-yellow solid (113 mg, 53%), mp 136–138 °C; $[\alpha]_D^{20}$ − 46.0 (*c* 0.28, DCM); IR (DCM) 1738, 1648 cm^{-1}; ^1H NMR (400 MHz, $CDCl_3$) δ 8.52 (s, 1H, *N-H*$_{indole}$), 8.49 (s, 1H, *N-H*$_{indole}$), 8.03 (d, *J* = 6.2 Hz, 1H, *H-6”’*), 7.98 (s, 1H, *H-2”’*), 7.63 (d, *J* = 7.9 Hz, 1H, Ar-H), 7.30 (t, *J* = 7.3 Hz, 2H *Ar-H*), 7.22 (d, *J* = 8.0 Hz, 1H, *Ar-H*), 7.04 (m, 6H, *4 x Ar*, *N-H*$_{Trp}$, *H-5 or H-5’*), 6.80 (s, 1H, *N-H*$_{Leu}$), 6.71 (s, 1H, *N-H*$_{Trp}$), 6.56 (s, 1H, *H-5 or H-5’*), 6.37 (d, *J* = 6.2 Hz, 1H, *H-5”’*), 4.82 (m, 1H, *H-2 or H-2’*), 4.73 (m, 1H, *H-2 or H-2’*), 4.55 (m, 1H, *H-2”*), 3.59 (s, 3H, *OMe*), 3.19 (m, 8H, *H-3*, *H-3’*, *H-7”’*, *H-10”’*), 1.81 (m, 4H, *H-8’”*, *H-9”’*), 1.66–1.42 (m, 3H, *H-3”*, *H-4”*), 0.87–0.80 (2 x d, *J* = 6.0 Hz, 6H, *H-5”*); ^{13}C NMR (400 MHz, $CDCl_3$) δ 171.9 (CO), 171.8 (CO), 170.8 (CO), 168.8 (CO), 150.2 (q), 148.9 148.3 136.2 (q), 136.1 (q), 127.4 (q), 127.2 (q), 123.8 (C-5 or C-5’), 123.2 (C-5 or C-5’), 122.0, 121.9, 119.6, 119.3, 118.8,118.3, 117.2 (q), 111.5, 111.3, 109.9 (q), 109.4 (q), 108.6 (C-5”’), 53.5 (C-2 or C-2’), 52.9 (C-2 or C-2’), 52.8 (C-2”), 52.3 ($O\underline{C}H_3$), 49.5 (C-7”’, C-10”’), 40.8 (C-3”), 28.0 (C-3 or C-3’), 27.4 (C-3 or C-3’), 25.4 (C-8”’, C-9”’), 25.0 (C-4”), 22.9 (C-5”), 21.6 (C-5).

Boc-Trp-Leu-OMe (147)[162]

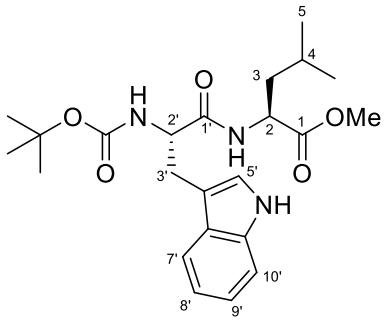

To a stirred solution of HCl-Leu-OMe (575 mg, 3.17 mmol) and Boc-Trp-OH (800 mg, 2.63 mmol), in pyridine (10 mL) at r.t., were added EDC (756 mg, 3.94 mmol) and HOBt (180 mg, 1.33 mmol). After 18 hrs, 1M HCl (5 mL) was added and the aqueous extracted with ethyl acetate. The combined organic extracts were washed with 1M HCl and dried over anhydrous $MgSO_4$ to give a crude product that was purified by column chromatography using ethyl acetate/hexane to yield **147** as a colourless solid (966 mg, 85%); $[\alpha]_D^{20}$ − 29.4 (*c* 0.49, MeOH); ^{1}H NMR (300 MHz, $CDCl_3$) δ 8.12 (s, 1H, *N-H*$_{indole}$), 7.67 (m, 1H, *H-7'*), 7.35 (m, 1H, *H-10'*), 7.24–7.06 (m, 3H, *H-8'*, *H-9'*, *H-5'*), 6.18 (d, *J* = 8.0 Hz, 1H, *N-H*), 5.14 (s, 1H, *N-H*), 4.52 (m, 1H, *H-2'*), 4.42 (m, 1H, *H-2*), 3.64 (s, 3H, *OMe*), 3.30–3.19 (m, 2H, H-3'), 1.54–1.36 (m, 12H, *H-3*, *H-4*, *t*-Bu) 0.86 (d, *J* = 4.3 Hz, 3H, *H-5*), 0.84 (d, *J* = 4.4 Hz, 3H, *H-5*).

NH_2-Trp-Leu-OMe (148)[154]

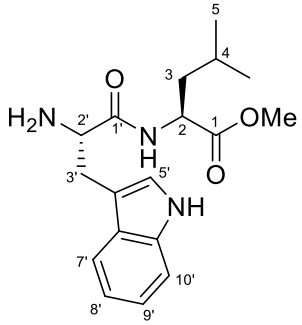

To a stirred solution of anisole (0.27 mL, 2.5 mmol), in 30% TFA/DCM (10 mL) at 0 °C was added **147** (533.8 mg, 1.237 mmol). After 2 hrs, sat. $NaHCO_3$ (25 mL) was added until a pH of approximately 9 was reached. The aqueous layer was washed with DCM (3 x 25 mL), the combined organic extracts were dried over anhydrous $MgSO_4$, and the solvent removed under reduced pressure to give a crude oil that was purified by column chromatography using

MeOH/DCM (10/90) to afford **148** as a clear oil (238 mg, 58%); $[\alpha]_D^{20}$ − 6.0 (*c* 0.50, MeOH) (lit.[154] $[\alpha]_D^{20}$ − 1.2 (*c* 0.50, MeOH); ^{1}H NMR (300 MHz, $CDCl_3$) δ 8.71 (s, 1H, *N-H$_{indole}$*), 7.70 (d, *J* = 8.4 Hz, 1H, *N-H$_{Trp}$*), 7.64 (d, *J* = 8.0 Hz, 1H, *H-7'*), 7.36 (d, *J* = 8.0 Hz, 1H, *H-10'*), 7.18 (m, 1H, *H-9'*), 7.09 (m, 1H, *H-8'*), 7.05 (d, *J* = 2.4 Hz, 1H, *H-5'*), 4.62 (m, 1H, *H-2'*), 3.71 (m, 4H, *H-2, OMe*), 3.37 (dd, *J* = 14.5, 4.1Hz, 1H, *H-3'*), 2.92 (dd, *J* = 14.5, 9.0 Hz, 1H, *H-3'*), 1.65–1.49 (m, 3H, *H-3, H-4*), 0.91 (m, 6H, *H-5*).

Fmoc-Leu-Trp-Leu-OMe (149)

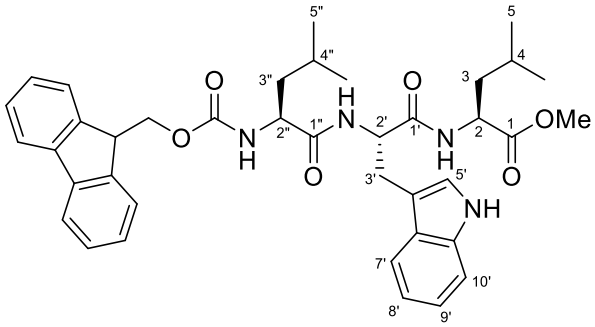

To a stirred solution of **148** (482.0 mg, 1.454 mmol) and Fmoc-Leu-OMe (666.2 mg, 1.885 mmol), in pyridine (6 mL), at r.t., were added EDC (408.3 mg, 2.130 mmol) and HOBt (196.0 mg, 1.450 mmol). After 18 hrs, 1M HCl (10 mL) was added followed by ethyl acetate (3 x 10 mL). The combined organic extracts were washed with 1M HCl (3 x 50 mL) and dried over anhydrous $MgSO_4$ to give a crude product that was purified by column chromatography using ethyl acetate/hexane (40/60) to afford **149** as a pale-yellow solid (584.2 mg, 60%), mp 170–172 °C; $[\alpha]_D^{20}$ − 39.5 (*c* 0.57, $CHCl_3$); ^{1}H NMR (300 MHz, $CDCl_3$) δ 7.93 (s, 1H, *N-H$_{indole}$*), 7.78 (d, *J* = 7.4 Hz, 2H, *H-6"', H-7"'*), 7.76 (m, 1H, *H-7'*), 7.56 (d, *J* = 7.4 Hz, 1H, *H-3"', H-10"'*), 7.41 (m, 2H, *H-9"', H-4"'*), 7.31 (m, 2H, *H-5"', H-8"'*), 7.24 (m, 1H, *H-10'*), 7.14 (ddd, *J* = 8.1, 7.1, 1.3 Hz, 1H, *H-9'*), 7.08 (ddd, *J* = 8.1, 7.1, 1.3 Hz, 1H, *H-9'*), 7.04 (d, *J* = 2.3 Hz, 1H, *H-5'*), 6.62 (s, 1H, *N-H$_{Trp}$*), 6.20 (d, *J* = 7.9 Hz, 1H, *N-H$_{Leu}$*), 4.98 (d, *J* = 8.0 Hz, 1H, *N-H$_{Leu}$*), 4.72 (m, 1H, *H-2'*), 4.48 (m, 1H, *H-2 or H-2'*), 4.42 (m, 1H, *H-1"'*), 4.31 (m, 1H, *H-1"'*), 4.18 (t, *J* = 6.8 Hz, 1H, *H-2"'*), 4.13 (m, 1H, *H-2, H-2'*), 3.66 (s, 3H, *OMe*), 3.30 (dd, *J* = 14.7, 7.5 Hz, 1H, *H-3'*), 3.18 (dd, *J* = 14.7, 7.5 Hz, 1H, *H-3'*), 1.59–1.34 (m, 6H, *H-3, H-3" and H-4, H-4"*), 0.89 (m, 6H, *H-5 or H-5"*), 0.82 (m, 6H, *H-5 or H-5"*); ^{13}C NMR (400 MHz, $CDCl_3$) δ 172.7 (CO), 172.0 (CO), 170.7 (CO), 143.9 (q), 141.4 (q), 136.4 (q), 127.8 (C-4"', C-9"'), 127.5 (q), 127.1 (C-5"', C-8"'), 125.1 (C-10"', C-3"'), 125.0 (C-10"', C-3"'), 123.3 (C-5"), 122.4 (C-9'), 120.0 (C-7"', C-6"'),

119.9 (C-8'), 118.9 (C-7') 111.2 (C-10'), 110.7 (q), 67.1 (C-1"'), 53.9 (C-2 or C-2"), 53.8 (C-2'), 52.1 ($O\underline{C}H_3$), 51.1 (C-2, C-2"), 47.3 (C-2"'), 41.5 (C-3, C-3"), 27.9 (C-3'), 24.8 (C-4, C-4"), 24.8(C-4, C-4"), 22.9 (C-5, C-5"), 22.6 (C-5, C-5"), 22.0 (C-5, C-5"), 21.9 (C-5, C-5"); HRMS (ES): *m/z* 667.3508 $[M + H]^+$. Calculated for $C_{39}H_{47}N_6O_6$, 667.3496 $[M + H]^+$; Chiralpak AD 30% isopropyl alcohol/hexane, 1.0 mL/min, 254 nm, 4.701 min;

NH_2-Leu-Trp-Leu-OMe (150)

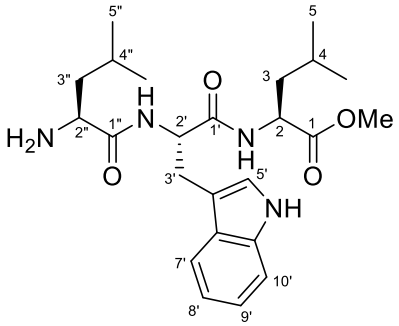

To a stirred solution of **149** (173.6 mg, 0.261 mmol) in DCM (2 mL) at 0 °C, was added piperidine (0.06 mL, 0.6 mmol). After 18 hrs, the solvent was removed *in vacuo* to give a crude product that was purified by column chromatography using MeOH/DCM (10/90) to afford **150** as a colourless solid (84.3 mg, 61%), mp 118–120 °C; $[\alpha]_D^{20}$ − 37.8 (*c* 0.51, $CHCl_3$); IR ($CHCl_3$) 3020 (NH_2), 1772 (CO_2Me), 1659 $(CO)_{amide}$, 1516 (NH) cm^{-1}; ^1H NMR (300 MHz, $CDCl_3$) δ 8.57 (s, 1H, *N-H*$_{indole}$), 7.83 (d, *J* = 8.1 Hz, 1H, *N-H*$_{Trp}$), 7.73–7.68 (d, *J* = 8.1 Hz, 1H, *H-7'*), 7.34 (d, *J* = 8.1 Hz, 1H, *H-10'*), 7.17 (m, 1H, *H-9'*), 7.14–7.07 (m, 2H, *H-5', H-8'*), 6.39 (d, *J* = 7.9 Hz, 1H, *N-H*$_{Leu}$), 4.76 (m, 1H, *H-2'*), 4.49 (m, 1H, *H-2*), 3.65 (s, 3H, *OMe*), 3.34 (dd, *J* = 9.6, 4.1 Hz, *H-2"*), 3.30–3.17 (m, 2H, *H-3'*), 1.59–1.38 (m, 6H, *H-3, H-3", H-4, H-4"*), 1.18 (m, 1H, *H-3,or H-3"*), 0.89 (d, *J* = 6.4 Hz, 3H, *H-5 or H-5"*), 0.87 (d, *J* = 6.4 Hz, 3H, *H-5, H-5"*), 0.84 (m, 6H, *H-5, H-5"*); ^{13}C NMR (400 MHz, $CDCl_3$) δ 175.7 (CO), 172.9 (CO), 171.2 (CO), 136.2 (q), 127.6 (q), 123.3 (C-5'), 122.1 (C-9), 119.6 (C-8'), 119.0 (C-7'), 111.1 (C-10), 110.9 (q), 53.6 (C-2') 53.5 (C-2, C-2"), 52.2 ($O\underline{C}H_3$) 51.0 (C-2, C-2"), 43.8 (C-3 or C-3"), 41.4 (C-3 or C-3"), 27.9 (C-3'), 24.8 (C-4, C-4"), 23.3 (C-5, C-5"), 22.6 (C-5, C-5"), 22.0 (C-5, C-5"), 21.4 (C-5, C-5"); HRMS (ES): *m/z* 445.2815 $[M + H]^+$. Calculated for $C_{24}H_{37}N_4O_4$, 445.2815 $[M + H]^+$; Chiralpak AD 30% isopropyl alcohol/hexane, 1.0 mL/min, 254 nm, 5.163 min.

_N_-4-Pyrrolidinyl nicotinamido-L-leucine-L-tryptophan-L-leucine methylester (140)

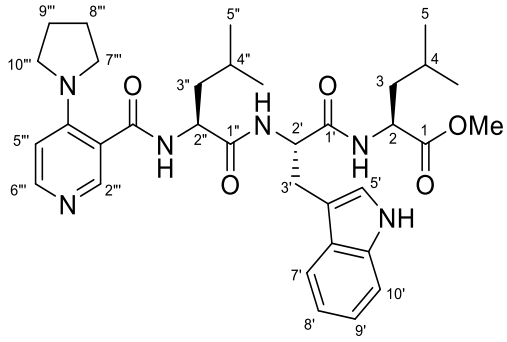

To a stirred solution of **107** (160 mg, 0.694 mmol) and **126** (365 mg, 0.821 mmol), in pyridine (5 mL) and DCM (4 mL), at r.t., were added EDC (200 mg, 1.04 mmol) followed by HOBt (47 mg, 0.35 mmol). After 12 hrs, (sat.) $NaHCO_3$ (20 mL) was added and the aqueous layer extracted with DCM (3 x 20 mL). The combined organic extracts were dried over anhydrous $MgSO_4$ and the solvent evaporated to afford a yellow oil that was purified by column chromatography using ethyl acetate/hexane (80/20), followed by MeOH/DCM (5/95) to provide **140** as a pale-yellow solid (188 mg, 44 %), mp 186–189 °C; $[\alpha]_D^{20}$ − 54.7 (*c* 0.5, CH_3OH); IR (DCM) 1741 (CO_2Me), 1641 $(CO)_{amide}$ cm^{-1}; ^1H NMR (400 MHz, $CDCl_3$) δ 8.60 (s, 1H, *N-H*$_{indole}$), 8.11 (d, *J* = 6.2 Hz, 1H, *H-6”’*), 8.05 (s, 1H, *H-2”’*), 7.62 (d, *J* = 8.1 Hz, 1H, *H-7’*), 7.30 (d, *J* = 8.1 Hz, 1H, *H-10’*), 7.13 (t, *J* = 7.1 Hz, 1H, *H-9’*), 7.09 (d, *J* = 2.2 Hz, 1H, *H-5’*), 7.05 (t, *J* = 7.1 Hz, 1H, *H-8’*), 6.93 (d, *J* = 7.9 Hz, 1H, *N-H*$_{Trp}$), 6.84 (d, *J* = 7.9 Hz, 1H, *N-H*$_{Leu}$), 6.73 (d, *J* = 7.9 Hz, 1H, *N-H*$_{Leu}$), 6.40 (d, *J* = 6.2 Hz, 1H, *H-5”’*), 4.81 (m, 1H, *H-2’*), 4.60 (m, 1H, *H-2 or H-2”*), 4.47 (m, 1 H, *H-2 or H-2”*), 3.63 (s, 1H, *OMe*), 3.21 (m, 6H, *H-3’, H-7”’, H-10”’*), 1.84 (m, 4H, *H-8”’, H-9”’*), 1.65 (m, 3H, *H-3, H-3”, H-4 or H-4”*), 1.44 (m, 3H, *H-3, H-3”, H-4 or H-4”*), 0.93 (m, 6H, *H-5 or H-5”*), 0.82 (d, *J* = 6.1 Hz, 3H, *H-5 or H-5”*), 0.79 (d, *J* = 6.1 Hz, 3H, *H-5 or H-5”*); ^{13}C NMR (400 MHz, $CDCl_3$) δ 172.9 (CO), 171.7 (CO), 170.9 (CO), 168.8 (CO), 150.1 (q), 149.4 (C-6”’), 148.7 (C-2”’), 136.3 (q), 127.4 (q), 123.5 (C-5’), 122.0 (C-9’), 119.5 (C-8’), 118.7 (C-7’), 117.2 (q), 111.4 (C-10’), 110.1 (q), 108.6 (C-5”’), 53.4 (C-2’), 52.5 (C-2 or C-2”), 52.1 ($O\underline{C}H_3$), 51.0 (C-2 or C-2”), 49.5 (C-7”’, C-10”’), 41.1 (C-3 or C-3”), 28.1 (C-3’), 25.5 (C-8”’ and C-9”’), 25.0 (C-4 or C-4”), 24.8 (C-4 or C-4”), 23.0 (C-5 or C-5”), 22.6 (C-5 or C-5”), 21.8 (C-5 or C-5”); HRMS (ES): *m/z* 619.3606 $[M + H]^+$. Calculated for $C_{34}H_{47}N_6O_5$, 619.3608 $[M + H]^+$; Chiralpak AD 30% isopropyl alcohol/hexane, 1.0 mL/min, 254 nm, 4.588 min;

_N_-4-Pyrrolidinyl nicotinamido-L-leucine-L-(_N-tert_-butyl-carboxylate)tryptophan methyl ester (141)

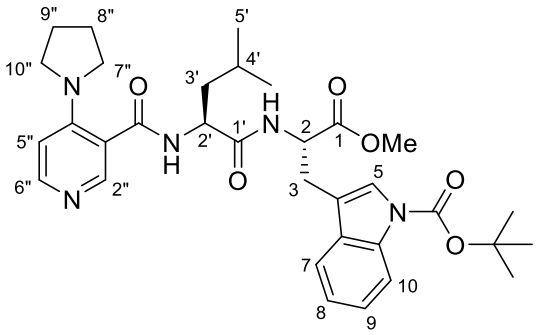

To a stirred solution of **128** (72 mg, 0.14 mmol) in THF (4 mL), was added di-*tert*-butyl dicarbonate (45 mg, 0.21 mmol). After 5 hrs, (sat.) $NaHCO_3$ (10 mL) was added and the THF removed *in vacuo*. The aqueous layer was extracted with ethyl acetate (3 x 10 mL), the combined organic extracts were dried over anhydrous $MgSO_4$ and the solvent evaporated to afford a yellow oil that was purified by column chromatography using MeOH/DCM (5/95) to provide **141** as a pale-yellow solid (44 mg, 51%), mp 102–104 °C; $[\alpha]_D^{20}$ − 4.5 (*c* 0.5, $CHCl_3$, 92% de); IR (DCM) 3420 (NH), 1736 (CO_2Me), 167 $(CO)_{amide}$ cm^{-1}; ^1H NMR (400 MHz, $CDCl_3$) δ 8.25 (s, 1H, *H-2”*), 8.14 (d, *J* = 6.1 Hz, 1H, *H-6”*), 8.08 (d, *J* = 8.2 Hz, 1H, *H-7*), 7.51 (d, *J* = 8.2 Hz, 1H, *H-10*), 7.46 (s, 1H, *H-5*), 7.26 (m, 1H, *H-9*), 7.21 (m, 1H, *H-8*), 6.79 (d, *J* = 6.1 Hz, 1H, *N-H*$_{Trp}$), 6.49 (d, *J* = 6.1 Hz, 1H, *N-H*$_{Leu}$), 6.44 (d, *J* = 6.1 Hz, 1H, *H-5”*),4.09 (m, 1H, *H-2*), 4.58 (m, 1H, *H-2’*), 3.67 (s, 3H, *OMe*), 3.24 (m, 6H, *H-3*, *H-7”*, *H-10”*), 1.86 (m, 4H, *H-8”*, *H-9”*), 1.71 (m, 2H, *H-3’*, *H-4’*), 1.64 (m, 10H, *H-3’*, *t-Bu*), 0.95 (m, 6H, *H-5’*); ^{13}C NMR (400 MHz, $CDCl_3$) δ 171.7 (CO), 171.6 (CO), 168.8 (CO), 150.1 (CO), 150.0 (C-6”), 149.5 (q), 149.2 (C-2”), 135.4 (q), 130.4 (q), 124.6 (C-9), 124.3 (C-5), 122.6 (C-8), 118.7 (C-10), 117.3 (q), 115.3 (C-7), 114.7 (q), 108.6 (C-5”), 83.8 (q), 52.8 (C-2), 52.4 (C-2’, O$\underline{C}H_3$), 49.5 (C-7”, C-10”), 41.2 (C-3’), 28.2 (C($\underline{C}H_3$)$_3$), 27.6 (C-3), 25.5 (C-8”, C-9”), 25.0 (C-4’), 23.0 (C-5’), 21.9 (C-5’); Chiralpak AD 30% isopropyl alcohol/hexane, 1.0 mL/min, 254 nm, 8.469 min; HRMS (ES): *m/z* 606.3290 $[M + H]^+$. Calculated for $C_{33}H_{44}N_5O_6$, 606.3291 $[M + H]^+$.

4-Pyrrolidinyl nicotinamido-L-leucine-L-(*N*-phenyl-carboxylate)tryptophan methyl ester (158)

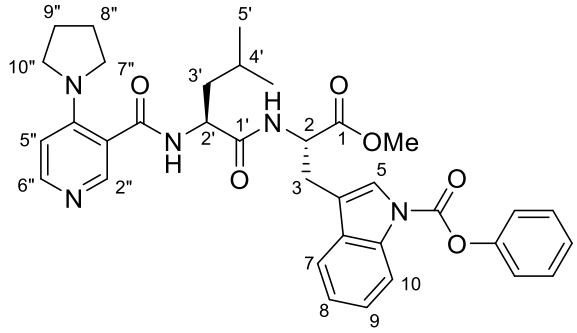

To a stirred solution of **128** (140 mg, 0.277 mmol) in DMF (1 mL) was added sodium hydride (10.4 mg, 0.26 mmol) at 0 °C. After 20 minutes, phenyl chloroformate (0.042 mL, 0.33 mmol) was added. After 1 hr (sat.) $NaHCO_3$ (2 mL) was added followed by ethyl acetate (3 x 3 mL). The combined organic layer was washed with water (3 x 10 mL). The organic layer was dried over anhydrous MgSO4 and the solvent removed to give a yellow residue that was purified by column chromatography using MeOH/DCM (5/95), to yield **158** as a pale-yellow solid (52 mg, 30%), mp 80–82 °C; $[\alpha]_D^{20}$ + 6.1 (*c* 0.72, $CHCl_3$, 45% de); IR (DCM) 3413 (NH), 1744 (CO_2Me), 1657 $(CO)_{amide}$ cm^{-1}; ^1H NMR (400 MHz, $CDCl_3$) δ 8.30 (s, 1H, *H-2”*), 8.20 (d, *J* = 8.0 Hz, 1H, *H-7*), 8.07 (s, 1H, *H-6”*), 7.70 (s, 1H, *H-5*), 7.61 (d, *J* = 7.1 Hz, 1H, *H-10*), 7.45 (t, *J* = 7.9 Hz, 2H, *H-8, H-9*), 7.38–7.29 (m, 5H, *Ar-H*), 7.12 (d, *J* = 7.8 Hz, 1H, *N-H*$_{Trp}$), 6.46 (s, 1H, *H-5”*), 4.97 (m, 1H, *H-2*), 4.63 (m, 1H, *H-2’*), 3.71 (s, 3H, *OMe*), 3.32 (m, 6H, *H-3’, H-7”, H-10”*), 1.90 (m, 4H, *H-8”, H-9”*), 1.78–1.69 (m, 3H, *H-3’, H-4’*), 0.97 (d, *J* = 4.8 Hz, 1H, *H-5’*), 0.95 (d, *J* = 4.8 Hz, 1H, *H-5’*); ^{13}C NMR (101 MHz, $CDCl_3$) δ 171.8 (CO), 171.6 (CO), 168.0 (CO), 157.7 (CO), 150.7 (q), 150.3 (q), 147.0 (C-2” or C-6”), 146.9 (C-2” or C-6”), 145.5 (q), 130.5 (q), 129.6 (C-8, C-9), 126.3, 125.2, 124.2, 123.4 (C-5), 121.5, 119.1 (C-10), 117.3 (q)116.6 (q), 115.5 (C-7), 108.6 (C-5”), 52.9 (C-2’, O$\underline{C}H_3$), 52.5 (C-2), 49.8 (C-7”, C-10”), 40.9 (C-3’), 27.6 (C-3), 25.4 (C-8”, C-9”), 25.0 (C-4’), 22.9 (C-5’), 21.8 (C-5’); HRMS (ES): *m/z* 626.2973 $[M + H]^+$, Calculated for $C_{35}H_{40}N_5O_6$, 626.2978 $[M + H]^+$.

_N_-4-Pyrrolidinyl nicotinamido-L-leucine-L-(_N_-4-methoxyphenyl-carboxylate) tryptophan methyl ester (159)

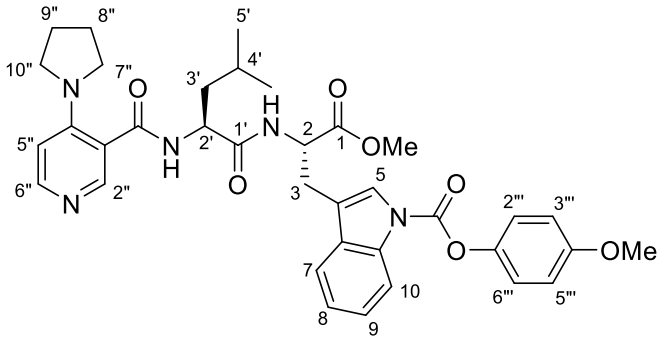

To a stirred solution of **128** (157 mg, 0.311 mmol) in DMF (1 mL) was added sodium hydride (11.2 mg, 0.28 mmol) at 0 °C. After 20 minutes, 4-methoxy-phenyl chloroformate (0.055 mL, 0.37 mmol) was added. After 1 hr, (sat.) $NaHCO_3$ (2 mL) was added followed by ethyl acetate (3 x 3 mL). The combined organic layer was washed with water (3 x 10 mL). The organic layer was dried over anhydrous $MgSO_4$ and the solvent removed to give a yellow residue that was purified by column chromatography using MeOH/DCM (5/95), to yield **159** as a pale-yellow solid (60.4 mg, 31%), mp 86–89 °C; $[\alpha]_D^{20}$ + 6.7 (*c* 0.52, $CHCl_3$, 85% de); IR (DCM) 3268 (NH), 1746 (CO_2Me), 1650 $(CO)_{amide}$, 1542 cm^{-1}; ^1H NMR (300 MHz, $CDCl_3$) δ 8.19 (m, 1H, *H-2”*), 8.16 (d, *J* = 7.2 Hz, 1H, *H-7*), 8.09–7.99 (m, 1H, *H-6”*), 7.65 (s, 1H, *H-5*), 7.57 (d, *J* = 7.2 Hz, 1H, *H-10*), 7.36–7.25 (m, 2H, *H-8*, *H-9*), 7.20–7.14 (m, 2H, *H-2”’*, *H-6”’*), 7.04 (d, *J* = 7.3 Hz, 1H, *N-*H_{Trp}), 6.93–6.87 (m, 2H, *H-3”’*, *H-5”’*), 6.42 (s, 1H, *H-5”*), 4.93 (m, 1H, *H-2*), 4.59 (m, 1H, *H-2’*), 3.82 (s, 3H, *OMe*), 3.67 (s, 3H, *OMe*), 3.28 (m, 6H, *H-3*, *H-7”*, *H-10”*), 1.86 (s, 4H, *H-8”*, *H-9”*), 1.74–1.61 (m, 3H, *H-3’*, *H-4’*), 0.94 (d, *J* = 4.0 Hz, 3H, *H-5’*), 0.92 (d, *J* = 4.0 Hz, 3H, *H-5’*); ^{13}C NMR (101 MHz, $CDCl_3$) δ 171.8 (CO), 171.7 (CO), 168.1 (CO), 157.7 (CO), 150.6 (q), 149.5 (q), 148.6 (q), 147.7 (C-2” or C-6”), 147.3 (C-2” or C-6”), 146.0 (q), 143.9 (q), 130.5 (q), 125.2 (C-8 or C-9), 124.1 (C-5), 123.4 (C-8 or C-9), 122.3 (C-2”’, C-6”’), 119.0 (C-10), 116.5 (q), 115.5 (C-7), 114.6 (C-3”’, C-5”’), 108.6 (C-5”), 55.7 ($O\underline{C}H_3$), 52.8 (C-2’), 52.5($O\underline{C}H_3$, C-2), 49.7 (C-7”, C-10”), 41.0 (C-3’), 27.6 (C-3), 25.4 (C-8”, C-9”), 25.0 (C-4’), 22.9 (C-5’), 21.8 (C-5’); HRMS (ES): *m/z* 656.3081 $[M + H]^+$, Calculated for $C_{36}H_{42}N_5O_7$, 656.30842 $[M + H]^+$.

_N_-4-Pyrrolidinyl nicotinamido-L-leucine-L-(_N_-Naphthalen-2-y-carboxylate l)tryptophan methyl ester (160)

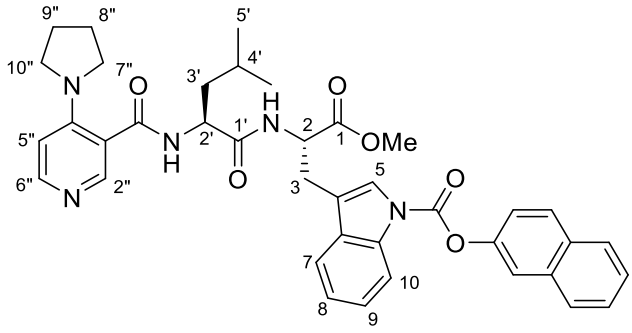

To a stirred solution of **128** (110 mg, 0.218 mmol) in DMF (1 mL) was added sodium hydride (7.8 mg, 0.20 mmol) at 0 °C. After 20 minutes, 2-naphthyl chloridocarbonate (54 mg, 0.26 mmol) was added. After 1 hr, (sat.) $NaHCO_3$ (2 mL) was added followed by ethyl acetate (3 x 3 mL). The combined organic layer was washed with water (3 x 10 mL). The organic layer was dried over anhydrous MgSO4 and the solvent removed to give a yellow residue that was purified by column chromatography using MeOH/DCM (5/95), to yield **160** as a pale-yellow solid (59 mg, 40 %), mp 96–99 °C; $[\alpha]_D^{20}$ + 9.4 (*c* 0.90, $CHCl_3$, 44% de); IR (DCM) 3408 (NH), 2959, 1746 (CO_2Me), 1657 $(CO)_{amide}$, 1455 cm^{-1}; ^1H NMR (400 MHz, $CDCl_3$) δ 8.26 (s, 1H, *H-2”*), 8.22 (d, *J* = 8.1 Hz, 1H, *H-7*), 8.09 (br. s, 1H, *H-6”*), 7.91–7.83 (m, 2H, *Naphth-H*), 7.79 (m, 1H, *Naphth-H*), 7.74 (s, 1H, *H-5*), 7.73 (s, 1H, *Naphth-H*), 7.59 (d, *J* = 8.1 Hz, 1H, *H-10*), 7.54–7.47 (m, 2H, *Naphth-H*), 7.40 (m, 1H, *Naphth-H*), 7.38–7.28 (m, 2H, *H-8*, *H-9*), 7.00 (d, *J* = 7.6 Hz, 1H, $N\text{-}H_{Trp}$), 6.78 (d, *J* = 6.8 Hz, 1H, $N\text{-}H_{Leu}$), 6.35 (d, *J* = 6.1 Hz, 1H, *H-5”*), 4.96 (m, 1H, *H-2*), 4.65–4.55 (m, 1H, *H-2’*), 3.71 (s, 3H, *OMe*), 3.38–3.25 (m, 2H, *H-3*), 3.20 (m, 4H, *H-7”*, *H-10”*), 1.80 (m, 4H, *H-8”*, *H-9”*), 1.76–1.66 (m, 3H, *H-3’*, *H-4’*), 0.95 (d, *J* = 8.0 Hz, 3H, *H-5’*), 0.93 (d, *J* = 8.0 Hz, 3H, *H-5’*); ^{13}C NMR (101 MHz, $CDCl_3$) δ 171.8 (CO), 171.7 (CO), 168.6 (CO), 150.2 (CO), 149.1 (C-6”), 148.5 (C-2”), 147.9 (q), 133.7 (q), 131.7 (q), 130.6 (q), 129.6 (C-Ar), 127.8 (C-5), 126.7 (C-Ar), 126.0 (C-Ar), 125.2 (C-Ar), 124.1 (C-Ar), 123.5 (C-9), 120.7 (C-8), 119.1 (C-Ar), 118.6 (C-10), 117.2 (q), 116.8 (q), 116.6 (q), 115.5 (C-7), 108.6 (C-5”), 52.6 (C-2), 52.5 (C-2’, O$\underline{C}H_3$), 49.53 (C-7”, C-10”), 41.0 (C-3’), 27.6 (C-3), 25.4 (C-4’), 25.0 (C-8”, C-9”), 23.0 (C-5’), 21.8 (C-5’); HRMS (ES): *m/z* 676.3142 $[M + H]^+$, Calculated for $C_{39}H_{42}N_5O_6$, 676.31351 $[M + H]^+$.

_N_-4-Pyrrolidinyl nicotinamido-L-leucine-L-(_N-tert_-butylcarbamothioyl) tryptophan methyl ester (161)

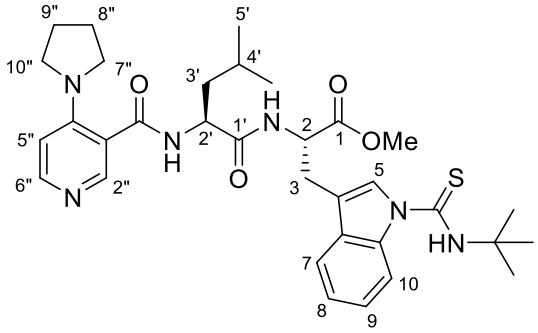

To a stirred solution of **128** (100 mg, 0.198 mmol) in DFM (0.8 mL) was added sodium hydride (7.1 mg, 0.178 mmol) at −5 °C. After 20 minutes, *tert*-butyl isothiocyanate (0.033 mg, 0.26 mmol) was added. After 2 hrs, the reaction was quenched with (sat.) $NaHCO_3$ (2 mL) and extracted with ethyl acetate (3 x 2 mL). The organic layer was washed with $NaHCO_3$ (3 x 5 mL), dried over anhydrous $MgSO_4$, and the solvent removed to give a yellow oil that was purified by column chromatography using MeOH/DCM (4/96), to yield **161** as a colourless solid (30 mg, 24%), mp 96–98°C; $[\alpha]_D^{20}$ + 24.4 (*c* 0.41, MeOH, 50% de); IR (DCM) 3054, 2986, 1742 (CO_2Me), 1679 $(CO)_{amide}$, 1422, 1266 (S=C) cm^{-1}; ^1H NMR (400 MHz, $CDCl_3$) δ 8.83 (s, 1H, *N-H*$_{Thiourea}$), 8.08 (d, *J* = 6.1 Hz, 1H, *H-6"*), 7.94 (m, 1H, *H-7*), 7.72 (s, 1H, *H-5*), 7.52 (m, 1H, *H-10*), 7.40 (s, 1H, *H-2"*), 7.25–7.13 (m, 2H, *H-8*, *H-9*), 6.86 (d, *J* = 7.5 Hz, 1H, *N-H*$_{Trp}$), 6.40 (d, *J* = 6.1 Hz, 1H, *H-5"*), 6.10 (d, *J* = 8.2 Hz, 1H, *N-H*$_{Leu}$), 4.92 (m, 1H, *H-2*), 4.54 (m, 1H, *H-2'*) 3.80 (s, 3H, *OMe*), 3.45 (m, 1H, *H-3*), 3.26–3.14 (m, 2H, *H-7*, *H-10*), 3.04 (m, 2H, *H-7*, *H-10*), 1.89–1.67 (m, 7H, *H-3'*, *H-4'*, *H-8"*, *H-9"*), 1.65 (s, 9H, *t-Bu*), 1.02 (d, *J* = 6.3 Hz, 3H, *H-5'*), 0.96 (d, *J* = 6.3 Hz, 3H, *H-5'*); ^{13}C NMR (101 MHz, $CDCl_3$) δ 178.0 (C=S), 171.7 (CO), 171.2 (CO), 169.0 (CO), 149.8 (q), 149.5 (C-6"), 148.4 (C-2"), 134.8 (q), 130.9 (q), 127.5 (C-5), 123.6 (C-8 or C-9), 121.8 (C-8 or C-9), 119.0 (C-10), 116.8 (q), 113.5 (C-7), 112.8 (q), 108.4 (C-5"), 52.6 ($O\underline{C}H_3$), 52.5 (C-2), 52.4 (C-2'), 49.4 (C-7", C-10"), 39.8 (C-3'), 28.1 ($C(\underline{C}H_3)_3$), 27.0 (C-3), 24.9 (C-4'), 23.1 (C-5'), 21.5 (C-5'), HRMS (ES): *m/z* 621.3219 $[M + H]^+$, Calculated for $C_{33}H_{45}N_6O_4S$, 621.32230 $[M + H]^+$.

3,5-bis(trifluoromethyl)phenyl isothiocyante (164)

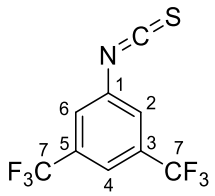

To a solution of 3,5-bis(trifluoromethyl)aniline (673.8 mg, 2.941 mmol) in DCM (8.7 mL) at 0 °C was added thiophosgene (406.0 mg, 3.532 mmol) followed by Hünig's base (802.7 mg, 6.210 mmol). After 5 hrs, aq. $NaHCO_3$ (15 mL) was added and the aqueous layer washed with DCM (3 x 15 mL). The combined organic extracts were dried over anhydrous $MgSO_4$ and the solvent removed *in vacuo* to afford a pale-yellow oil that was purified by column chromatography using heptane (100%) to give **164** as a clear oil (570 mg, 71%), ^{1}H NMR (300 MHz, $CDCl_3$) δ 7.76 (s, 1H, *H-4*), 7.64 (s, 2H, *H-2*, *H-6*); ^{13}C NMR (101 MHz, $CDCl_3$) δ 141.0 (N=C=S), 134.1 (q), 133.5 (quart., J_{CF} = 34.3 Hz, C-3, C-5), 125.7 (d, J_{CF} = 2.9 Hz, C-2, C-6), 120.5 (dt, J_{CF} = 7.5, 3.8 Hz, C-4), 118.4–126.6 (q, J_{CF} = 273.0 Hz, C-7).

***N*-4-Pyrrolidinyl nicotinamido-L-leucine-L-(*N*-3,5-bis(trifluoromethyl)phenyl)carbamothioyl) tryptophan methyl ester (162)**

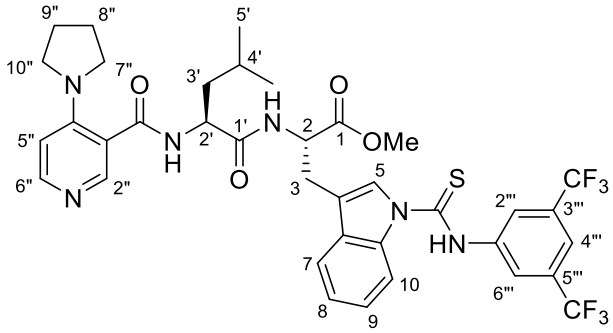

To a stirred solution of **128** (70.0 mg, 0.138 mmol) in DFM (1.5 mL) was added sodum hydride (9.5 mg, 0.24 mmol) at 0 °C. After 20 minutes, 3,5-bis(trifluoromethyl)phenyl isocyanate (0.043 mg,0.097 mmol) was added and the solution warmed to r.t. After 4 hrs, the reaction was quencehed with (sat.) $NaHCO_3$ (5 mL) and extracted with ethyl acetate (5 mL). The organic layer was washed with $NaHCO_3$ (3 x 5 mL), dried over anhydrous $MgSO_4$, and the solvent removed to give a brown oil that was purified by column chromatography using MeOH/DCM (5/95), to yield **162** as a pale-yellow solid (18 mg, 17%); $[\alpha]_D^{20}$ − 20.8 (*c* 0.36, $CHCl_3$, 53% de); IR (DCM) 3402 (NH), 1742 (CO_2Me), 1659 $(CO)_{amide}$, 1266 (C=S); ^{1}H NMR (400 MHz, $CDCl_3$) δ 8.17 (br. s , 2H, *H-2"'*, *H-6"'*), 8.14 (m, 1H, *H-7*),7.92 (d, *J* = 6.2

Hz, 1H, *H-6”*),7.74 (s, 1H, *H-5*),7.71 (s, 1H, *H-4”’*), 7.51 (m, 1H, *H*-10), 7.18 (m, 2H, *H-8*, *H-9*), 6.94 (s, 1H, *H-2”*), 6.68 (d, *J* = 7.5 Hz, 1H, *N-H*$_{Trp}$), 6.30 (d, *J* = 6.2 Hz, 1H, *H-5”*), 5.74 (d, *J* = 7.9 Hz, 1H, *N-H*$_{Leu}$), 4.96 (m, 1H, *H-2*), 4.55 (m, 1H, *H-2’*), 3.83 (s, 3H, *OMe*), 3.59 (dd, *J* = 14.7, 4.7 Hz, 1H, *H-3*), 3.20 (m, 3H, *H-3*, *H-7” or H-10”*), 2.98 (m, 2H, *H-7” or H-10”*), 1.88 (m, 3H, *H-3’*, *H-8” or H-9”*), 1.73–1.58 (m, 4H, *H-3’*, *H-4’*, *H8” or H-9”*), 1.00 (d, *J* = 6.4 Hz, 3H, *H-5’*),0.93 (d, *J* = 6.4 Hz, 3H, *H-5’*); ^{13}C NMR (101 MHz, $CDCl_3$) δ 179.4 (C=S), 171.6 (CO),170.9 (CO), 169.2 (CO),149.7 (q), 149.0 (C-6”), 147.6 (C-2”), 141.3 (q), 135.3 (q), 132.1 (quart., J_{CF} = 33.0 Hz, C-3”’, C-5”’), 131.5 (q), 126.7 (C-5), 124.2 (C-8 or C-9), 124.1 (C-8”’ or C-9”’, C-2”’ and C-6””),124.0 (C-8”’ or C-9”’, C-2”’ and C-6”’), 122.5 (C-8 or C-9), 119.1 (C-10, C-4”’), 119.0 (C-2”), 116.5 (q),115.1 (C-7), 114.8 (C-7), 108.6 (C-5”), 52.9 ($O\underline{C}H_3$), 52.6 (C-2), 52.2 (C-2’), 49.3 (C-7”, C-10”), 39.5 (C-8”, C-9”), 26.5 (C-3), 25.3 (C-3’), 25.0 (C-4’), 23.1 (C-5’), 21.4 (C-5’); HRMS (ES): *m/z* 777.2668 [M + H]$^+$, Calculated for $C_{37}H_{39}F_6N_6O_4S$, 777.2657 [M + H] $^+$.

5.5 α–Substituted Catalysts

4,8-Dihydroxyquinoline (168) [156]

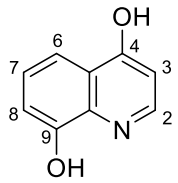

A solution of Xanthurenic acid (5.00 g, 24.4 mmol) in diphenyl ether was heated to reflux temperature. After 3 hrs the reaction mixture was cooled to r.t., and the crude product was filtered and washed with hexane to give **168** as a brown solid (3.60 g, 92%), which was used in the next step without further purification, ^{1}H NMR (400 MHz, DMSO- d_6) δ 11.21 (br. s, 1H, *OH*), 10.61 (br. s, 1H, *OH*), 7.73 (d, 1H, *J* = 7.2 *Hz*, *H-2*), 7.52 (dd, 1H, *J* = 7.8, 1.5 *Hz*, *H-6*), 7.11 (t, 1H, *J* = 7.8 *Hz*, *H-7*), 7.05 (dd, 1H, *J* = 7.8, 1.5 *Hz*, *H-8*), 6.01 (d, 1H, *J* = 7.2 *Hz*, *H-3*).

4-Hydroxy-8-tosyloxyquinoline (169)

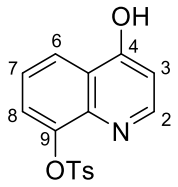

To a stirred solution of **168** in 1M NaOH (3.9 mL) at r.t was added (*p*-toluenesulfonyl chloride (710 mg, 3.73 mmol) dropwise in acetone (1.5 mL). After 18 hrs a further aliquot of *p*-toluenesulfonyl chloride (140 mg 0.75 mmol) in acetone (1 mL) was added. The mixture was stirred for an additional 2 hrs after which water (5 mL) was added to the solution resulting in the formation of a precipitate that was filtered and washed with water (10 mL) followed by acetone (10 mL) to afford **169** as a grey precipitate (1.12 g, 96%) that was used directly in the next step without further purification, ^{1}H NMR (400 MHz, DMSO) δ 11.43 (s, 1H, *OH*), 7.98 (d, *J* = 7.8 Hz, 1H, *H-2*), 7.78 (d, *J* = 8.3 Hz, 2H, *Ar-H*), 7.69 (m, 1H, *Ar-H*), 7.39 (m, 3H, *Ar-H*), 7.26 (t, *J* = 8.1 Hz, 1H, *Ar-H*), 6.03 (d, *J* = 7.8 Hz, 1H, *H-3*), 2.36 (s, 3H, *CH_3*).

4-Chloro-8-tosyloxyquinoline (170)

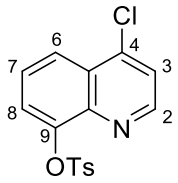

A solution of **169** (500 mg, 1.59 mmol) in phosphoryl chloride (4 mL) was heated to reflux temperature. After 3 hrs the resulting solution was cooled and carefully added to a beaker containing a small portion of ethyl acetate and ice slurry. The mixture was then slowly added to a large separatory funnel containing (sat.) $NaHCO_3$ and ethyl acetate, and extracted with ethyl acetate (3 x 200 mL). The combined organic extracts were washed with (sat.) $NaHCO_3$ and dried over anhydrous $MgSO_4$. The solvent was removed under reduced pressure to afford the crude chloride that was purified using column chromatography using ethyl acetate and hexane (25/75) to give **170** as a pale-yellow solid (390 mg, 74 %), mp 140–141°C (lit.[156] value 141–142 °C); ^{1}H NMR (400 MHz, $CDCl_3$) δ 8.67 (d, *J* = 4.6 Hz, 1H, *H-2*), 8.16 (dd, *J* = 8.4, 1.5 Hz, 1H, *H-8*), 7.87 (m, 2H, *Ar-H*), 7.70–7.55 (m, 2H, *H-6*, *H-7*), 7.47 (d, *J* = 4.6 Hz, 1H, *H-3*), 7.26 (s, 2H, *Ar-H*), 2.41 (s, 3H, *CH_3*).

4-(Pyrrolidin-1-yl)-8-tosyloxyquinoline (171)

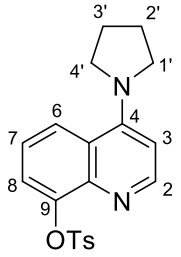

To a solution of **170** (200 mg, 0.60 mmol), in toluene (4 mL), at 100 °C, were added pyrrolidine (0.25 mL, 3.0 mmol) and K_2CO_3 (83 mg, 0.6 mmol). After 18 hrs the solution was cooled to r.t., filtered through Celite®, and washed with MeOH (20 mL). The filtrate was concentrated under reduced pressure to give a crude residue that was purified by column chromatography using ethyl acetate to afford **171** as colourless solid (150 mg, 67 %), mp 159–161°C; ^{1}H NMR (400 MHz, DMSO) δ 8.22 (d, *J* = 6.8 Hz, 1H, *H-2*), 7.94 (d, *J* = 8.5 Hz, 1H, *H-8*), 7.49 (d, *J* = 7.9 Hz, 2H, *Ar-H*), 7.41 (t, *J* = 8.5 Hz, 1H, *H-7*), 7.30 (d, *J* = 7.6 Hz, 1H, *H-6*), 7.11 (d, *J* = 7.9 Hz, 2H, *Ar-H*), 6.71 (d, *J* = 6.8 Hz, 1H, *H-3*), 3.90 (m, 4H, *H-1', H-4'*), 2.28 (s, 3H, CH_3), 2.01 (m, 4H, *H-2', H-3'*).

4-(Pyrrolidin-1-yl)-8-hydroxyquinoline tosylate (172)

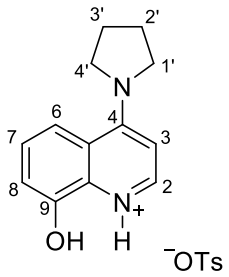

A solution of **171** (200 mg, 0.54 mmol) in ethanol (2 mL) and 2M NaOH (1.4 mL, 2.7 mmol) was heated to reflux temperature. After 3 hrs the mixture was cooled to r.t. followed by the addition of deionized water (1 mL). The pH was adjusted to 7 with 1M HCl, and the solvent removed to give a crude product that was purified by column chromatography using MeOH/DCM (10/90) to afford the purified tosylate salt **172** as a dark-green solid (193 mg, 97 %), mp decomposes > 285 °C; ^{1}H NMR (400 MHz, DMSO) δ 8.22 (d, *J* = 6.8 Hz, 1H, *H-2*), 7.94 (d, *J* = 8.5 Hz, 1H, *H-8*), 7.49 (d, *J* = 7.9 Hz, 2H, *Ar-H*), 7.41 (t, *J* = 8.5 Hz, 1H, *H-7*), 7.30 (d, *J* = 7.6 Hz, 2H, *H-6*), 7.11 (d, *J* = 7.9 Hz, 1H *Ar-H*), 6.71 (d, *J* = 6.8 Hz, 1H, *H-3*), 3.79 (m, 4H, *H-1', H-4'*), 2.28 (s, 3H, CH_3), 2.01 (br. s, 4H, *H-2', H-3'*).

Methyl (2-chloroacetyl)-L-leu-L-tryp (173)

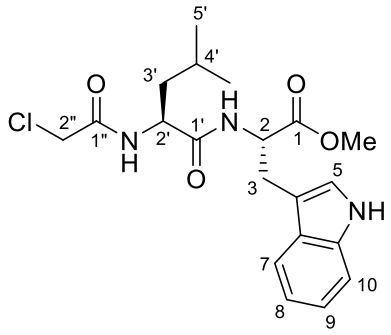

To a solution of the **104** (100 mg, 0.3 mmol) in dry DCM (5 mL) at 0 °C, was added chloroacetic acid (19 mg, 0.2 mmol), HOBt (27 mg, 0.20 mmol), and DCC (54 mg, 0.26 mmol). After 18 hrs, the mixture was filtered through Celite ® and washed with DCM (50 mL). The filtrate was concentrated under reduced pressure to give a crude residue that was purified by column chromatography using ethyl acetate/hexane (30/70) to give **173** as a colourless solid (75 mg, 92%), mp 73–75 °C; $[\alpha]_D^{20}$ + 26.5 (*c* 1.0, DCM); IR (DCM) 3407, 3055, 1743 (CO_2Me), 1661$(CO)_{amide}$, 1266 cm^{-1}; ^1H NMR (400 MHz, $CDCl_3$) δ 8.31 (br. s, 1H, *N-H*$_{indole}$), 7.50 (m, 1H, *H-7*), 7.34 (m, 1H, *H-10*), 7.17 (m, 1H, *H-9*), 7.10 (m, 1H, *H-8*), 6.98 (s, 1H, *H-5*), 6.91 (d, *J* = 8.4 Hz, 1H, *N-H*$_{Leu}$), 6.86 (d, *J* = 7.7 Hz, 1H, *N-H*$_{Trp}$), 4.90 (m, 1H, *H-2*), 4.52 (m, 1H, *H-2'*), 3.87 (d, *J* = 15.0 Hz, 1H, *H-2"*), 3.65 (d, *J* = 15.0 Hz, 1H, *H-2"*), 3.68 (s, 3H, *OMe*), 3.31 (d, *J* = 5.3 Hz, 2H, *H-3*), 1.70–1.57 (m, 3H, *H-3', H-4'*), 0.90 (d, *J* = 80 Hz, 3H, *H-5'*), 0.86 (d, *J* = 80 Hz, 3H, *H-5'*). ^{13}C NMR (101 MHz, $CDCl_3$) δ 171.9 (CO), 171.3 (CO), 166.2 (CO), 136.1 (q), 127.4 (q), 123.2 (C-5), 122.2 (C-9), 119.7 (C-8), 118.3 (C-7), 111.4 (C-10), 109.3 (q), 52.9 (C-2), 52.4 ($O\underline{C}H_3$), 51.9 (C-2'), 42.3 (C-2"), 41.1 (C-3'), 27.4 (C-3), 24.7 (C-4') 22.8 (C-5'), 22.0 (C-5'); HRMS (ES): *m/z* 408.1691 $[M + H]^+$, Calculated for $C_{20}H_{27}ClN_3O_4$, 408.1690 $[M + H]^+$; Chiralpak AD 30% isopropyl alcohol/hexane, 1.0 mL/min, 254 nm, 4.537 min.

Methyl (2-((4-(pyrrolidin-1-yl)quinolin-8-yl)oxy)acetyl)-*L*-leucyl-*L*-tryptophanate (165)

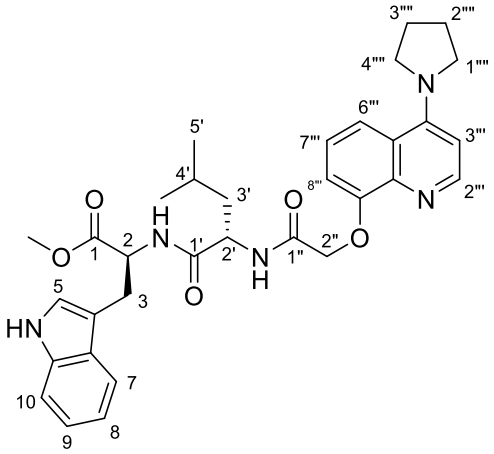

To a solution of **172** (200 mg, 0.54 mmol) in dry acetonitrile (10 mL) at r.t., were added **173** (329 mg, 0.81 mmol) and cesium carbonate (352 mg, 1.08 mmol). The temperature was increased to 60 °C, and after 7 hrs the reaction mixture was cooled, filtered through Celite®, rinsed with MeOH, and the solvent removed to afford a crude residue that was purified by column chromatography using MeOH/DCM (3/97) to afford **165** as a pale-green (180 mg, 60%), mp 106–109 °C; $[\alpha]_D^{20}$ + 13.1 (*c* 0.75, DCM); IR (DCM) 3055, 2309, 1742 (CO_2Me), 1670 $(CO)_{amide}$, 1266 cm^{-1}; ^1H NMR (400 MHz, $CDCl_3$) δ 9.22 (s, 1H, *N-H*$_{Leu}$), 9.20 (s, 1H, *N-H*$_{indole}$), 8.33 (d, *J* = 6.6 Hz, 1H, *H-2”’*), 7.85 (d, *J* = 8.8 Hz, 1H, *H-8”’*), 7.50 (d, *J* = 7.7 Hz, 1H, *N-H*$_{Trp}$), 7.47–7.41 (m, 1H, *H-7*), 7.31 (t, *J* = 8.3 Hz, 1H, *H-7”’*), 7.17 (br. s, 1H, *H-5*), 7.16–7.09 (m, 2H, *H-10*, *H-6”’*), 6.96–6.84 (m, 1H, *H-8*, *H-9*), 6.42 (d, *J* = 6.6 Hz, 1H, *H-3”’*), 4.80 (m, 1H, *H-2*), 4.70–4.60 (m, 2H, *H-2’*, *H-2”*), 4.53 (d, *J* = 14.6 Hz, 1H, *H-2”*), 3.75 (m, 4H, *H-1””*, *H-4”’*), 3.58 (s, 3H, *OMe*), 3.30–3.17 (m, 2H, *H-3*), 2.11–2.05 (m, 4H, *H-2””*, *H-3””*), 1.90 (m, 1H, *H-3’*), 1.75 (m, 1H, *H-3’*), 1.64–1.53 (m, 1H, *H-4’*), 0.87 (d, *J* = 6.6 Hz, 6H, *H-5’*), 0.83 (d, *J* = 6.6 Hz, 6H, *H-5’*); ^{13}C NMR (101 MHz, $CDCl_3$) δ 172.4 (CO), 172.1 (CO), 167.8 (CO), 154.9 (q), 149.2 (q), 142.3 (C-3”’), 136.1 (q), 133.7 (q), 127.4 (q), 124.5 (C-7”’), 124.0 (C-5), 121.2 (C-8 or C-9), 119.7 (q), 118.8 (C-8 or C-9), 118.6 (C-8”’), 118.2 (C-7), 112.8 (C-6”’), 111.2 (C-10), 109.5 (q), 102.4 (C-2”’), 69.0 (C-2”), 53.2 (C-1””, C-4””), 52.8 (C-2), 52.5 (C-2’), 52.1 ($O\underline{C}H_3$), 39.5 (C-3’), 27.4 (C-3), 25.7 (C-2””, C-3””), 24.8 (C-4’), 22.9 (C-5’), 21.7 (C-5’); HRMS (ES): *m/z* 586.3038 $[M + H]^+$, Calculated for $C_{33}H_{40}N_5O_5$, 586.3029 $[M + H]^+$; Chiralpak AD 30% isopropyl alcohol/hexane, 1.0 mL/min, 254 nm, 13.778 min.

(*S*)-2-Chloro-1-(2-(hydroxydiphenylmethyl)pyrrolidin-1-yl)ethanone (175)

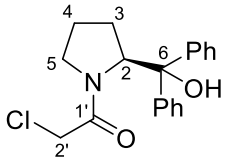

To a solution of (*S*)-(-)-α,α-diphenyl-2-pyrrolidinemethanol (300 mg, 1.18 mmol) in dry DCM at 0 °C, were added chloroacetyl chloride (267 mg, 2.36 mmol) and triethylamine (0.16 mL, 1.18 mml). After 1hr (sat.) $NaHCO_3$ was added followed by DCM (3 x 20 mL). The combined organic layers were dried over $MgSO_4$ and solvent removed at reduced pressure to give a crude residue that was purified by column chromatography using ethyl acetate/hexane mixtures (30/70) to afford **175** as a colourless solid (350 mg, 90%), $[\alpha]_D^{20}$ − 129.7 (*c* 1, DCM); ^{1}H NMR (300 MHz, $CDCl_3$) δ 7.44–7.36 (m, 4H, *Ar-H*), 7.35–7.28 (m, 6H, *Ar-H*), 6.13 (s, 1H, *OH*), 5.21 (m, 1H, *H-2*), 3.99 (s, 2H, *H-2'*), 3.45 (m, 1H, *H-5*), 3.05 (m, 1H, *H-5*), 2.14 (m, 1H, *H-3*), 2.00 (m, 1H, *H-3*), 1.62 (m, 1H, *H-4*), 1.09 (m, 1H, *H-4*); ^{13}C NMR (75 MHz, $CDCl_3$) δ 168.6 (CO), 145.8 (q), 143.0 (q), 128.0, 127.4, 81.9 (q), 67.3 (C-2), 48.5 (C-5), 42.1 (C-2'), 29.2 (C-3), 23.3 (C-4).

(*S*)-1-(2-(hydroxydiphenylmethyl)pyrrolidin-1-yl)-2-iodoethanone (176)

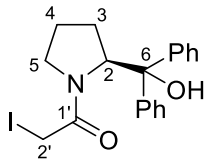

To a solution of **175** (300 mg, 0.91 mmol) in dry acetonitrile (20 mL) at 80 °C was added KI (755 mg, 4.55 mmol). After 18 hrs (sat.) $NaHCO_3$ was added followed by extraction with DCM(3 x 20 mL). The combined organic layers were dried over MgSO4 and the solvent removed at reduced pressure to give a crude residue that was purified by column chromatography using ethyl acetate/hexane mixtures (30/70) to afford **176** as a light-brown oil(320 mg, 83%), $[\alpha]_D^{20}$ − 146.1 (*c* 1.0, DCM); IR (DCM) 1619 $(CO)_{amide}$, 1215 (C–O) cm^{-1}; ^{1}H NMR (400 MHz, $CDCl_3$) δ 7.46–7.37 (m, 4H, *Ar-H*), 7.35–7.27 (s, 6H, *Ar-H*), 6.34 (s, 1H, *OH*), 5.18 (dd, *J* = 8.8, 4.2 Hz, 1H, *H-2*), 3.75 (d, *J* = 9.6 Hz, 1H, *H-2'*), 3.63 (d, *J* = 9.6 Hz, 1H, *H-2'*), 3.38 (m, 1H, *H-5*), 2.98 (m, 1H, *H-5*), 2.13 (m, 1H, *H-3*), 2.00 (m, 1H, *H-3*), 1.60 (m, 1H, *H-4*), 0.92 (m, 1H, *H-4*); ^{13}C NMR (101 MHz, $CDCl_3$) δ 170.5 (CO), 146.1 (q), 143.2 (q), 128.2–127.2 (Ar), 82.1 (C-6), 67.2 (C-2), 49.3 (C-5), 29.8 (C-3), 23.1 (C-4), −2.1 (C-2'); HRMS (ES): *m/z* 422.0614 $[M + H]^+$, Calculated for $C_{19}H_{21}INO_2$, 422.0617 $[M + H]^+$.

(*S*)-1-(2-(hydroxydiphenylmethyl)pyrrolidin-1-yl)-2-((4-(pyrrolidin-1-yl)quinolin-8-yl)oxyethan-1-one (166)

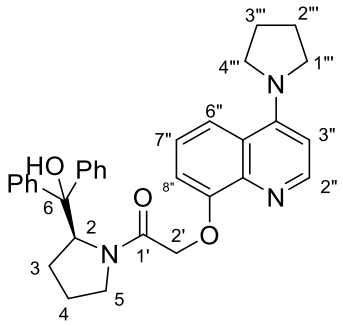

To a solution of **172** (120 mg, 0.33 mmol) in dry actonitrile (4 mL) at r.t., were added **158** (208 mg, 0.5 mmol) and cesium carbonate (215 mg, 0.66 mmol) and the temperature increased to 120 °C. Every 24 hrs iodide **167** (30 mg, 0.07 mmol) was added, and after seven days, the mixture was cooled and filtered through Celite®, rinsed with MeOH and the solvent removed to give a crude residue that was purified by column chromatography using MeOH/dihloromethane (7/93) to afford **166** as a colourless solid (73 mg, 44%), mp 139–142 °C; $[\alpha]_D^{20}$ − 76.5 (*c* 1, DCM); IR (DCM) 1638, 1347, 1265 cm^{-1}; ^1H NMR (400 MHz, $CDCl_3$) δ 8.10 (d, *J* = 8.0 Hz, 1H, *H-2”*), 7.92 (d, *J* = 8.0 Hz, 1H, *H-8”*), 7.20–7.50 (m, 11H, *H-7”*, *Ar-H*), 6.91 (d, *J* = 8.0 Hz, 1H, *H-6”*), 6.53 (d, *J* = 8.0 Hz, 1H, *H-3”*), 6.34 (s, 1H, *OH*), 5.34 (d, *J* = 15.3 Hz, 1H, *H-2’*), 5.14 (dd, *J* = 8.0, 4.0 Hz, 1H, *H-2*), 4.88 (d, *J* = 15.3 Hz, 1H, *H-2’*), 3.95 (m, 5H, *H-5*, *H-1”’*, *H-4”’*), 3.24 (m, 1H, *H-5*), 2.15 (m, 4H, *H-2”’*, *H-3”’*), 2.06 (m, 1H, *H-3*), 1.93 (m, 1H, *H-3*), 1.77 (m, 1H, *H-4*), 1.25(m, 1H, *H-4*); ^{13}C NMR (100.6 MHz, $CDCl_3$) δ 169.3 (CO), 155.1 (q), 147.5 (q), 145.9 (q), 143.4 (q), 139.3 (C-2”), 130.7 (q), 127.9, 127.6, 127.4, 127.3, 127.2, 125.6 (C-7”), 118.7, 118.6 (C-8”), 113.7 (C-6”), 102.2 (C-3”), 81.3 (q), 68.3 (C-2, C-2’), 54.1 (C-1”’, C-4”’), 48.5 (C-5). 29.6 (C-3), 25.6 (C-2”’, C-3”’), 23.5 (C-4); HRMS (ES): *m/z* 508.2607 $[M + H]^+$, Calculated for $C_{32}H_{34}N_3O_3$, 508.2600 $[M + H]^+$; Chiralpak AD 30% isopropyl alcohol/hexane, 1.0 mL/min, 254 nm, 8.300 min.

5.6 Synthesis of Alcohols

9-(1-Hydroxyethyl)anthracene (154)[163]

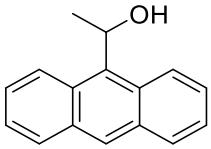

To a stirred solution of 9-anthraldehyde (1.014 g, 4.917 mmol) in diethyl ether (30 mL) at 0 °C was added CH_3Li (1.6 M in toluene, 4 mL, 6.4 mmol). After 4 hrs, sat. NH_4Cl (5 mL) was added and the layers separated. The aqueous layer was extracted with diethyl ether (1 x 10 mL) and the combined organic layer was dried over anhydrous $MgSO_4$ and the solvent removed under reduced pressure to give **154** as a yellow solid (1.033 g, 94%) that used in the next step without further purification, ^{1}H NMR (400 MHz, $CDCl_3$) δ 8.62 (d, *J* = 8.6 Hz, 1H), 8.23 (d, *J* = 81.5 Hz, 1H), 7.94 (d, *J* = 8.0 Hz, 1H), 7.41 (m, 1H), 6.42 (dd, *J* = 13.5, 6.8 Hz, 1H), 1.87 (d, *J* = 6.8 Hz, 1H); CHIRALPACK AD (4.6 mm x 25 cm), isopropyl alcohol/hexane (2.5/97.5), 1.0 mL/min, 254 nm, 11.479 min, 16.462 min.

(1S,2R)-2-hydroxycyclohexyl 4-(dimethylamino)benzoate (134)

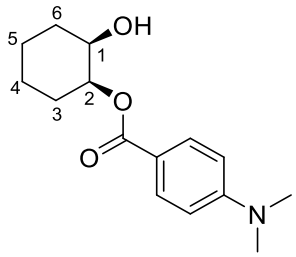

To a stirred solution of 1,2-cyclohexenediol (316.4 mg, 2.724 mmol) in pyridine (4 mL), at 0 °C, was added 4-(dimethylamino)benzoyl chloride (201.2 mg, 1.096 mmol) and the temperature increased to r.t. After 18 hrs, 1M HCl (15 mL) was added, followed by extraction with ethyl acetate (3 x 15 mL). The combined organic layer was washed with 1M HCl (3 x 45 mL), dried over anhydrous $MgSO_4$, and the solvent removed *in vauo* to give a crude residue that was purified by column chromatography using ethyl acetate/hexane (40/60) to afford **134** as a colourless solid (172.9 mg, 60%), ^{1}H NMR (300 MHz, $CDCl_3$) δ 7.94 (d, *J* = 8.0 Hz, 2H, *Ar-H*), 6.65 (d, *J* = 8.0 Hz, 2H, *Ar-H*), 5.16 (m, 1H, *H-2*), 3.92 (m, 1H, *H-1*), 3.04 (m, 6H, 2 x *CH*$_3$), 1.95 (m, 2H, *H-2*), 1.79 (m, 2H, *H-6*), 1.67 (m, 2H, *H-4 or*

H-5), 1.40 (m, 2H, *H-4 or H-5*), Chiralpak AD (4.6 mm x 25 cm), isopropyl alcohol/hexane (10/90), 1.0 mL/min, 254 nm, 25.373 min, 31.684 min.

General Procedure for the reduction of ketones: To a stirred solution of ketone in (3.0 mmol) in MeOH (5 mL), at 0 °C was added $NaBH_4$ (3.6 mmol). After 3 hrs, (sat). NH_4Cl (10 mL) was added and the layers separated. The aqueous layer was washed with ethyl acetate (3 x 30 mL). The combined organic extracts were dried over anhydrous $MgSO_4$ and the solvent removed under reduced pressure to afford the crude product that was purified by column chromatography using ethyl acetate/hexane to give the pure product.

1-(4-Methoxyphenyl)ethanol (130)

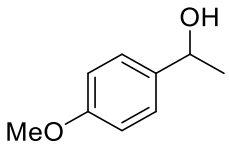

(colourless oil, 76%), ^{1}H NMR (400 MHz, $CDCl_3$) δ 7.30 (m, 2H, *Ar-H*), 6.88 (m, 2H, *Ar-H*), 4.85 (q, *J* = 6.5 Hz, 1H, *C-H*), 3.80 (s, 3H, *OMe*), 1.81 (s, 1H, *OH*), 1.48 (d, *J* = 6.4 Hz, 3H, *CH_3*); Chiralpak AD (4.6 mm x 25 cm), isopropyl alcohol/hexane (10/90), 1.0 mL/min, 254 nm, 8.136 min, 8.587 min.

1-(4-Nitrophenyl)ethanol (131)

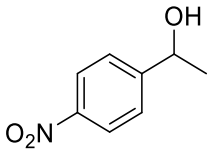

(orange oil, 80%) ^{1}H NMR (300 MHz, $CDCl_3$) δ 8.03–7.98 (d, *J* = 8.4 Hz, 2H, *Ar-H*), 7.40 (d, *J* = 8.4 Hz, 2H, d, *J* = 8.4 Hz, 2H), 4.87 (q, *J* = 6.5 Hz, 1H, *C-H*), 1.37 (d, *J* = 6.5 Hz, 3H, *CH_3*); Chiralpak IC (4.6 mm x 25 cm), isopropyl alcohol/hexane (7/93), 0.8 mL/min, 254 nm, 12.366 min, 12.926 min.

1-(4-Bromophenyl)ethanol (155)

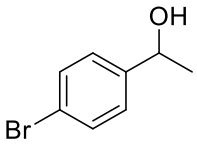

(oil, 79%), ^{1}H NMR (400 MHz, $CDCl_3$) δ 7.36 (m, 2H, *Ar-H*), 7.13 (m, 2H, *Ar-H*), 4.74 (q, *J* = 6.5 Hz, 1H, *C-H*), 1.93 (s, 1H, *OH*), 1.36 (d, *J* = 6.5 Hz, 3H, CH_3); Chiralcel OD (4.6 mm x 25 cm), isopropyl alcohol/hexane (10/90), 1.0 mL/min, 254 nm, 5.877 min, 6.301 min.

1-(2,4,6-trimethylphenyl)ethan-1-ol (133)

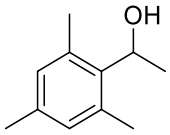

(colourless solid, 88%), ^{1}H NMR (400 MHz, $CDCl_3$) δ 6.80 (s, 2H, *Ar-H*), 5.37 (q, *J* = 6.8 Hz, 1H, *C-H*), 2.42 (s, 3H, CH_3), 2.26 (s, 3H, CH_3), 1.68 (s, 1H, *OH*), 1.53 (m, 3H, CH_3); Chiralpak AD (4.6 mm x 25 cm), isopropyl alcohol/hexane (9.5/90.5), 1.0 mL/min, 254 nm, 4.453 min, 4.854 min.

2-Methyl-1-phenyl-1-propanol (129)

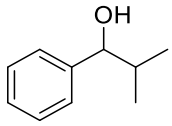

(clear oil, 85%), ^{1}H NMR (300 MHz, $CDCl_3$) δ 7.23 (m, 5H, *Ar-H*), 4.29 (d, *J* = 6.8 Hz, 1H, *C-H*), 1.90 (m, 1H, *C-H*), 1.78 (s, 1H, *OH*), 0.94 (d, *J* = 6.7 Hz, 2H, CH_3), 0.73 (d, *J* = 6.7 Hz, 2H, CH_3); Chiralpak AD (4.6 mm x 25 cm), isopropyl alcohol/hexane (2.5/97.5), 2.5 mL/min, 254 m, 11.483 min, 12.095 min.

5.7 Kinetic Resolution Experiments

General procedure for the catalytic kinetic resolution of *sec*-alcohols: To a stirred solution of the *sec*-alcohol (0.5 mmol), catalyst (0.025 mmol), and triethylamine (0.45 mmol) in DCM (2 mL) at −78 °C, was added *iso*-butyic anhydride (0.35 mmol). After 3 hrs, the reaction was quenched with MeOH (1 mL), followed by the addition of sat. $NaHCO_3$ (5 mL). The organic layer was separated and the aqueous layer was washed with DCM (2 x 5 mL). The combined organic layer was dried over anhydrous $MgSO_4$ and the solvent removed *in vacuo*. The alcohol and ester mixture was purified by column chromatography using ethyl acetate/hexane (20/80). The isolated ester was hydrolysed using 1M NaOH in MeOH (2 mL). After 6 hrs, the solvent was removed *in vacuo* and the residue purified by column chromatography using ethyl acetate/hexane (50/50).

Determination of enantiomeric excesses, conversion and selectivities: All unreacted alcohols recovered from kinetic resolutions using catalyst were found to be enriched in the (*R*)-enantiomer, as determined by the sign of the optical rotation, while esters were enriched in the (*S*)-enantiomer (also determined by measuring optical rotation). The enantiomeric excess of the unreacted alcohol and the ester (after hydrolysis) were determined by analytical chiral HPLC (Chiracel OD, Chiralpak AD, or Chiralpak IC).

Selectivity[164] was calculated according to:

$$S = \frac{\ln\left((1- C_{HPLC})(1 - ee_A)\right)}{\ln\left((1 - C_{HPLC})(1 + ee_A)\right)}$$

C_{HPLC} was calculated according to:

$$C_{HPLC} = \frac{ee_A}{ee_A + ee_E}$$

References

1. Crosby, J. In *Introduction;* Collins, A. N., Sheldrake, G. N. and Crosby, J., Eds.; Chirality in Industry II: Developments in the Manufacture and Applications of Optically Active Compounds; John Wiley & Sons Ltd: West Sussex, 1997; pp 1-10.
2. Aitken, R. A.; Gopal, J. In *Sources and Strategies for the Formation of Chiral Compounds;* Aitken, R. A., Kilényi, S. N., Eds.; Asymmetric Synthesis; Blackie Academic & Professional: London, 1992; pp 64-82.
3. Blumenstein, J. J. In *Chiral Drugs: Regulatory Aspects;* Collins, A. N., Sheldrake, G. N. and Crosby, J., Eds.; Chirality in Industry II: Developments in the Manufacture and Applications of Optically Active Compounds; Wiley & Sons Ltd: West Sussex, 1997; pp 11-18.
4. Nelson, C. G.; Burke, T. R. *J. Org. Chem.* **2012**, *77*, 733-738.
5. Walsh, P. J.; Kozlowski, M. C. *Fundamentals of Asymmetric Catalysis;* University Science Books: California, 2009.
6. Keith, J. M.; Larrow, J. F.; Jacobsen, E. N. *Adv. Synth. Catal.* **2001**, *343*, 5-26.
7. Allen, S. E.; Hsieh, S.; Gutierrez, O.; Bode, J. W.; Kozlowski, M. C. *J. Am. Chem. Soc.* **2014**, *136*, 11783-11791.
8. Lihammar, R.; Millet, R.; Baeckvall, J. *J. Org. Chem.* **2013**, *78*, 12114-12120.
9. Dalko, P. I.; Moisan, L. *Angew. Chem., Int. Ed.* **2001**, *40*, 3726-3748.
10. Berkessel, A.; Gröger, H. *Asymmetric Organocatalysis;* Wiley-VCH: Weinheim, 2005.
11. Dalko, P. I.; Moisan, L. *Angew. Chem., Int. Ed.* **2004**, *43*, 5138-5175.
12. Bredig, G.; Fiske, P. S. *Biochem. Z.* **1913**, *46*, 7-23.
13. Brown, S. P.; Brochu, M. P.; Sinz, C. J.; MacMillan, D. W. C. *J. Am. Chem. Soc.* **2003**, *125*, 10808-10809.
14. Wilson, J. E.; Casarez, A. D.; MacMillan, D. W. C. *J. Am. Chem. Soc.* **2009**, *131*, 11332-11334.
15. Wang, Z.; Ye, X.; Wei, S.; Wu, P.; Zhang, A.; Sun, J. *Org. Lett.* **2006**, *8*, 999-1001.
16. Connon, S. J. *Org. Biomol. Chem.* **2007**, *5*, 3407-3417.
17. Sigman, M. S.; Jacobsen, E. N. *J. Am. Chem. Soc.* **1998**, *120*, 4901-4902.
18. Sigman, M. S.; Vachal, P.; Jacobsen, E. N. *Angew. Chem., Int. Ed.* **2000**, *39*, 1279-1281.

19. Bartoli, G.; Bosco, M.; Carlone, A.; Locatelli, M.; Melchiorre, P.; Sambri, L. *Angew. Chem., Int. Ed.* **2005**, *44*, 6219-6222.
20. Beeson, T. D.; MacMillan, D. W. C. *J. Am. Chem. Soc.* **2005**, *127*, 8826-8828.
21. Ueda, M.; Kano, T.; Maruoka, K. *Org. Biomol. Chem.* **2009**, *7*, 2005-2012.
22. Enders, D.; Seki, A. *Synlett* **2002**, 26-28.
23. List, B.; Pojarliev, P.; Martin, H. J. *Org. Lett.* **2001**, *3*, 2423-2425.
24. Denmark, S. E.; Coe, D. M.; Pratt, N. E.; Griedel, B. D. *J. Org. Chem.* **1994**, *59*, 6161-6163.
25. Franzen, J.; Marigo, M.; Fielenbach, D.; Wabnitz, T. C.; Kjrsgaard, A.; Jørgensen, K. A. *J. Am. Chem. Soc.* **2005**, *127*, 18296-18304.
26. Bartoli, G.; Bosco, M.; Carlone, A.; Pesciaioli, F.; Sambri, L.; Melchiorre, P. *Org. Lett.* **2007**, *9*, 1403-1405.
27. Seayad, J.; List, B. *Org. Biomol. Chem.* **2005**, *3*, 719-724.
28. Höefle, G.; Steglich, W.; Vorbrueggen, H. *Angew. Chem.* **1978**, *90*, 602-615.
29. Scriven, E. F. V. *Chem. Soc. Rev.* **1983**, *12*, 129-161.
30. Grondal, C. *Synlett* **2003**, *10*, 1568-1569.
31. Murugan, R.; Scriven, E. F. V. *Aldrichimica Acta* **2003**, *36*, 21-27.
32. Litvinenko, L. M.; Kirichenko, A. I. *Doklady Chemistry (Engl. Transl.)* **1967**, 763-766.
33. Steglich, W.; Höefle, G. *Angew. Chem., Int. Ed. Engl.* **1969**, *8*, 981.
34. Spivey, A. C.; Arseniyadis, S. *Angew. Chem., Int. Ed.* **2004**, *43*, 5436-5441.
35. Singh, S.; Das, G.; Singh, O. V.; Han, H. *Org. Lett.* **2007**, *9*, 401-404.
36. De, R. N.; Berionni, G.; Couty, F.; Mayr, H.; Goumont, R.; David Olivier, R. P. *Org. Lett.* **2011**, *13*, 530-533.
37. Nicolaou, K. C.; Baran, P. S. *Angew. Chem. Int. Ed. Engl.* **2002**, *41*, 2678-2720.
38. Yao, Q. *Org. Lett.* **2002**, *4*, 2197-2199.
39. Wurz, R. P. *Chem. Rev.* **2007**, *107*, 5570-5595.
40. Müller, C. E.; Schreiner, P. R. *Angew. Chem. Int. Ed. Engl.* **2011**, *50*, 6012-6042.
41. Wei, Y.; Held, I.; Zipse, H. *Org. Biomol. Chem.* **2006**, *4*, 4223-4230.
42. Moitessier, N.; Chapleur, Y. *Tetrahedron Lett.* **2003**, *44*, 1731-1735.
43. Kattnig, E.; Albert, M. *Org. Lett.* **2004**, *6*, 945-948.
44. Xu, S.; Held, I.; Kempf, B.; Mayr, H.; Steglich, W.; Zipse, H. *Chem. Eur. J.* **2005**, *11*, 4751-4757.

45. Kagan, H. B.; Fiaud, J. C. In Eliel, E. L., Fiaud, J. C., Eds.; Topics in Stereochemistry; Wiley: New York, 1988; pp 249-330.
46. Gawley, R. E. *J. Org. Chem.* **2006**, *71*, 2411-2416.
47. Vedejs, E.; Chen, X. *J. Am. Chem. Soc.* **1996**, *118*, 1809-1810.
48. Bondarenko, L. I.; Kirichenko, A. I.; Litvinenko, L. M.; Dmitrenko, I. N.; Kobets, V. D. *Zh. Org. Khim.* **1981**, *17*, 2588-2594.
49. Kawabata, T.; Nagato, M.; Takasu, K.; Fuji, K. *J. Am. Chem. Soc.* **1997**, *119*, 3169-3170.
50. Spivey, A. C.; Maddaford, A.; Fekner, T.; Redgrave, A. J.; Frampton, C. S. *J. Chem. Soc., Perkin Trans. 1* **2000**, 3460-3468.
51. Díez, D.; Gil, M. J.; Moro, R. F.; Garrido, N. M.; Marcos, I. S.; Basabe, P.; Sanz, F.; Broughton, H. B.; Urones, J. G. *Tetrahedron: Asymmetry* **2005**, *16*, 2980-2985.
52. Jeong, K.; Kim, S.; Park, H.; Chang, K.; Kim, K. S. *Chem. Lett.* **2002**, 1114-1115.
53. Yamada, S.; Misono, T.; Iwai, Y.; Masumizu, A.; Akiyama, Y. *J. Org. Chem.* **2006**, *71*, 6872-6880.
54. Yamada, S.; Misono, T.; Tsuzuki, S. *J. Am. Chem. Soc.* **2004**, *126*, 9862-9872.
55. Dalaigh, C. O.; Hynes, S. J.; O'Brien, J. E.; McCabe, T.; Maher, D. J.; Watson, G. W.; Connon, S. J. *Org. Biomol. Chem.* **2006**, *4*, 2785-2793.
56. Poisson, T.; Penhoat, M.; Papamicael, C.; Dupas, G.; Dalla, V.; Marsais, F.; Levacher, V. *Synlett* **2005**, 2285-2288.
57. Nguyen, H. V.; Butler, D. C. D.; Richards, C. J. *Org. Lett.* **2006**, *8*, 769-772.
58. Nguyen, H. V.; Motevalli, M.; Richards, C. J. A *Synlett* **2007**, 725-728.
59. Ma, G.; Deng, J.; Sibi, M. P. *Angew. Chem., Int. Ed.* **2014**, *44*, 12012-12015.
60. Bull, S. D.; Davies, S. G.; Fox, D. J.; Garner, A. C.; Sellers, T. G. R. *Pure Appl. Chem.* **1998**, *70*, 1501-1506.
61. Sibi, M. P.; Zhang, R.; Manyem, S. A *J. Am. Chem. Soc.* **2003**, *125*, 9306-9307.
62. Arseniyadis, S.; Mahesh, M.; McDaid, P.; Hampel, T.; Davey, S. G.; Spivey, A. C. *Collect. Czech. Chem. Commun.* **2011**, *76*, 1239-1253.
63. Spivey, A. C.; Fekner, T.; *Tetrahedron Lett.* **1998**, *39*, 8919-8922.
64. Spivey, A. C.; Charbonneau, P.; Fekner, T.; Hochmuth, D. H.; Maddaford, A.; Malardier-Jugroot, C.; Redgrave, A. J.; Whitehead, M. A. *J. Org. Chem.* **2001**, *66*, 7394-7401.
65. Spivey, A. C.; Zhu, F.; Mitchell, M. B.; Davey, S. G.; Jarvest, R. L. *J. Org. Chem.* **2003**, *68*, 7379-7385.

66. Spivey, A. C.; Leese, D. P.; Zhu, F.; Davey, S. G.; Jarvest, R. L. *Tetrahedron* **2004**, *60*, 4513-4525.
67. Spivey, A. C.; Maddaford, A.; Leese, D. P.; Redgrave, A. J. *J. Chem. Soc., Perkin Trans. 1* **2001**, 1785-1794.
68. Sammakia, T.; Hurley, T. B. *J. Org. Chem.* **1999**, *64*, 4652-4664.
69. Larionov, E.; Mahesh, M.; Spivey, A. C.; Wei, Y.; Zipse, H. *J. Am. Chem. Soc.* **2012**, *134*, 9390-9399.
70. Ruble, J. C.; Fu, G. C. *J. Org. Chem.* **1996**, *61*, 7230-7231.
71. Dalko, P. I.; Editor Enantioselective Organocatalysis: Reactions and Experimental Procedures. **2007**, 536.
72. Garrett, C. E.; Fu, G. C. *J. Am. Chem. Soc.* **1998**, *120*, 7479-7483.
73. Garrett, C. E.; Lo, M. M. -C.; Fu, G. C. *J. Am. Chem. Soc.* **1998**, *120*, 10276.
74. Hill, E. A.; Richards, J. H. *J. Am. Chem. Soc.* **1961**, *83*, 3840-3846.
75. Turbitt, T. D.; Watts, W. E. *J. Chem. Soc., Perkin Trans. 2* **1974**, 185-189.
76. Wurz, R. P.; Lee, E. C.; Ruble, J. C.; Fu, G. C. *Adv. Synth. Catal.* **2007**, *349*, 2345-2352.
77. Ruble, J. C.; Latham, H. A.; Fu, G. C. *J. Am. Chem. Soc.* **1997**, *119*, 1492-1493.
78. Ruble, J. C.; Tweddell, J.; Fu, G. C. *J. Org. Chem.* **1998**, *63*, 2794-2795.
79. Bellemin-Laponnaz, S.; Tweddell, J.; Ruble, J. C.; Breitling, F. M.; Fu, G. C. *Chem. Commun.* **2000**, 1009-1010.
80. Tao, B.; Ruble, J. C.; Hoic, D. A.; Fu, G. C. *J. Am. Chem. Soc.* **1999**, *121*, 5091-5092.
81. Brenna, E.; Caraccia, N.; Fuganti, C.; Fuganti, D.; Grasselli, P. *Tetrahedron: Asymmetry* **1997**, *8*, 3801-3805.
82. Sinha, S. C.; Barbas, C. F.,III; Lerner, R. A. *Proc. Natl. Acad. Sci. U. S. A.* **1998**, *95*, 14603-14608.
83. Francais, A.; Leyva, A.; Etxebarria-Jardi, G.; Ley, S. V. *Org. Lett.* **2010**, *12*, 340-343.
84. Seitzberg, J. G.; Dissing, C.; Sotofte, I.; Norrby, P.; Johannsen, M. *J. Org. Chem.* **2005**, *70*, 8332-8337.
85. Seitzberg, J. G.; Dissing, C.; Sotofte, I.; Norrby, P.; Johannsen, M. *J. Org. Chem.* **2005**, *70*, 10890.
86. Crittall, M. R.; Rzepa, H. S.; Carbery, D. R. *Org. Lett.* **2011**, *13*, 1250-1253.
87. Crittall, M. R.; Fairhurst, N. W. G.; Carbery, D. R. *Chem. Commun.* **2012**, *48*, 11181-11183.
88. Briere, J.; Oudeyer, S.; Dalla, V.; Levacher, V. *Chem. Soc. Rev.* **2012**, *41*, 1696-1707.

89. Mayer, S.; List, B. *Angew. Chem. Int. Ed. Engl.* **2006**, *45*, 4193-4195.
90. Martin, N. J. A.; List, B. *J. Am. Chem. Soc.* **2006**, *128*, 13368-13369.
91. Schreiner, P. R. *Chem. Soc. Rev.* **2003**, *32*, 289-296.
92. Zhang, Z.; Schreiner, P. R. *Chem. Soc. Rev.* **2009**, *38*, 1187-1198.
93. Doyle, A. G.; Jacobsen, E. N. *Chem. Rev.* **2007**, *107*, 5713-5743.
94. De, C. K.; Klauber, E. G.; Seidel, D. *J. Am. Chem. Soc.* **2009**, *131*, 17060-17061.
95. Seidel, D. *Synlett* **2014**, *25*, 783-794.
96. Klauber, E. G.; De, C. K.; Shah, T. K.; Seidel, D. *J. Am. Chem. Soc.* **2010**, *132*, 13624-13626.
97. De, C. K.; Mittal, N.; Seidel, D. *J. Am. Chem. Soc.* **2011**, *133*, 16802-16805.
98. De, C. K.; Seidel, D. *J. Am. Chem. Soc.* **2011**, *133*, 14538-14541.
99. De, C. K.; Mittal, N.; Seidel, D. *J. Am. Chem. Soc.* **2011**, *133*, 16802-16805.
100. Mittal, N.; Sun, D. X.; Seidel, D. *Org. Lett.* **2012**, *14*, 3084-3087.
101. Min, C.; Mittal, N.; De, C. K.; Seidel, D. *Chem. Commun.* **2012**, *48*, 10853-10855.
102. Wennemers, H. *Chem. Commun.* **2011**, *47*, 12036-12041.
103. Miller, S. J. *Acc. Chem. Res.* **2004**, *37*, 601-610.
104. Tsogoeva, S. B. *Lett. Org. Chem.* **2005**, *2*, 208-213.
105. Freund, M.; Tsogoeva, S. B. In *Peptides for Asymmetric Catalysis;* Methods in Asymmetric Synthesis: Advanced Materials, Techniques, and Applications; John Wiley & Sons, Inc: New Jersey, 2011; pp 529-578.
106. Oku, J.; Ito, N.; Inoue, S. *Makromol. Chem.* **1979**, *180*, 1089-1091.
107. Oku, J.; Inoue, S. *J. Chem. Soc., Chem. Commun.* **1981**, 229-230.
108. Juliá, S.; Masana, J.; Vega, J. C. *Angew. Chem.* **1980**, *92*, 968-969.
109. Juliá, S.; Guixer, J.; Masana, J.; Rocas, J.; Colonna, S.; Annuziata, R.; Molinari, H. *J. Chem. Soc., Perkin Trans. 1* **1982**, 1317-1324.
110. Eder, U.; Sauer, G.; Wiechert, R. *Angew. Chem., Int. Ed. Engl.* **1971**, *10*, 496-497.
111. Hajos, Z. G.; Parrish, D. R. *J. Org. Chem.* **1974**, *39*, 1615-1621.
112. Miller, S. J.; Copeland, G. T.; Papaioannou, N.; Horstmann, T. E.; Ruel, E. M. *J. Am. Chem. Soc.* **1998**, *120*, 1629-1630.
113. Lewis, P. N.; Momany, F. A.; Scheraga, H. A. *Proc. Nat. Acad. Sci. U. S. A.* **1971**, *68*, 2293-2297.
114. Copeland, G. T.; Jarvo, E. R.; Miller, S. J. *J. Org. Chem.* **1998**, *63*, 6784-6785.
115. Jarvo, E. R.; Copeland, G. T.; Papaioannou, N.; Bonitatebus, P. J., Jr.; Miller, S. J. *J. Am. Chem. Soc.* **1999**, *121*, 11638-11643.

116. a) Vasbinder, M. M.; Jarvo, E. R.; Miller, S. J. *Angew. Chem., Int. Ed.* **2001**, *40*, 2824-2827; b). Copeland, G. T.; Miller, S. J. *J. Am. Chem. Soc.* **2001**, *123*, 6496-6502.

117. a) Papaioannou, N.; Evans, C. A.; Blank, J. T.; Miller, S. J. *Org. Lett.* **2001**, *3*, 2879-2882; b) Papaioannou, N.; Blank, J. T.; Miller, S. J. *J. Org. Chem.* **2003**, *68*, 2728-2734.

118. a) Hrdina, R.; Mueller, C. E.; Schreiner, P. R. *Chem. Commun.* **2010**, *46*, 2689-2690; b) Muller, C. E.; Wanka, L.; Jewell, K.; Schreiner, P. R. *Angew. Chem. Int. Ed.* **2008**, *47*, 6180-6183.

119. a) Birman, V. B.; Uffman, E. W.; Jiang, H.; Li, X.; Kilbane, C. J. *J. Am. Chem. Soc*, **2004**, *126*, 12226-12227; b) Birman, V. B.; Jiang, H. *Org. Lett.* **2005**, *7*, 3445-3447; c) Li, X.; Liu, P.; Houk, K. N.; Birman, V. B. *J. Am. Chem. Soc*, **2008**, *130*, 13836-13867; d) Li, X.; Jiang, H.; Uffman, E. W.; Guo, L.; Zhang, Y.; Yang, X.; Birman, V. B. *J. Org. Chem.* **2012**, *77*, 1722-1737.

120. Mandai, H.; Irie, S.; Akehi, M.; Yuri, K.; Yoden, M.; Mitsudo, K.; Suga, S. *Heterocycles* **2013**, *87*, 329-340.

121. a) Kawabata, T.; Stragies, R.; Fukaya, T.; Nagaoka, Y.; Schedel, H.; Fuji, K. *Tetrahedron Lett.* **2003**, *44*, 1545-1548; b) Kawabata, T.; Stragies, R.; Fukaya, T.; Fuji, K. *Chirality*, **2003**, *15*, 71-76; c) Kawabata, T.; Muramatsu, W.; Nishio, T.; Shibata, T.; Shedel, H. *J. Am. Chem. Soc.* **2007**, *129*, 12890-12895; d) Ueda, Y.; Muramatsu, W.; Mishiro, K.; Furuta, T.; Kawabata, T. *J. Org. Chem.* **2009**, *74*, 8802-8805; e) Schedel, H.; Kan, K.; Ueda, Y.; Mishiro, K.; Yoshida, K.; Futura, T.; Kawabata, T. *Beilstein J. Org. Chem.* **2012**, *8*, 1778-1787; f) Ueda, Y.; Furuta, T.; Kawabata, T. *Angew. Chem. Int. Ed.* **2015**, *54*, 11966-11970; g) Pelotier, B.; Priem, G.; MacdonaldS. F.; Anson, M. S.; Upton, R. J.; Campbell, I. B. *Tetrahedron Lett*., **2005**, *46*, 9005.

122. Schneider, C. *Synthesis* **2006**, 3919-3944.

123. Matsunaga, S.; Das, J.; Roels, J.; Vogl, E. M.; Yamamoto, N.; Iida, T.; Yamaguchi, K.; Shibasaki, M. *J. Am. Chem. Soc.* **2000**, *122*, 2252-2260.

124. Wang, Z.; Law, W. K.; Sun, J. *Org. Lett.* **2013**, *15*, 5964-5966.

125. Denmark, S. E.; Barsanti, P. A.; Wong, K.; Stavenger, R. A. *J. Org. Chem.* **1998**, *63*, 2428-2429.

126. Kobayashi, S.; Hachiya, I.; Araki, M.; Ishitani, H. *Tetrahedron Lett.* **1993**, *34*, 3755-3758.

127. Kobayashi, S. *Eur. J. Org. Chem.* **1999**, 15-27.
128. Berkessel, A.; Ashkenazi, E.; Andreae, M. R. M. *Appl. Catal., A* **2003**, *254*, 27-34.
129. Choudary, B. M.; Jyothi, K.; Madhi, S.; Kantam, M. L. *Synlett* **2004**, 231-234.
130. Oriyama, T.; Imai, K.; Sano, T.; Hosoya, T. *Tetrahedron Lett.* **1998**, *39*, 3529-3532.
131. Jacobsen, E. N. *Acc. Chem. Res.* **2000**, *33*, 421-431.
132. Jacobsen, E. N.; Kakiuchi, F.; Konsler, R. G.; Larrow, J. F.; Tokunaga, M. *Tetrahedron Lett.* **1997**, *38*, 773-776.
133. Matsunaga, S.; Das, J.; Roels, J.; Vogl, E. M.; Yamamoto, N.; Iida, T.; Yamaguchi, K.; Shibasaki, M. *J. Am. Chem. Soc.* **2000**, *122*, 2252-2260.
134. Schneider, C.; Sreekanth, A. R.; Mai, E. *Angew. Chem., Int. Ed.* **2004**, *43*, 5691-5694.
135. Cole, B. M.; Shimizu, K. D.; Krueger, C. A.; Harrity, J. P. A.; Snapper, M. L.; Hoveyda, A. H. *Angew. Chem., Int. Ed. Engl.* **1996**, *35*, 1668-1671.
136. Fahrni, C. J.; Pfaltz, A. *Helv. Chim. Acta* **1998**, *81*, 491-506.
137. Fahrni, C. J. *Tetrahedron* **1998**, *54*, 5465-5470.
138. Trost, B. M.; Ito, H. *J. Am. Chem. Soc.* **2000**, *122*, 12003-12004.
139. Trost, B. M.; Yeh, V. S. C.; Ito, H.; Bremeyer, N. *Org. Lett.* **2002**, *4*, 2621-2623.
140. Pfaltz, A. *Acc. Chem. Res.* **1993**, *26*, 339-345.
141. Koenig, W.; Geiger, R. *Chem. Ber.* **1970**, *103*, 788-798.
142. Chen, F. M. F.; Benoiton, N. L. *Can. J. Chem.* **1987**, *65*, 1224-1227.
143. Trost, B. M.; Yeh, V. S. C.; Ito, H.; Bremeyer, N. *Org. Lett.* **2002**, *4*, 2621-2623.
144. Harper, K. C.; Sigman, M. S. *Proc. Natl. Acad. Sci. U. S. A.* **2011**, *108*, 2179-2183.
145. Copp, F. C.; Timmis, G. M. *J. Chem. Soc.* **1955**, 2021-2027.
146. Mitsunobu, O.; Yamada, M. *Bull. Chem. Soc. Jpn.* **1967**, *40*, 2380-2382.
147. Mancilla, T.; Carrillo, L.; Zamudio-Rivera, L. S.; Beltran, H. I.; Farfan, N. *Org. Prep. Proced. Int.* **2001**, *33*, 341-349.
148. Han, Z.; Da, C.; Qiu, L.; Ni, M.; Zhou, Y.; Wang, R. *Lett. Org. Chem.* **2006**, *3*, 143-148.
149. Richter, J. M.; Whitefield, B. W.; Maimone, T. J.; Lin, D. W.; Castroviejo, M. P.; Baran, P. S. *J. Am. Chem. Soc.* **2007**, *129*, 12857-12869.
150. Groselj, U.; Bevk, D.; Jakse, R.; Meden, A.; Pirc, S.; Recnik, S.; Stanovnik, B.; Svete, J. *Tetrahedron: Asymmetry* **2004**, *15*, 2367-2383.
151. Halgren, T. *J. Comp. Chem.* **1996**, *17*, 490.
152. Sperry, J.; Moody, C. J. *Tetrahedron* **2010**, *66*, 6483-6495.

153. Appleton, D. R.; Babcock, R. C.; Copp, B. R. *Tetrahedron* **2001**, *57*, 10181-10189.
154. Deng, G.; Liu, Z.; Ye, F.; Luo, X.; Zhmu, W.; Shen, X.; Liu, H.; Jiang, H. *Eur. J. Med. Chem.* **2008**, *43*, 2699-2716.
155. Chai, J.; Head-Gordon, M. *Phys. Chem. Chem. Phys.* **2008**, *10*, 6615-6620.
156. Heiskanen, J. P.; Omar, W. A. E.; Ylikunnari, M. K.; Haavisto, K. M.; Juan, M. J.; Hormi, O. E. O. *J. Org. Chem.* **2007**, *72*, 920-922.
157. Franzen, J.; Marigo, M.; Fielenbach, D.; Wabnitz, T. C.; Kjaersgaard, A.; Jørgensen, K. A. *J. Am. Chem. Soc.* **2005**, *127*, 18296-18304.
158. Sumiyoshi, H.; Shimizu, T.; Katoh, M.; Baba, Y.; Sodeoka, M. *Org. Lett.* **2002**, *4*, 3923-3926.
159. Page, P. C. B.; Buckley, B. R.; Farah, M. M.; Blacker, A. J. *Eur. J. Org. Chem.* **2009**, 3413-3426.
160. Yamada, S.; Misono, T.; Iwai, Y.; Masumizu, A.; Akiyama, Y. *J. Org. Chem.* **2006**, *71*, 6872-6880.
161. Sperry, J.; Moody, C. J. *Tetrahedron* **2010**, *66*, 6483-6495.
162. Dahiya, R.; Kumar, A. *J. Zhejiang Univ., Sci. , B* **2008**, *9*, 391-400.
163. Sanyal, A.; Snyder, J. K. *Org. Lett.* **2000**, *2*, 2527-2530.
164. Vedejs, E.; Daugulis, O. *J. Am. Chem. Soc.* **1999**, *121*, 5813-5814.